Design and synthesis of metallo-β-lactamase inhibitors

Ricky Michael Cain

Submitted in accordance with the requirements for the degree of
Doctor of Philosophy

The University of Leeds
School of Chemistry

July 2015

The candidate confirms that the work submitted is his own, except where work which has formed part of jointly-authored publications has been included. The contribution of the candidate and the other authors to this work has been explicitly indicated below. The candidate confirms that appropriate credit has been given within the thesis where reference has been made to the work of others.

Chapter 4 contains work described in the publication 'Applications of structure-based design to antibacterial drug discovery', as published in the journal, Bio-organic Chemistry. The candidate carried out the literature review and manuscript preparation with S. Narramore. The candidate also conducted all work relating to metallo-β-lactamase inhibitor discovery. M. McPhillie and K. Simmons provided information on triclosan derivative and DHODH respectively, and C. Fishwick helped with manuscript preparation.

Chapter 8 contains work described in the publication 'Assay Platform for Clinically Relevant Metallo-β-lactamases', as published in the journal, Journal of Medicinal Chemistry. The candidate contributed *in silico* studies, S. van Berkel, J. Brem and A. Rydzik carried out biological evaluation, R.Salimraj, A. Verma and R. Owens expressed the relevant proteins., and C. Fishwick, J. Spencer and C. Schofield prepared the manuscript.

Acknowledgements

Abstract

Bacterial resistance is a continuously evolving threat to our most common antibiotics; the β-lactams. Most recently, the production of β-lactamase enzymes by bacteria rendered many of our current antibiotics unusable threatening to plunge us into a 'pre-antibiotic' era. Metallo-β-lactamases (MBLs) play a key role in bacterial resistance to β-lactam antibiotics by efficiently catalysing the hydrolysis of the β-lactam amide bond. Since their discovery, the clinically relevant MBLs, Verona integrin-encoded metallo-β-lactamase (VIM-2), Imipenemase (IMP-1), New Delhi metallo-β-lactamase (NDM-1) and Sao Paulo metallo-β-lactamase (SPM-1), have spread across the world with cases reported in almost all countries.

This thesis describes a number of approaches to the identification of inhibitors of MBLs. A combination of structure-based drug design, chemical synthesis and biological evaluation has been used to rationally identify novel inhibitors of VIM-2, IMP-1, NDM-1 and SPM-1 which have also been co administered with a current β-lactam antibiotic and been found to re-sensitise the bacteria to the antibiotic. Four novel classes of inhibitor have been investigated by taking different approaches to inhibitor discovery.

A vHTS screening campaign was conducted to identify potential inhibitors from libraries of known compounds. The campaign identified some weak binding inhibitors. Boronic acid-based inhibitors were identified by using vHTS and *de novo* design respectively and were synthesised which gave IC_{50}'s in the region of 10 nM against VIM-2 and NDM-1. Additionally, a new computational method for the identification of peptides which bind to enzymes has been developed which found Pro-Cys-Phe to be the most active peptide for binding to NDM-1 with an IC_{50} of 183 µM. This method could be applied to many other systems. In the final approach, *de novo* design using SPROUT led to the design of a novel thiol based inhibitor class. The inhibitor class has been co-crystallised in VIM-2 and gives IC_{50} values in the range of 200 nM. The inhibitor class has also successfully shown a 100 fold recovery of the MIC of meropenem against NDM-1 expressing bacteria.

Table of Contents

List of Abbreviations and Symbols

aq.	Aqueous
bp.	Boiling point
BSAC	British Society for Antimicrobial Chemotherapy
BuLi	Butyl lithium
Cat.	Catalytic
DCM	Dichloromethane
DIPA	Di-isopropylamine
DIPEA	Di-isopropylethylamine
DMSO	Dimethyl sulfoxide
DMF	Dimethylformamide
EDC	1-Ethyl-3-(3-dimethylaminopropyl) carbodiimide
eHiTS	Electronic high throughput screening
EI	Electron impact
eq.	Equivalent (s)
EtOAc	Ethyl acetate
ESI	Electrospray ionisation
g	Grams
h	Hours
HATU	O-(7-Aza-1H-benzotriazol-1-yl)-N,N,N',N'-tetramethyluronium hexafluorophosphate
HCTU	O-(6-Chlorobenzotriazol-1-yl)-N,N,N′,N′-tetramethyluronium hexafluorophosphate
HMBC	Heteronuclear Multiple Bond Correlation
HMQC	Heteronuclear Multiple-Quantum Correlation
HOBt	N-hydroxybenzotriazole
HPLC	High Performance Liquid Chromatography

HRMS	High Resolution Mass Spectroscopy
HTS	High throughput screening
IC_{50}	Concentration of a drug that is required for 50% inhibition *in vitro*
IMP-1	Imipenemase
IR	Infra-red
K_d	Dissociation constant
K_m	Substrate concentration at half-maximum reaction speed
L	Litre
LCMS	Liquid chromatography- mass spectrometry
LDA	Lithium di-isopropylamine
LiHMDS	Lithium hexamethyldisilazine
Lit.	Literature
MBL	Metallo-β-lactamase
MIC	Minimum inhibition concentration
μM	Micromolar
min	Minutes
ml	Millilitre
mmol	Milimole
mol	Mole
mp.	Melting point
MRSA	Methicillin-resistant Staphylococcus aureus
NDM-1	New Delhi metallo-β-lactamase
NMR	Nuclear magnetic resonance
PBP	Penicillin binding protein
PDB	Protein data bank
PDB-ID	Protein data bank identification number
ppm	Parts per million

RCSB	The research collaborator for structural Bioinformatics
rt	Room temperature
R_f	Retardation factor
SAR	Structure activity relationship
SBDD	Structure based drug design
SPM-1	Sao Paulo metallo-β-lactamase
T3P	Propylphosphonic anhydride solution
TFA	Trifluoroacetic acid
THF	Tetrahydrofuran
TLC	Thin layer chromatography
TMS	Trimethylsilane
T_r	Retention time
vHTS	Virtual high throughput screening
VIM-2	Verona integrin-encoded metallo-β-lactamase

Amino Acids

Alanine	Ala	A
Arginine	Arg	R
Aspartic acid	Asp	D
Asparagine	Asn	N
Cysteine	Cys	C
Glutamic acid	Glu	E
Glutamine	Gln	Q
Glycine	Gly	G
Histidine	His	H
Isoleucine	Ile	I
Leucine	Leu	L
Lysine	Lys	K
Methionine	Met	M
Phenylalanine	Phe	F
Proline	Pro	P
Serine	Ser	S
Threonine	Thr	T
Tryptophan	Trp	W
Tyrosine	Tyr	Y
Valine	Val	V

Part I
Introduction

Chapter 1
Bacterial Resistance

Bacterial infections cause seventeen million deaths per year worldwide and it is estimated that currently one third of the world's population is likely to be infected by bacterial pathogens.[1] Bacteria continue to develop resistance to new antibiotics with the result that antibiotics have a short and finite lifetime. Considerable research is therefore needed to find new antibiotics or ways to slow the development of resistance in bacteria.

Beginning with the production of penicillin in the late 1930s and running right up until the discovery of daptomycin in 1987, was a period of time which generated almost all of the antibiotic classes which are used in the clinic today. This period, which was later known as the 'golden age' of antibacterial drug discovery, has been hailed as one of the most important advancements in modern medicine.[2] However since 1987, the majority of large pharmaceutical companies have focussed their efforts on other therapeutic areas which has indirectly allowed bacteria to develop widespread resistance to our most commonly used antibiotics.

The term 'antibiotic' was first used to classify natural products that inhibited the growth of, or killed microorganisms.[3] This definition has now been extended to include synthetic and semi-synthetic antibacterial agents. These natural products were secondary metabolites of *actinomycetes*, microbes isolated from soil samples and marine deposits, a rich source of structurally complex chemical entities which are produced to protect the microbes from other bacteria. The use of nature's natural products in herbal medicines has occurred for centuries, but isolating and characterising these compounds required modern techniques to produce the quantities required to satisfy medical need during the 20th century.

1.1 The structure of bacteria

Bacteria are part of a large group of unicellular prokaryotic micro-organisms. Many bacteria have beneficial effects for humans. However, infection with others can have detrimental effects, and, in the most extreme cases can lead to death.
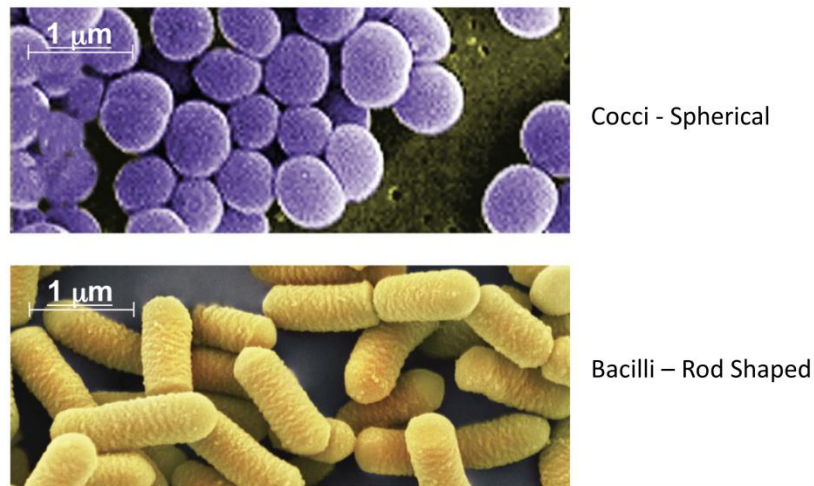
Figure 1: Bacterial cell shapes, adapted from[4]

Two main bacterial cell shapes are common; cocci which are spherical, and bacilli, which are rod shaped (**Figure 1**). Eubacteria and archaebacteria are the two subgroups bacteria can be divided into. The eubacteria subgroup includes *Escherichia coli* and *Klebsiella pneumoniae*. The archaebacteria are a diverse group of organisms which have very different cell walls and membranes compared to eubacteria. They include bacteria capable of existing in extreme conditions such as *Sulfolobas* and *Pyroccus*. This review concentrates on eubacteria as this encompasses most of the human pathogenic bacteria.

Bacteria are small, single cell prokaryotic microorganisms which have a simple internal cell structure; however the cell surface is considerably more complex.[5] Bacteria have no mitochondria or chloroplasts which are associated with energy production in eukaryotic cells, and additionally have a cell wall consisting of peptidoglycan. Peptidoglycan is a polymer of sugars and amino acids, unique to prokaryotic cells, that contributes to cell wall rigidity and shape. The cell wall is a tough multifunctional layer, protecting the cell from mechanical damage and osmotic lysis. The cell wall also acts

as a barrier to exclude various molecules, including polar drugs, *via* the cytoplasmic membrane. In certain bacteria, there can be a capsule formed around the bacterial cell formed of polysaccharide or another protein. Fibrils can be found on the cell surface which aid the adhesion of bacteria to surfaces. A flagellum will be present if the bacteria is required to move and become mobile (**Figure 2**).[6]
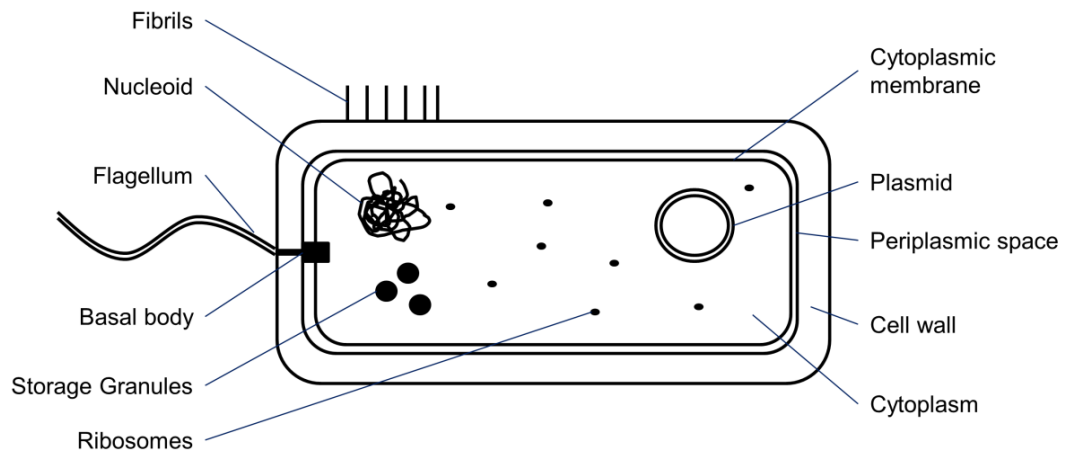
Figure 2: The structural components of a bacterial cell.

There are two subclasses of bacteria, which can be distinguished by their response to the Gram stain.[7] Bacteria which are stained violet or blue by the crystal Gram stain are defined as Gram-positive bacteria. Their ability to retain the stain is due to the high content of peptidoglycan in their thick cell wall. *Bacillus subtilis*, *Staphylococcus epidermidis*, and *Clostridium botulinum* are all Gram-positive bacteria.

Bacteria which are not stained *via* the Gram test but are stained by the counterstain (safranin) and appear red or pink are defined as Gram-negative bacteria. The result is due to the relative amounts of peptidoglycan found in the cell wall. Gram-positive bacteria has a thick peptidoglycan layer usually between 20-80 nm thick whereas Gram-negative bacteria have a much thinner peptidoglycan layer, about 7-8 nm thick (**Figure 3**). Gram-negative bacteria also have an additional lipopolysaccharide outer membrane, an orthogonal barrier to the cytoplasmic barrier, which excludes hydrophobic molecules with >600 Da molecular mass. *Escherichia Coli*, *Pseudomonas*, and *Stenotrophomonas* are all Gram-negative bacteria.

Gram-positive cell wall

Gram-negative cell wall
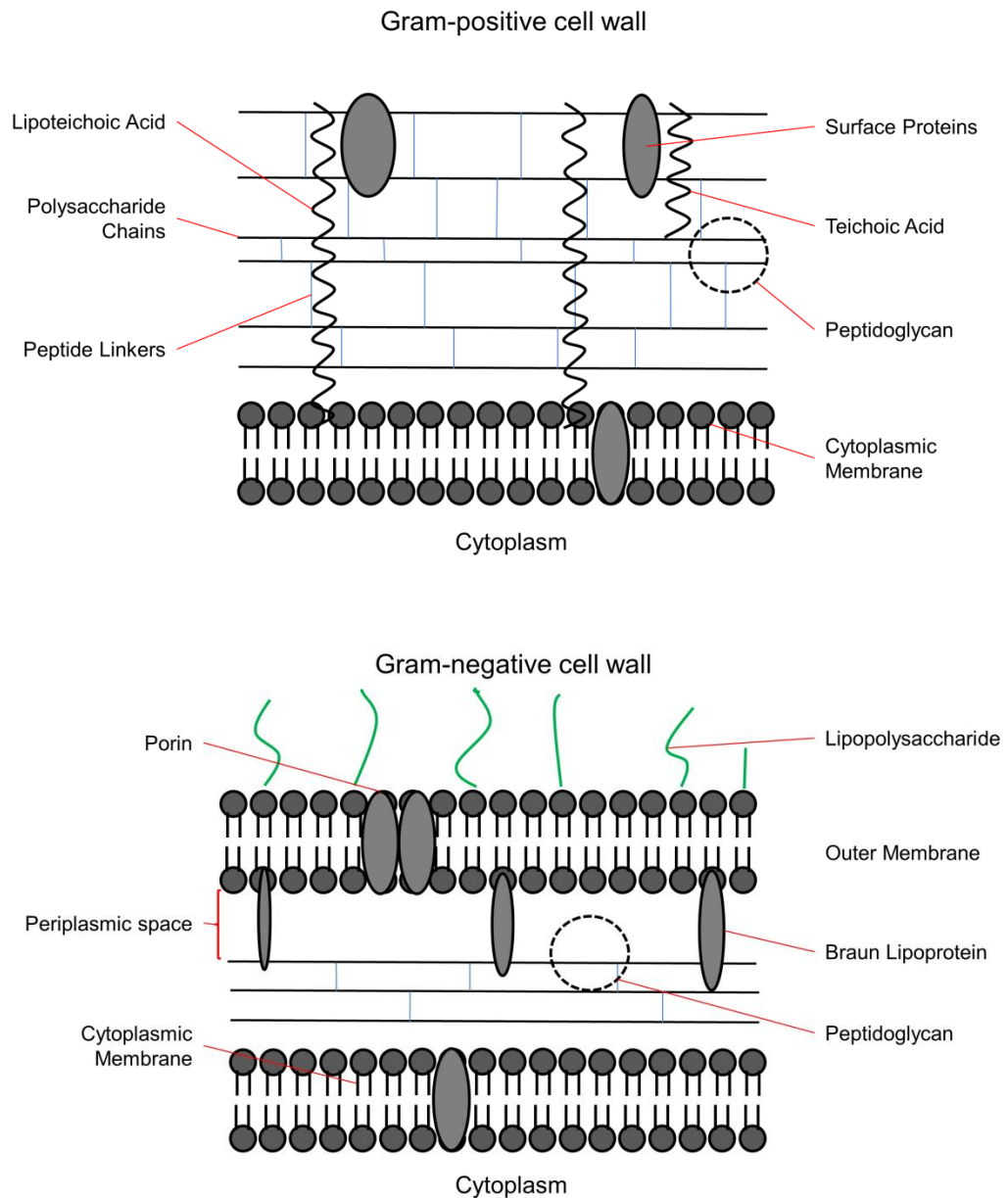
Figure 3: The structure of the cell wall a) Gram-positive cell b) Gram-negative cell

The great challenge for agents acting on Gram-negative bacteria is to penetrate both the outer and cytoplasmic membranes since different physiochemical properties are required to pass through each layer. This task is no easier for agents acting on Gram-positive bacteria since cell walls vary greatly between bacterial species. Not only do antibacterial agents require affinity for a certain biological target, but they need to be membrane permeable to accumulate inside bacterial cells and exert their function. This is the defining feature of antibiotics which sets them apart from other therapeutic drugs.

1.2 Antibacterial agents

Fatalities from bacterial infections have become relatively rare occurrences in the developed world over the last 50 years. This is due to overall improvements in medication, increased levels of sanitation, good housing and better nutrition. Antibacterial agents have become key to fighting many bacterial infections which would have previously been life threatening. Antibacterial agents are defined as natural or synthetic chemical compounds used to impede the growth of, or kill, bacteria.[8] If the compound is isolated from microbes, they are referred to as antibiotics. In 2009 the global antibiotic market generated an estimated $42 billion USD in sales. Experts predict with an average annual growth rate of ~4%, antibiotic sales could reach $60 billion USD by 2015.[9]

From around 1987 the majority of large pharmaceutical companies focussed their research on other therapeutic areas. It was generally agreed that due to the large number of antibiotics available, it was not commercially viable to spend time and money researching new antibiotics. Antibacterial research is now returning as a focus of many pharmaceutical companies due to the increase in hospital acquired diseases and antibiotic resistance in the community, threatening a return to a 'pre-antibiotic era'. Legislation has also been altered in order to help with the fast track and streamlining of approval of new antibacterial agents. In 2013 the FDA announced the Antibiotic Development to Advance Patient Treatment Act (ADAPT) which allows the approval of drugs to the market for the most serious cases of resistant bacterial infections which require a much smaller set of clinical testing data.

1.2.1 History of antibacterial agents

The first recognised antibacterial agent was salvarsan, an arsenic-containing compound used for the treatment of syphilis, discovered in 1909 by Paul Ehrlich, a pioneer of chemotherapy.[10] This was an early example of his 'magic bullet' theory, whereby a chemical agent could selectively cure a particular disease. The discovery of penicillin by Fleming in 1928 changed modern medicine, as penicillin was effective against a wide range of Gram-positive bacteria.[11] In 1935 Gerhard Domagk discovered the sulfonamides, the first effective drug administered against bacterial infections, for which

Domagk won the Nobel prize in 1939.[12] These two discoveries marked the beginning of the golden age of antibacterial drug discovery (**Figure 4**).

During this time actinomycetes provided a great source of antibacterial agents, discovered through the empirical screening of fermentation broths and extracts of microorganisms containing secondary metabolites which inhibited bacterial growth. Over 20 antibiotic classes used today were discovered from the actinomycetes during the 'golden age' of antibacterial drug discovery. During this period of high antibacterial agent discovery, clinicians were effectively able to deal with any bacterial resistance which arose.
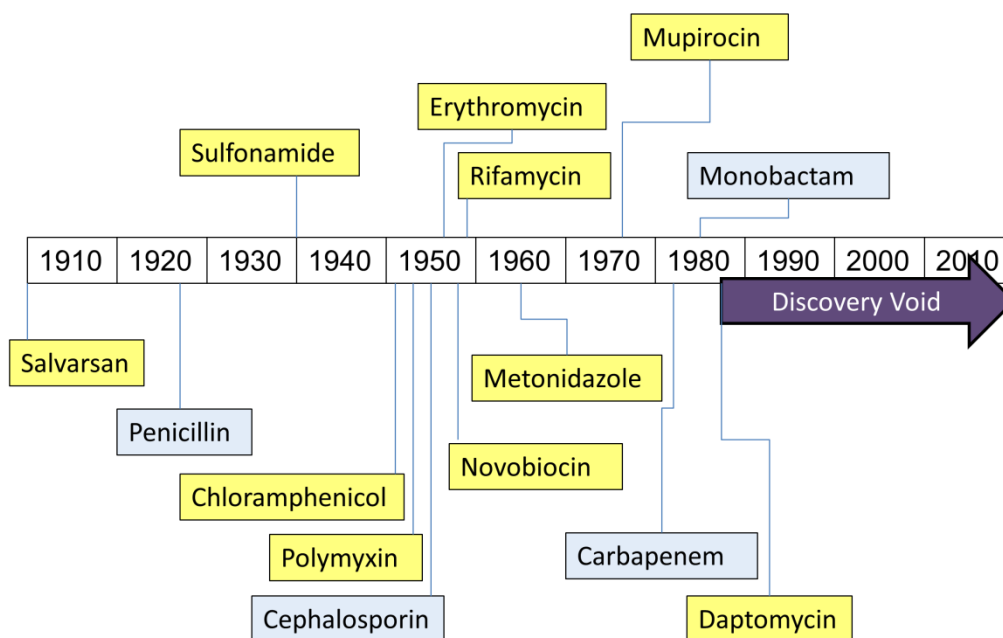
Figure 4: A timeline of the initial discoveries of antibiotic classes. Showing the key introductions of β-lactam antibiotics (blue) and the discovery void since the late 1980s. Adapted from[13]

Since the discovery of daptomycin in 1987, no new classes of antibiotics have been identified and successfully delivered to the clinic, leading to a period known as the 'discovery void' (**Figure 4**). The emphasis on discovering antibacterial agents with better whole cell activity and pharmacokinetic properties switched to finding analogues of previously identified classes rather than previous methods of identifying new antibacterial agents and classes from natural products. Eighteen of the

twenty newly approved antibiotics between 2000 and 2011 are analogues of either the β-lactam or quinolone classes. From 1995, a target-based approach was been employed by many companies looking to identify drugs specific to the desired bacteria. Screening of natural products was seen as time consuming and expensive. However, high throughput screening (HTS) and genomic methods have so far failed to deliver a drug to the market. As described by Spellberg *et al.,*[14] the number of antibiotics accepted in the clinic has dropped but resistance has continued to rise. A review of recent literature suggests that the current rate of antibacterial drug discovery cannot meet clinical needs.[15]

1.2.2 Mechanisms of action

Different antibacterial families have different mechanisms of action against bacteria; (**Table 1**).

Table 1: Antibacterial classes and their enzyme targets

Antibiotic Family	Enzyme Target	Source	Date Discovered
Inhibitors of cell wall biosynthesis			
Penicillins (β-lactams)	Transpeptidase	Actinomycete	1932
Cephalosporins (β-lactams)	Transpeptidase	Fungus	1948
Carbapenems (β-lactams)	Transpeptidase	Actinomycete	1976
Glycopeptides	Transpeptidase	Actinomycete	1952
Inhibitors of protein biosynthesis			
Tetracyclines	30S ribosome subunit	Actinomycete	1945
Aminoglycosides	30S ribosome subunit	Actinomycete	1943
Oxazolidinones	50S ribosome subunit	Oxazolidinone	1990s
Macrolides	50S ribosome subunit	Actinomycete	1949
Chloramphenicol	50S ribosome subunit	Natural product derived	1949
Inhibitors of DNA/RNA biosynthesis			
Fluoroquinolones	DNA gyrase	Synthetic	1962
Novobiocin	DNA gyrase	Natural product derived	1955
Rifamycins	RNA polymerase	Actinomycete	1957
Inhibitors of cell membrane structure and function			
Lipopeptides	n/a	Actinomycete	1986
Polymyxin	n/a	Natural product derived	1947
Inhibitors of cell metabolism			
Sulfonamides	Dihydropteroate synthase	Synthetic	1932
Trimethoprim	Dihydrofolate reductase	Synthetic	1950s
Triclosan	FabI	Synthetic	1972

The mechanisms in **Table 1** show how bacteria are targeted by antibacterial agents. Below is a general description of the five bacterial targeting mechanisms:

- Inhibition of bacterial cell wall synthesis: This leads to bacterial cell lysis and death. Mammalian cells do not have a cell wall composed of primarily peptidoglycan and are therefore not affected by these agents.
- Disruption / inhibition of protein synthesis: The proteins and enzymes needed for bacterial cell survival are no longer produced, leading to cell death.
- Inhibition of nucleic acid transcription and replication: This prevents cell division and or synthesis of essential proteins.
- Interactions with the plasma membrane: Antibacterial agents interact with the plasma membrane of the bacterial cell to affect membrane permeability.
- Inhibition of cell wall metabolism: Antibacterial agents which inhibit cell metabolism are termed antimetabolites. These compounds inhibit the metabolism of a microorganism, but not the metabolism of the host. This can be done by inhibiting an enzyme catalysed reaction which is present in the bacterial cell, but not in animal cells.

1.2.3 β-lactam antibiotics

Seventy years from their first use, β-lactam antibiotics remain the single most important type of antibiotic in the clinic in terms of sales[9] and prescriptions.[16] As one of the few antibiotic classes which show a broad-spectrum activity, β-lactam antibiotics are of particular importance in the treatment of infections by Gram-negative pathogens. In particular these drugs have retained their importance as resistance to other broad spectrum antibiotics such as fluoroquinolones has increased.[17]

β-Lactam antibiotics derive their name from their four-membered cyclic amide rings motif. The most well-known β-lactam antibiotics are the penicillin family which are classified as part of the penams (**Figure 5**).
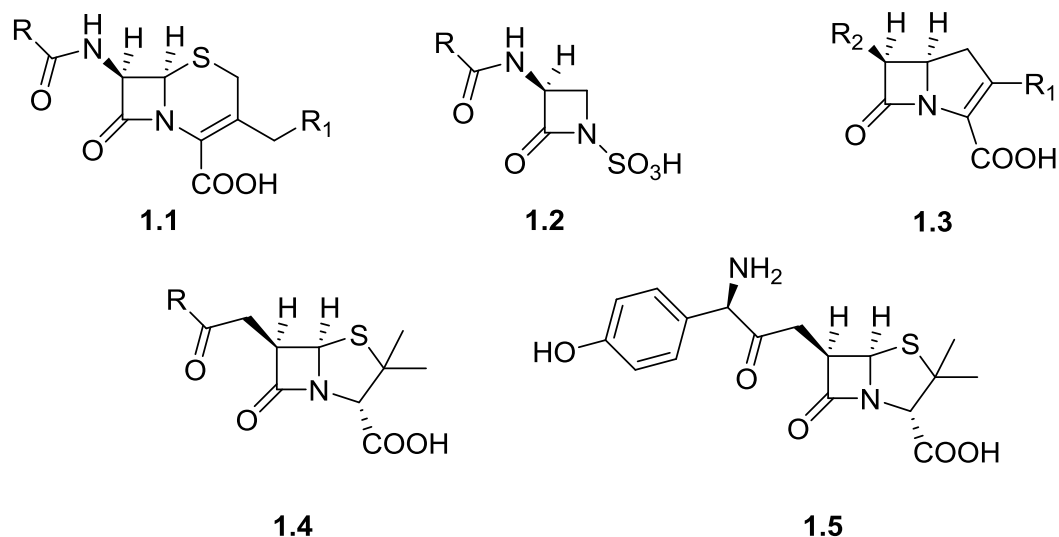
Figure 5: β-lactam antibiotics: a) Cephalosporin **1.1**, b) Monobactam **1.2**, c) Carbapenem **1.3**, d) Penicillin **1.4**, e) Amoxicillin **1.5**.

1.2.3.1 History of the β-lactam antibiotics

In 1928, Fleming noted that a bacterial culture on the surface of an agar plate that had been left for several weeks open to air had become contaminated by a fungal colony. He noted that there was an area on the surface around the fungal growth where the bacterial colonies were dying. He concluded that the fungal colony was producing an antibacterial agent which was spreading to the surrounding area. Fleming set about identifying the fungus and showed it to be from the *Penicillium* genus and he termed the active agent 'penicillin'.[11]

Penicillin was first isolated in 1938 by Florey and Chain using processes such as freeze drying and chromatography which allowed for isolation under much milder conditions than previously had been available.[18] By 1941 Florey and Chain had produced sufficient penicillin in order to enable the clinical trials and achieved spectacular success. The structure of penicillin was finally confirmed in 1945 when Dorothy Hodgkin successfully performed X-ray crystallographic analysis. The first full synthesis was conducted by Sheehan in 1957 however this route was deemed commercially unviable.[19] Beechams isolated a biosynthetic intermediate of penicillin called 6-aminopenicillanic acid which revolutionised the field of penicillins opening up a huge range of semi-synthetic penicillins.

1.6
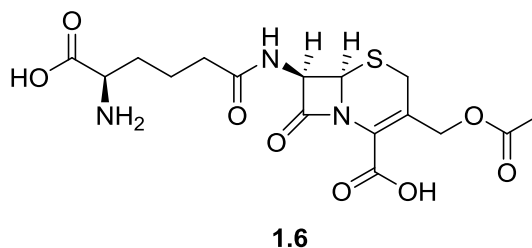
Figure 6: The structure of cephalosporin C **1.6**

The second major group of β-lactam antibiotics is the cephalosporins. The first cephalosporin (cephalosporin C, **Figure 6**) was identified within a fungus obtained in the mid-1940s from sewer waters on the island of Sardinia. The first isolation was achieved in 1948 by workers at the University of Oxford but it was not until 1961 that the X-ray crystal structure was confirmed. As shown in **Figure 5**, the cephalosporin (**1.1**) structure has clear similarities to penicillin (**1.4**) with containing a bicyclic system and four membered β-lactam ring. The β-lactam ring in the cephalosporin is fused to a six membered ring rather than a five membered ring in the penicillins.

1.2.3.2 Mechanism of action.

β-lactam antibiotics act upon the peptidoglycan component of the cell wall of bacteria. The cell wall is a peptidoglycan structure consisting of peptide and sugar units (**Figure 7**). The structure of the wall consists of a parallel series of sugar backbones consisting of two types of sugar, (N-acetylmuramic acid (NAM) and N-acetylglucosamine (NAG)). Peptide chains are bound to the NAM sugars which contain both L-and D-amino acids. In the final stage of cell wall biosynthesis, the peptide chains are linked together by the displacement of D-alanine from one chain and glycine in another. This final stage is where the β-lactam antibiotics act by disrupting the cross-linking. This results in the wall becoming fragile and it can no longer prevent water continually entering the cell as a result of osmotic pressure causing the cell to swell and eventually burst. The enzymes responsible for the cross linking reaction are known as the transpeptidase enzyme or Penicillin Binding Protein (PBPs).
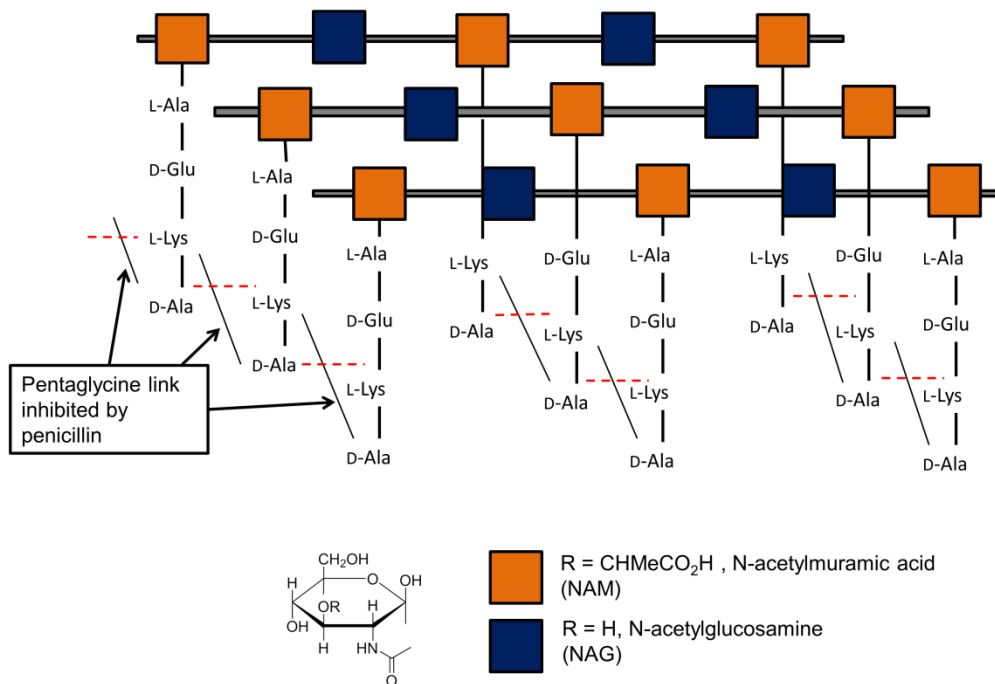
Figure 7: Peptidoglycan structure of bacterial cell walls, adapted from[20]

The transpeptidase enzymes are bound to the outer surface of the cytoplasmic membrane. In the cross-linking mechanism (**Figure 8**), a serine residue acts as a nucleophile to split the peptide bond between the two D-Ala units (**A**). The terminal D-Ala departs leaving the peptide chain bound to the enzyme. The pentaglycyl moiety of another peptide chain now enters the active site and forms a new peptide bond with the D-Ala displacing the enzyme bound through the serine residue (**B**). The cell wall is then cross linked and much stronger (**C**).

The β-lactam antibiotic has a conformation which is similar to the transition-state conformation taken up by the D-Ala-D-Ala moiety during the cross-linking reaction. The enzyme binds the β-lactam antibiotic to the active site in place of the D-Ala-D-Ala through the serine residue (**D**). The enzyme hydrolyses the β-lactam ring, however as the β-lactam is a cyclic molecule it is not split into two, so nothing leaves the active site. Subsequent hydrolysis of the β-lactam antibiotic does not occur as the antibiotic structure blocks access to the pentaglyine chain (**F**) and water (**G**).
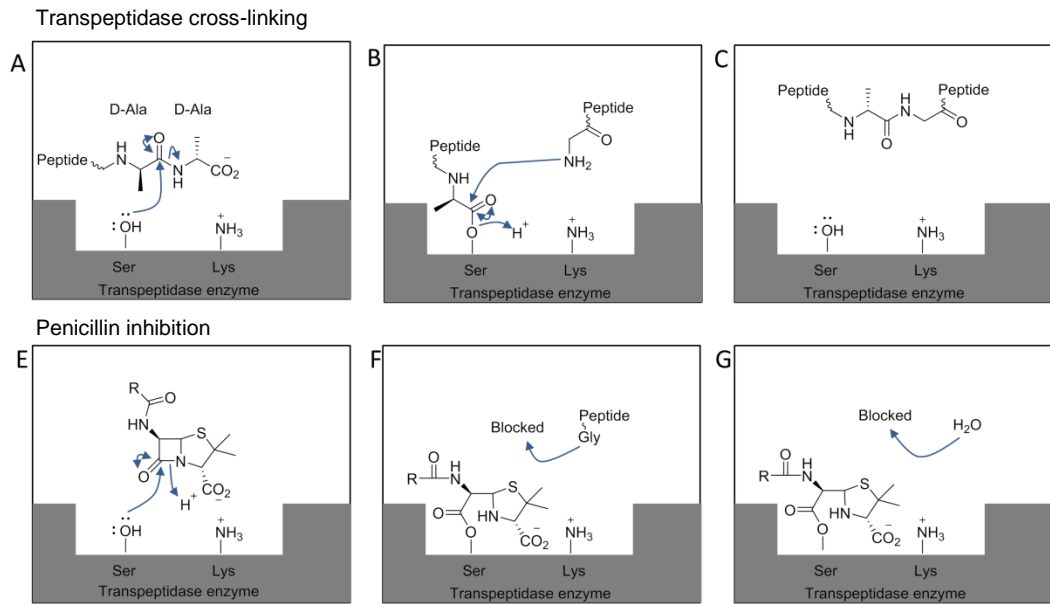
Figure 8 : Mechanisms of transpeptidase cross-linking and penicillin inhibition, reproduced from[20]

1.3 Bacterial resistance

Hospital-acquired infections are a major and growing threat to public health.[21] Multi-drug resistant bacteria compromise the ability to perform what are now considered routine surgical procedures. More worrying is the fact that these infections are becoming more prevalent in the community and are no longer solely a hospital-based problem.[22] Bacterial resistance complicates treatments and increases the likelihood of death and financial cost.

There are two broad resistance mechanisms seen: Inherent or natural resistance where the bacterium is inherently resistant to an antibiotic, or acquired resistance by genetic mutation or gene transfer. Acquired resistance can occur by vertical evolution which is a classical Darwinian type of evolution, or horizontal evolution, which involves genetic transfer between strains and species.

These two broad classes of resistance can be subdivided into different mechanisms by which the resistance can arise (**Figure 9**):[8, 23, 24]

1. Enzymic destruction or inactivation of the antibiotic – includes the most common modes of resistance to penicillins and cephalosporins.

2. Alteration of the target site, or protection of a new site – this is seen in β-lactam antibiotics and others including glycopeptides.

3. Reduced antibiotic uptake – this is important for tetracycline and β-lactam antibiotics.

4. Increased efflux of the antibiotic from the bacteria – this is often seen with macrolides, tetracyclines and quinolones.

5. Over-expression of the drug target

6. Acquisition of a replacement for the metabolic step initiated by the antibiotic – known examples include sulphonamides and trimethoprim
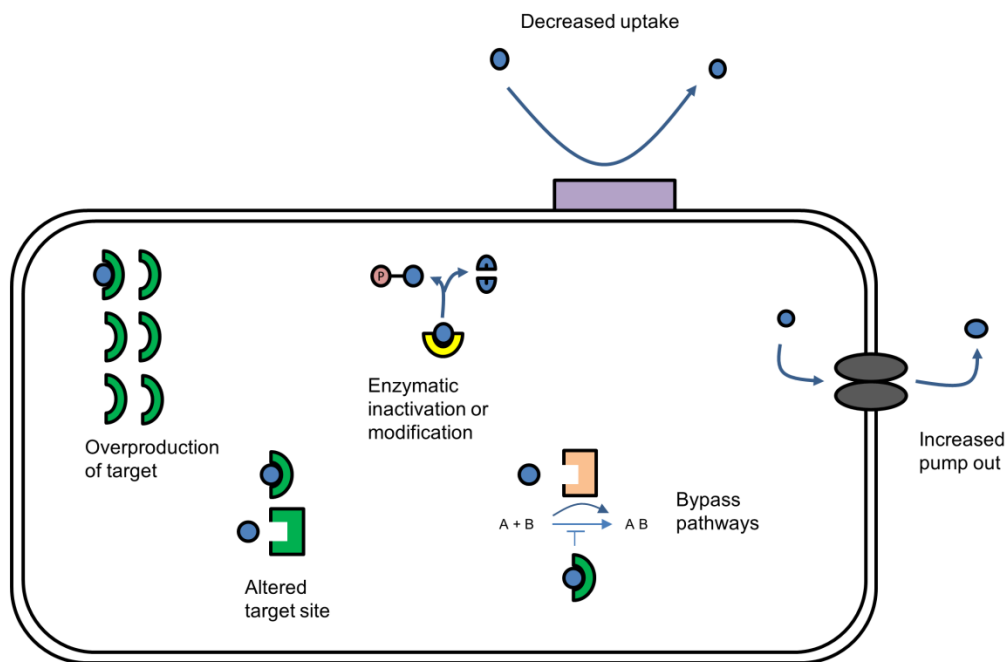
Figure 9: Resistance mechanisms, adapted from[25]

Many different classes of antibiotics have been administered to patients in the clinic to treat bacterial infections, and for each class at least one mechanism of resistance has been observed. Resistance has been observed within fifteen years for many antibiotics. (**Table 2**). Resistance to penicillin was observed soon after its introduction into the clinic in 1943 with the first cases of resistance reported in 1946. By the late 1960s, almost 80%

of people with a *S. aureus* infection were resistant to penicillin.[26] Bacterial resistance has emerged at almost a parallel rate to the design and introduction to the clinic of new antibiotics which drastically reduced the efficiency of many antibiotics.[8] This is increasingly worrying as no new antibiotic classes with Gram-negative activity are currently close to the clinic.[17] Linezolid, an oxazolidinone, was the first entirely synthetically derived class to be introduced but resistance was seen in less than a year after its clinical introduction in 2000.[26]

Table 2: Antibiotics and drug resistance

Antibiotic	Introduced	Resistance observed
Sulfonamides	1930s	1940s
Penicillin	1943	1946
Streptomycin	1943	1959
Chloramphenicol	1947	1959
Tetracycline	1948	1953
Erythromycin	1952	1988
Vancomycin	1956	1988
Methicillin	1960	1961
Ampicillin	1961	1973
Cephalosporins	1960s	late 1960s
Linezolid	2000	2001

There has been a steady decline in the number of FDA approved antibacterial agents, both acting against Gram-positive and Gram-negative bacteria, in the last 20 years. (**Figure 10**)
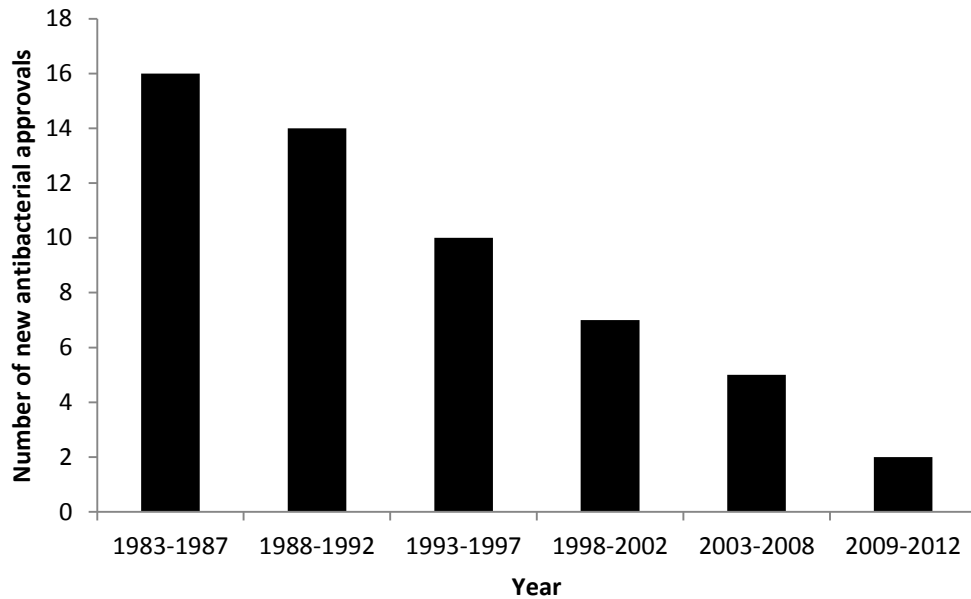
Figure 10: The decline of antibacterial drug approvals by the FDA, adapted from[14]

It can be deduced that if a new highly effective antibiotic is found, its widespread usage will increase the chance of resistance developing.[8]

The aim to reduce the amount of bacterial resistance to antibacterial agents can be approached from two directions:

1. The rejuvenation of existing antibiotics by constant modification of existing antibiotics to stay ahead of resistance.

2. The search for new drugs with novel modes of action as a result of identification of a biological target.

Due to recent developments this report will focus on β-lactamase bacterial resistance and the methods being used to combat this form of bacterial resistance.

Chapter 2

β-lactamases

Bacteria have developed resistance to β-lactam antibiotics by producing a specific family of enzymes, the β-lactamases. They catalytically hydrolyse the β-lactam antibiotics rendering them unable to inhibit peptidoglycan biosynthesis.

The first β-lactamase enzyme was identified in *Escherichia coli* before the clinical use of penicillin.[27] The enzyme was not thought to be clinically relevant, since penicillin was used to treat *Staphylococcal* and *Streptococcal* infections. β-Lactamase enzymes have mutated from the transpeptidase enzyme and therefore are quite similar in nature. Along with the ability to hydrolyse the β-lactam ring, the β-lactamase enzymes also possess the ability to hydrolyse the ester linkage to the enzyme to shed the hydrolysed moiety. This is so efficient that they can hydrolyse 1000 penicillin molecules per second (**2.1**, **Figure 11**).
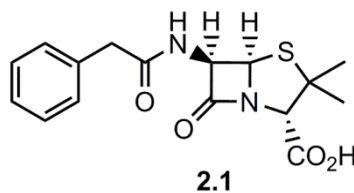
Figure 11: Structure of penicillin G (**2.1**)

Many Gram-positive strains of bacteria are resistant to penicillin as they can produce β-lactamase enzymes which are released into the surrounding area to intercept the antibiotics before they reach the cell membrane. The enzyme eventually dissipates through the cell wall and is lost so the bacteria has to keep producing the enzyme in order to remain resistant.

Most if not all Gram-negative bacteria produce β-lactamase enzymes which makes them more resistant to penicillin than Gram-positive bacteria. The released β-lactamase enzymes are trapped within the periplasmic space between the cell membrane and the outer cell membrane as they cannot permeate through the latter. As a result, β-lactam antibiotics which pass

through the outer membrane encounter a higher concentration of β-lactamase than in Gram-positive bacteria.

There are a number of β-lactamase enzymes which vary in their substrate selectivity. Penicillinases are selective to penicillin and cephalosporinases are selective to cephalosporins. There are also enzymes which are not selective between classes of β-lactam antibiotics. The differing levels of enzymes produced and the different affinities for each β-lactam antibiotic accounts for the varying susceptibility of different Gram-negative species to different β-lactam antibiotics.

β-Lactamase enzymes have been grouped into four major classes (A-D) as defined by Ambler, based on amino acid sequence homology.[28] Class A, C, and D belong to the serine-β-lactamase family as they use an active site serine as a nucleophile. Class B belongs to the metallo-β-lactamase family of enzymes which use zinc atoms in the active site to help ionize and coordinate a nucleophilic hydroxide ion to mediate hydrolysis.

2.1 Serine-β-lactamases

The serine β-lactamase class have evolved directly from the transpeptidase enzymes and are very similar in structure with active site lysine and serine residues helping to co-ordinate and hydrolyse the β-lactam antibiotics. The three classes of serine-β-lactamases (A, C and D) are described below:

Class A[29] serine-β-lactamases, often referred to as penicillinases, were the first β-lactamases to be identified in penicillin resistant isolates of bacteria and are still the most common β-lactamases today. In 1963, the plasmid-borne class A resistant gene, TEM-1 was discovered. TEM-1 has spread through many different species of bacteria and spread throughout the globe. The TEM enzymes have demonstrated an ability to evolve resistance to molecules specifically designed to inhibit class A β-lactamases.

Class C[30] serine-β-lactamases are often termed cephalosporinases on account of their preference towards cephalosporins as a substrate even though they are also highly active against penicillins. Class C enzymes are the second most common class of serine-β-lactamase enzymes behind

class A. Class C enzymes are most commonly found in Gram-negative bacteria and are chromosomally encoded.

Class D[31] serine-β-lactamases are called oxicillinases because of their ability to hydrolyse oxacillin (**Figure 12**) and cloxacillin about three times faster than penicillins. Class D are the least well known serine-β-lactamases and have <20% amino acid identity with classes A and C. Almost 30 class D enzymes are known and have been designated OXA-1, OXA-2, etc. Class D enzymes have been found as dimeric enzymes.
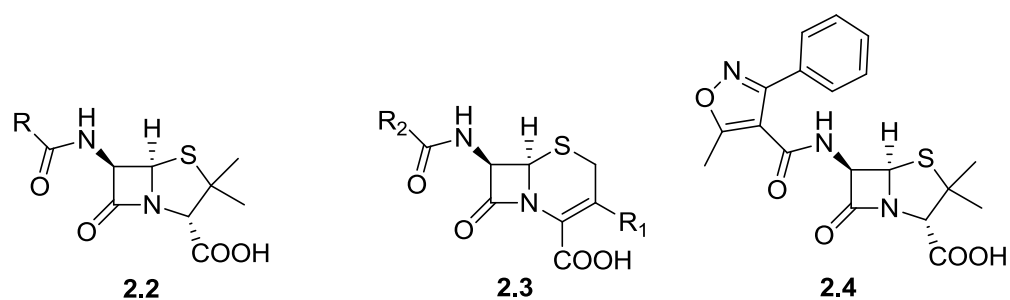
Figure 12: Antibiotics hydrolysed by serine-β-lactamases. a) penicillin, **2.2** b) cephalosporin **2.3** and c) oxacillin **2.4**.

2.1.1 Hydrolysis mechanism

In the serine β-lactamases, an active site serine is used to hydrolyse the β-lactam ring (**Scheme 1**). A conserved Ser-X-X-Lys motif is conserved through all the serine β-lactamase enzymes. The lysine residue helps to co-ordinate the antibiotic in position to enable nucleophilic attack by the serine residue, by forming a hydrogen bonding interaction with the carboxylic acid present in many antibiotics **2.6**. The hydrolysed antibiotic is cleaved from the enzyme by hydrolysis of the formed ester bond by a water molecule **2.7**. The enzyme then expels the antibiotic and is ready to accept another molecule for hydrolysis **2.8**.
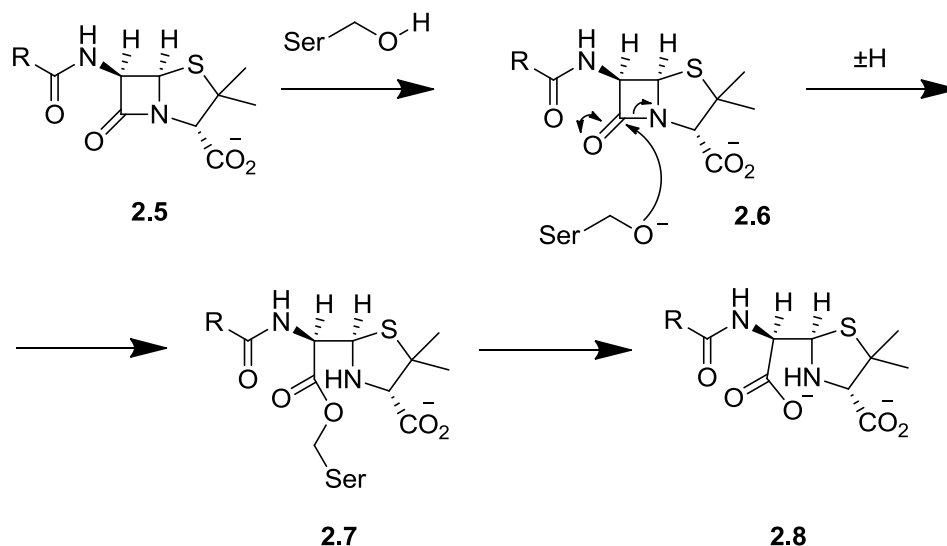
Scheme 1: Mechanism of hydrolysis of β-lactam antibiotics by serine-β-lactamases

2.1.2 Serine-β-lactamase inhibitors

A large number of class A enzyme inhibitors have been developed. These inhibitors have substantially extended the spectrum of activity of otherwise class A β-lactamase-susceptible partner penicillins. Examples already used in the clinic are Clavulanic acid (**2.9**)[32], Tazobactam (**2.10**)[33] and Sulbactam (**2.11**)[34] (**Figure 13**). These inhibitors protect the β-lactam antibiotic from the activity of the β-lactamase and have widely been used for the treatment of human infections.
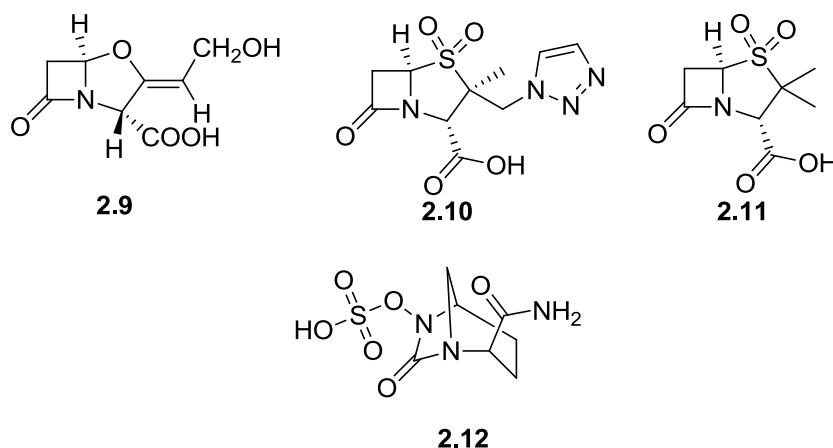
Figure 13: Structures of serine-β-lactamase inhibitors: Clavulanic acid (**2.9**), Tazobactam (**2.10**), Sulbactam (**2.11**) and Avibactam (**2.12**).

These inhibitors act as suicide inhibitors, covalently bonding to the active site serine residue. This re-structures the inhibitor molecule, creating a much more reactive species which is attacked by another amino acid in the active site, permanently inactivating it, and thus inactivating the enzyme.

An example of how clavulanic acid (**2.9**) inhibits a serine-β-lactamase (SHV-1) is shown in **Scheme 2**.[20] Clavulanic acid (**2.9**) covalently binds to the active site serine residue Ser-70 in the active site of the SHV-1 enzyme. Upon hydrolysis of the β-lactam to form the covalently bound species, the resulting cascade results in the formation of more reactive species which is attacked by the serine residue Ser-130. Hydrolysis of the bond to the Ser-70 residue occurs but the inhibitor remains covalently bound to Ser-130 permanently inactivating the SHV-1 enzyme.
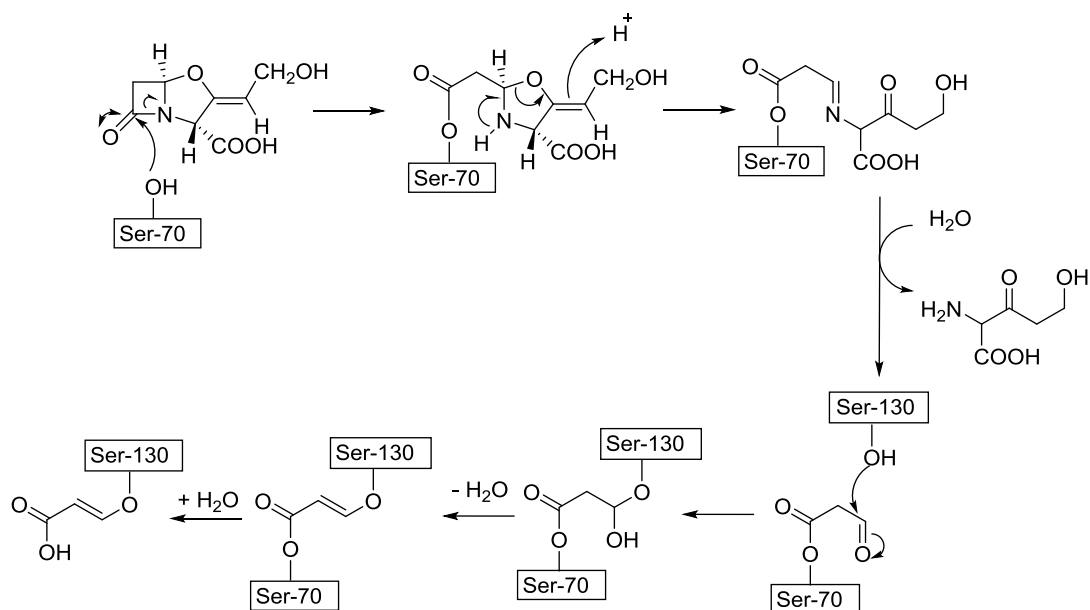
Scheme 2: Inhibition mechanism of SHV-1 serine-β-lactamase by clavulanic acid showing binding to key residues Ser-70 and Ser-130.

Class C inhibitors are also being developed for use in the clinic. Avibactam (**2.12, Figure 13**)[35] is in late stage clinical trials for the treatment of infections caused by bacteria expressing Class C β-lactamases. Avibactam is given in combination with a cephalosporin to combat the β-lactamase enzymes. Avibactam has also been shown to have activity against Class A and some Class D enzymes but not the Class B metallo-β-lactamases.

There are very few examples of Class D inhibitors and as yet there are no reports of clinically useful inhibitors of the class B MBLs.

2.2 Metallo-β-lactamases (MBLs)

Metallo-β-lactamases are divided into three subclasses B1, B2, and B3. Subclasses B1 and B3 contain two zinc ions in the active site while subclass B2 contains only one zinc ion.[36] Subclass B1 β-lactamases are active in both the mono-zinc and di-zinc forms although binding of a second zinc atom improves activity. B2 are only active in the mono-zinc form, with the binding of a second zinc atom inhibiting the hydrolysis activity, and B3 are only active in the di-zinc form.[37,38]

Each subclass has several different types of metallo-β-lactamase, many of which have several allelic variants.[36] A value of at least 30% amino acid diversity is used as a cut off for classification of new metallo-β-lactamases.[39]

MBLs are encoded either by genes which are part of the chromosomal framework in some bacterial species (resident metallo-β-lactamases) or by heterologous genes acquired by horizontal gene transfer (acquired metallo-β-lactamases). Almost all acquired types belong to the B1 subclass. This implies B1 subclass MBLs have more mobile genetic elements than subclasses B2 and B3.

Due to the broad nature of β-lactam antibiotics and the increase in number and spread of MBLs, it is desirable to produce metallo-β-lactamase inhibitors that can restore the activity of the β-lactam antibiotics against MBL-producing bacteria.

A few of the most prevalent MBLs for which potential inhibitors have been sought are Imipenemase (IMP-1),[40] Verona integrin-encoded metallo-β-lactamase (VIM-2)[41] and *Bacillus cereus* β-lactamase.[42] A common feature of many reported MBL inhibitors is the inclusion of metal chelators such as thiols[40] and hydroxamic[43] acids. Problems are often seen as these inhibitors are not selective for the desired enzymes and bind to other metal centres in the body. Selective inhibitors have been found for individual enzymes such as NH-1,2,3-triazole inhibitors of VIM-2[41], however a broad spectrum inhibitor which is only selective for MBLs is still to be found.

2.2.1 The Spread of MBLs

MBLs have become widespread throughout the world. (**Figure 14**).[37] It is believed that the un-regulated prescription of β-lactam antibiotics in the developing world and the increased use of air travel has helped to facilitate transmission of the metallo-β-lactamase enzymes across the world. There is limited clinical data available from African countries leading to the lack of information on **Figure 14** in this area of the world although it is predicted that MBLs will be present in these countries.

IMP and VIM MBL isolates have been found to be the most widespread with most countries in the world seeing infections of bacteria expressing these enzymes. For NDM-1, although originally isolated in India and the UK, rapid spread has been seen across the world (see Section 2.3.1). There are limited cases of SPM-1 which have been identified, and these have been restricted to Brazil and central Europe. There are a number of reasons for this (see Section 2.4.1.3)
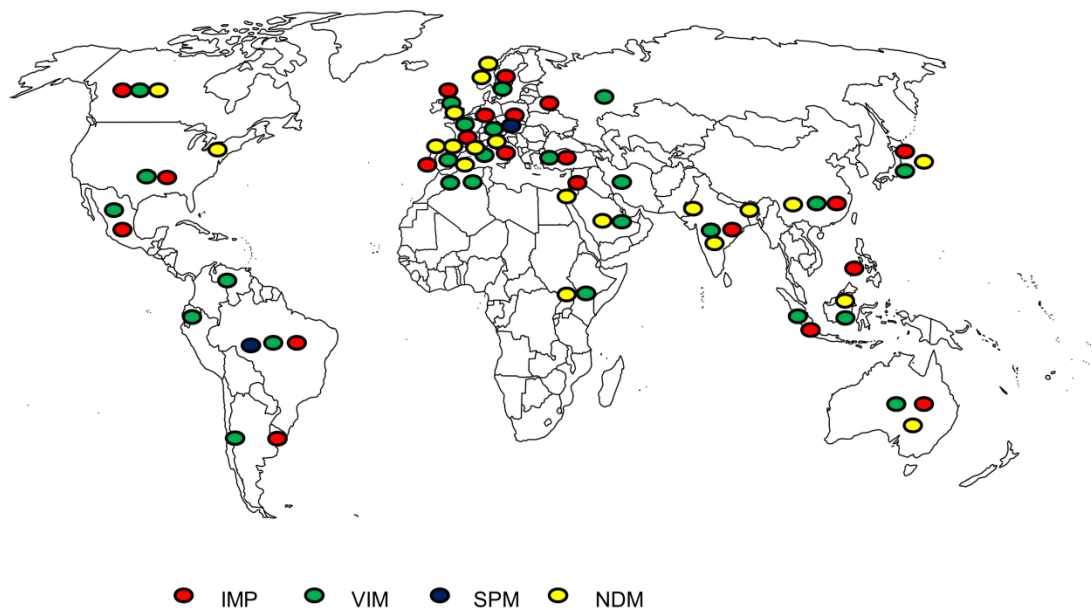
Figure 14: The spread of key clinically relevant MBLs throughout the world, Adapted from.[9]

2.2.2 Hydrolysis mechanism
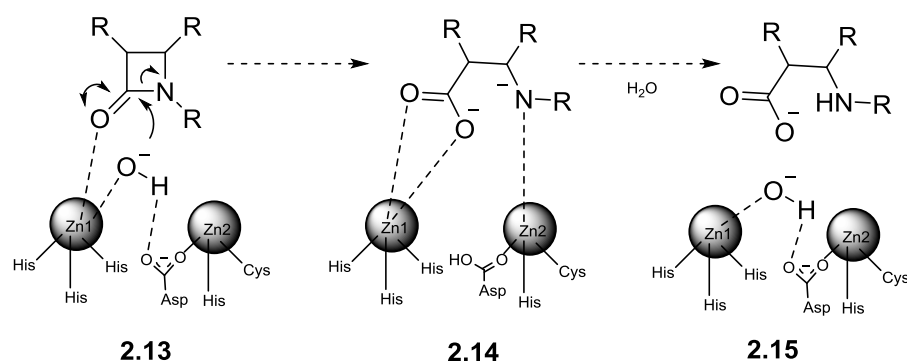
Scheme 3: Schematic drawing of the proposed mechanism of β-lactam hydrolysis by NDM-1, adapted from[44]

In the proposed mechanism, Zn1 functions to orientate the substrate carbonyl bond, whereas Zn2 is required for interaction with the amide nitrogen of the substrate **2.13**[45] (**Scheme 3**). The shared hydroxide attacks the carbonyl carbon as the nucleophile. It is suggested (and supported by crystallographic evidence), that the hydroxide ion is generated from the bound water by the putative general base Asp-120.[46] This results in a tetrahedral species which is short lived as the C-N bond breaks immediately with Zn2 acting as a Lewis acid to stabilise the charge on the nitrogen leaving group **2.14**.[38] The proton coming from the hydroxide is close to the nitrogen of the hydrolysed substrate and is acidic in its microenvironment bound to Asp-120 and is therefore easily transferred to the nitrogen. This mechanism appears plausible for all three subclasses of metallo-β-lactamase. In the B1 and B3 subclasses when the Zn-Zn bond distance increases following hydrolysis there is a weakening in the interaction with the former amide nitrogen which leads to the departure of the product from the active site **2.15**. The interatomic bond distance between Zn1 and Zn2 returns to the shortened form as the enzyme returns to its apo form. This helps to make this mechanism catalytic so that one enzyme can turn over many molecules.

2.3 New Delhi metallo-β-lactamase 1 (NDM-1)

New Delhi metallo-β-lactamase (NDM-1) is a broad spectrum β-lactamase that is able to inactivate all β-lactams except aztreonam, as is typical of metallo-β-lactamases.[47] The first recorded case of an NDM-1 producing bacteria was reported in 2008 in a Swedish patient who had previously been hospitalised in New Delhi in 2007. The first case was found to be *Klebsiella pneumonia* from a urinary tract infection.[48] NDM-1 has increasingly become a worldwide concern with reported cases in the UK, India and Pakistan.[49] The link between hospitalisation in India and Pakistan and development of infections in the UK was established in fourteen of thirty seven hospitalised patients in 2010.[49]

NDM-1 is not only restricted to a single strain of bacteria and has been identified in a number of unrelated species, the most common of which have been found are *E. coli* and *K. pneumonia*.[49] NDM-1 producers have recently also been reported in *E. cloacae, Providencia rettgeri and Morganella morganii.[50]* NDM-1 producers cause a range of infections such as urinary tract, diarrhoea and soft tissue infections.[51]

2.3.1 Spread of NDM-1 producers

As of the 1st November 2010, around seventy cases of NDM-1- producing bacteria have been reported in the UK, one hundred and fifty in India and Pakistan,[49] and four in Canada.[52] Positive cases have not only been restricted to these countries as shown in **Figure 15**. Several fatal cases have been reported in UK, India and Belgium. In most cases, patients have been hospitalised in India, Pakistan or Bangladesh, or were of South Asian origin or had spent some time in that part of the world.[51] It is suspected that overcrowding, poor sanitation, poor personal health and the sale of non-prescribed antibiotics may all be factors in facilitating the spread of NDM-1.
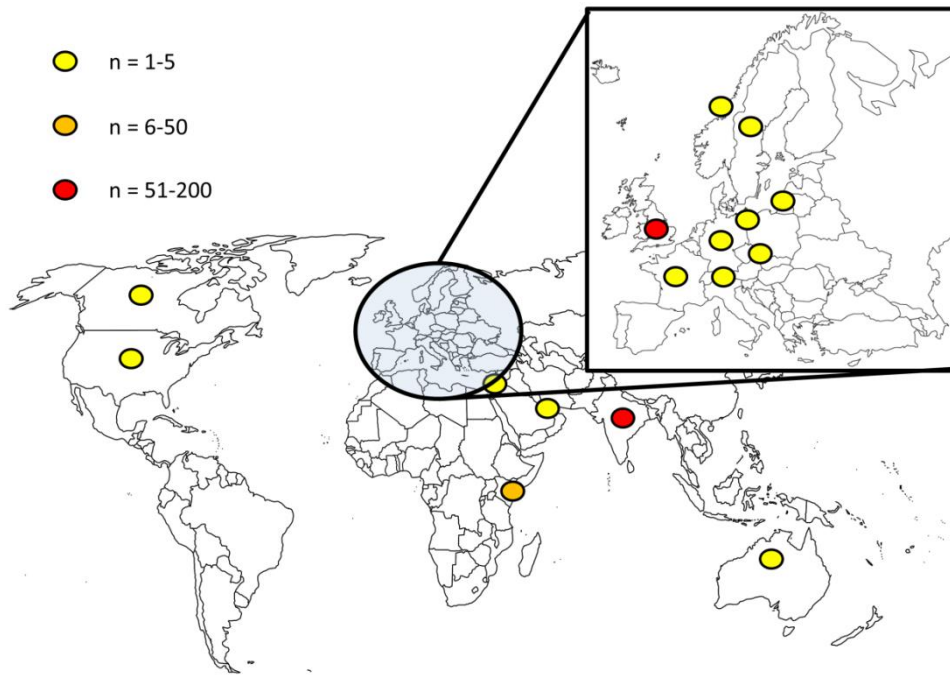
Figure 15: Worldwide distribution of identified cases of NDM-1 producers (1st December 2010). Adapted from.[51]

It is difficult to predict the rate of spread of the gene encoding NDM-1 within the less developed world. Exchange of the Bla_{NDM-1} gene between unrelated bacterial isolates and species has already been seen.[53] It is suspected, like many other carbapenemases, that NDM-1 has a carrier state. It is important to estimate the amount of people who carry the inactive state and predict the genetic spread. It is predicted that like other carbapenemases NDM-1 will spread across the world due to the increased amount of human air travel.

Bacteria become able to produce NDM-1 through the process of acquired resistance. This is when a particular microorganism gains the ability to resist the activity of a particular antimicrobial agent that it was previously susceptible to. This can result from mutation of genes involved in normal physiological processes and cellular structures (vertical evolution), from the acquisition of foreign resistance genes (horizontal evolution) or from a combination of these two mechanisms. The spread of NDM-1 is an example of horizontal evolution as genetic information is transferred between different bacterial species. **Figure 16** describes the spread of the NDM-1 gene from the first isolate in *K. pneumoniae* in 2008. Genes for producing MBLs are transferred from the *K. pneumoniae* DNA. The genetic elements are spread easily to other strains of Enterobacteriacease or another *K. pneumoniae*.

NDM-1 has shown that it has all the properties necessary to turn organisms that contain it into 'superbugs'.[54] There is increasing concern over how easily NDM-1 can spread between species through gene transcription.

K.pneumoniae resistant to multiple antibiotics discovered in 2008 in a patient who acquired the organism in New Delhi

K.pneumoniae DNA

180-kb transmissible genetic element

Novel metallo-beta-lactamase that hydrolyses penicillins, cephalosporins, and carbapenems

Variety of determinants including another broad spectrum beta lactamase (CYM-4) and genes inactivating erythromycin, ciprofloxacin, rifampicin and chloramphenicol

Genetic element that also encodes efflux pump and promoters that ensure the transcription of its genes

Transmissible genetic elements spread rapidly among other strains of Enterobacteriaceae

Figure 16: The origin and spread of NDM-1, adapted from**[55]**

2.3.2 Structure of NDM-1

A number of crystal structures of NDM-1 have recently become available: Apo-structure (PDB-ID: 3SPU),[56] monometalated (PDB-ID: 3SPF)[57] and containing a bound hydrolysed ampicillin molecule (PDB-ID: 3Q6X).[38] All of the crystal structures are of good resolution, between 2-2.5 Å. The crystal structures are also in good agreement with the homology models which were generated before high resolution crystal structures were available.[58]

2.3.2.1 Overall structure

NDM-1 is a single-chain polypeptide consisting of 270 amino acids.[38] NDM-1 adopts a characteristic metallo-β-lactamase αβ/βα fold as observed in the previously characterised VIM-2 and IMP-1[56] enzymes (**Figure 17**). The structure consists of two β-sheets (red); one is made up of seven antiparallel strands and the other five antiparallel strands. Each β sheet is flanked on its outer face by two α helices (cyan). A further α helix bridges the two β-sheets. NDM-1 shows about 32% sequence identity with VIM-2 and IMP-1. Notable variations are that the N-terminus of NDM-1 is much longer, forming two more β-strands but not part of the N-terminal β-sheet.

In NDM-1 loop L3 appears to be more open than in VIM-2 and IMP-1 (see Section 2.4.2.1) (**Figure 17**). The open face suggests a broader profile of substrates can bind there. It has been found that the substrate binding face of this loop is more hydrophobic than in other metallo-β-lactamases. NDM-1 is closely related to the B1 sub-class of metallo-β-lactamases as it has been found to be active in both the mono-zinc and di-zinc forms.[59]
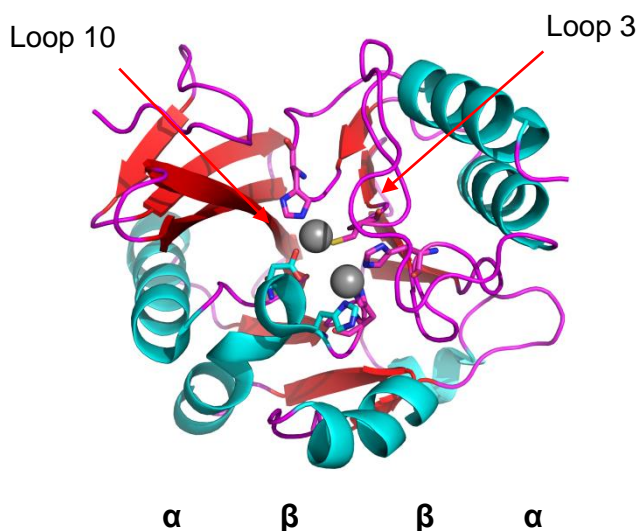
Figure 17: PDB entry 3Q6X shown with ribbon representation and coloured by secondary structure. α-helix (red), β-sheet (cyan), and loops (purple)

2.3.2.2 Active site of NDM-1

The active site of NDM-1 is located at the bottom of a shallow groove enclosed by two important loops L3 and L10. In the same way as other subclass B1 metallo-β-lactamases, two zinc atoms are located in the active site. NDM-1 has a larger active site cleft than VIM-2 with a surface area of 520 Å^2 compared to 450 Å^2. The larger surface area comes from the orientation of the L3 and L10 loops which are further away from the zinc active centre than in other metallo-β-lactamases. The large surface area allows for many more larger β-lactam substrates to be accommodated in the active site for hydrolysis (**Figure 18b**).

In the zinc active centre, Zn1 is tightly coordinated with tetrahedral geometry by three histidine residues and a bridging water (His-120, His-122 and His-189). Zn2 is coordinated in an octahedral environment by His-250 Cys-208, Asp-124 and three water molecules, one of which is the catalytic water which bridges to Zn1.[60] The binding region is shown in **Figure 18a**.
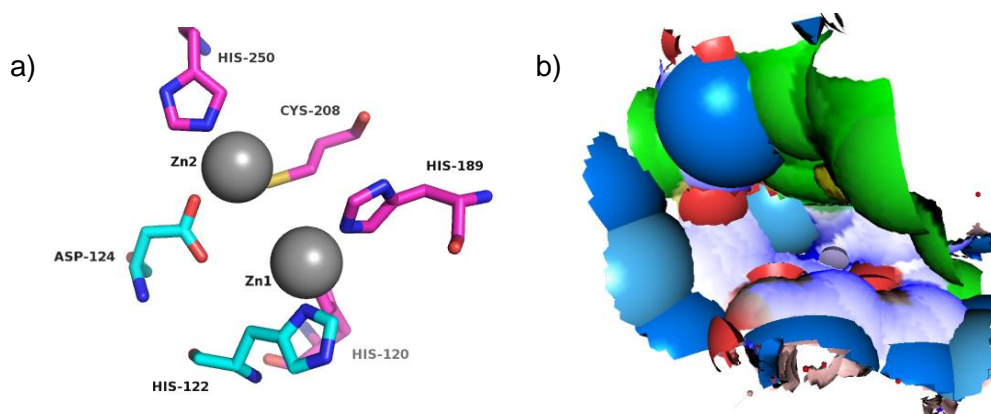
Figure 18: NDM-1 active site. a) amino acid residues binding to zinc atoms. b) SPROUT generated boundary surface of active site showing hydrophobic wall (green), hydrogen bond acceptor sites (red) and hydrogen bond donor sites (blue).

It has been observed that NDM-1 has an enhanced positively charged electrostatic profile around Zn1 compared with VIM-2, which may serve to attract and orientate the negatively charged β-lactam carboxylate during hydrolysis.[56]

The Zn-Zn interatomic bond distance is seen to be ~3.8 Å in the apo-structures. Upon binding with a hydrolysed substrate it has been seen that the interatomic bond distance is substantially longer at ~4.6 Å. It has been

suggested that the larger Zn-Zn bond distance observed in the hydrolysed form of NDM-1 is required for the release of the hydrolysed substrate.[38]

2.4 The other clinically relevant MBLs

2.4.1 Spread

2.4.1.1 Verona integron-encoded metallo-β-lactamase (VIM-2)

VIM-2 has been identified in clinical isolates worldwide as shown in Section 2.2.1. When focussing in on Europe, almost all European countries have seen an outbreak of VIM producing isolates. Spain and Italy have seen spread of VIM-2 outbreaks between hospitals. Greece shows a high prevalence of VIM enzymes within bacteria from patients (**Figure 19**). The bla_{VIM-2} gene has rapidly spread into many pathogenic bacteria with isolates found in *E. coli* and *K. pneumoniae.* As with NDM-1, bla_{VIM-2} is spread *via* horizontal gene transfer, giving acquired resistance to the bacteria that receive the gene.
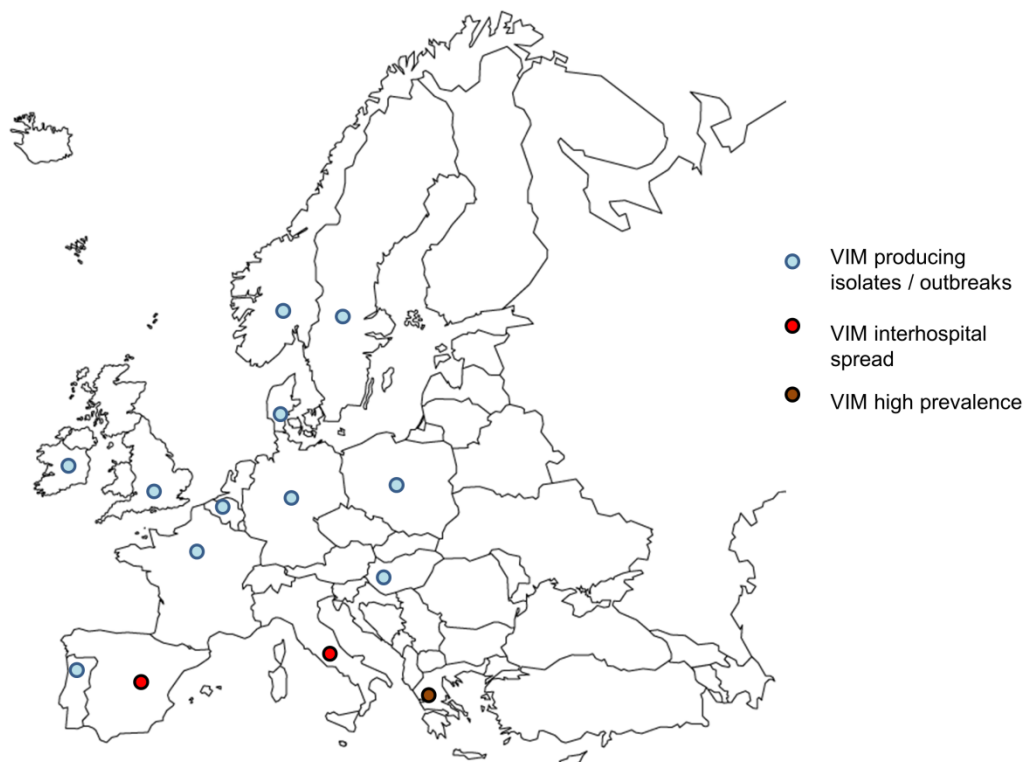
Figure 19: Locations of VIM in Europe.

2.4.1.2 Imipenemase (IMP-1)

IMP-1 was initially isolated in the early 1990s from *Pseudomonas aeruginosa* and *Serratia marcescens*. Since this time IMP-1 has been detected in a number of different strains of bacterial isolates. Due to the ability of the bla_{IMP} gene to spread rapidly by horizontal transfer, isolates have been identified across the globe.[61] IMP-1, like the other MBL, exhibits broad substrate specificity, with high affinities for cephalosporin and carbapenems as opposed to penicillins. IMP-1 is considered to be one of the most clinically important MBL for several reasons: IMP variants hydrolyse all β-lactam containing antibiotics, except monobactams, including carbapenems like imipenem. The gene for IMP, bla_{IMP} has rapidly spread into many pathogenic bacteria. IMP has spread across the globe but a high prevalence has been identified in Japan and Indonesia. The high prevalence in Japan can be partially attributed to the high population density which leads to ease of the spread of IMP (**Figure 20**).
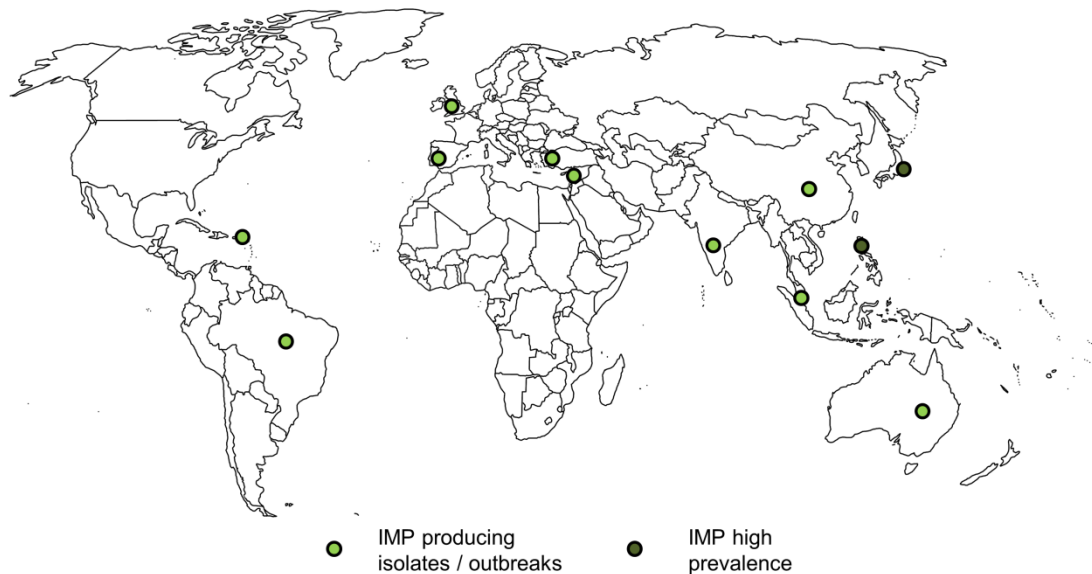
Figure 20: Worldwide spread of IMP metallo-beta lactamase.

2.4.1.3 São Paulo metallo-β-lactamase (SPM-1)

SPM-1 was purified for a highly resistant *P. aeruginosa* isolate from a 4 year old leukemic girl in São Paulo, Brazil.[62] A subsequent screening program confirmed the presence of SPM-1-producing stains in a high proportion (~35%) of carbapenem-resistant isolates from seven geographically widespread Brazilian hospitals. This elevated SPM-1 to be viewed as

significantly clinically relevant. So far SPM-1 spread has been limited to South America and central Europe. (see Section 2.2.1) SPM-1 does have the potential to spread as rapidly as the other metallo-β-lactamase enzymes.

2.4.2 Structural comparison

2.4.2.1 VIM-2 and IMP-1

VIM-2[63],[64] and IMP-1 along with NDM-1 belong to the B1 subclass of the MBLs. The crystal structures reveal the αβ/βα sandwich seen in NDM-1 and feature a catalytic di-nuclear zinc binding site which lies at the interface of the two αβ domains. VIM-2[63],[64] is the closest analogue to the NDM-1 enzyme (~33%), and as for NDM-1, the active sites of VIM-2 and IMP-1 contain two zinc atoms (**Figure 21**). The first Zn (Zn1 site) is coordinated in a tetrahedral geometry by three His residues and a bridging water molecule as in NDM-1. (His-116, His-119, His-196 and a bridging water in IMP-1 and His-116, His-118, His-196 and a bridging water in VIM-2) The second Zn (Zn2 site) is bound in an octahedral environment by an Asp, Cys, His, terminal water and a bridging water. (Asp-120, Cys-221, His-263, two terminally bound waters and the bridging water molecule in IMP-1 and Asp-120, Cys-221, His-263, two terminal waters and a bridging water in VIM-2). The inter atomic Zn-Zn distance is very similar to NDM-1 at around 3.5-3.7 Å in length in the unbound form a distance which is seen to increase on binding of a substrate.
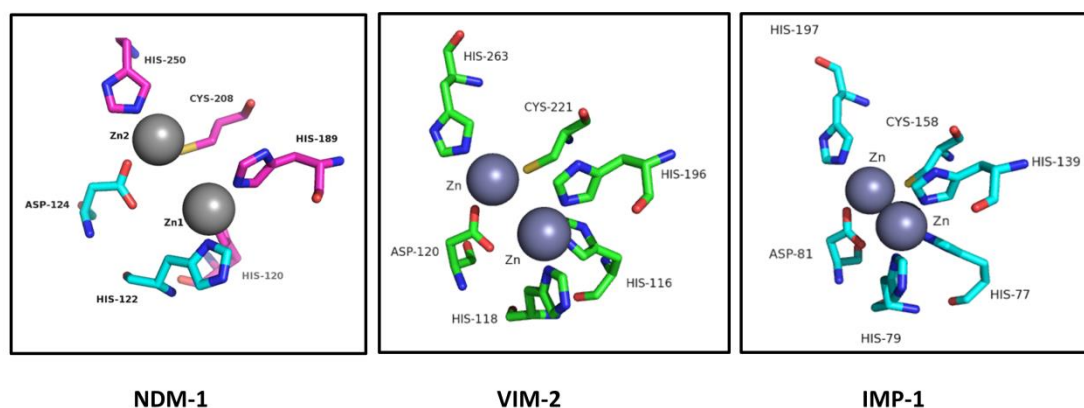
Figure 21: Comparison of the co-ordination of the Zn ions in NDM-1, VIM-2 and IMP-1

The active site of VIM-2 has a surface area of 450 Å^2 which is slightly more closed than in NDM-1 which shows a larger surface area of 520 Å^2. As seen

in **Figure 22** in VIM-2, there is a Phe-61 residue which protrudes into the active site which is not present in NDM-1. This narrows the amount of space in the active site and reduces the overall surface area. IMP-1 has an even smaller active site surface area of 399 Å^2. As is highlighted in **Figure 22** there is a significant reduction in the size of the active site cleft in IMP-1. The IMP-1 active site has almost a completely closed loop, which forms a hydrophobic pocket, increasing the affinity to hydrophobic molecules. The Trp-28 residue of the active site loop is seen to create a π stacking interaction with compounds helping to orientate them for hydrolysis in the active site.
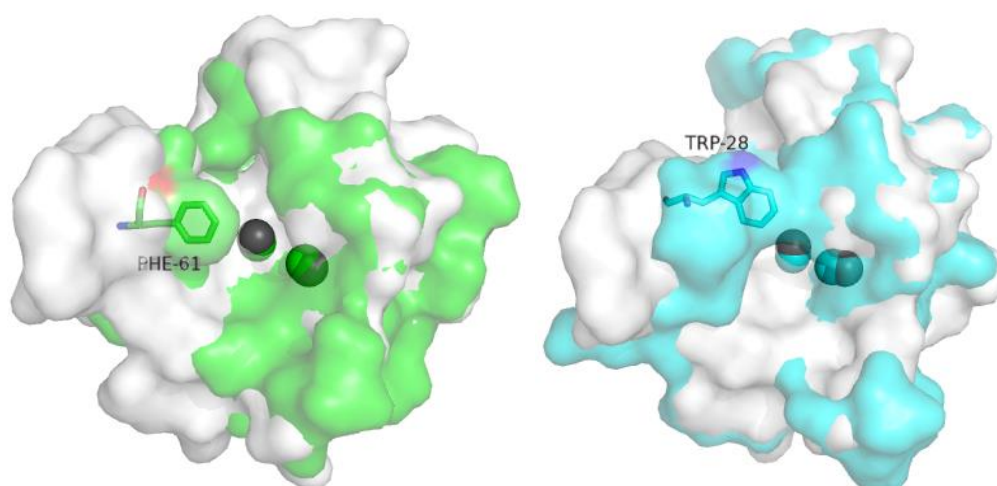
Figure 22: Overlays of the MBL active sites against NDM-1 (White with grey Zn). a) VIM-2 showing key Phe-61 residue (Green) and b) IMP-1 showing key Trp-28 residue (Blue).

2.4.2.2 SPM-1

Unusually, SPM-1 has high sequence similarity with MBLs from both B1 and B2 subclasses. In solution SPM-1 is reported to have a Zn (II) ratio of 1.5 : 1 however in the first available crystal structure there is only one zinc atom in the active site which is surrounded by three His residues, His-116, His-118, His-196 and a terminal water molecule (PDB ID: 2FHX).[62] The Cys residue which would be expected to bind the Zn$_2$ atom has been oxidised (CSO-221, **Figure 23**). Brem *et al.* conducted a number of studies and concluded that in terms of its Zn (II) usage and catalytic mechanism, SPM-1 is best defined as a B1 MBL.[65] However in terms of structure and in particular the flexible loop region, SPM-1 has features typical of a B2 enzyme.
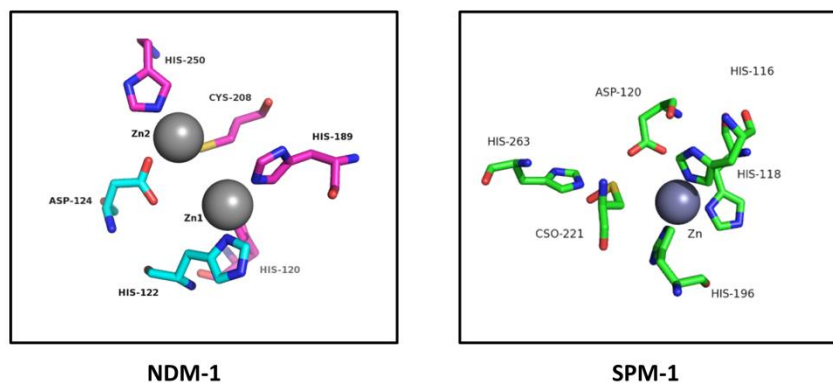
Figure 23: Comparison of the active sites of NDM-1 and SPM-1 showing Single Zn occupancy in SPM-1

The active site cleft is seen to be smaller than in other enzymes with a flexible loop covering part of the active site. The flexible loop is able to move into both a closed (PDB ID: 4BP0) and an open (PDB ID: 2FHX) form which enables or disables access to the active site of the molecule (**Figure 24**). The crystal structure of the closed form shows two zinc atoms present in the active site which again shows the strange nature of the SPM-1 enzyme having cross subclass characteristics. SPM-1 shows the lowest similarity to the active site of NDM-1.
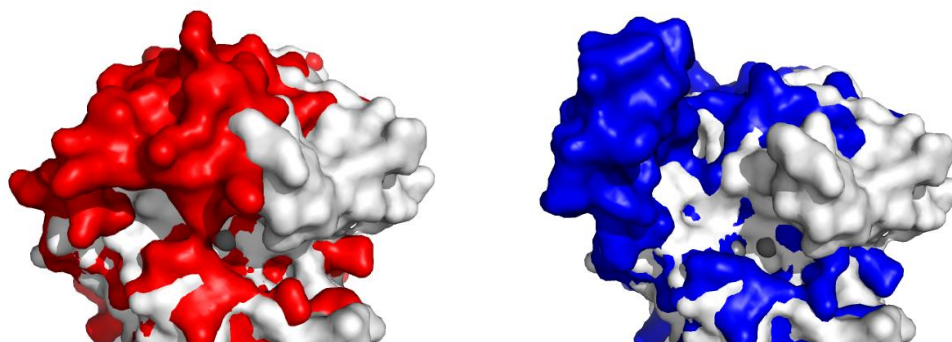
Figure 24: Overlay of NDM-1 (White) (PDB ID: 3Q6X) and SPM-1 in both closed (Red) (PDB ID: 4BP0) and open (Blue) (PDB ID: 2FHX) showing the enclosed active site of the SPM-1 enzyme in the closed form believed to be the cause of its differing properties to the other B1 MBLs.

2.5 Inhibitors of MBLs

As NDM-1 is one of the most recent MBLs to be identified in bacteria from hospital acquired infections, there has been limited work conducted into finding new inhibitors. Currently there are no known clinically relevant inhibitors of the MBLs however there are a few classes of inhibitors in development. These include metal extractors, thiols and transition state mimics all of which are designed to be given in a combination with a current β-lactam antibiotic.

2.5.1 Metal extractors

The metal chelator EDTA (**2.16**) has been shown to inhibit NDM-1 by binding strongly to the zinc atoms present in the active site[44] (**Figure 25**). However EDTA is non-selective in nature meaning it binds to other metal sites in the body as well as the NDM-1 enzyme which causes many potential issues with its use.
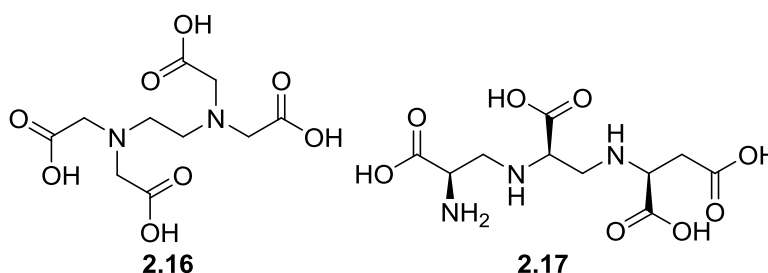
Figure 25: Structures of metal extractors EDTA (**2.16**) and Aspergillomarasimine A (**2.17**)

Aspergillomarasmine A (AMA, **2.17**)[66], has recently been identified as an NDM-1 inhibitor. It acts by coordinating to the zinc ions in the active site of the enzyme. This compound, which is similar structure to EDTA, acts as a 'suicide' inhibitor by removing the zinc ions from the active site of the enzyme, leaving the enzyme unable to function. Wright *et al.,* who identified AMA, showed it can overcome bacterial resistance in NDM-1 producers towards the carbapenem antibiotic meropenem. Although initial studies show promising results, limited selectivity data is available to show whether the molecule will be selective towards its target or have a detrimental effect by coordinating to other zinc-containing enzymes in the body.

2.5.2 Thiols

Captopril (**2.18**, **Figure 26**) is one of the few compounds that effectively inhibit NDM-1. Chen *et al.* investigated scaling back captopril to simpler derivatives to identify the pharmacophore for NDM-1 inhibition. Captopril is a peptide mimic consisting of a proline residue and a 3-mercapto-2-methylpropanoic acid subunit (**2.19**). They concluded that the captopril 3-mercapto-2-methylpropanoic acid subunit demonstrated inhibitory activity against the NDM-1 enzyme. This highlighted the potential for thiol containing compounds which could bind strongly to zinc containing systems. Even the smallest of thiols have been seen to give an inhibitory effect such as mercaptoacetate (**2.20**) which was used to help elucidate the structure of B3 MBL SMB-1.[67]
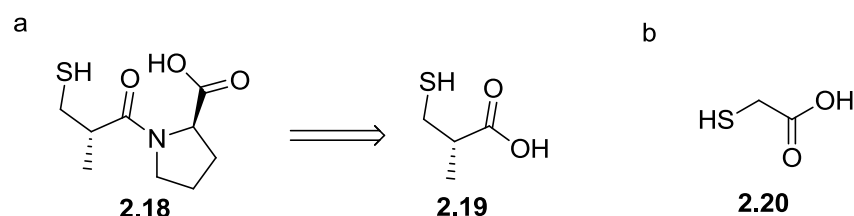
Figure 26: Thiol-based inhibitors. a) Captopril (**2.18**) and active 3-mercapto-2-methylpropanoic acid subunit (**2.19**). b) mercaptoacetate (**2.20**)

Work has also been conducted into using cysteine-containing peptides. The 3-mercapto-2-methylpropanoic acid subunit seen in captopril is a peptide mimic of cysteine so activity is also expected to be observed with cysteine. Page *et al.* showed that micromolar inhibition can be achieved against *Bacillus cereus* zinc β-lactamase using cysteine-containing peptides.[42] This class of compound is discussed further in Chapter 6.

Recently Klingler *et al.* showed that a number of existing FDA approved thiol-containing drugs can inhibit a range of MBLs.[68] The study found that four compounds DL-captopril (**2.18**), DL-Thiorphan (**2.21**, **Figure 27**) , 2,3-Dimercaprol (**2.22**) and Tiopronin (**2.23**) showed micromolar levels of affinity against the MBLs. Further studies using thermal shift measurements confirmed that the inhibitors were co-ordinating to the zinc after observing higher melting temperatures than the enzyme with no inhibitor as the enzyme gained increased stability. This is in contrast to EDTA, which gave a

lower melting temperature due to the increased instability of the enzyme once the zincs had been abstracted.
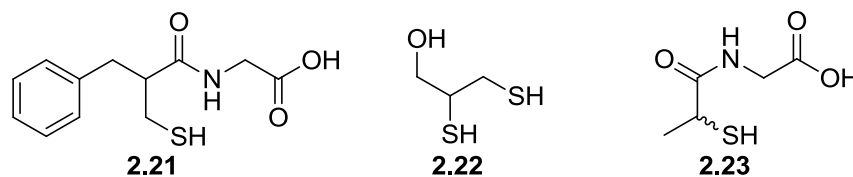
Figure 27: The structures of thiol based inhibitors DL-Thiorphan (**2.21**), 2,3-Dimecarpol (**2.22**) and Tiopronin (**2.23**)

Rhodanines are known to inhibit class A and C β-lactamases and some PBP.[69] Although rhodanines have often been identified as pan-assay interference compounds (PAINS),[70] a recent report of a broadly active rhodanine based inhibitor claims the inhibitor to be an uncompetitive/non-competitive submicromolar inhibitor of clinically relevant MBLs: VIM-2 (Ki = 183 ± 24 nM) and IMP-1 (Ki = 930 ± 97 nM).[71] The inhibitor is also seen to recover the activity of imipenem against clinical isolates of VIM-2, IMP-1 and NDM-1. Brem *et al.* conducted crystallographic and biological studies to elucidate the mechanism by which the inhibitor works.[72] They showed the rhodanine (**2.24**) hydrolyses to form a thioenolate (**2.25**) active species which binds through the thiol to the zinc atoms (**Figure 28**).
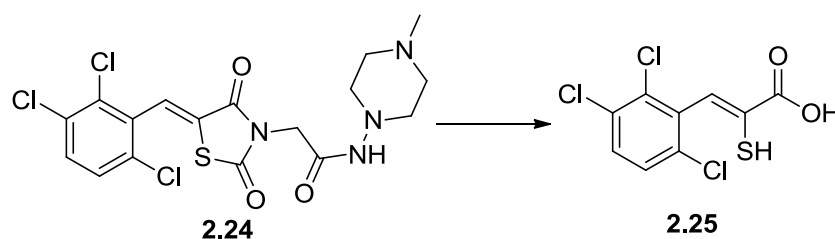
Figure 28: Rhodanine inhibitor (**2.24**) undergoes hydrolysis to give active thioenolate (**2.25**).

2.5.3 Transition state mimics

A number of 'suicide' inhibitors have been designed which mimic the β-lactam antibiotics transition state on hydrolysis. Since β-lactam-containing antibiotics are peptide mimics and since β-lactamases catalyse peptide bond cleavage, researchers hypothesised that a tetrahedral transition state may be formed during the hydrolysis mechanism. It was thought that a chemically stable β-phospholactam transition state mimic may be a good inhibitor of the MBLs (**2.26**, **Figure 29**) Examples have seen β-phospholactams used to

inhibit ~50 % of NDM-1's activity at 100 µM.[73] Although inhibition through this type of mimic was seen it was significantly weaker than binding with metal chelators or thiols.

The same principle has been applied with boron containing compounds forming a boronic acid transition state inhibitor (BATSI) (**2.27**, **Figure 29**).[74] In these compounds, the boronic acid acts as the tetrahedral intermediate.[75] These compounds have been shown to inhibit serine-β-lactamases and VIM-2 in the nanomolar region but have yet to be tested against NDM-1, IMP-1 and SPM-1 (See Chapter 6).
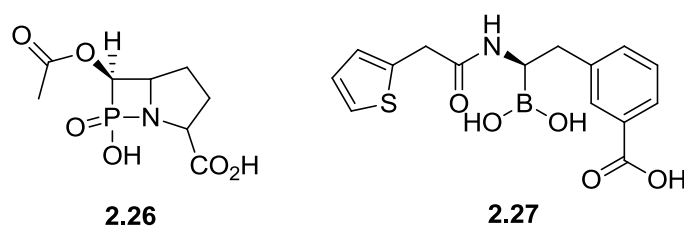
Figure 29: Transition state β-lactamase inhibitors. Phospholactam (**2.26**) and BATSI (**2.27**)

2.5.4 Other MBL inhibitors

Recently Worthington *et al.* have identified a 2-aminoimidazole-derived small molecule (**2.28**) that is able to suppress resistance of a NDM-1 producing strain of *K. pneumoniae*[76] (**Figure 30**). This small molecule is able to lower carbapenem MICs by up to 16 fold, while exhibiting little anti-bacterial activity itself. The molecule was derived by examination of previously reported inhibitors of MRSA, an example of drug repurposing.[77] The mechanism of action of this compound has yet to be determined.
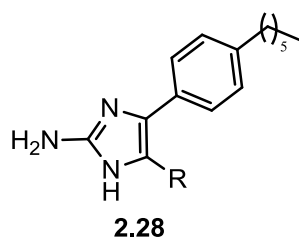
Figure 30: 2-aminoimidazole scaffold (**2.28**)

A study was carried out by Weide *et al.* to identify selective VIM-2 inhibitors[41] The most potent compound (**Figure 31**), a NH-1,2,3-triazole-based inhibitor (**2.29**), was found to have a K_i of 0.41 ± 0.03 µM activity against VIM-2. The same compound was seen to be inactive when screened against IMP-1.

Minond *et al.* discussed the click chemistry synthesis of these compounds and studied further derivatives to look for more potent inhibitors.[78]

2.29
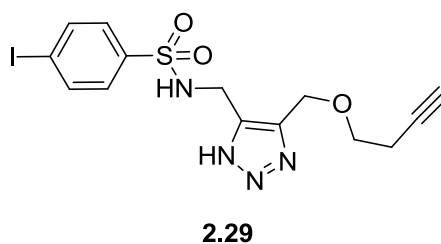
Figure 31: Selective VIM-2 inhibitor (**2.29**) identified by Weide *et al.*

Toney *et al.* identified a number of 2,3-(S,S)-di-substituted succinic acid inhibitors (**2.30**).[79] The identified best succinic acid inhibitor, which contained aromatic groups at R_1 and R_3, gave an IC_{50} value of 9 nM against IMP-1 (**Figure 32**) It is expected that the aromatic portions form good π stacking interactions within the enclosed hydrophobic pocket.

2.30
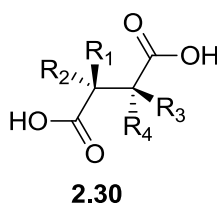
Figure 32: Succinic acid inhibitor (**2.30**) identified by Toney *et al.*

As well as the described inhibitors above, which would be given in combination with a current β-lactam antibiotic, a number of combinations of non β-lactam containing drugs have been used to treat infections caused by NDM-1 producing bacteria, such as tigecycline and colistin. In 2011 Stone *et al.* reported a patient with calciphylaxis and co-infection with NDM-1 producing *E. coli* and *K. pneumoniae*, both being susceptible to tigecycline and colistin.[80] Colistin is an antimicrobial agent composed of a complex mixture of polymyxins which inhibits the cell membrane structure and function. Tigecycline is a glycylcycline with a wide spectrum of activity against bacteria, which inhibits protein biosynthesis. This work highlights that resistance was being observed when treatment was with tigecycline alone and that the colistin was required to fully treat the patient.[81]

Chapter 3
Project goals

The work presented in this thesis aims to rationally identify novel inhibitors of the clinically relevant metallo-β-lactamases, VIM-2, IMP-1, NDM-1 and SPM-1, using a combination of structure-based drug design, chemical synthesis and biological evaluation.

3.1 Molecular design stage

- Understand the principles of structure-based drug design

- Become proficient at using SPROUT modelling software and AutoDock, eHiTS and Glide docking programs

- Use SPROUT to design novel inhibitors of the metallo-β-lactamases, NDM-1, VIM-2, IMP-1 and SPM-1.

- Apply a consensus docking approach to the designed compounds.

3.2 Chemical synthesis

- Use modern organic synthesis to prepare the designed compounds

- Produce libraries of analogues based upon hit compound(s) to enable SAR

- Ensure all compounds are of suitable purity for biological evaluation

3.3 Biological evaluation

- An enzymatic assay will be used to determine the IC_{50} value of any potential inhibitors against each enzyme

- Significantly potent inhibitors will be used in a cell based assay to determine if they rescue the Minimum Inhibitory Concentration (MIC) of meropenem against MBL producing bacteria.

When an IC_{50} value of better than 1 µM is achieved in the enzymatic assay, the inhibitors go on for MIC testing. 1 µM has been chosen as a cut off as captopril has an IC_{50} of 36 µM against NDM-1 and 12 µM against IMP-1. Any inhibitor designed specifically to interact with MBL would be expected to have a better potency than captopril against the enzymes.

The inhibitors themselves should not have an MIC as they are not designed intentionally to be anti-bacterial but should give an MIC when used in combination with an established anti-bacterial agent such as meropenem. It would be expected that a compound would restore the meropenem MIC to less than 64 µg/ml before being taken further for *in vivo* testing.

The design of new inhibitors goes through a number of cycles making improvements on compounds whose IC_{50}'s and MICs fall below the desired acceptable ranges until a good inhibitor meeting the desired criteria is found. (**Figure 33**)
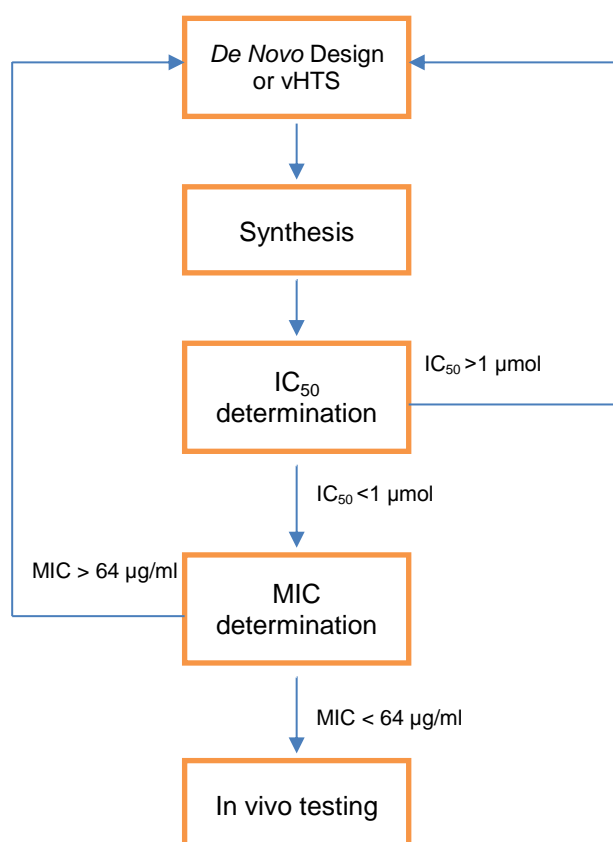
Figure 33: Flow diagram of biological testing protocol for potential MBL inhibitors.

Screening of the compounds to determine the IC_{50}'s was conducted by a collaborating partner; Dr Jürgen Brem at the University of Oxford. The enzymes used in the assays were expressed and purified by a collaborating partner; Dr James Spencer at the University of Bristol.

The enzymatic assay is based upon the hydrolysis of chromogenic cephalosporin nitrocefins as a reporter of enzyme inhibition (ie. assaying at multiple substrate/inhibitor concentrations and / or analysing the complete time course for the hydrolysis reaction.)[82] (see Appendix A1.1) The reaction is monitored at 485 nm as this is the absorbance band of the hydrolysed nitrocefin. The absorbance seen is due to the n →π* electronic transition in the di-nitro benzene ring seen in the nitrocefin. (**Figure 34**)
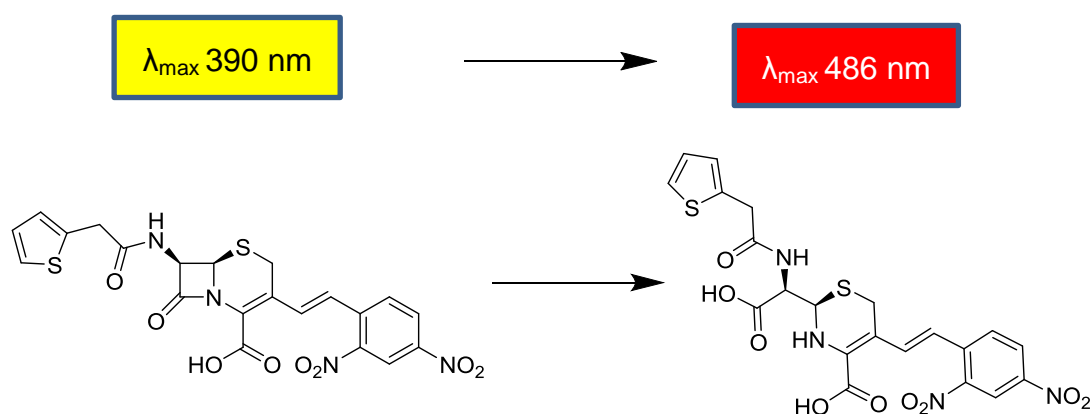
Figure 34: Hydrolysis of nitrocefin showing the change in λ_{max} between the hydrolysed and unhydrolysed forms.

Compounds which displayed an IC_{50} of less than 1 µM against the enzymes in the enzymatic assay were sent to Dr James Spencer at the University of Bristol where they were tested against NDM-1-producing bacteria with antibacterial agent meropenem to determine the recovery in the MIC. The broth dilution method was used according to standard Clinical Laboratory Standards Institute (CLSI)[83] protocols were used to determine MICs. (see Appendix A1.2)

Part 2

Results and Discussion

Chapter 4
Application of vHTS to inhibitor discovery.[84]

Virtual High-Throughput Screening (vHTS) both reduces the time and the cost of identifying potential inhibitors for a given target. In virtual screening, available databases of compounds are searched to identify novel hit molecules.[85] The potential molecules predicted using vHTS can be used to obtain a highly focussed library of compounds to be assayed against the protein target.[86] Libraries generated using vHTS have been shown to give hit rates of 20-30% which is much higher than the hit rates of traditional HTS which generally give a hit rate of less than 1%.[87] Two of the vHTS packages used at Leeds are AutoDock[88] and eHiTS.[89]

Recent advances in computation technology have made the docking of very large collections of small molecules into a desired molecular target a very rapid and time efficient process. Some libraries which are available for screening are the ZINC library[90], chemnavigator library[91] and the Chembridge compound library[92]. Some of the most prominent pieces of docking software currently in use for virtual screening include AutoDock[88], Glide[93], Gold[94], Dock[95], FRED[96] and eHiTS[89]. A selection from these programs is discussed below in the context of their recent use in antibacterial drug discovery. In a typical vHTS (**Figure 35**), a library of >10,000 compounds is docked using one of the docking programs. Very large libraries such as the ZINC database may be pre-screened using a program such as Pipeline Pilot.[97] Conditions such as the Lipinski rules[98] can be used to reduce the computational time required to dock the whole library by removing molecules that don't match the desired criteria. From the results generated by the scoring function in such programs, the top 10% of the 'virtual hits' is usually then visually inspected to assess synthetic accessibility, as well as calculate physiochemical properties such as cLogP. From these, a small library of compounds will be synthesised or purchased and screened against the enzyme. If an active compound is identified, a SAR study can be conducted around this molecule.
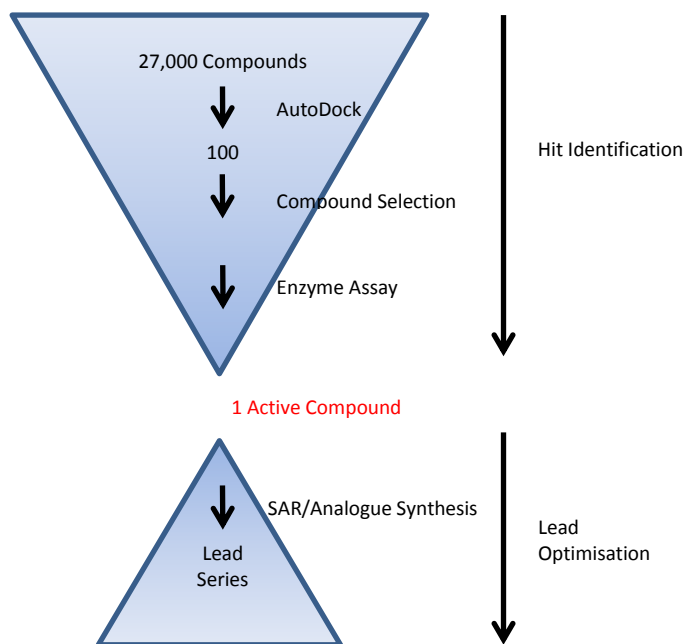
Figure 35: Typical vHTS screening protocol based upon using the Peakdale molecular screening library of 27,000 compounds[99]

4.1 Docking programs

4.1.1 AutoDock

AutoDock is a suite of automated docking tools designed to predict how small molecules bind to a protein of known three-dimensional structure.[100] AutoDock consists of two main programmes: '*autodock*' which carries out the docking of the desired ligand to a set of grids describing the protein. The grids are pre-calculated in '*autogrid*' from a designated grid box as shown in **Figure 36**. In '*autodock*' the ligand explores six spatial degrees of freedom, rotation and translation, and an arbitrary number of torsional degrees of freedom within the grid. After docking, AutoDockTools can be used to visualise and analyse the results.[88]

AutoDock uses a Lamarckian genetic algorithm to generate a range of docking poses that can be clustered together based on energetic similarity. A number of studies have shown that, rather than the lowest energy cluster, the most populated cluster of docked ligand conformations are better predictors of the native state.[101] The clustering of results is displayed in bar chart form (**Figure 36**).
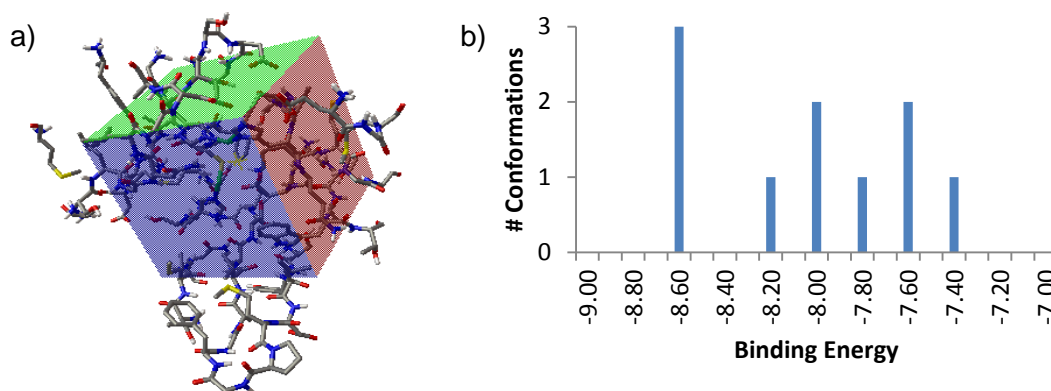
Figure 36: AutoDock results generation. a) Formation of a grid box. b) AutoDock tools results clustering.

4.1.2 eHiTS

eHiTS (designed and released by SimBioSys)[102] takes a unique approach to docking, by having an innovative algorithm and novel scoring function.[89] The approach breaks ligands into rigid fragments and connecting flexible chains. Each rigid fragment is docked independently and exhaustively within the receptor. A post-match algorithm finds all the matching solutions and reconstructs the original molecules (**Figure 37**). The solutions generated are automatically 'scored' by the eHiTS scoring function. This scoring function is based upon the interactions made between surface points on the receptor and ligand. Complementary surface points give a positive score while repulsive points give negative scores. Scoring components include hydrogen bonding, hydrophobicity, VDW contact energy, steric clash and entropy lost due to restricted rotatable bonds. Recent examples of the use of eHiTS include the identification of inhibitors of BACE-1[103] and the bacterial leucine transporter, LeuT respectively.[104]

eHiTS has also been previously been used in the identification of inhibitors for staphylococcal pyruvate kinase. Work in the Cherkasov group focussed on discovering inhibitors of methicillin-resistant *Staphylococcus aureus* (MRSA).[105] An in-house collection of 255 chemically diverse compounds that were selected from the ZINC library using "antibiotic like" criteria[106] were screened in a MRSA pyruvate kinase enzymatic assay and docked using eHiTS (PDB ID: 3TOT). The molecular docking used eHiTS operating with

the standard parameters. eHiTS successfully identified the selection of inhibitors which were found to be the most active in the enzymatic assay.
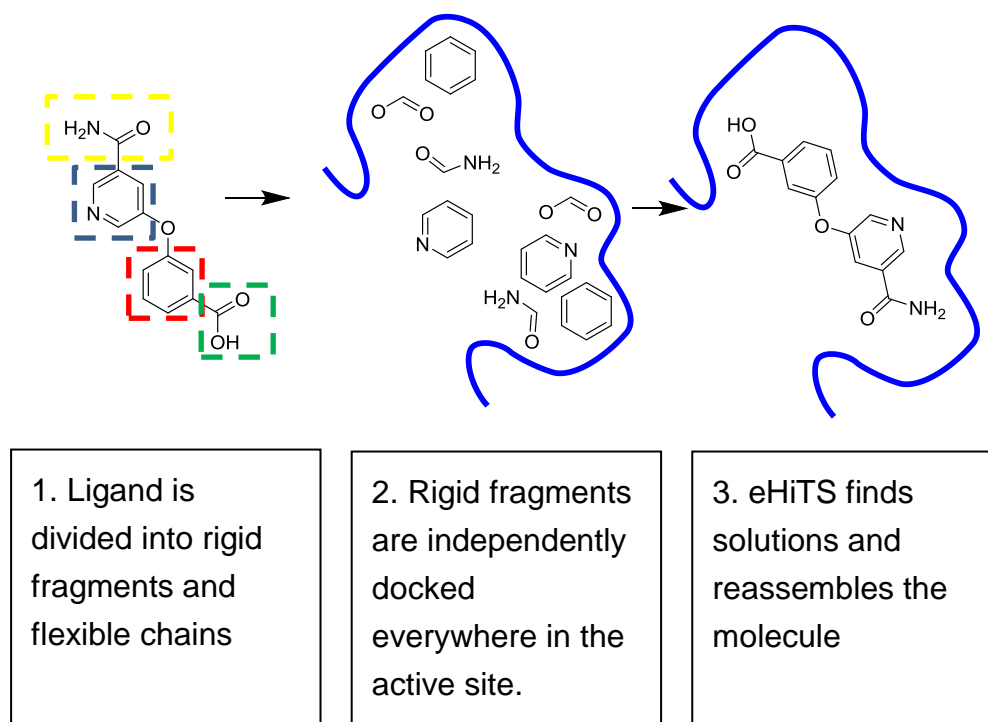
Figure 37: Schematic representation of eHiTS docking.

4.1.3 Glide

Glide[93,107] is an add-on to the Schrödinger package Maestro. Glide approximates a complete systematic search of the conformational, orientation, and positional space of the docked ligand. In this search, an initial rough positioning and scoring phase that dramatically narrows the search space is followed by torsionally flexible energy optimization on an OPLS-AA[108] non-bonded potential grid for a few hundred surviving candidate poses. The very best candidates are further refined *via* a Monte Carlo sampling of pose conformation;[109] in some cases, this is crucial to obtaining an accurate docked pose. Selection of the best pose uses a model energy function that combines empirical and force-field based terms.

Glide has been used by the Legler group in the design of inhibitors of *Francisella tuarensis*.[110] This facultative intracellular Gram-negative bacterium is responsible for the disease tularemia. Without treatment, the mortality rate can be as high as 5-15% for type A strains and 30-60% for the severe systemic and pneumonic forms of the disease.

4.2 Program choice

The choice of docking program is important as each utilises a different docking algorithm as described in Sections 4.1.1-4.1.3.

In order to investigate the best docking algorithm to use for docking proteins containing zinc atoms, as is the case for the MBLs, 4 known zinc binding ligands from crystal structures were sourced from the Protein Databank.[111] The selected zinc-containing crystal structures were chosen to cover a range of different ways ligands bind directly to the zinc atoms. (e.g. hydroxamic acid or thiol). The following crystal structures were selected:

1. 2FV9- TNF-alpha converting enzyme (TACE) complex[112]

2. 2HOC- Human carbonic anhydrase complex[113]

3. 2IWE- Structure of a cavity mutant CH117G of Pseudomonas aeruginosa azurin[114]

4. 3B92- Novel thiol based TACE inhibitor[115]

Each of the four ligands as well as ampicillin (from 3Q6X[38]) were re-docked into their native crystal structure using eHiTS, glide[93] and AutoDock respectively to see which docking program provided the closest match to the observed native co-crystallised ligand.
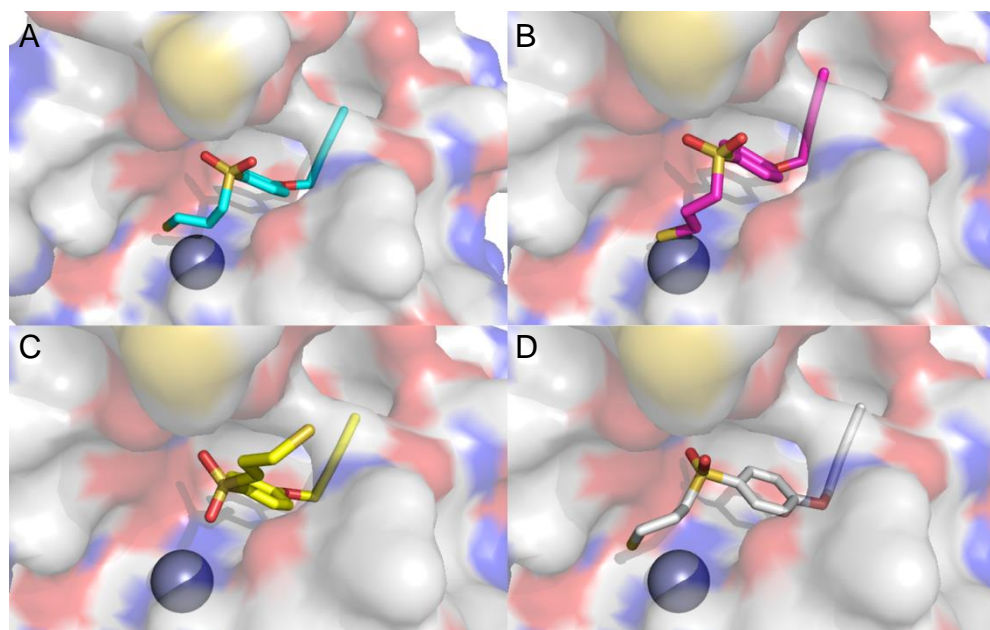
Figure 38: Novel thiol inhibitor in PDB ID: 3B92 a) crystal structure (cyan) b) eHiTS docked pose (pink) c) Glide docked pose (yellow) d) AutoDock docked pose (grey).

When conducting re-docking of the ligands into the native crystal structure using eHiTS. It was observed that the bond lengths between the zinc atoms of the enzyme active site and heteroatoms on the ligands from which binding occurs were consistently in the region of 1-1.5 Å (**Figure 38b**). This observed bond length for a covalent bond to a zinc atom is unrealistically small with typical bond lengths observed in crystal structures to be around 1.8-2.5 Å.[116] From these results, it can be deduced that eHiTS was not parameterised adequately for docking to proteins containing zinc atoms and therefore would not be suitable to use for vHTS.

The Glide docking algorithm provided more reasonable docking poses. However many of the poses involved the ligands binding at other locations within the active site rather than making a direct contact to the zinc atom as observed in the actual co-crystal structures. (**Figure 38c**). Overall Glide recognised the zinc atoms in the active site but would preferentially bind to other locations in the active site rather than by the zinc as observed in the native crystal structures.
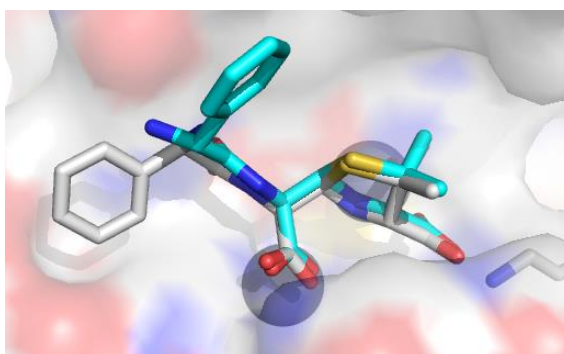
Figure 39: Overlay of ampicillin co-crystalized in NDM-1 (PDB ID: 3Q6X) (Cyan) and docked ampicillin (Grey)

The AutoDock docking algorithm gave the closest docking results to the native crystal structures. The bond lengths of the carboxylic acid of the ampicillin to the Lys-211 and carboxylic acid formed by the hydrolysis of the β-lactam ring to Zn1, predicted by AutoDock, were in a similar range to those seen in the crystal structures. AutoDock was the only programme to re-dock the hydrolysed ampicillin back into the crystal structure in a very similar position to that seen in the native crystal structure. The only observed change is the position of the phenyl ring where AutoDock places this deep into the active site pocket minimising solvent interactions whereas in the

native crystal structure the phenyl ring is positioned up away from the base of the active site. (**Figure 39**). The decision was then taken that AutoDock would be the programme used to conduct vHTS of compound libraries and used to dock new SPROUT designs.

4.3 Protocol for vHTS screening using AutoDock

In this work, the same protocol was used for all vHTS screening runs using AutoDock. The protocol is described below:

1. A crystal structure of the target protein is chosen from the Protein Databank.[111] Suitable crystal structures are those that have been resolved to less than 3 Å and have a co-crystallised small molecule inhibitor which can be used to define the screening volume of the enzyme.

2. The active site was defined using SPROUT (see Section 7.2.1). A 10 Å cut of the protein surrounding the active site was designated as the protein receptor.

3. A library of three-dimensional structures of commercially available compounds is created from the two-dimensional structures provided by the chemical supplier using the Corina software.[117] These were used as the ligand file for AutoDock screening. Suitable databases include the Peakdale Molecular[99], Chembridge[92], Maybridge[118] and KeyOrganics[119] databases.

4. At Leeds, AutoDock is run on an array of parallel processors which enables ~27,000 compounds to be screened against a particular protein in around 48 hours.

5. Once the AutoDock run was complete, any structures which have a score value of less than -7.000 in AutoDock were then analysed using SPROUT.

6. These structures were scored in the HIPPO module. Structures which had a score better than -5.50 using SPROUT were then evaluated to assess the predicted H-bonding and hydrophobic interactions within the protein. It was preferable for compounds to be making at least one H-bonding interaction with the protein, as well as a hydrophobic interaction.

The following factors are important when considering compounds for purchase/ synthesis prior to actual screening:

LogP: The partition coefficient P is a measure of the differential solubility of a compound in octanol and water. The log ratio of the concentrations of the solute in the solvent is called LogP. In the context of drug-like substances, hydrophobicity is related to absorption, bioavailability, hydrophobic drug-receptor interactions, metabolism and toxicity. The preferred limits for compounds LogP are in the range of +5.5 to -0.5.[98]

Toxicity: Evaluation of lead compounds using the Advanced Chemistry Development, Inc.(ACD/Percepta)[120] examined each molecule for toxicity and gave it an overall toxicity value based upon its predicted mutagenicity, tumourogenicity, irritating and teratogenic effects.

The ACD/Percepta Platform provides prediction and modelling of physicochemical (pKa, logD, Solubility), ADME (Blood-Brain Barrier[121] CYP 450 Regioselectivity) and toxicity (Genotoxicity, hERG Inhibition) endpoints by the use of a number of computational algorithms. From the results the user has the ability to design or modify structures to attain a desired property profile.

Solubility: The aqueous solubility of a compound significantly affects its absorption and distribution characteristics. Typically, a low aqueous solubility goes along with poor absorption. ACD/Percepta[120] gives an estimated LogS value for each compound by incremental addition of each atom's solubility. LogS is an estimate of the solubility measured in mol dm^{-3}. More than 80% of drugs on the market have an estimated LogS value greater than -4.

Molecular Weight: Compounds with high molecular weights are less likely to be absorbed. Over 80% of all marketed drugs have a molecular weight below 450 g mol^{-1}.

Promiscuity[122]: A promiscuous drug is a term used for drugs that may bind to many different molecular targets or receptors in the body, and so tend to have a wide range of effects and the potential for adverse drug reactions.[123]

At micromolar and sometimes submicromolar concentrations, many drug-like organic molecules aggregate into colloid-like particles in aqueous media,

termed 'colloidal aggregation'. These aggregates can block off protein targets from their desired substrate, thereby inhibiting them. Aggregating inhibitors are often unrelated chemically, although they typically share certain physical properties. Like colloids and vesicles, they are sensitive to assay conditions, the presence or absence of adjuvants, such as detergents or serum proteins, and target concentration.

Pharmaceutical companies try to make new drugs as selective as possible to minimise binding to undesired targets and hence reduce the occurrence of side effects and risk of adverse reactions.

Once a short list of compounds has been identified the desired compounds can be purchased from the supplier and tested for enzyme inhibition. Several vHTS screenings were conducted against NDM-1 were carried out and are discussed in sections 4.4 and 4.5.

4.4 Molecular docking of the Peakdale Molecular screening collection

Molecular docking was conducted using the method described in Section 4.3, using the Peakdale Molecular[99] database as the ligand files and the NDM-1 crystal structure PDBID: 3Q6X.[38] A set of ten possible inhibitors of NDM-1 was identified from the Peakdale Molecular database for purchase. Details of compound structures and predicted binding affinities are shown in Appendix A2.2.

4.4.1 Preliminary 'hit' molecule

Compound **4.1** (**Figure 40**) was identified from a preliminary biological evaluation, which was conducted at the University of Bristol by Dr. James Spencer. The preliminary biological evaluation was to give an indication of an inhibitory effect but not to quantify it. Of the top ten scoring compounds from the vHTS runs only compound **4.1** showed inhibition at 100 μM. Compound **4.1** showed limited solubility in 10% DMSO solution.
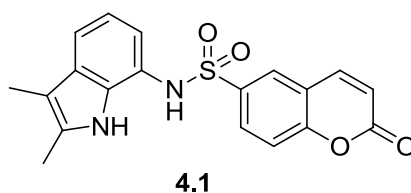
Figure 40: Structure of inhibitor **4.1** identified from Peakdale screen

Figure 41 shows that the main interactions between the 'hit' molecule and NDM-1 are predicted to come from the coumarin portion of the molecule interacting through the carbonyl to Gln-123 and the sulfonyl to Lys-211, Asn-220 and Zn2 respectively. The indole portion of the scaffold is seen to extend into a hydrophobic region of the binding site and is therefore a good place to investigate the effects of substituents in this region and attempt to make the molecule more soluble and more potent.
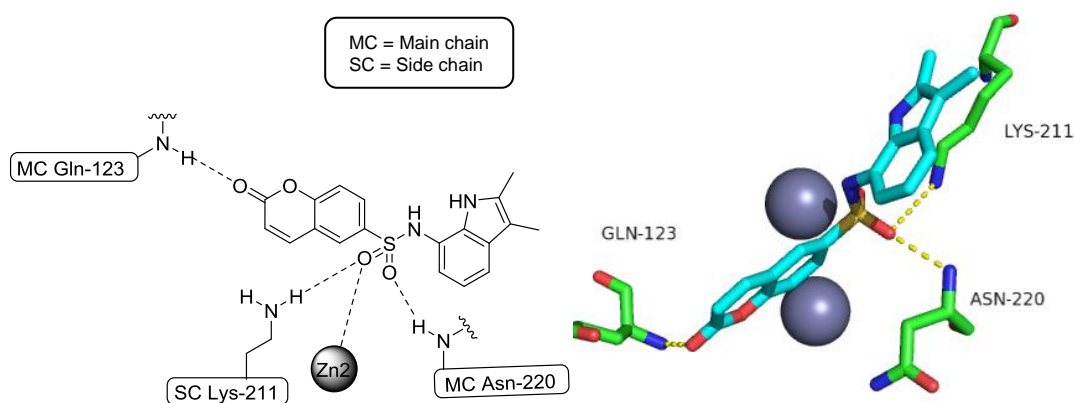
Figure 41: Binding interactions of **4.1** in a) 2D skeletal representation and b) 3D representation

In order to confirm these results, a re-synthesis of the hit molecule **4.1** was conducted as shown below (**Scheme 4**).

Coumarin **4.2** was reacted with chlorosulfonic acid to form sulfonyl chloride **4.3**. The reaction proceeded with moderate yields due to the formation of the undesired isomer with the sulfonyl chloride group on the 8 position of the coumarin (41%). In order to form nitro indole **4.5,** a Fisher indole synthesis[124] was conducted from hydrazine **4.4** and butan-2-one in moderate yield (52%). Nitro indole **4.4** was reduced under an atmosphere of hydrogen to produce amine **4.6** in high yield (83%). Finally sulfonyl chloride **4.3** and amine **4.6** were coupled in the presence of base to produce **4.1** in good yield (70%)(**Scheme 4**).
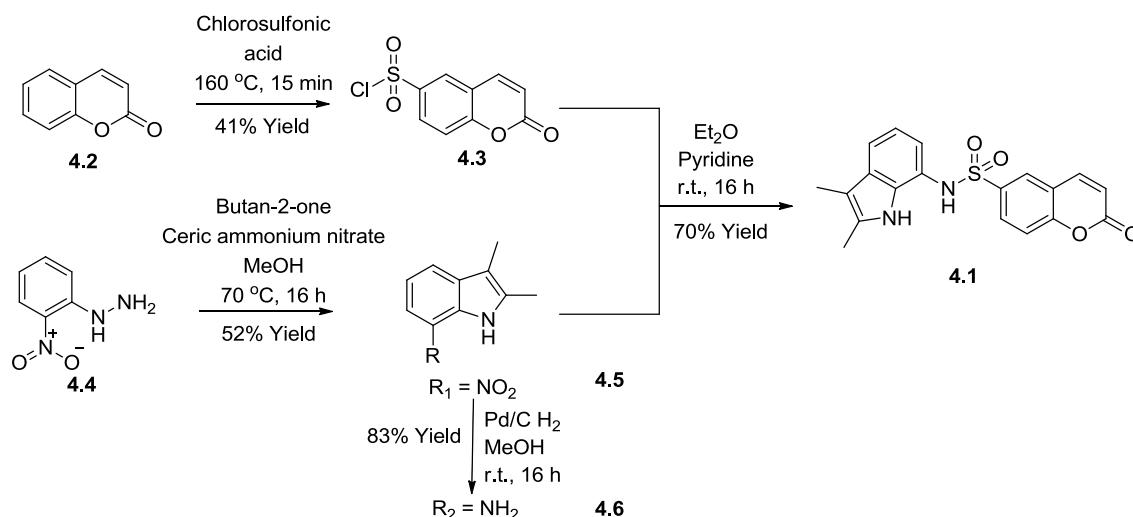
Scheme 4: Synthetic route to **4.1**

4.4.2 SAR investigation

The 'Hit' molecule **4.1** was re-examined in SPROUT[125] to look at the predicted interactions with NDM-1 and sites of potential interactions where a SAR investigation could be conducted to increase potency and solubility.

SPROUT identified three potential areas where a structure activity relationship exploration could be conducted around **4.1** with the aim of identifying a more potent inhibitor (**Figure 42**)
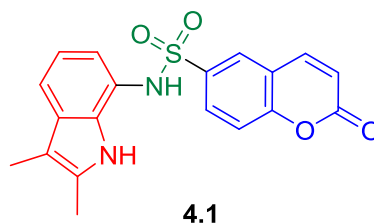
Figure 42: Areas for SAR investigation of **4.1**

All synthesised compounds (**4.13-4.18, 4.20, 4.22, 4.25, 4.27**) were biologically evaluated against NDM-1 by Dr Jürgen Brem at the University of Oxford, and the results are reported in Section 4.4.2. IC$_{50}$ values were determined on compounds which showed less than 30% residual enzyme activity at 100 µM.

4.4.2.1 Structure activity relationship of the N-aryl ring substituent.

The first SAR series containing compounds (**4.13-4.18**) was designed to examine the effects of changing the electron density of the aromatic ring attached directly to the amine side of the sulfonamide (previously the indole in **4.1**).

Compound **4.13** was synthesised as an analogue of **4.1** with the methyl groups on the indole portion of the molecule removed in an attempt to reduce the hydrophobicity of the molecule and make it more soluble in the assay without reducing the potency. Compounds **4.14-4.18** are simpler analogues of **4.1** looking at the effects of changing the electron density of the ring.
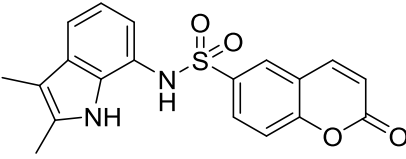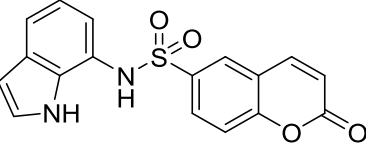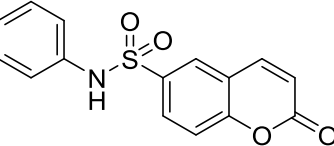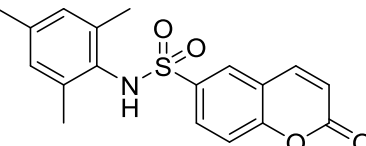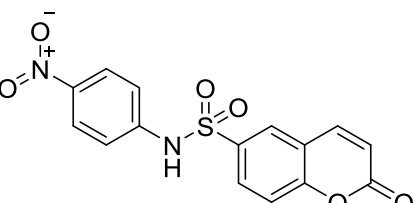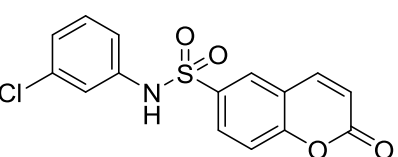
Scheme 5: Synthetic route to compounds **4.13-4.18**

The synthesis of compounds (**4.13-4.18**) investigating the N-aryl substituent was conducted as shown in **Scheme 5**. Each amine (**4.7-4.12**) was coupled to sulfonyl chloride **4.3** in the presence of base to produce compounds **4.13-4.18** respectivly in good yields (90-68%)(**Scheme 5**)

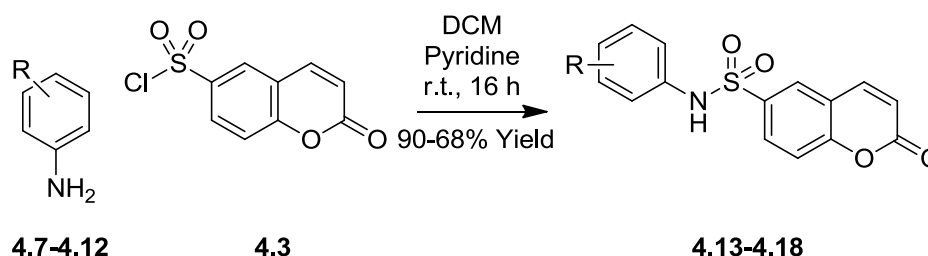Biological evaluation of compounds **4.13-4.18** against NDM-1 was conducted by Dr Jürgen Brem at the University of Oxford using the nitrocefin based assay described in Appendix A1.1.

From the residual activity it appears that the addition of electron withdrawing groups (rendering the aromatic ring electron deficient) helps to slightly increase the potency (**Table 3**). The substitution to a pyridine ring helps to both increase the potency and solubility (as in compound **4.15**). Although there is a significant reduction in the residual activity it is not below the desired level of <30% and therefore the IC_{50} of the compound was not calculated.

Table 3: SAR Study of N-aryl ring substituent of **4.1** against NDM-1

Compound Number	Structure	RA[%], 100 μM
4.1		83
4.13		86
4.14		89
4.15		40
4.16		89
4.17		81
4.18		92

4.4.2.2 Structure activity relationship of the dihedral angle of the linker.

The second series of compounds was designed to investigate the role of the dihedral angle of the N-aryl ring from the coumarin in order to explore if there are specific π stacking interactions occurring within the binding site due to the position of these groups.

The nitrogen from the sulfonamide was substituted for a carbon (**4.20**) and an oxygen (**4.22**). The substitutions were conducted in order to change the dihedral angle due to the change in bond angles around the individual atoms.

The synthesis of compound **4.20** investigating the role of the dihedral angle of the N-aryl ring from the coumarin where the nitrogen was substituted for a carbon was conducted as shown in **Scheme 6**. Benzyl bromide (**4.19**) was coupled to sulfonyl chloride **4.3** in the presence of base to produce compound **4.20** in moderate yield (29%)(**Scheme 6**).
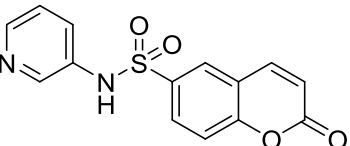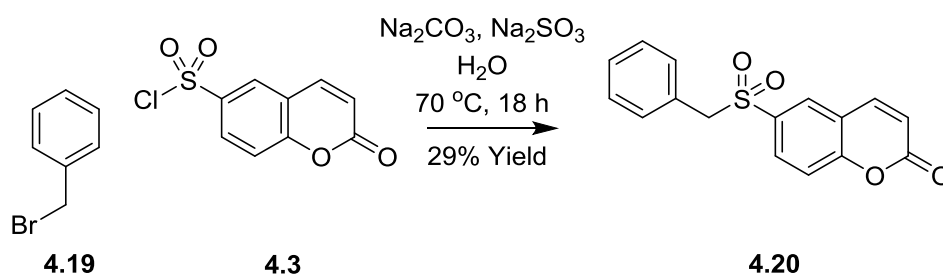

Scheme 6: Synthetic route to compound **4.20**

The synthesis of compound **4.22** investigating the role of the dihedral angle of the N-aryl ring from the coumarin where the nitrogen was substituted for a oxygen was conducted as shown in **Scheme 7**. Phenol (**4.21**) was coupled to sulfonyl chloride **4.3** in the presence of base to produce compound **4.22** in good yield (73%)(**Scheme 7**).
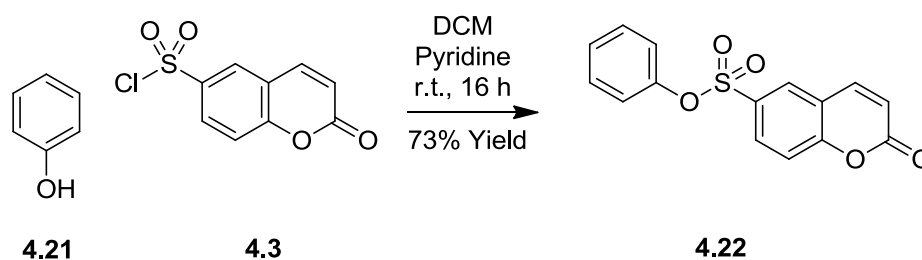
Scheme 7: Synthetic route to compound **4.22**

Biological evaluation of compounds **4.20** and **4.22** against NDM-1 was conducted by Dr Jürgen Brem at the University of Oxford using the nitrocefin based assay described in Appendix A1.1.

Table 4: SAR investigation of linker against NDM-1

Compound Number	Structure	RA[%], 100 µM
4.14		83
4.20		95
4.22		98

It can be seen that substitution of the sulfonamide nitrogen for an oxygen or a carbon has a negative effect on the potency of the compound (**Table 4**). The dihedral angle created by the sulfonamide must be required for good binding.

4.4.2.3 Structure activity relationship of the aryl sulfonyl group.

The third series was designed to investigate the importance of the predicted interaction between the coumarin carbonyl to the main chain amine of the Gln-123 residue.

Compound **4.27** was therefore designed to remove this interaction completely and compound **4.25** to change the nature of the bonding due to the tautomerisation to the hydroxyquinoline. The synthesis of compound **4.25** investigating the importance of the predicted interaction between the coumarin carbonyl to the main chain amine of the Gln-123 residue by changing the nature of the bonding was conducted as shown in **Scheme 8**.

1,2-dihydroquinolin-2-one **4.23** was reacted with chlorosulfonic acid to form sulfonyl chloride **4.24**. The reaction proceeded with moderate yields due to the formation of the undesired isomer with the sulfonyl chloride group on the 8 position of the quinoline (39%). Sulfonyl chloride **4.24** and amine **4.6** were coupled in the presence of base to produce **4.25** in moderate yield (31%)(**Scheme 8**).
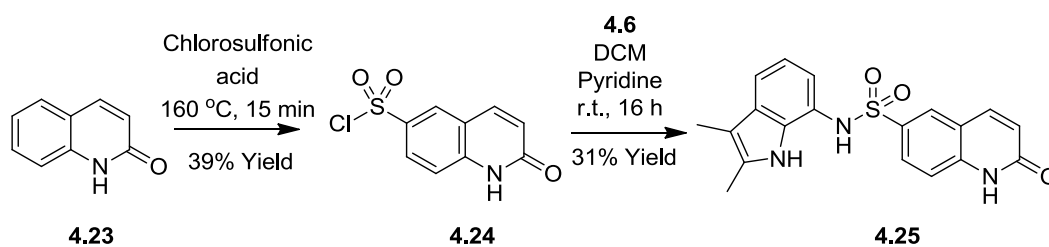
Scheme 8: Synthetic route to compound **4.25**

The synthesis of compound **4.27** investigating the importance of the predicted interaction between the coumarin carbonyl to the main chain amine of the Gln-123 residue by completely removing the interaction was conducted as shown in **Scheme 9**. Benzene sulfonyl chloride (**4.26**) was coupled to amine **4.6** in the presence of base to produce compound **4.27** in good yield (57%)(**Scheme 9**).
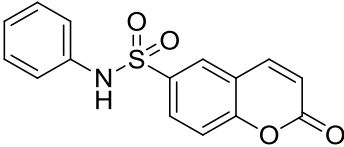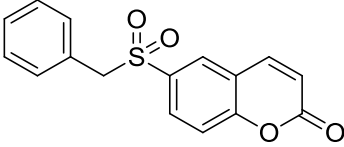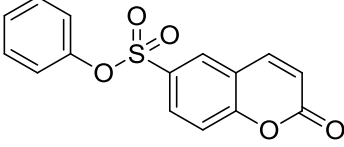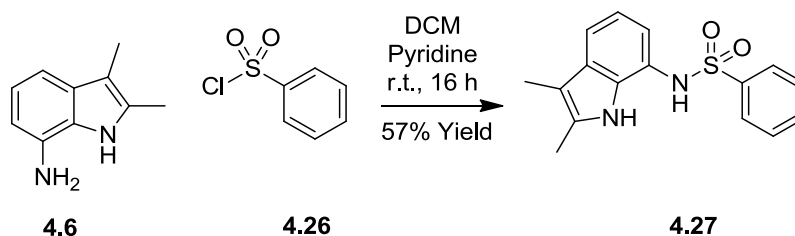

Scheme 9: Synthetic route to compounds **4.27**

Biological evaluation of compounds **4.25** and **4.27** against NDM-1 was conducted by Dr Jürgen Brem at the University of Oxford using the nitrocefin based assay described in Appendix A1.1.

Table 5: SAR investigation of coumarin portion of **4.1** against NDM-1

Compound Number	Structure	RA[%], 100 µM
4.1		83
4.25		82
4.27		93

The substitution of the coumarin to 2-hydroxyquinoline and a simple phenyl ring appeared to have no effect upon binding to the enzyme (**Table 5**). The residual activity of the enzyme remained almost constant for all of the compounds.
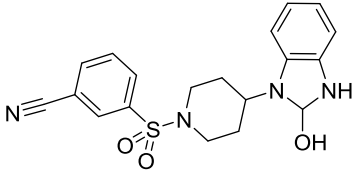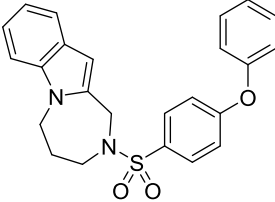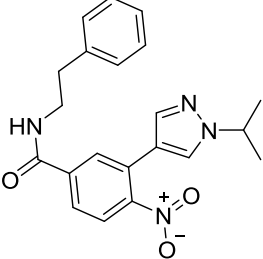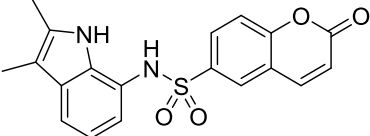
4.4.3 Biological evaluation of the hits identified from the Peakdale Molecular screening collection

Biological evaluation of the identified potential inhibitors against NDM-1 was conducted by Dr Jürgen Brem at the University of Oxford using the nitrocefin based assay described in Appendix A1.1.

The top four results from the biological evaluation of the selected inhibitors from the Peakdale molecular library against NDM-1 are shown in **Table 6**.

As the residual activity was greater than 30% at 100 µM in all cases, no IC_{50} values were determined. Although these compounds showed some activity against the enzyme, they were not pursued due to the activity levels being well above the desired levels of less than 30% residual activity at 100 µM.

Table 6: Peakdale molecular potential inhibitors and residual activities against NDM-1

Inhibitor	Structure	RA[%], 100 µM
4.28		75
4.29		78
4.30		80
4.1		83

4.5 Molecular docking of the Chembridge screening collection
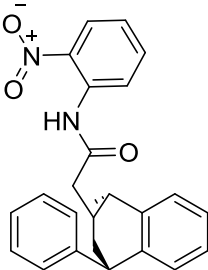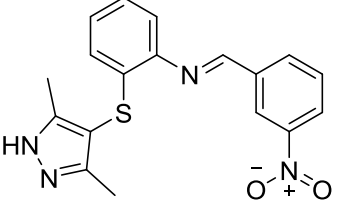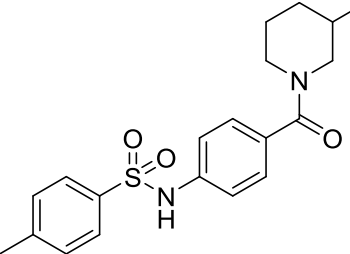
Screening was conducted using the method described in Section 4.3, using the Chembridge[92] database as the ligand files and the NDM-1 crystal structure 3Q6X.[38] A set of eight possible inhibitors of NDM-1 was identified from the Chembridge database, for purchase. Details of compound structures and predicted binding affinities are shown in Appendix A2.1.

4.5.1 Biological evaluation of the hits identified from the Chembridge screening collection

Biological evaluation of the identified potential inhibitors against NDM-1 was conducted by Dr Jürgen Brem at the University of Oxford using the nitrocefin based assay described in Appendix A1.1.

The top three results from the biological evaluation of the selected inhibitors from the Chembridge diversity library against NDM-1 are shown in **Table 7**.

Table 7: Chembridge identified compounds and their residual activity against NDM-1

Inhibitor	Structure	RA[%], 100 μM
4.31		81
4.32		81
4.33		82

As the residual activity was greater than 30% in all cases, no IC_{50} values were determined. Although these compounds showed some activity against the enzyme, they were not pursued due to the activity levels being well below the desired levels of lower than 30% residual activity.

4.6 Conclusions

An extensive vHTS campaign was carried out in an attempt to identify novel inhibitors of NDM-1. Initial evaluation of a number of docking algorithms using known zinc binding ligands determined AutoDock to be the best program to use for docking studies investigating MBLs . Biological evaluation at the University of Bristol of the top 10 scoring compounds from the Peakdale molecular compound library lead to the identification of a moderate hit from which a limited SAR investigation was conducted. When the initial putative inhibitors were re-screened along with the Chembridge compounds and SAR series at the University of Oxford, some inhibition was seen against NDM-1. However there was not significant enough inhibition to warrant a more detailed SAR investigation to be carried out around these compounds.

One of the limitations of the vHTS screening approach is that AutoDock relies upon a single high-resolution crystal structure. It is important to take into account that a protein, when in solution, is flexible and will often undergo conformational changes upon substrate binding. A number of studies have shown the importance of allowing both the protein and the ligand to have free movement in binding.[126] Increasing the protein flexibility also rapidly increases the computational time to process the dockings and therefore most programs, such as AutoDock, only allow the ligand to be flexible. It would not be possible, with the current computational power available, to conduct high throughput docking where both the ligand and protein are allowed to move.

Therefore if vHTS was to be used further in the identification of inhibitors of MBLs it would be sensible to use a number of crystal structures and select compounds which are identified as hits for a number of them. Further avenues to investigate would be to look at known inhibitors of the MBLs and

subject them to development (Chapter 6) and the design of *de novo* compounds which would be specifically designed for this biological target (Chapter 7). Both of these methods of compound identification would move away from the restrictions imposed by using a commercially available library for screening.

Chapter 5
Boronic acid inhibitors

Traditionally due to a common belief that boron and boron-containing compounds are toxic, many medicinal chemists in both industry and academia have overlooked using boron in drug molecules and have only used them as molecular tools.[127] The belief that boron is a toxic element is thought to have come from the fact that boric acid is an ingredient in ant poisons. It has however been proven that boric acid has a median lethal dose (LD_{50}) of 2660 mg/kg (rat, oral) which is comparable to regular table salt (NaCl) which has a LD_{50} of 3000 mg/kg (rat, oral).[128] People have also questioned the toxicity of boron from the side effects of taking Bortezomib, which is marketed as Velcade (**Figure 43**).[129] Velcade is the only boron-based therapeutic on the market, widely prescribed for the treatment of multiple myeloma. Velcade was slow to be taken into the clinic due to the high rate of side effects such as peripheral neuropathy in 30% of patients. Myelosuppression causing neutropenia and thrombocytopenia can also occur and can be dose limiting. The side effects are however usually mild relative to the side effects of bone marrow transplantation and other treatment options available for patients with this type of cancer. Recent studies have shown that the side effects of taking Velcade are not from the presence of a boron atom but the mechanism of action.[130]

5.1
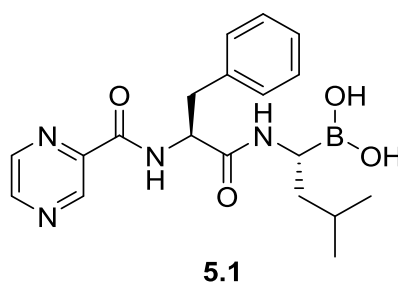
Figure 43: The structure of the boronic acid-based drug Velcade (**5.1**)

Boron-containing compounds have begun to receive increased attention over the past few years as potential drugs. This interest comes from a better understanding of the unique electronic properties of boron, which for example, allow it to act as a transition-state mimetic for the tetrahedral intermediate of peptide bond cleavage observed in the β-lactamase enzymes.

Boron contains an empty p-orbital which makes it a strong electrophile and a Lewis acid. Boron can easily form dative bonds with nucleophiles which changes the structure from being uncharged in a trigonal-planar geometry to an anionic tetrahedral geometry (**Figure 44**).[131] The formation of dative bonds to inhibitors in the β-lactamase active site provides additional binding affinity of the inhibitor to the enzyme. The advantage of a dative bond is that they provide stronger binding than non-covalent and hydrophobic interactions but are reversible, unlike many covalent bonds generated by 'suicide inhibitors' such as EDTA. The formation of the tetrahedral geometry allows inhibitors to be designed which mimic the tetrahedral transition state in the hydrolysis of β-lactams. The formation of the dative covalent bond makes this type of inhibitor a reversible competitive inhibitor which is preferable to 'suicide inhibitors' are which are often non-selective in nature and co-ordinate to a wide number of sites.
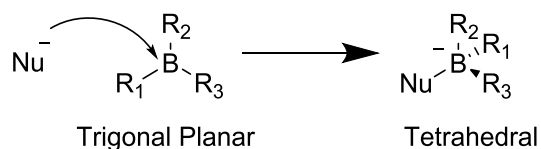
Figure 44: Trigonal-planar boronic acid species forms dative bond with nucleophile to generate tetrahedral structure

In addition to boronic acids, which has been explored by numerous research groups, the benzoxaboroles, a class of compounds wherein the boron atom is incorporated into a heteroaromatic ring system, have provided a number of interesting anti-inflammatory, antifungal and antibacterial drug candidates (see Section 5.1).

5.1 Known boron-containing drugs

The first natural product found to contain boron was Boromycin (**5.2**, **Figure 45**), a polyether macrolide antibiotic active against Gram positive bacteria.[132] It is effective against most Gram-positive bacteria, but is ineffective against Gram negative bacteria. Boromycin kills bacteria by negatively affecting the cytoplasmic membrane, resulting in the loss of potassium ions from the cell. The discovery of boromycin led to scientists realising that boron could be incorporated into clinically administered drugs.
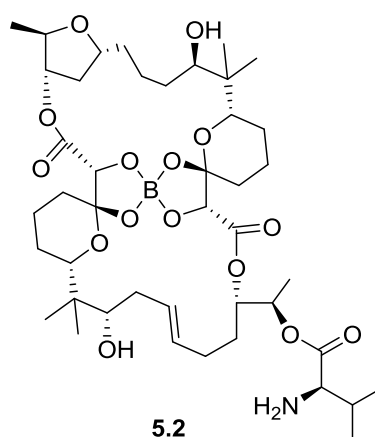
Figure 45: Natural product Boromycin (**5.2**)

There has also been research into the use of boronic acids as electrophiles targeting enzymes such as arginase[133] (**5.3**) and serine proteases (a class which includes the serine-β-lactamases) (**5.4**)[131] (**Figure 46**).
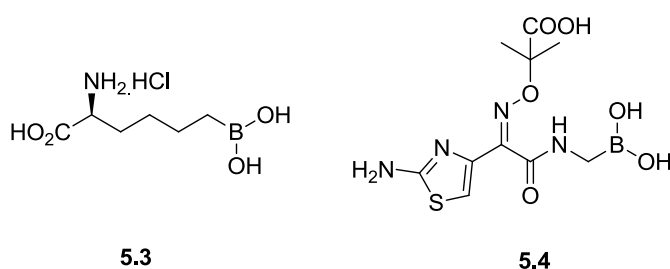
Figure 46: Boronic acid containing therapeutics clinical trials. a) Arginase inhibitor (**5.3**), b) beta-lactamase inhibitor (**5.4**).

The oxaboroles were first synthesised and characterised by Torssell *et al.* and were found to possess a high hydrolytic stability.[134] The oxaborole class of compounds have recently seen an upsurge in interest with almost half of the publications and patents based on this class of compound having appeared after 2005. The physical properties of the oxaboroles differ from

simple aryl-boronic acids mainly in their pK_a. Cyclising the boron into an oxaborole ring reduces the pK_a by 1-2 pK_a units. A compound of this class which is on the market is AN2690 (**5.5**). AN2690 (**Figure 47**), which is commercially marketed as Tavaborole, was the result of a medicinal chemistry program conducted at Anacor Pharmaceuticals.[135] Tavaborole was designed to be a small, water soluble antifungal agent that could penetrate human toe and finger nails to treat onychomycosis.
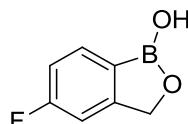
5.5

Figure 47: The structure of Tavaborole

5.2 Boron containing β-lactamase inhibitors

Several years ago it was recognised that boronic acid-containing compounds could be developed as β-lactamase inhibitors. The boronic acid-containing inhibitors do not contain a β-lactam ring and can therefore not be hydrolysed[136] however due to the nature of the boron element they have the ability to accept a pair of electrons from a nucleophile in the active site of the β-lactamase to form a strong dative covalent bond giving good binding affinity. However this research has mainly focused on the serine-β-lactamases, in particular the Class C β-lactamase, AmpC, where a variety of boronic acids have been tested for their biological activity.[137] Compound **5.6** (**Figure 48**), identified by Anacor, has a K_i of 35 nM against AmpC. Compound **5.4** (**Figure 46**), a glycylboronic acid bearing a side chain of ceftazidime, has proven to be a competitive reversible inhibitor of CTX-M β-lactamases giving a K_i's of 15 and 4 nM against CTX-M-9 and CTX-M-16 respectively.
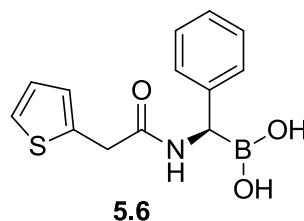
Figure 48: Anacor AmpC inhibitor (**5.6**).

In 2000, Burns *et al.* patented a large number of boronic acid based inhibitors which act on the β-lactamase enzymes.[138] Each of the compounds was screened against SHV-5, KPC-2 and CTX-M-15 (Class A), P99 AmpC (Class C), VIM-2 (Class B) and OXA-23 (Class D) in enzymatic assays.

Almost all of the inhibitors show low nano-molar IC_{50} values against the CTX-M-15, P99 AmpC and KPC-2 enzymes. There was a significant increase in the IC_{50} values against VIM-2, SHV-5 and OXA-23 enzymes with almost no activity seen against the OXA-23 enzymes. The results for VIM-2 range from 22 nM through to no inhibition being seen at all. The low nano-molar IC_{50} values raised the question of whether, with further modification, these compounds could become potent pan MBL enzyme inhibitors. The compounds were identified as good potential inhibitors and therefore a synthesis was required in order that the compounds could be screened against the panel of clinically relevant MBLs. The synthetic route which was used to make the boronic acid based inhibitors in the patent is shown in **Scheme 10**.

The synthesis begins with a tert-butyl protection of acid **5.7** followed by reaction of the boronic acid with (+)-pinanediol to form **5.8**. A homologation was then conducted on **5.8** to produce **5.9**. Molecule **5.9** was then converted to compound **5.11** *via* intermediate **5.10** by conducting a homologation before introducing the amine using lithium hexamethyldisilane. The TMS groups were then removed before an amide coupling was conducted yielding **5.11**. Finally a global deprotection was conducted using BCl_3 to yield boronic acid inhibitor **5.12**.
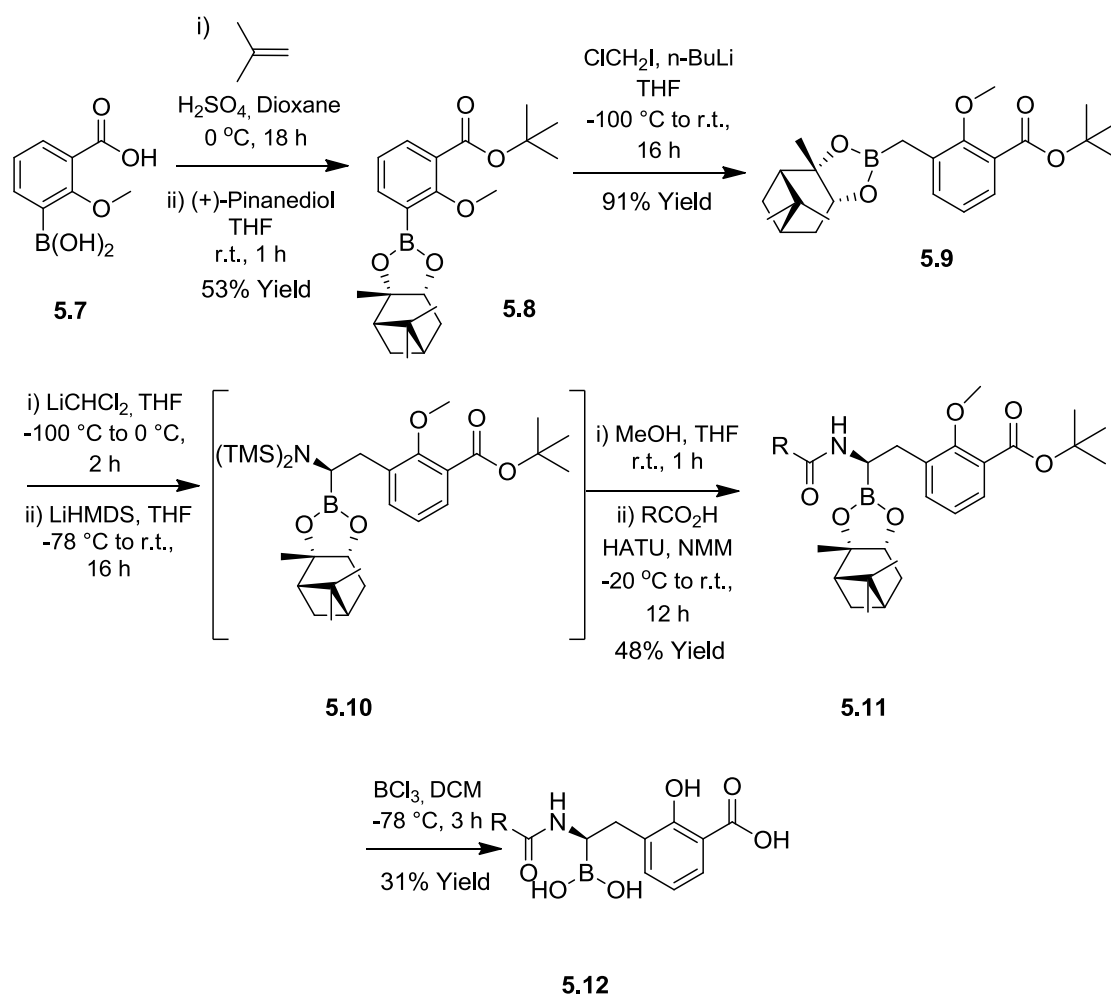
Scheme 10: The synthetic route to produce the boronic acid-based inhibitors[138]

The patent does not confirm how the compounds bind to the VIM-2 enzyme and there has been no co-crystal structures published in the literature of this class of compound binding to the MBLs.

5.3 Targeting the MBLs with boron-containing inhibitors

Initial biological screening data against VIM-2, from the patent by Burns *et al,* suggests that this boron containing inhibitor class could be strongly active against the MBLs as well as the serine-β-lactamases. The aim was to identify, using a number of *in silico* techniques, a small sample of five strongly binding boronic acid-containing inhibitors which would be synthesised and screened against the panel of clinically relevant MBLs. Any of the boronic acid containing compounds which show good activity against the MBLs will be co-crystallised in an MBL in order to investigate how the boronic acid based inhibitors bind to the MBL enzymes.

The five boronic acid-based inhibitors were selected using the following reasoning: The first compound (**5.13**) was selected because it gave the best biological result against the VIM-2 MBL with an IC_{50} of 22 nM in the patent (see Section 5.3.1). The next two compounds (**5.14** and **5.15**) were selected as the best predicted binding compounds from docking the 45 compounds stated in the patent into the active site of NDM-1 (see Section 5.3.2). The final two compounds (**5.17** and **5.18**) were identified using *de novo* design, building up from a scaled down portion of the boronic acid with the aim of increasing the binding affinity of the inhibitor to the MBL compared to inhibitor compound **5.13** (see Section 5.3.3).

5.3.1 VIM-2 active compound

Compound (**5.13, Figure 49**) was selected because it reported the best biological result against the VIM-2 MBL with an IC_{50} of 22 nM in the patent. It is expected that by having good biological activity against VIM-2 there will also be good biological activity against the other clinically relevant MBLs.

5.13
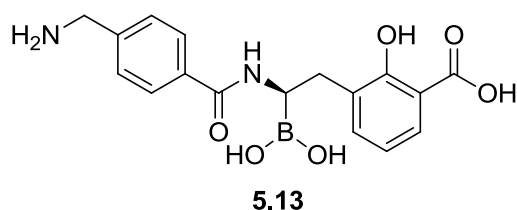
Figure 49: Structure of compound **5.13** with IC_{50} of 22 nM against VIM-2

Molecular docking of compound **5.13** was conducted as part of the docking of the 45 patented compounds, as described in Section 5.3.2. Compound **5.13** is predicted to bind to both zinc atoms and a number of residues within VIM-2 (**Figure 50**). The free carboxylic acid is predicted to bind to the side chain amine of Lys-211, main chain amide of Asn-220 and Zn2. The hydroxyl group binds to Zn1 along with the boronic acid group which also has interactions with the main chain amides of Gln-123 and Asp-124. The docking poses do not show the free amine making any contacts with the enzyme. It is however expected that the free amine would bind to the side chain carboxylic acid of Glu-152 which is located in close proximity to the free amine.
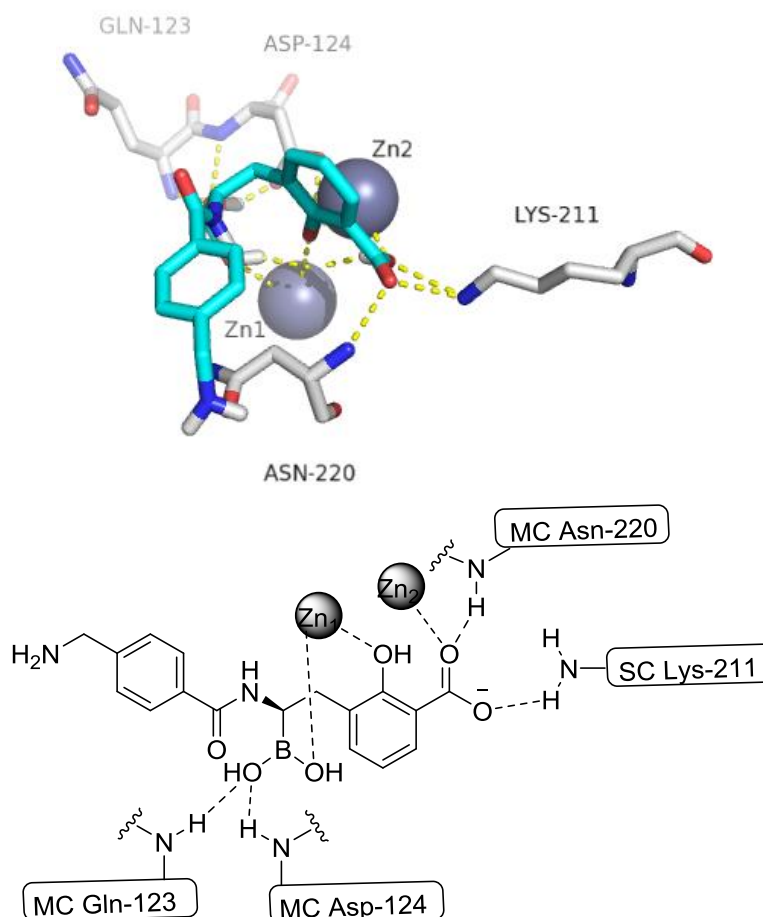
Figure 50: Docking of compound **5.13** into NDM1 showing key binding contacts: a) 3D spatial representation, b) 2D representation (PDB ID: 3Q6X).

5.3.2 Docking of patented compounds

In silico docking of the 45 compounds described in the patent, into the NDM-1 enzyme (PDB ID: 3Q6X), was conducted to identify the two compounds which gave the best predicted AutoDock[88, 100] and SPROUT[125] binding scores. The compounds would be biologically screened after synthesis against the panel of clinically relevant MBLs to see if these compounds exhibit strong inhibitory effects. The procedure for molecular docking was carried out as described below.

The following protocol was used:

1. Each of the 45 boronic acid based inhibitors were constructed in maestro.[139] The resulting structures were then fully energy minimised using the multiple minimisation tool (MM).

2. Each compound was then docked using the AutoDock program and docked into the di-zinc containing active site of the crystal structure of NDM-1 (PDB ID: 3Q6X[38]).

3. The resulting docking 'poses' were scored, both within AutoDock and also using the SPROUT scoring function for comparison.

The top two results, compound **5.14** and **5.15** (**Figure 51**), were selected based upon consideration of the best AutoDock score, AutoDock pose clustering and SPROUT score respectively.

5.14   **5.15**
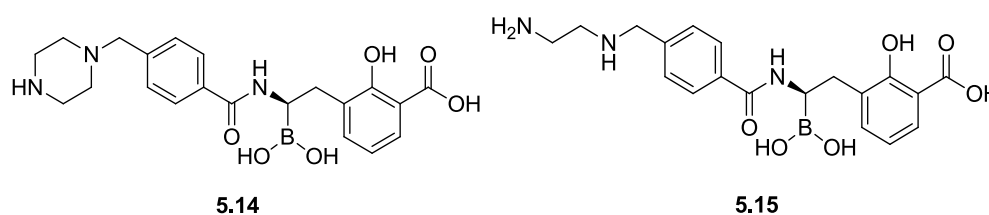
Figure 51: Structure of best scoring compounds (**5.14** and **5.15**) identified from docking to NDM-1 in AutoDock

Compound **5.14** contains a piperazine unit in place of the free amine of compound **5.13**. Compound **5.14** is predicted to bind in a slightly different position to **5.13** with the boronic acid now being the key binding portion of the molecule as it binds to main chain amide of Asn-220, side chain amine of Lys-211 and Zn2 (**Figure 52**). The hydroxyl group can be seen to bind to main chain amide of Asn-220. The carbonyl of the amide bond is placed between the two zinc atoms binding to both. The piperazine binds to the side chain carboxylic acid of the Glu-152 residue which the free amine of **5.13** did not bind to in the predicted docking pose.

Compound **5.15** is predicted to bind in almost identical position to compound **5.14** (**Figure 53**). The amine-containing alkyl chain is positioned down deeper into the active site of the NDM-1 enzyme than the piperazine amine of compound **5.14** and therefore, as well as picking up the side chain carboxylic acid of the Glu-152 residue, there is also an interaction with the side chain carboxylic acid of the Asp-223 residue. From the patent, the IC_{50} against VIM-2 is 47 nM for compound **5.15** and 510 nM for compound **5.14** which could show that making this extra interaction is key to good potency.
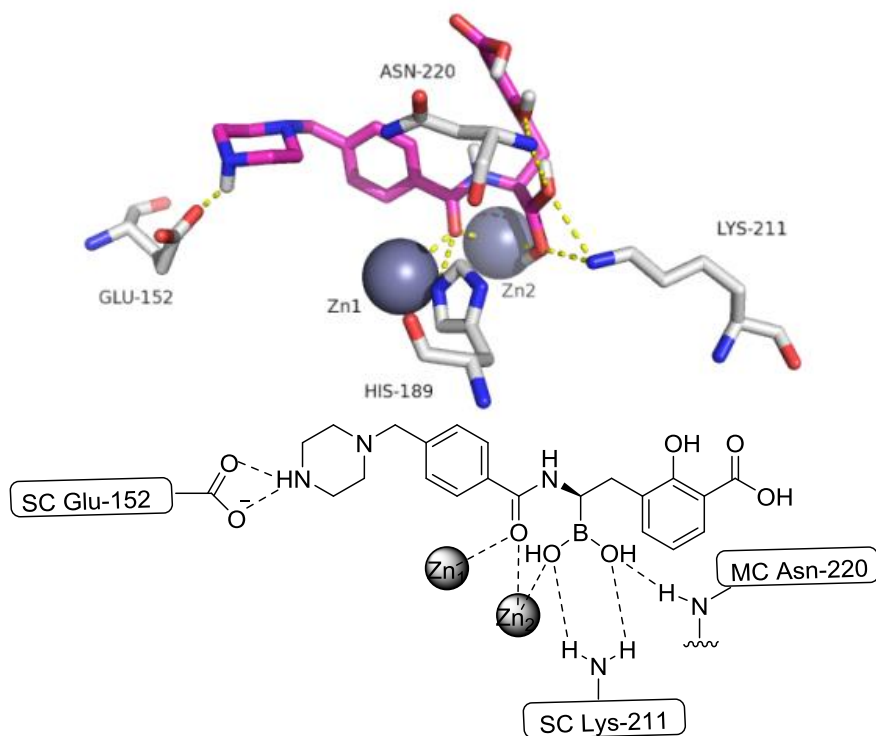
Figure 52: Docking of compound **5.14** into NDM1 showing key binding contacts: a) 3D spatial representation, b) 2D representation (PDB ID: 3Q6X).
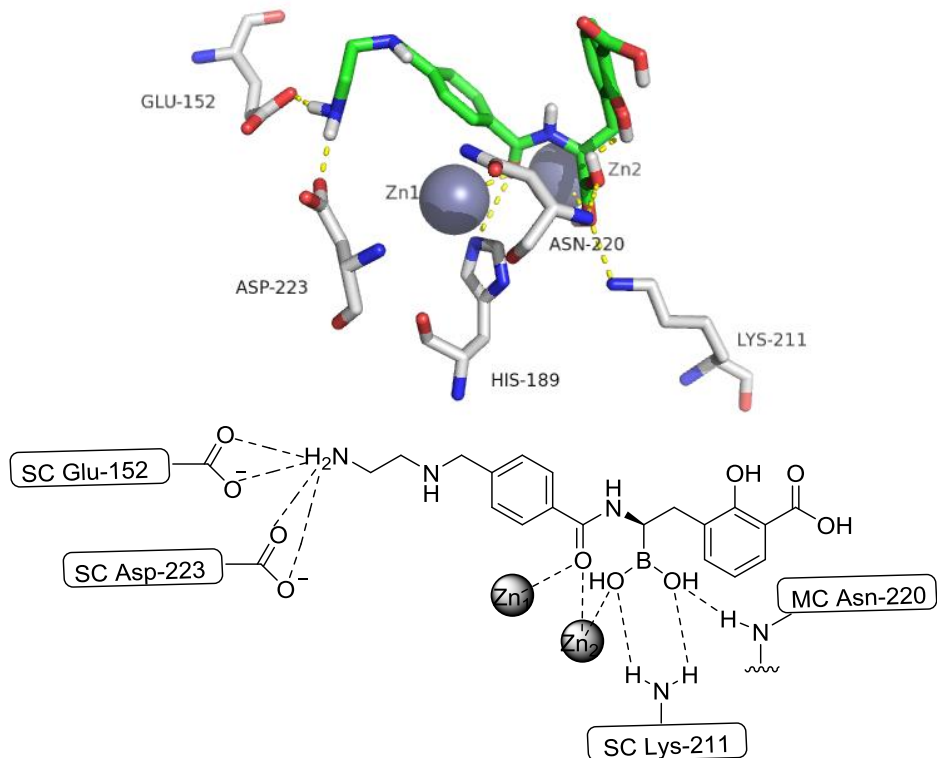

Figure 53: Docking of compound **5.15** into NDM1 showing key binding contacts: a) 3D spatial representation, b) 2D representation (PDB ID: 3Q6X).

5.4.3 *De novo* design of novel compounds.

Two compounds were to be made with the use of *de novo* design to attempt to increase the potency of the boron-containing inhibitors against the MBLs. A scaled back fragment of compound **5.13** disconnected at the amide bond leaving an amine was used as the starting point for *de novo* design (**5.16**, **Figure 54**). This was selected as the fragment **5.16** was a common motif seen in all of the boronic acid based inhibitors from the patent. The aim was to grow out from this free amine using the SPROUT *de novo* design program in an attempt to pick up further interactions within the binding site therefore increasing the potency of the inhibitor (see Section 7.2 for explanation of SPROUT). Once designed the molecules would be synthesised and screened against the panel of clinically relevant MBLs.
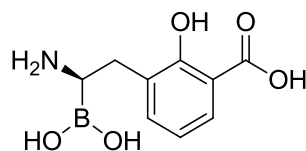
5.16

Figure 54: Scaled back starting point for de novo design (**5.16**)

A number of SPROUT runs were conducted growing from the free amine of fragment **5.16** out into the active site of NDM-1. A number of runs were conducted attempting to bind fragment **5.16** to a number of residues in the active site including Glu-152 where previous interactions have been see in the docking of patented compounds **5.14** and **5.15**. The SPROUT runs identified a selection of 30 potential inhibitor compounds which were re-docked into the active site of NDM-1 (PDB ID: 3Q6X) using AutoDock to increase confidence in the predicted binding pose. The results of the AutoDock dockings were visually inspected to identify the top two scoring compounds. The two compounds predicted to bind the best, **5.17** and **5.18**, were selected for synthesis (**Figure 55**).
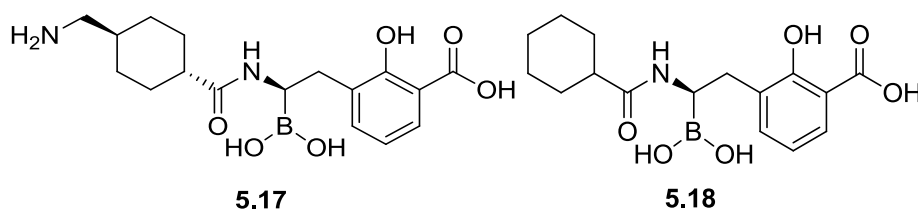
5.17   **5.18**

Figure 55: *De novo* designed boronic acid based inhibitors (**5.17** and **5.18**)

Compound **5.17** was predicted to bind mainly through the boronic acid which is predicted to bind to main chain amide of Asn-220, the side chain amine of Lys-211 and Zn2 (**Figure 56**). There are further binding interactions predicted from the amide nitrogen to the carboxylic acid side chain of Asp-124 and the amide carboxylate to the side chain amide of Asn-220. Finally the free amine is predicted to bind the side chain carboxylic acid of the Glu-152 residue as seen in previous examples.
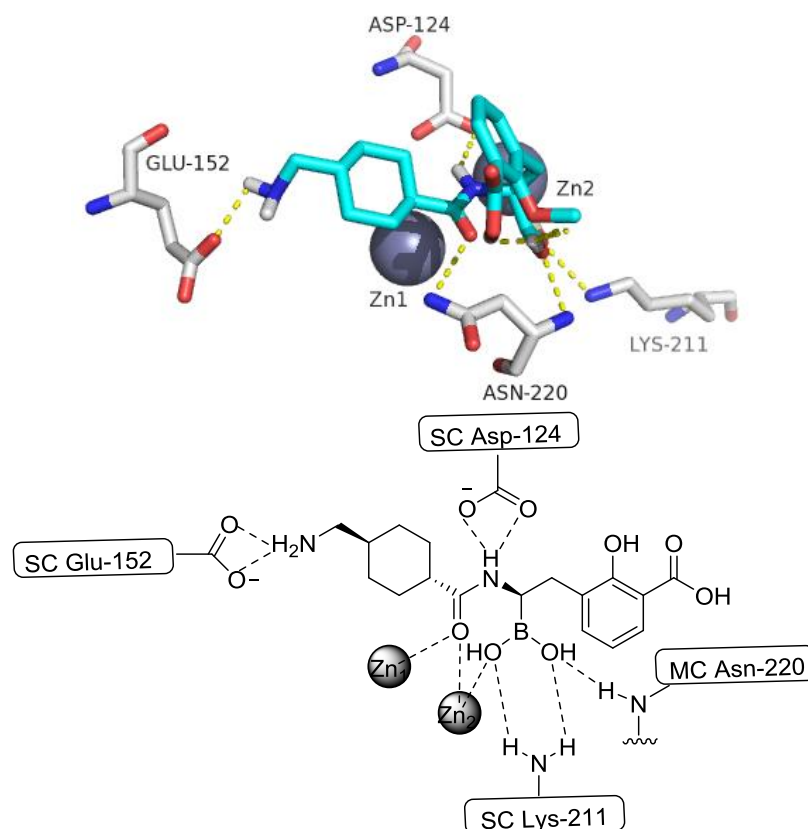

Figure 56: Docking of SPROUT identified compound **5.17** into NDM1 showing key binding contacts: a) 3D spatial representation, b) 2D representation (PDB ID: 3Q6X).

Compound **5.18** has a rather different predicted binding pose when compared to the other boronic acid compounds. The boronic acid is now expected to bind to side chain carboxylic acid of Asp-124, main chain amide of Asp-124 and main chain amide of Gln-123. The carbonyl of the amide is predicted to bind to the side chain amide of Asn-220 (**Figure 57**). The carboxylic acid is predicted to bind to both the side chain amine of Lys-211 and the main chain amide of Asn-220. The final predicted contact is from the phenol to the Zn1 atom. The cyclohexyl group lies up against the hydrophobic wall of the NDM-1 active site.
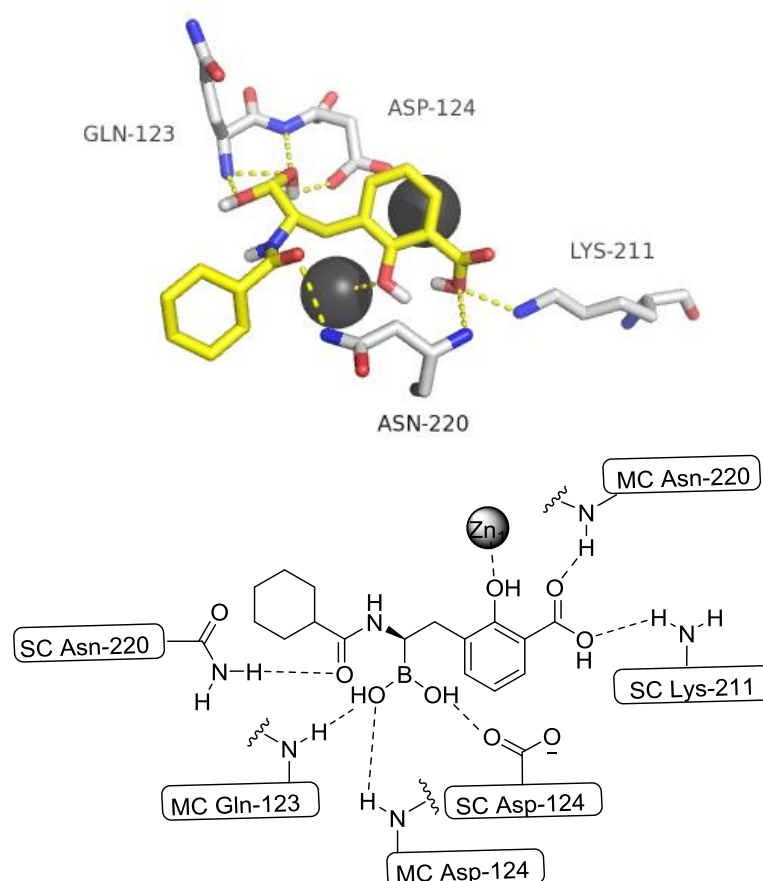
Figure 57: Docking of SPROUT identified compound **5.18** into NDM1 showing key binding contacts: a) 3D spatial representation, b) 2D representation (PDB ID: 3Q6X).

5.5 Synthetic route development

In order to produce the compounds required for biological evaluation and crystallisation studies, some synthetic route development work was required to make the reasonable quantities of the desired compounds.

The first change that was made to the route described in the patent by Burns *et al* was the choice of starting material. Rather than using 3-(dihydroxyboranyl)-2-methoxybenzoic acid (**5.7**) which costs >£500 per g (Combi-blocks) a switch was made to 3-bromo-2-methoxy benzoic acid (**5.19**) which costs ~£75 per g (Sigma-Aldrich). This change in starting material changed the first few steps of the synthesis as the boronic acid was now needed to be introduced to the starting molecule. Although there is an increase in the number of synthetic steps the developed route is preferred as it uses cheaper starting materials. Many of the steps show slightly improved

yields over the patent route. The complete modified synthetic route is shown in **Scheme 11**.
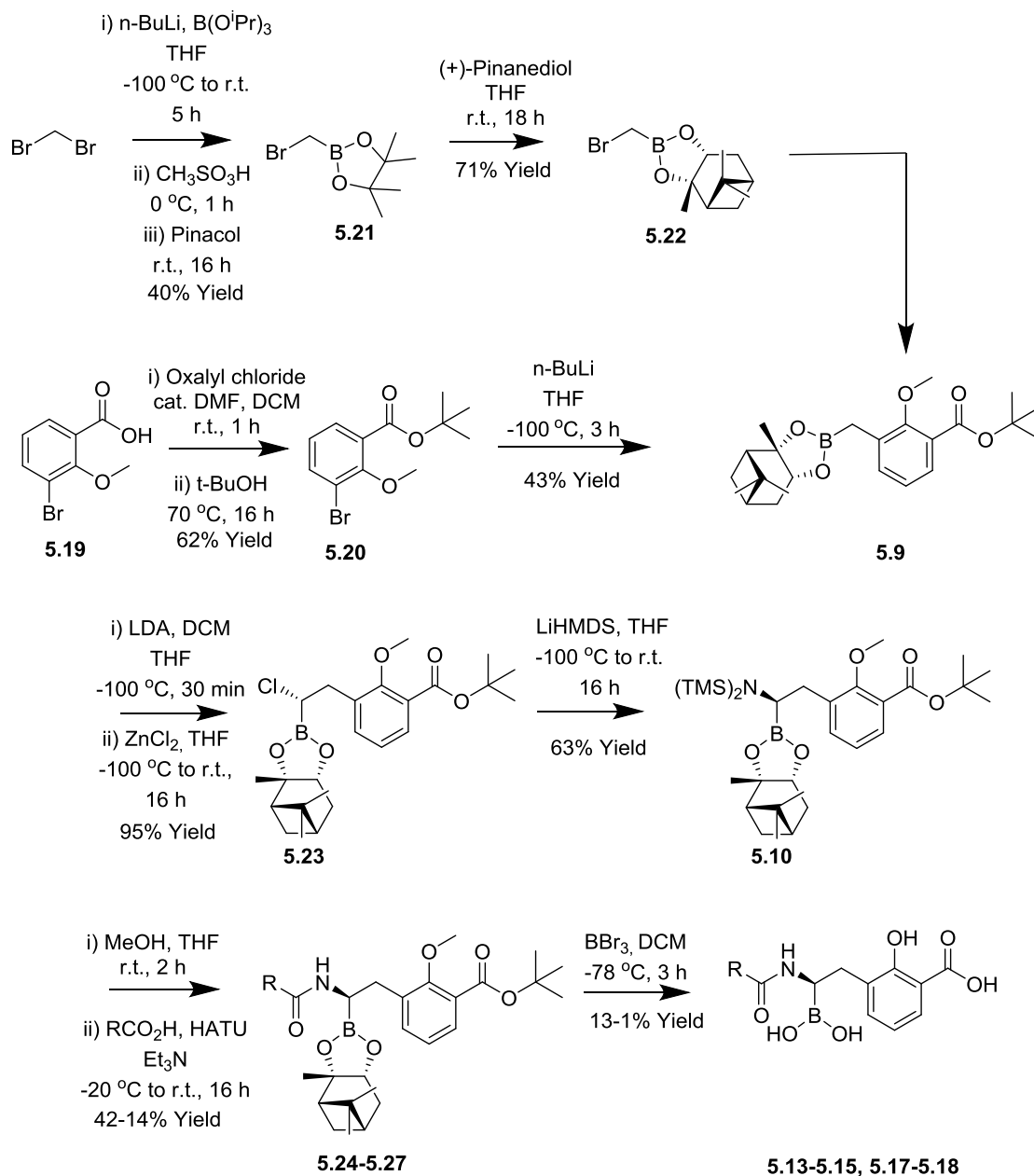
Scheme 11: Synthetic route to boronic acid based inhibitors

The first reaction, protecting the acid (**5.19**) as a tert-butyl ester (**5.20**) was initially conducted as described in the patent (**Scheme 12**). This reaction provided low conversion to yield ester **5.20** (12%). In order avoid the use of 2-methylpropene gas and to use milder conditions, the reaction was repeated with the use of oxalyl chloride to form the acid chloride and then reaction with t-BuOH (**Scheme 12**). The reaction gave an improved yield of

ester (62%). This route was therefore chosen as the preferred route to be used.

a) H$_2$SO$_4$, Dioxane
0 °C, 18 h
12 % Yield

b) i) Oxalyl Chloride
cat. DMF, DCM
r.t., 1 h
ii) t-BuOH
70 °C, 16 h
62% Yield

5.19

5.20
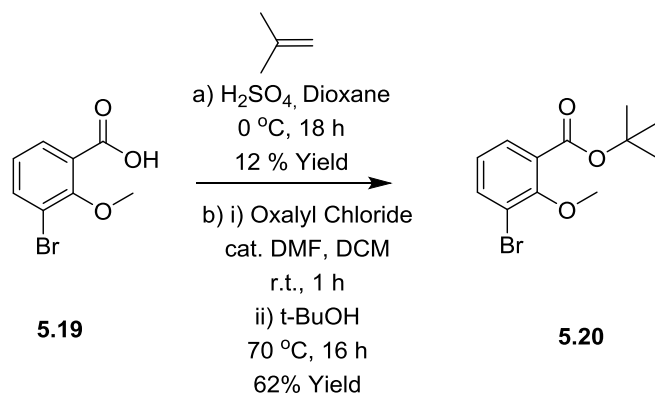
Scheme 12: Formation of tert-butyl ester (**5.20**)

The second reaction was a one pot conversion of dibromomethane to the pinacol boronate (**5.21**) (**Scheme 13**).[140] This was conducted *via* the addition of *n*-BuLi to a mixture of dibromomethane and triisopropylborate to form the triisopropyl borate intermediate. This was then hydrolysed with methane sulfonic acid to form the boronic acid and trans-esterified with pinacol to form **5.21**. Compound **5.21** is isolated rather than proceeding straight to **5.22** as **5.21** is easier to purify using distillation to remove the salts and reaction by-products. The product was formed in moderate yield (40%). The second stage was a transesterification of **5.21** with (+)-pinanediol which was conducted over 18 h to give **5.22** in good yield (71%).[141]

i) n-BuLi, B(O^{i}Pr)$_3$
THF
-100 °C to r.t.
5 h

ii) CH$_3$SO$_3$H
0 °C, 1 h
iii) pinacol
r.t., 16 h
40% Yield

(+)-pinanediol
THF
r.t., 18 h
71% Yield

5.21

5.22
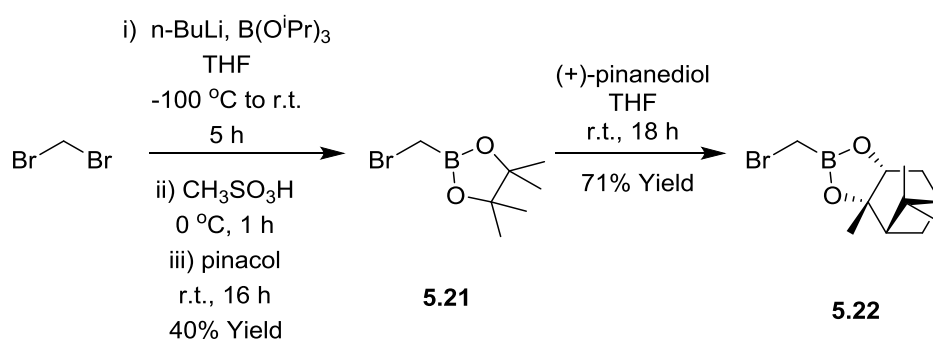
Scheme 13: Formation of pinaneboron species (**5.22**)

The joining of **5.20** and **5.22** to form coupled product **5.23** was conducted by lithium halogen exchange on **5.20** before the addition of the borane species **5.22.** Presumably, the reaction proceeds *via* a Matteson type homologation (**Scheme 14**).[142] The lithiated **5.20** attaches to **5.22** to form a borate complex

which rearranges on warming to give the product **5.9**. Typically, the reaction gives low to moderate yields (~40-50%).
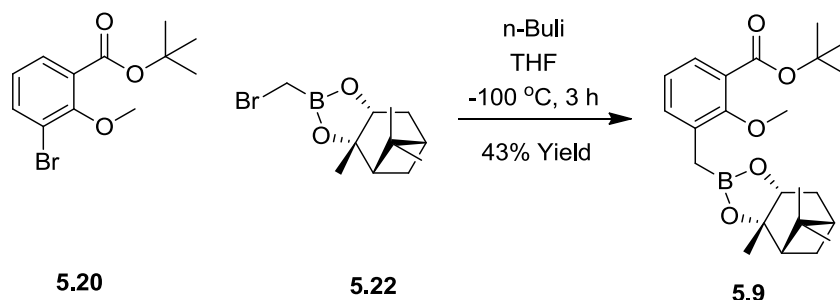
Scheme 14: Mattesen type homologation of **5.20** and **5.22** to form compound **5.9**

The next step was another Matteson type homologation of **5.9** to **5.23**.[142] The reaction was initially conducted as described in the patent using chloroiodomethane but this afforded low yield (20%). The reaction was then conducted using the conditions described by Inglis *et al.* at Oxford using freshly produced LDA, DCM and ZnCl$_2$.[141] The ZnCl$_2$ catalyses the rearrangement giving improved diastereoselection. The altered conditions gave an improved yield of product (95%, **Scheme 15**). The introduction of the TMS amine by a S$_N$2 reaction *via* the use of LiHMDS was conducted as described in the patent to yield amine **5.10** in moderate yield (63%).
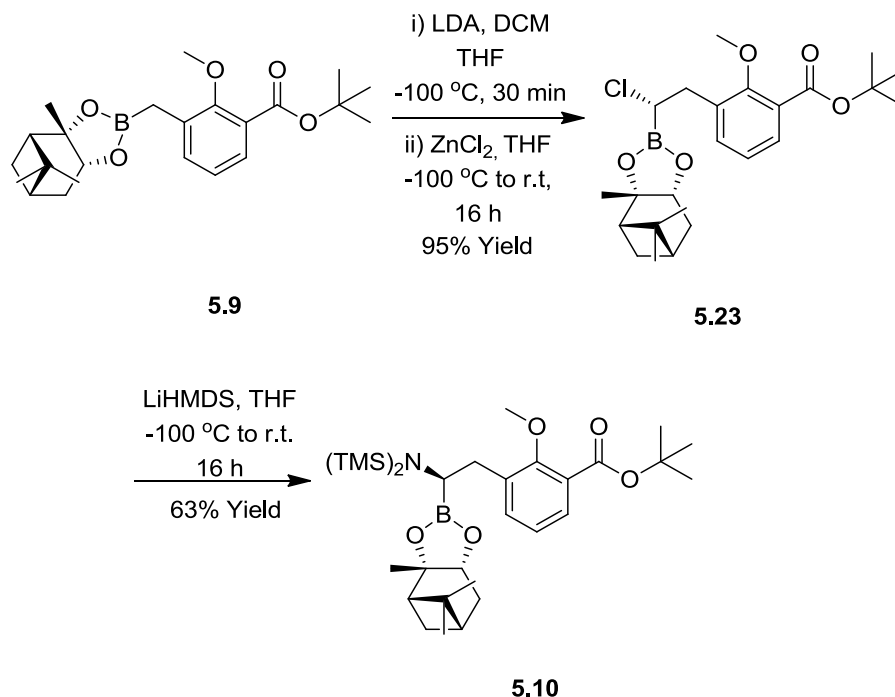
Scheme 15: Homologation and amine introduction to give **5.10**

Removal of the TMS groups from **5.10** proved difficult to monitor so was assumed to proceed with quantitative conversion to the free amine. The amide coupling with different carboxylic acids, to give compounds **5.24-5.27** respectively, was conducted using HATU as the coupling agent. The amide coupling reactions proceeded in low yield (40-14%, **Scheme 16**). A number of different coupling agents were tested including EDC/HOBt, T3P and the use of an acid chloride. However, all of these methods gave significantly lower yields than the HATU conditions.
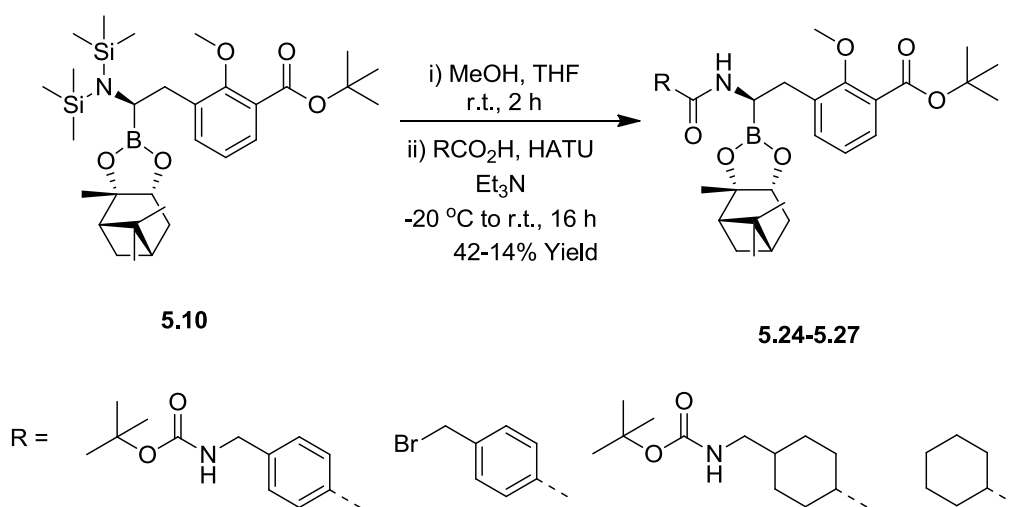
Scheme 16: Amine deprotection and amide coupling

In order to produce compounds **5.14** and **5.15** an extra step was required in the synthetic route. An S_N2 reaction was carried out on the bromine of compound **5.25** with 1-Boc piperazine and N-Boc-ethylenediamine respectively in the presence of base (**Scheme 17**) to give compounds **5.28** and **5.29** respectively in low yield (18-17%)
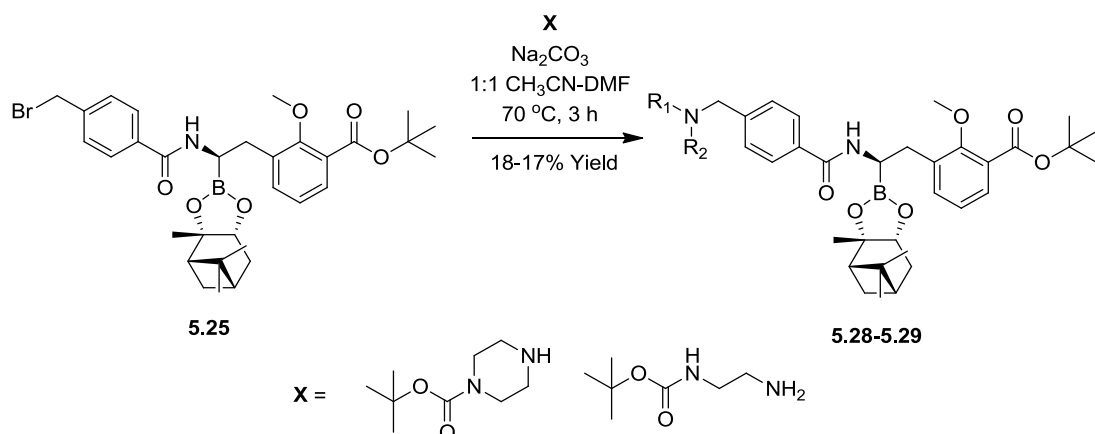
Scheme 17: S_N2 reaction of compound **5.25** with amine **X** to form compounds **5.28** and **5.29**

The global deprotection of the protecting groups from compounds **5.24, 5.26-5.29** to give compounds **5.13-5.15, 5.17** and **5.18** was attempted as described in the patent with the exception of substituting BCl_3 with BBr_3. Additionally an alternative deprotection method used in a second patent by Burns *et al.* using 3N HCl was tested. However, in this case no deprotected product was seen using LCMS.[143] The deprotected inhibitors were purified using reverse phase C_{18} biotage column chromatography in low yield (13-1%). (**Scheme 18**).
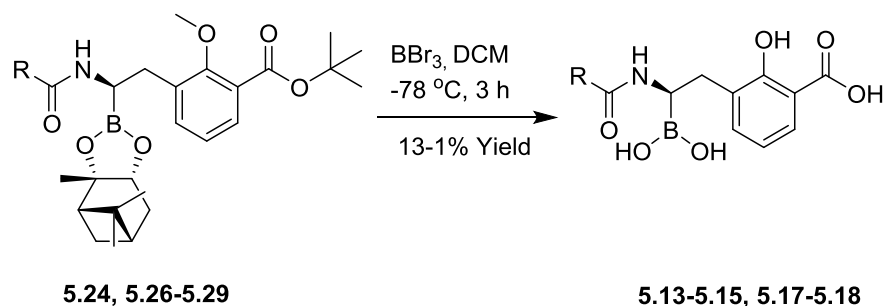
Scheme 18: Global deprotection of compounds **5.24, 5.26-5.29**
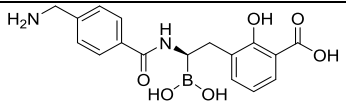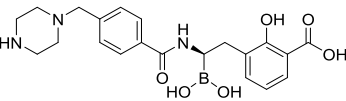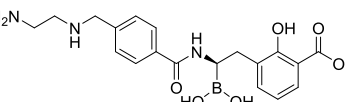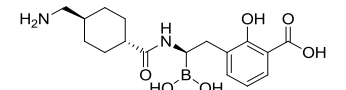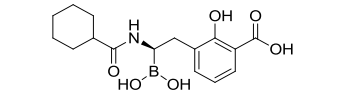
Compounds **5.13-5.15**, **5.17-5.18** were formed in low quantities as the HCl salt. Due to the low quantities produced a satisfactory ^{13}C NMR spectrum was unable to be obtained for characterisation.

5.6 Biological evaluation

Biological evaluation of the identified potential inhibitors of NDM-1 was conducted by Dr Jürgen Brem at the University of Oxford using the nitrocefin based assay described in Appendix A1.1.

The results of the biological evaluation against NDM-1 are reported in **Table 8**.

Table 8: Biological evaluation of boronic acid based compounds against VIM-2, IMP-1 and NDM-1

Compound Number	Structure	IC_{50} VIM-2 (µM)	IC_{50} IMP-1 (µM)	IC_{50} NDM-1 (µM)
5.13		0.003 ± 0.058	10.0 ± 0.09	0.029 ± 0.020
5.14		0.014 ± 0.045	16.3 ± 0.13	0.040 ± 0.021
5.15		0.002 ± 0.114	26.0 ± 0.13	0.004 ± 0.052
5.17		0.011 ± 0.029	32.0 ± 0.11	0.687 ± 0.068
5.18		0.051 ± 0.035	27.6 ± 0.12	2.04 ± 0.028

Generally all of the boronic acid based inhibitors **5.13-5.15**, **5.17-5.18** exhibited < 50 µM inhibition against the MBL enzymes. Inhibitor **5.15** was the most potent inhibitor against VIM-2 and NDM-1 giving IC_{50}'s of 2 nM and 4 nM respectively.

The five boronic acid-containing inhibitors (**5.13-5.15**, **5.17-5.18**) have poorer IC_{50}'s against IMP-1 than against the other MBL enzymes. The IC_{50}'s for IMP-1 are in the micro-molar range as opposed to IC_{50}'s in the nano-molar range observed for the other enzymes. This is rationalised by the much more enclosed active site of the IMP-1 enzyme when compared to the active sites of VIM-2 and NDM-1 (see Section 2.4.2.1). In comparison to IMP-1 the IC_{50}'s of each inhibitor against NDM-1 and VIM-2 are in a similar range to each other.

A trend is visible within the IMP-1 IC_{50} data showing that the shorter in length the inhibitor molecule the better the inhibition the enzyme. The same trend is not observed in either the VIM-2 or NDM-1 IC_{50} results.

The cyclohexyl containing compound **5.18,** which does not have the free amine is predicted to bind to Glu-152 in NDM-1 as seen in compounds **5.13-5.15** and **5.17**, has weaker IC_{50}'s against all of the MBL enzymes. This shows that the amine in this position has a positive effect on the binding affinity of the boronic acid-containing inhibitors.

Poorer IC_{50} values are observed for the SPROUT derived compounds **5.17** and **5.18** which contain a cyclohexyl ring in the place of an aryl ring next to the amide bond. This implies either that a positive π-stacking interaction is being formed between the MBL enzyme side wall and the aromatic ring in compounds **5.13-5.15,** there is not enough space in the active site to accommodate the cyclohexyl ring, or the direction of the amine emanating from the cyclohexyl ring compared to coming off of an aryl ring has a large effect on the binding affinity. This effect is more prominent in NDM-1 than the other enzymes.

5.7 Conclusions

Boron has been shown to be a useful atom which can be used in medicinal chemistry and is slowly beginning to be incorporated into a number of therapeutics including inhibitors of the β-lactamases. Traditionally boron was avoided due to the perception it was toxic but now many of these misconceptions are being dispelled leading to boron being viewed as another useful atom to use in medicinal chemistry.

Using the patent by Burns *et al.* as a starting point five compounds were identified for synthesis by the use of vHTS and *de novo* design. A number of significant changes were made to the synthetic route in order to both reduce the overall cost of the synthesis and to improve the yields on a number of steps.

The compounds were biologically screened against the enzymes showing pan inhibition across the panel of MBL enzymes. IMP-1 gave significantly poorer IC_{50}'s for the inhibitors with low micro-molar results for each inhibitor

compared to nano-molar results for each inhibitor against the VIM-2 and NDM-1. Inhibitor **5.15** gave IC_{50}'s of 2 nM, 26 µM and 4 nM against VIM-2, IMP-1 and NDM-1 respectively.

The results backed up the predictions with each of the five inhibitors being active against the panel of MBL enzymes. The *de novo* designed inhibitors **5.17** and **5.18** did not provide any extra binding affinity compared to the compound identified from the patent (**5.13**) and the vHTS identified compounds (**5.14**-**5.15**). It is predicted this is due to the cyclohexyl portion of the molecule and **5.18** having no free amine which could bind to the Gln-152 residue in NDM-1.

A crystal structure of compound **5.13** in VIM-2 is currently being solved by Dr Michael MacDonough at the University of Oxford who will be looking to see how the boronic acid binds to the enzyme. From this data more active inhibitors can be designed and synthesised. The availability of a crystal structure will greatly increase the accuracy of the structure based drug design techniques.

Chapter 6
Cysteine-containing peptides

Inhibition of enzymes by peptides and the evolution of peptide ligands to small molecule mimetics is a common approach in drug discovery, with several notable successes. Some well-known examples where peptides or peptide mimetics have been used in drug discovery include Captopril[144] (ACE inhibitor), Epifibatide[145] (anticoagulant) and Ziconotide[146] (N-type Ca channel blocker).

Peptides would therefore seem to be ideal drug leads with a large number of advantages to the use of peptides as drugs including: high potency, high selectivity, broad range of targets, potentially lower toxicity than small molecules, low accumulation in tissue and high chemical and biological diversity. However there are also a large number of disadvantages to peptides including: poor metabolic stability due to protease cleavage of the peptide backbone, poor membrane permeability, poor oral bioavailability, high production cost, rapid clearance and sometimes poor solubility. A large number of peptide based drugs fail in clinical trials before making it to the clinic.[147]

6.1 Methods of identifying the active peptides

The starting point for peptide and peptide mimetic research is the identification of a peptide that is active in the relevant assay. There are a number of techniques which could be used to probe peptide binding to the enzyme target. These included phage display, peptide microarrays and HTS.

Phage display is a technique used for the study of protein–protein, protein–peptide, and protein–DNA interactions. The technique uses bacteriophages (viruses that infect bacteria) to connect proteins with the genetic information that encodes them.[148] In this method, a gene which encodes the protein (or in this case peptide) of interest is inserted into a phage coat protein gene, causing the phage to "display" the peptide on its outside while containing the gene for the peptide on its inside, resulting in a connection between genotype and phenotype.[149] The displaying phages are then screened

against the enzyme, in order to detect interactions between the displayed peptide and the enzyme. In this way, large libraries of proteins can be screened and amplified in a process called *in vitro* selection, which is analogous to natural selection. **Figure 58** shows the sequence of identifying a hit from Phage display screening.[150]
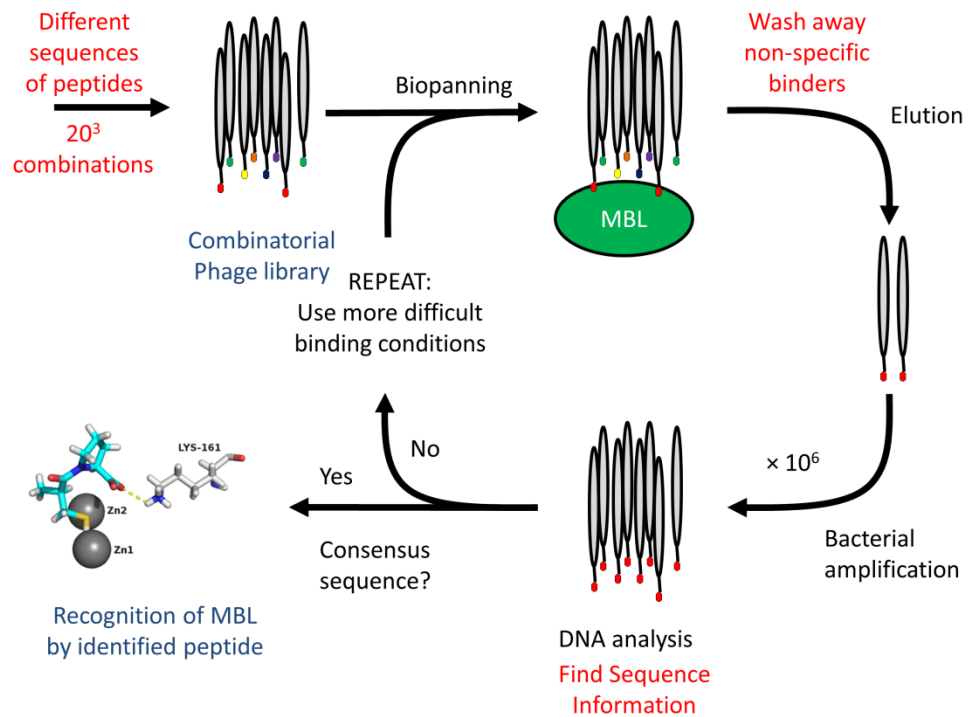
Figure 58: Phage display screening sequence based upon identification of trimer peptides against a MBL, adapted from[150]

A second technique is the peptide microarray (also referred to as peptide spot array) which is a collection of peptides displayed on a solid surface of silica or glass, which is often termed a 'peptide chip'.[151] A peptide microarray is assembled directly on the surface of the peptide chip by *in situ* synthesis. Synthesis on a chip allows the parallel synthesis of tens of thousands of peptides providing larger peptide libraries with relatively low synthesis costs.[152] Peptide chips are then used by scientists in biochemistry to study binding properties, functionality and kinetics of protein-protein interactions. Peptide microarrays are often used to profile an enzyme to find key residues for binding. **Figure 59** shows an example row on a peptide microarray for trimer peptides.
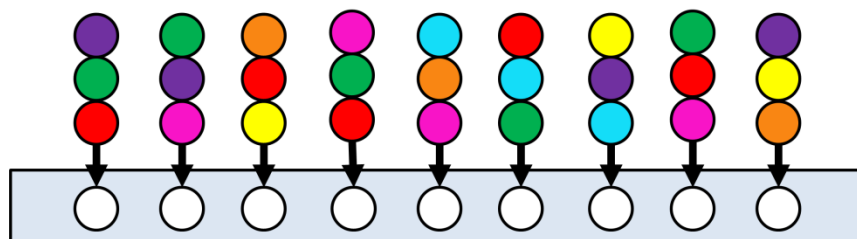
Figure 59: Simplified representation of a peptide microarray for the identification of trimer peptides which would bind to a MBL. Each colour represents a different amino acid.

High Throughput Screening (HTS) has become an important way of screening peptides and proteins against a biological target. HTS significantly reduces the cost and time required to identify active molecules from a large library of compounds. In the case of peptides a large library can be screened in a short amount of time against the target. HTS does, however, have some disadvantages when compared to the other techniques. These include storage of a large number of compounds as well as the cost of the run. HTS is, however, used by a number of researchers against a wide range of biological targets with a large number of compounds.

As HTS is a commonly used process to identify new peptides, there is no reason why this process could not be switched to vHTS for all the advantages set out in Section 4.1. Computational libraries of peptides could be constructed and docked into crystal structures in significantly smaller timescales with greatly reduced cost over traditional HTS. The computationally generated peptide libraries could be made into more bespoke libraries by applying filters such as ensuring one residue type such as Cys is present in all the peptides (see Section 6.3). This chapter of work describes the process of converting the standard HTS protocol into a vHTS protocol with its application to the NDM-1 enzyme.

6.2 Peptides as inhibitors of MBLs

Captopril, an angiotensin-converting-enzyme inhibitor (ACE inhibitor), is a known peptide mimic of a Cys-Pro di-peptide.[144] ACE indirectly increases blood pressure by causing blood vessels to constrict. For this reason, drugs known as ACE inhibitors (such as captopril) are used to lower blood pressure.[153] ACE is a zinc-containing enzyme which makes it interesting to

potentially screen its inhibitors against the MBLs. D-captopril was screened against IMP-1 and NDM-1 and has been shown to exhibit moderate inhibition of NDM-1 with an IC_{50} of 36 μM and IMP-1 with an IC_{50} of 12 μM.

A crystal structure of D-captopril co-crystalised in IMP-1 was obtained by Brem *et al.*[154] at the University of Oxford. The key feature in the binding of captopril is the sulfur displacing the bridging water between the zinc atoms and forming a strong zinc-sulfur bond to both zincs (**Figure 60**). A secondary interaction is seen from the carboxylic acid group of the captopril to the Lys-161 residue.

From this knowledge it was decided to include cysteine in each designed putative inhibitor peptide, due to the potential to form a strong zinc-sulfur bond similar to that seen in captopril.
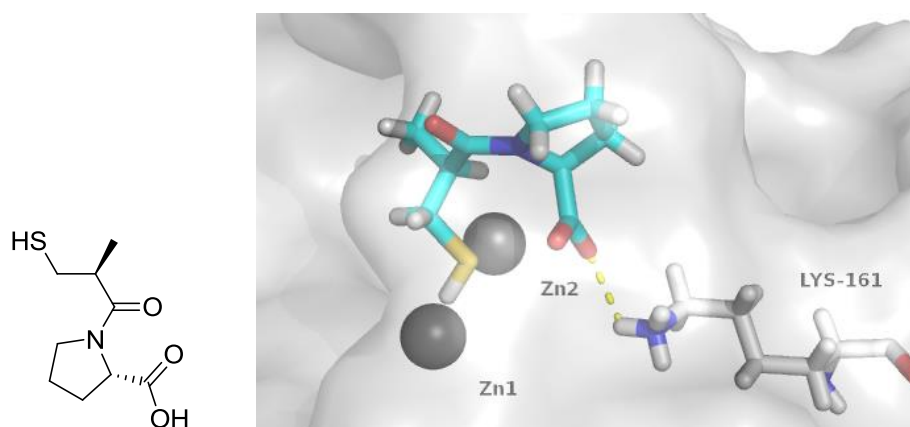
Figure 60: Captopril co-crystallised in IMP-1 Brem *et al.* Unpublished data[154]

Page *et al.* at the University of Huddersfield, screened a small number of substituted thiols and cysteinyl dipeptides as potential inhibitors of *Bacillus cereus* zinc β-lactamase. The simplest thiol, N(2-mercaptoethyl)-phenylacetamide, was found to be a competitive inhibitor of the enzyme. Competitive inhibition was also seen for all the other compounds tested. The thiol group was observed to be necessary for inhibition as removal of the group led to a significant decrease in potency. This work confirmed the key nature of the zinc-sulfur interaction and that cysteine-containing dipeptides have a moderate binding affinity to MBL enzymes.

In the current study the length of the peptide will be investigated to see if a di-, tri- or tetramer peptide length gives the best binding to the target. This work focuses on targeting the peptide for the NDM-1 system so slightly weaker binding would be expected due to the larger active site than the *Bacillus cereus* zinc β-lactamase enzyme investigated by Page *et al.* The full range of di-, tri- and tetramer cysteine containing peptides will be docked to identify the best binding compounds rather than only docking a small selection of each length of peptide.

6.3 Peptide library generation

A computational library containing all of the possible molecular structures of the L-amino acid-containing trimer peptides was required. This study was initially performed on the L-amino acid enantiomers because this absolute configuration represents the majority of peptides *in vivo*. The required conditions were that there was one cysteine residue in the trimer peptide and the other two residues could consist of any of the other 19 common amino acids. Multiple cysteine residues were not allowed due the toxicity of many thiol containing compounds. The generated library would contain 1,083 trimer peptides. The library was first created using a Python[155] script (Appendix A3.1), written by Joshua Meyers (MChem student at the University of Leeds), which generated all possible trimers meeting the criteria firstly as three letter code (**Figure 61**, **A**) and then in SMILES strings[156] (**B**). The SMILES strings were then fed into Openeye's BABEL[157] program which converted the SMILES strings into 2D structures in SDF file format (**C**)(Appendix A3.2). The 2D structures were then converted into lowest energy 3D conformers using the OMEGA[158] programs (**D**)(Appendix A3.3). The same process was repeated for the di-peptides and tetramer peptides respectively.
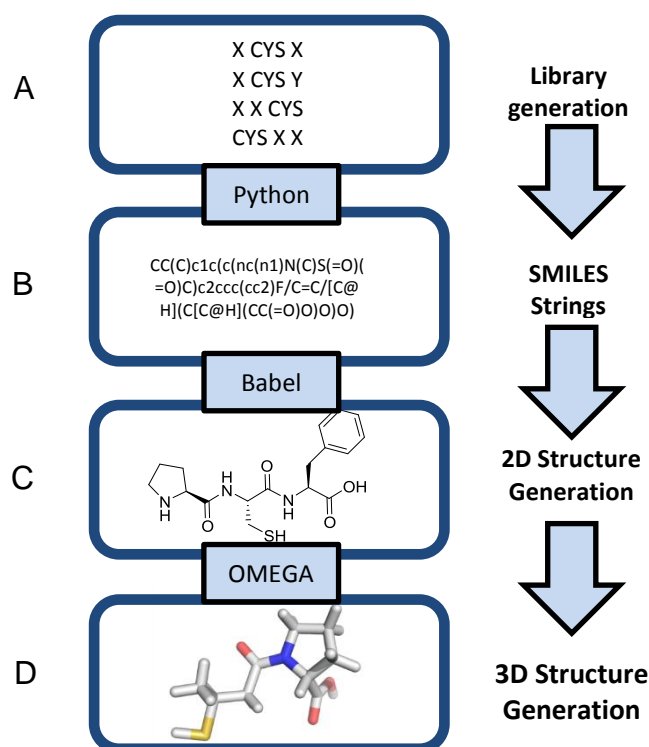
Figure 61: Schematic of peptide library production

6.4 Docking protocol

The computational library of trimers was docked into the crystal structure of NDM-1 (PDB ID: 3Q6X[38]) using AutoDock 4.2 (see Section 4.1.1). AutoDock, uses a Lamarckian genetic algorithm to generate a range of docking poses. The resulting docking poses were scored, both within AutoDock and also using the SPROUT scoring function for comparison. **Figure 62** below shows the correlation between the two scores for both the tri- and tetra-peptides respectively. The scores have been normalised to allow a direct comparison of the two scoring functions, with the best scoring peptide being normalised to one. It can be seen that there is a possible weak correlation between the two scores with almost no correlation when looking at the tri-peptides but a clearer correlation with the tetra-peptides. The major variances are seen due to the different weighting of different components in the scoring functions. This highlights the need for a consensus approach when interpreting the results taking into account both scores to find the best inhibitors.
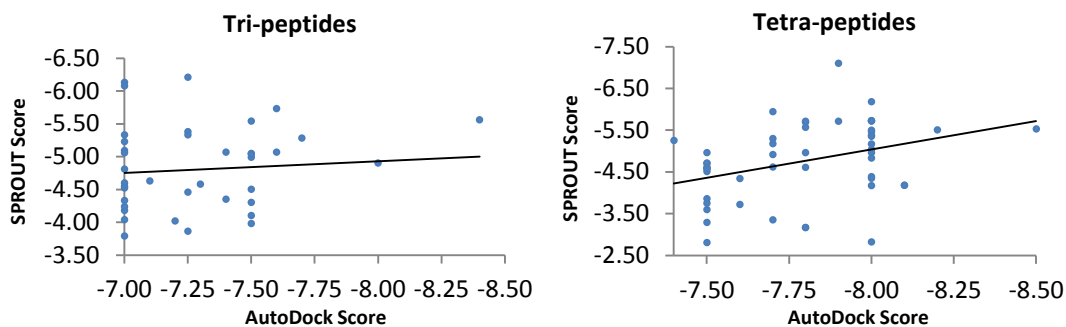
Figure 62: Graphs comparing the AutoDock and SPROUT scores of the top 40 hits of the tri- and tetra-peptides.

6.5 Docking results

The docking of the di-, tri- and tetramer peptides respectively were conducted as described in Section 6.4. The results of the docking studies can be seen in Appendix A4.1-A4.3. Overall the dipeptides gave the weakest binding scores which was to be expected due to the lower molecular weight of these systems. As the task was to look for the best binding peptides and the trimers and tetramers gave a significant enhancement on the binding, the di-peptides were not investigated any further.

Initially it appeared that the scores of both the trimer and tetramer peptides are very similar, however considering that the tri-peptides have a lower molecular weight, and that a greater average number of possible docking poses were found than in the four membered peptides, the tri-peptides performed significantly better. Visual inspection of the docking poses for the tri- and tetramer peptides revealed that the tri-peptide molecules docked deep into the pocket making contacts with residues in the pocket whereas the tetra-peptides often protrudes into the solvent exposed region of the open cavity (**Figure 63**). Taking these results into account, it was decided to progress the trimer peptides only.
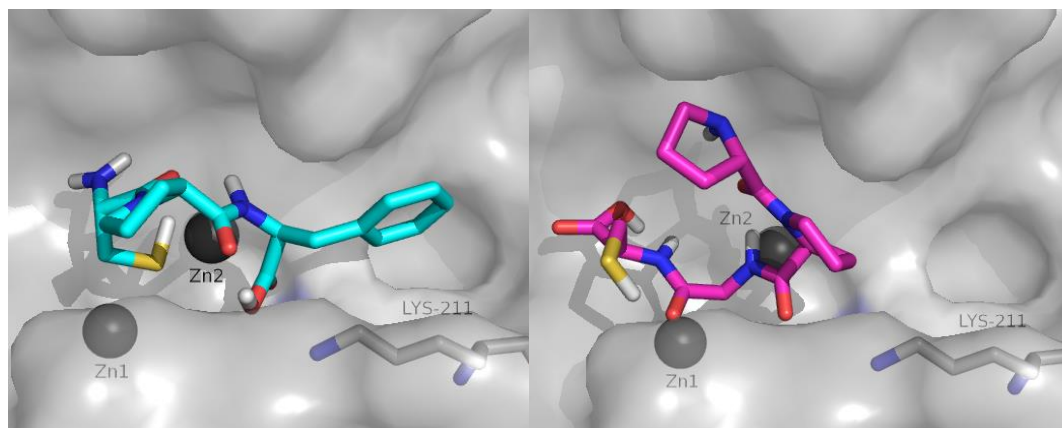
Figure 63: Example docking of a trimer **6.1** (cyan) and tetramer **6.2** (magenta) showing the tetramer extending up into open space

It was observed that in almost all of the top ten trimer peptides, a Pro attached to a Cys is a common feature. It is predicted that this motif orientates the binding functional groups on the peptide towards the Lys and Zn thus reducing the energy required for binding. An example of this is shown by the docking of compound **6.1** (**Figure 63**)

In a large number of the docking results, the sulfur atom within the cysteine residue is not predicted to make a direct contact with the zinc atom and is placed into the solvent-exposed region of the cavity rather than in a position to make a direct contact to the zinc atoms. This issue stems from one of the limitations in the AutoDock docking parameters where the zinc is assumed to have zero charge. Docking also only provides a score of a pre-covalent event, therefore not taking into account the strength of a covalent bond that could be formed from sulfur to the zinc atoms. It is predicted that upon binding, there would be rotation of the molecule to place the sulfur in a position where it can make a strong covalent bond with the zinc atoms. Part of the visual inspection of the results ensures that with rotation, a zinc-sulfur bond could be formed without disruption of the other bonds already predicted to take place.

Figure 64 shows a high scoring example where the sulfur is in a good orientation to make a zinc-sulfur bond. However, this bond is not taken into account in the score of the docking pose.
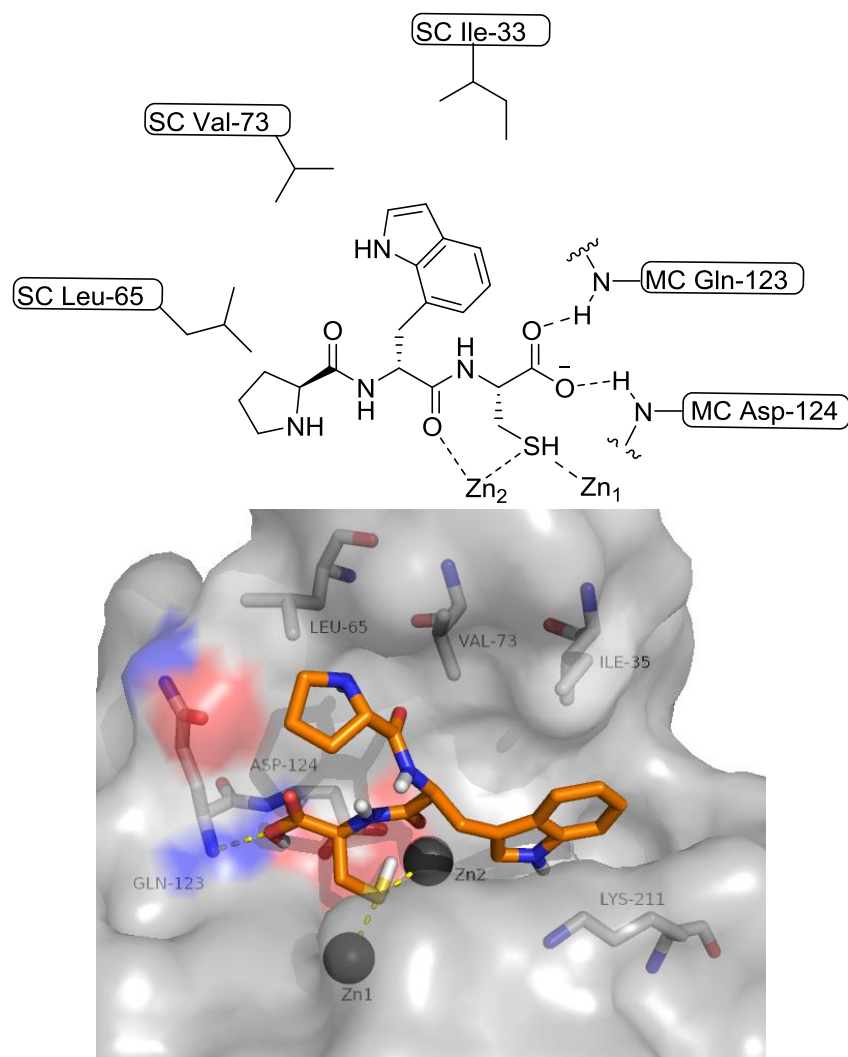
Figure 64: 2D and 3D representations of trimer peptide **6.3** (Pro-Trp-Cys) docked into NDM-1. PDB ID: 3Q6X

The ten worst binding trimer peptides were identified in order to synthesise them along with the top ten to ensure that the screening identifying pre-covalent inhibitors was sucessful, and the formation of the zinc-sulfur bond is not the exclusive factor contributing to the binding affinity of the inhibitors. The predicted worst ten trimer peptides contained a number of charged functional groups such as Asp and Arg which gave poor scores. Predictions implied that many of them would have problems reaching the active site to form binding interactions. **Figure 65** shows an example of the poor binding peptide **6.4**.
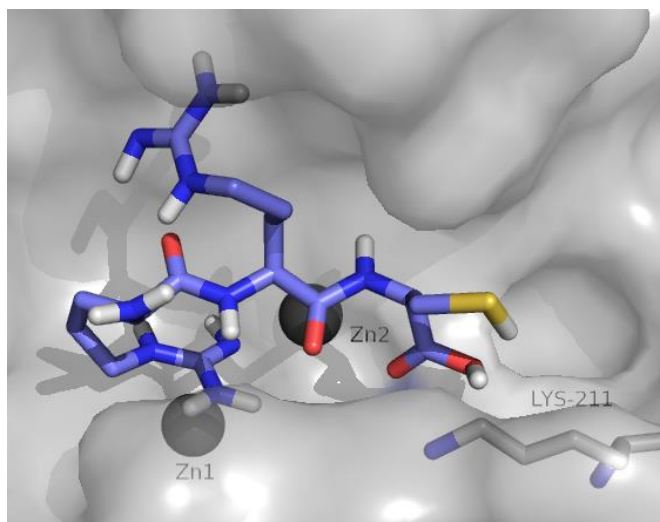
Figure 65: Poor binding peptide **6.4** (Arg-Arg-Cys)

6.6 Biological evaluation

The ten trimer peptides which gave the strongest predicted binding were identified for synthesis along with the ten trimer peptides which gave the weakest predicted binding.

The selected trimer peptides were synthesised using Solid Phase Peptide Synthesis (SPPS)[159] and purified using preparative mass-directed HPLC. Biological evaluation against NDM-1 was conducted at the University of Oxford in a nitrocefin based fluorescence assay as described in Appendix A1.1.

The results of biological screening for the top ten scoring trimers are shown in **Table 9**.

Table 9: Top 10 scoring trimer peptides and their biological activity against NDM-1

Compound No.	Sequence	RA [%], 100 µM
6.5	Pro-Ile-Cys	100 ± 2.3
6.6	Asn-Pro-Cys	77 ± 11.5
6.7	Pro-Pro-Cys	100 ± 2.8
6.8	Pro-Trp-Cys	100 ± 10.6
6.9	Pro-Cys-Phe	59 ± 4.3
6.10	Cys-Pro-Phe	100 ± 12.2
6.11	Cys-Gly-Trp	100 ± 7.8
6.12	Cys-Pro-Trp	100 ± 4.0
6.13	Cys-Phe-Tyr	64 ± 1.9
6.14	Cys-Pro-Tyr	100 ± 2.4

Peptide **6.9** and Peptide **6.13** showed moderate inhibition of the NDM-1 enzyme. Both contain a Cys-Pro motif and an aromatic-containing amino acid residue. Compounds **6.9** and **6.13** displayed IC_{50} values against NDM-1 of 183 ± 0.1 μM and 219 ± 0.1 μM respectively. Peptide **6.6** showed low inhibition of the NDM-1 enzyme however this was not deemed significant for IC_{50} determination. No inhibition was seen for the other top-scoring peptides which exhibited 100% residual activity (RA) at 100 μM.

The predicted ten worst peptides were also biologically evaluated against NDM-1 and the results are shown below in **Table 10**.

Table 10: Worst Scoring compounds and their biological results against NDM-1

Compound No.	Sequence	RA [%], 100 μM
6.15	Cys-Arg-Arg	100 ± 2.5
6.16	Arg-Cys-Arg	100 ± 6.9
6.17	Gln-Cys-Arg	100 ± 6.2
6.18	Lys-Cys-Arg	100 ± 12.1
6.19	Asp-Cys-Asp	88 ± 5.9
6.20	Arg-Arg-Cys	100 ± 4.2
6.21	Cys-Lys-Glu	100 ± 5.4
6.22	Cys-Arg-Glu	100 ± 3.5
6.23	Lys-Cys-Gln	100 ± 2.8
6.24	Arg-Cys-Tyr	100 ± 3.0

Overall it is observed that there is poorer binding with these peptides than the best binding top ten with all compounds apart from **6.19** exhibiting 100% residual activity at 100 μM against NDM-1. This indicates that the screening is broadly consistent with the predictions. The peptide based inhibitors have been identified in their pre-covalent docking state. The docking predictions does not take into account the strength of the zinc sulfur bond and therefore should distinguish between strong and weak binding inhibitors by the other binding interactions with the active site. The results show that the formation of the zinc-sulfur bond is not the exclusive factor in the inhibitors binding affinity as some of the top scoring peptides are biologically active.

Compound **6.19** gives a slightly anomalous result with higher than predicted inhibition relative to the other peptides. This is potentially rationalised by the preference of the Asp residues to bind strongly to the Lys-211 residue found in the active site. **Figure 66** shows the predicted contact made by compound **6.19**.
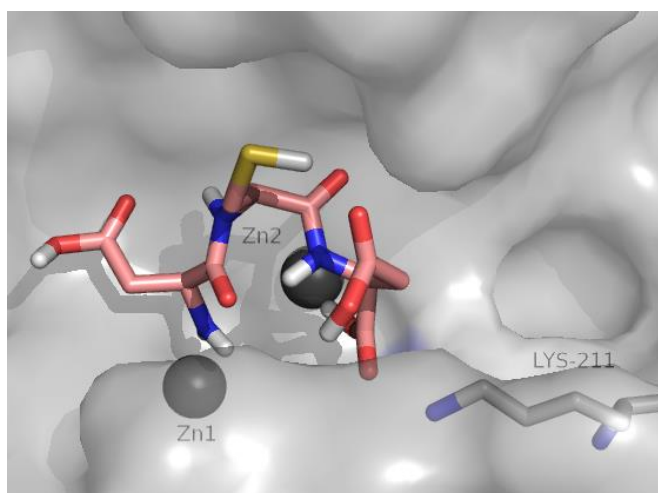
Figure 66: Binding of compound **6.19** to the Lys-211 in the active site

6.7 D and DL combination trimers

The research into thiol- and cysteinyl peptide inhibitors by Page *et al.* suggested that, for dipeptides in the BCII model system, that the strongest binders have a D absolute stereochemistry at the cysteine residue and at the C-terminal chiral centre respectively. The above process was therefore repeated using libraries of just D-amino acids and of all DL combinations.

The virtual libraries of all D-amino acids (1,083 compounds) and the DL combinations (8,432 compounds) were produced as described in Section 6.3. The four top scoring peptides were identified by docking each of the libraries into the crystal structure of NDM-1 using AutoDock. The docking results can be found in Appendix A4.5. As with the all L amino acid trimers, the common Cys-Pro motif was observed in many of the high scoring compounds. It was also noted that all of the four top scoring trimer peptides consisted of all D-amino acids. From the research by *Page et al.* these would therefore be expected to give better binding than the already tested L-amino acid trimers. The top scoring peptide was **6.25** which is shown in **Figure 67**.
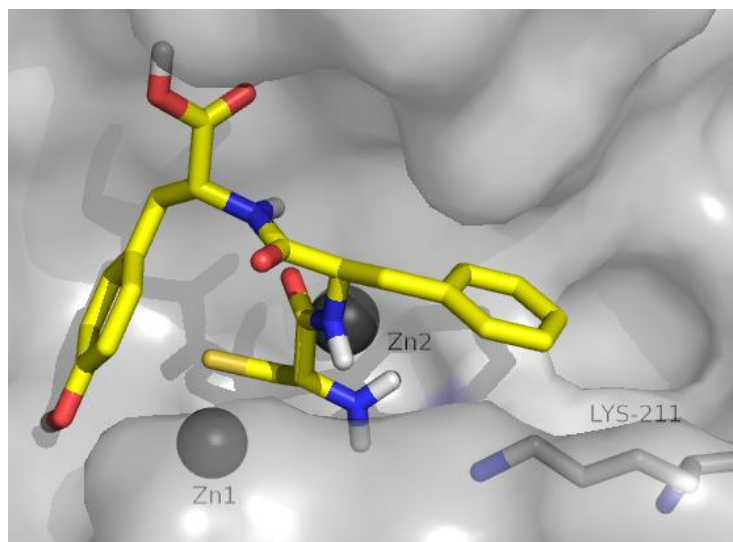
Figure 67: Best binding DL combination trimer peptide **6.25**

The top four peptides were then synthesised and biologically evaluated against the NDM-1 enzyme at the University of Oxford

The results of the biological evaluation are shown below in **Table 11**.

Table 11: Top scoring D and DL combination trimers and their biological activity against NDM-1

Compound No.	Sequence	RA[%], 100 µM
6.25	D-Cys-D-Phe-D-Tyr	91 ± 3.6
6.26	D-Pro-D-Trp-D-Cys	72 ± 5.7
6.27	D-Cys-D-Pro-D-Tyr	84 ± 5.1
6.28	D-Pro-D-Cys-D-Phe	77 ± 3.2

Given the limited range of the activities it is hard to draw firm conclusions from the results. However, generally the all D- absolute stereochemistry containing peptides **6.25-6.28** show better inhibition of the NDM-1 enzyme at 100 µM than the all L- absolute stereochemistry peptides.

The all L-absolute stereochemistry peptides **6.9** and **6.13** exhibit the best overall inhibition at 183 µM and 219 µM against NDM-1 respectively

6.8 Peptide mimics

After a strong binding peptide has been identified using one of the techniques described in Section 6.1, a peptide mimic can be designed. Designing a peptide mimic involves deconstructing the original peptide and reassembling the essential features on a new mimetic scaffold that retains the ability to interact with the enzyme target, but circumvents the problems associated with a natural peptide. By this process, the peptide is reduced to its 'information content', the basis for a pharmacophore model that defines the critical features and their arrangement in space. This model supports the re-assembly of the critical elements and non-peptide variants on a modified scaffold that presents the optimized pharmacophore to the receptor. The optimized peptide-hybrid may be valuable as a lead, in addition to its role as a tool for further evolution to a mimetic.

For the peptides identified as active in the current research, a study was conducted to find compounds from a known commercial library which are similar in structure and electron density to the identified peptide but without the biological liabilities of peptides. The virtual screening of the Zinc database's 'Drug like molecules' against the peptide **6.25** was conducted using the shape similarity software ROCS[160] and electron density comparison software EON.[161]

6.8.1 ROCS[160]

ROCS stands for Rapid Overlay of Chemical Structures and is a ligand-based docking software, marketed by OpenEye, which uses shape comparison to identify potential inhibitors from large databases of compounds. ROCS works on the idea that molecules similar in shape to active molecules are more likely to be active molecules than randomly selected molecules. ROCS considers 3D similarity and chemical functionality such as hydrogen bond acceptors and donors, positive and negative charges. Results are ranked based upon the ROCS scoring function which includes the shape and chemical similarity.

6.8.2 EON[161]

EON is a program designed to compare the electrostatics of a compound to a database of known compounds to find similarity matches. EON compares electrostatic potential maps of pre-aligned molecules and determines the Tanimoto measures for the comparison. The results from the top slice of the ROCS result can be directly used as the input file for the EON run.

6.8.3 Process for identifying peptide mimics

A three-dimensional library of the Zinc databases 'Drug-Like Molecules' collection was created from the available two-dimensional structure library using the OMEGA software.[162] The Zinc 'Drug-Like' library contains 1,064,843 compounds. The 'Drug-Like' library is based upon the Lipinski rule of 5 being applied to the full zinc library database.[163] This library was used for comparison to the query molecule **6.25**. ROCS was used to identify the top 1000 compounds which scored highly. The results were visually inspected in VIDA[164], OpenEye's molecular modelling visualising software, to ensure there were no major variations from **6.25**. **Figure 68** shows an overlay of one of the library compounds with the desired query.
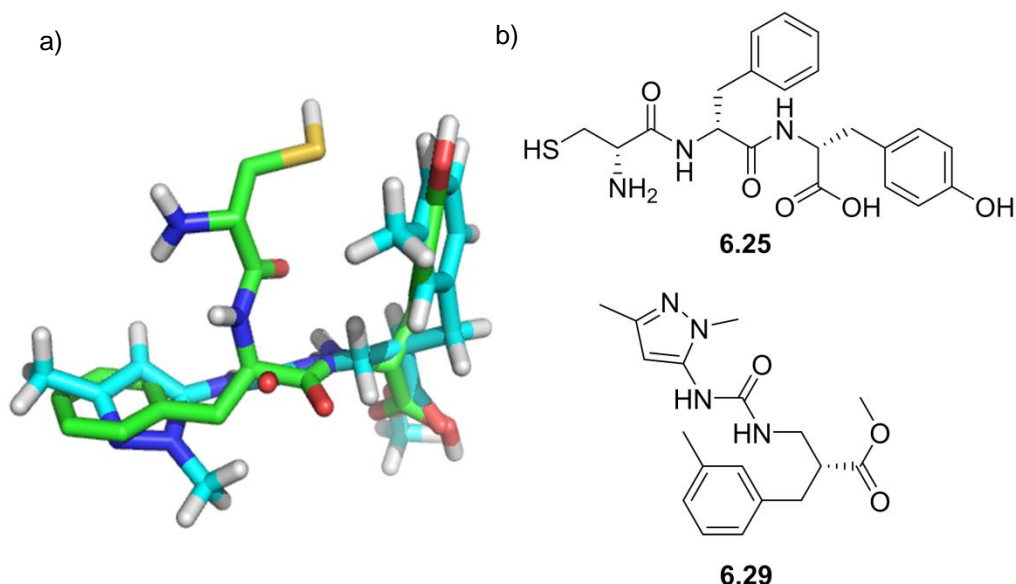

Figure 68 ROCS and EON screening identified compound **6.29**: a) overlay of **6.29** (cyan) onto query molecule **6.25** (green). b) 2D structures of **6.25** and **6.29**

The electrostatic comparison was conducted using EON which identified the top 50 compounds with the best electrostatic overlay to query molecule **6.25**.

The top 50 compounds were visually inspected using SPROUT to ensure there were no surface boundary violations.

6.8.4 Compound results

The top six scoring compounds are shown in **Figure 69**.
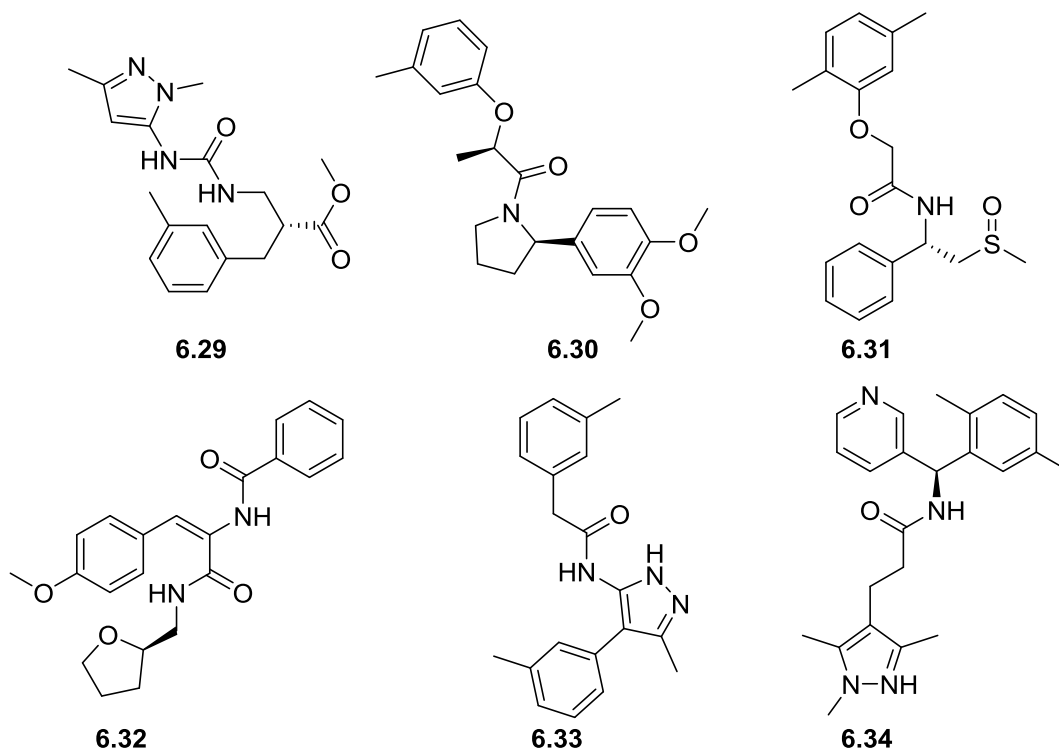
Figure 69: Structures of the top six scaffold hopping results (**6.29-6.34**)

From all of the selected compounds it is clear to see that ROCS and EON try to mimic the peptide backbone but do not mimic the side chain containing the thiol. When looking at the electrostatic map generated in VIDA there are no interactions around the thiol. This would be an issue if the thiol was wanted to be included as part of the designed inhibitor. An inhibitor could however be designed that does not require this functionality and therefore forms a cover over the active site zincs preventing the β-lactam from reaching the active site. Further research is therefore required to find a good peptide mimetic for this peptide structure if direct binding to the zinc is required as has previously been suggested.

6.9 Conclusions

A new method coupling *in silico* predictions to peptide screening to identify strong binding peptides to biological targets by making custom-built peptide libraries has been developed which could be a great improvement on the current methods of peptide identification. The method has been shown to work by identifying active peptides against the MBL NDM-1.

When docking to NDM-1 it was observed that trimer peptides provide the best predicted binding scores when compared with di and tetramer peptides. The L-amino acid trimer peptides give moderate activity against the NDM-1 enzyme with the best giving an IC_{50} of 183 µM. This result is not as good as was initially hoped for but does show moderate binding to the enzyme which could be further developed into a drug compound.

The all D-absolute stereochemistry peptides are in general better inhibitors of the NDM-1 enzyme however due to the tight range of the results a firm conclusion on the extent of the improved binding affinity cannot be drawn. The best L-amino acid trimer had better inhibitory activity than the all D-trimers however was still a way off the inhibitory activity of known peptide mimic captopril.

There are still a number of limitations to this technique including the zinc atoms being given no charge in the docking runs but the zinc atoms in the MBLs are known to be in the 2+ charged state. Docking is also only conducted on a single crystal structure which is deemed to be rigid. In the biological environment the enzyme would have much more movement however as previously this would greatly increase the computational time required to complete the dockings.

There is a great potential that this method could be used to identify binding peptides for a large number of different biological targets. The libraries can be made to be tailored for each individual task increasing the chance of getting a hit which can be further developed into a peptide mimetic drug. This coupled with the reduced time to identify the hits and the reduced cost of compound production and storage needing to only make the best identified compounds makes this a very attractive hit finding method.

Chapter 7
De novo designed inhibitors

The term *de novo* means starting from the beginning or anew. *De novo* drug design is an iterative process in which the three-dimensional structure of the receptor is used to design new inhibitor molecules.[165] The inhibitor molecule is designed from scratch to bind in the active site. Fragments are docked into sub-sites, and then joined to create full molecules. These molecules are scored and ranked *in silico* based on the interactions present with the target protein.[84] The top scoring lead molecules can be taken on for full synthesis reducing the overall number of compounds produced saving both time and money.

The first examples of software produced specifically for *de novo* drug design were reported in the early 90s. Developments in computing power and increased availability to high-resolution crystal structures has led to the development of more programs to conduct *de novo* design.[166] The use of such programs has been increasing as people look for easy starting points for lab synthesis and aim to reduce the time and cost spent conducting high throughput screening to produce a hit compound. A general description of the steps involved in *de novo* design is given in **Scheme 19**.
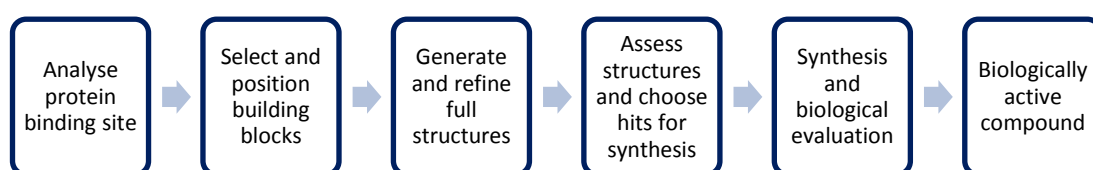
Scheme 19: General summary of the *de novo* process to obtain a biologically active compound.

Chemical space[167] is defined as the total number of possible small organic molecules and is estimated to exceed 10^{60}. When designing new molecules from scratch it is possible to come up with almost infinite possibilities. Therefore, design of molecules must be constrained to those which fit certain spatial and electronic characteristics which will allow them to bind favourably within the target protein.

The first step carried out by many *de novo* design programs is the analysis of the target site of the desired protein. Some programs, such as SPROUT[168] and LUDI[169], identify regions where favourable interactions could form between an appropriately functionalised ligand and the protein by looking for hydrogen bond donors and acceptors and hydrophobic residues in the protein structure. Other programs such as GRID[170] and LigBuilder[171] use a grid-based approach moving probe fragments around a grid of points in the binding site and calculating the energy at each position to determine regions where favourable interactions might occur.

Once a binding site has been identified and analysed to identify possible interactions, building blocks are chosen to begin designing new ligands. The type of building blocks used varies from program to program. A number of programs such as SPROUT, have a database of small, simple fragments such as aromatic rings and linker fragments such as amides or alkyl chains which can be combined to give a wide range of structures. Other programs can take known molecules, break them down into functional groups and dock these within the binding site.

The ways in which building blocks are connected varies immensely between programs. Some programs start from a single fragment positioned in the binding site and grow out from there by directly linking fragments to the start fragment one at a time. Others start with several building blocks positioned in favourable positions in the binding site and then connect them using linker fragments, e. g. SPROUT[168]. Once an appropriately sized small molecule has been produced further improvements to the structure might be carried out by evolution or substitution at various positions. This is often conducted with the use of the programs scoring function

An essential part of any *de novo* design software is a method for determining the relative binding affinity of the designed structures which is often referred to as the scoring function. Most programs contain methods for calculating the free energy of the designed structures within the protein binding site as a way of predicting the binding affinity and thus determining which putative ligands designed by the program are the most promising candidates. Often structures generated by *de novo* design can be complex and difficult to

synthesise, so many *de novo* design packages include a method for analysing the complexity or synthetic accessibility of the designed structures.

Several detailed reviews cover the different software tools available which provide a more detailed account of the various techniques used and their application to different areas of drug discovery.[166, 172] This report focuses upon the SPROUT package which has been employed in the project work.

7.1 SPROUT

SPROUT was created at the Institute for Computer Applications in Molecular Sciences (ICAMS) at the University of Leeds. SPROUT is a unique program that uses a multidirectional tree search to build up templates from functional groups that are predicted to have the best possible interactions with the target site.[168,125b] SPROUT has already been used successfully to design inhibitors of a number of enzymes such as Dihydroorotate dehydrogenase (DHODH)[173] and RNA polymerase (RNAP).[174]

A problem in *de novo* design is the generation of a large number of structures. SPROUT uses many constraints such as steric and electrostatic properties on the molecule to limit the number of structures generated.
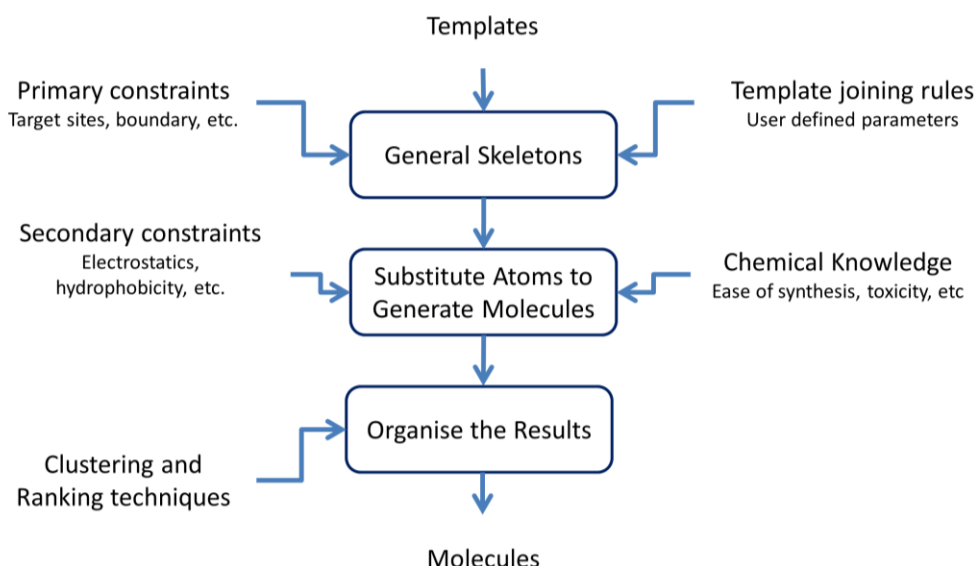
Figure 70: Overview of the components of SPROUT.

7.2 Components of SPROUT

SPROUT consists of a series of individual modules, each of which controls a section of the overall process outlined in **Figure 70**. These are as follows;

- CANGAROO – Definition of constraints for primary structure generation i.e. receptor volume, boundary
- HIPPO – Analysis of localities for favourable interaction (target sites)
- ELEFANT – Docking of atoms or fragments (as defined by the user) into chosen target sites
- SPIDER – Connection of target sites using user defined spacer templates to produce molecular scaffolds
- ALLIGATOR – Scoring and ranking output

7.2.1 CANGAROO

CANGAROO stands for **C**left **AN**alysis by **G**eometry based **A**lgorithm **R**egardless **O**f the **O**rientation. In this module the primary constraints are defined. The X-ray crystal structure of the target protein is imported into the module (i.e. pdb). CANGAROO identifies potential binding pockets or clefts based upon the protein surface curvature. The user then selects the desired cleft in which structure generation is to occur and reassigns this as a receptor site comprising of a set distance (usually 10 Å) from the centre of the cleft. In the ideal case the X-ray crystal structure will contain a known ligand co-crystallised within the protein. (**Figure 71**). The receptor site can then be assigned as the area directly around the ligand. The ligand is then removed from the receptor leaving and empty pocket for *de novo* structure generation.
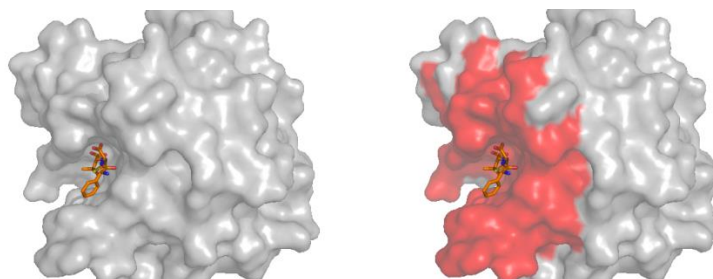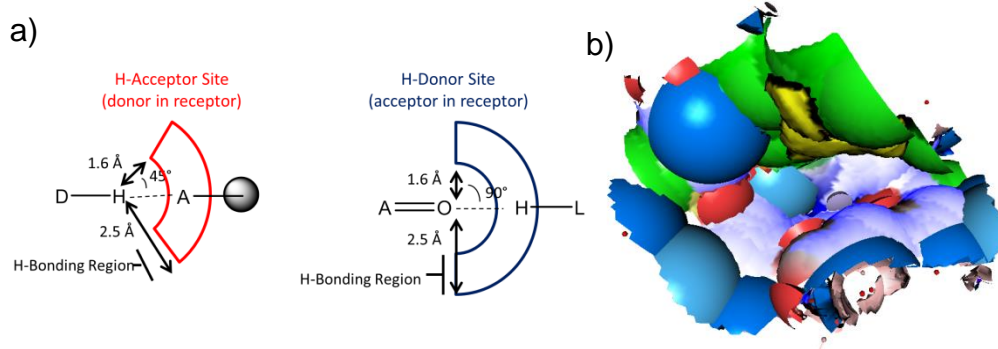

Figure 71: Cangaroo identification of active site in NDM-1. a) Hydrolysed ampicillin (Orange) bound in the active site (Grey) identified as binding cavity. b) 10 Å cut around the cavity defined as the receptor (Red).

7.2.2 HIPPO

HIPPO stands for **H**ydrogen-bonding **I**nteraction site **P**rediction as **P**ositions with **O**rientations. In this module the interaction sites within the receptor are identified. The receptor is analysed for its electrostatic and hydrophobic features which are determined by the amino acids found on the receptor surface. A boundary surface is added to the receptor based upon van der Waals radii of each protein atom and this is coloured as follows; red for an area where hydrogen bond donors exist in the protein, blue for an area where hydrogen bond acceptors exist in the protein, purple for a complex hydrogen bonding area (i.e overlapping acceptor and donor sites) and green for a non-polar hydrophobic area. HIPPO then creates a loci around each polar atom in the receptor defining an area of space where a favourable polar contact might be made if a complementary moiety in the generated structure were placed there. This locus is calculated based on statistical analysis of H-bonding geometry in published crystal structures. As with the boundary surface colouring, areas around H-acceptors in the receptor are coloured blue and around H-bond donors coloured red. (**Figure 72**). HIPPO also has the ability to create a spherical site which is a user defined area within the receptor in which ready-made fragments which are not part of the template library can be docked. This is useful if the user wishes to grow from a known core or part of an existing ligand.


Figure 72: Hippo identification of surface interaction sites. a) Donor and acceptor site loci generation. b) SPROUT generated surface of NDM-1 active site showing identified interaction sites.

7.2.3 ELEFANT

ELEFANT stands for **ELE**ction of **F**unctional groups and **AN**choring them to **T**arget sites. Atoms and fragments are selected from the SPROUT template library based upon complementarity to the target sites generated in HIPPO. (**Figure 73**) The choice of fragments and atoms to be included are defined by the user. All available conformations are considered for flexible fragments whilst atom hybridisation governs the directional nature of fragment growth.
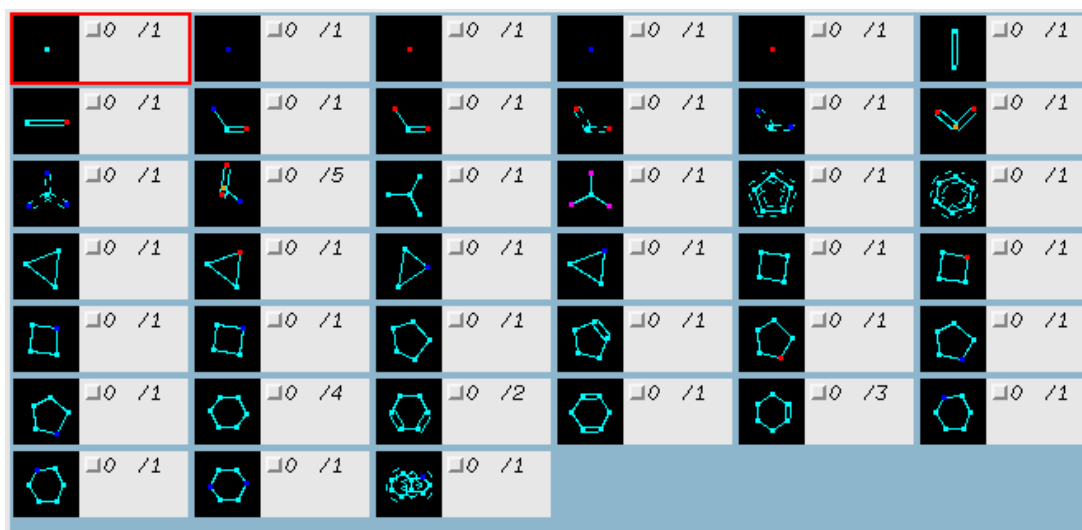
Figure 73: Template fragments available in the SPROUT Elefant module

7.2.4 SPIDER
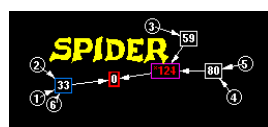
SPIDER stands for **S**tructure **P**roduction with **I**nteractive **DE**sign of **R**esults. Structures are generated by joining the fragments docked in the ELEFANT module to produce scaffolds. The fragments are connected in a stepwise manner where violations of the primary constraints is monitored at each step. The SPROUT template library is again used to define the spacers, which controls the potential combinatorial explosion of results. In the connection of two starting fragments, templates (as chosen by the user) are added simultaneously to each starting fragment in the direction of the other fragment (as governed by joining rules creating 'partial skeletons') As mentioned above, a final solution is found when an overlapping template common to both partial skeletons is found. The newly created scaffold

connecting the two sites is now grown in the same way towards the remaining receptor target sites to produce the final ligand.
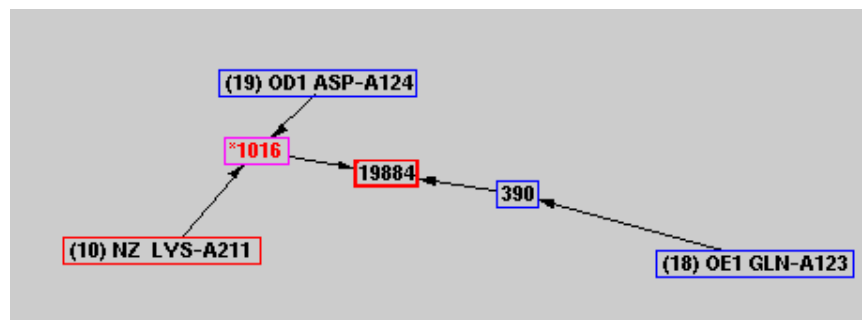

Figure 74: Example tree diagram of connections made in SPIDER module of SPROUT

7.2.5 ALLIGATOR

 ALLIGATOR stands for **A**nalyse **L**ots of **LIGA**nds, **T**est and **O**rder **R**esults. This module sorts out the generated results into sets by various user imposed criteria. This enables easy identification of groups of molecules which contain either desired or undesired characteristics. The module assigns each new scaffold a score which is then used to rank the output in order to predict binding affinity and identify the molecules with the best potential for good *in vitro* binding. The SPROUT score attempts to estimate binding affinity through considering the combined contribution of hydrogen bonding, hydrophobic interactions, van der Waals interactions and the number of rotatable bonds. These estimates are derived from real-life measurements involving ligand-protein complexes making this an empirical scoring function. Ligand and receptor desolvation is not considered in the SPROUT scoring function. (**Scheme 20**).

$$\Delta G_{Score} = \Delta G_{hbonds} + \Delta G_{hydrophobic} + \Delta G_{VdW} + \Delta G_{rotatable}$$

Scheme 20: SPROUT scoring function components

Naturally, it is unrealistic to expect a scoring function to predict the experimental potency of a ligand to any great degree of accuracy, however, the SPROUT scores serves more as a ranking system, directing the user to the ligands which have the most potential to show activity.

7.3 Compound selection

A SPROUT run was conducted which involved all of the steps described in Section 7.2. This yielded a selection of possible inhibitors scaffolds of which the top ten-scoring motifs were docked back into the NDM-1 active site (PDB ID: 3Q6X) using AutoDock to ensure the compounds bound as expected from the SPROUT design. Visual inspection of the docking poses generated for the top ten SPROUT-designed compounds led to the identification of structure **7.1** as a potential NDM-1 enzyme inhibitor which gave a SPROUT score of -6.90 (**7.1**, **Figure 75**).
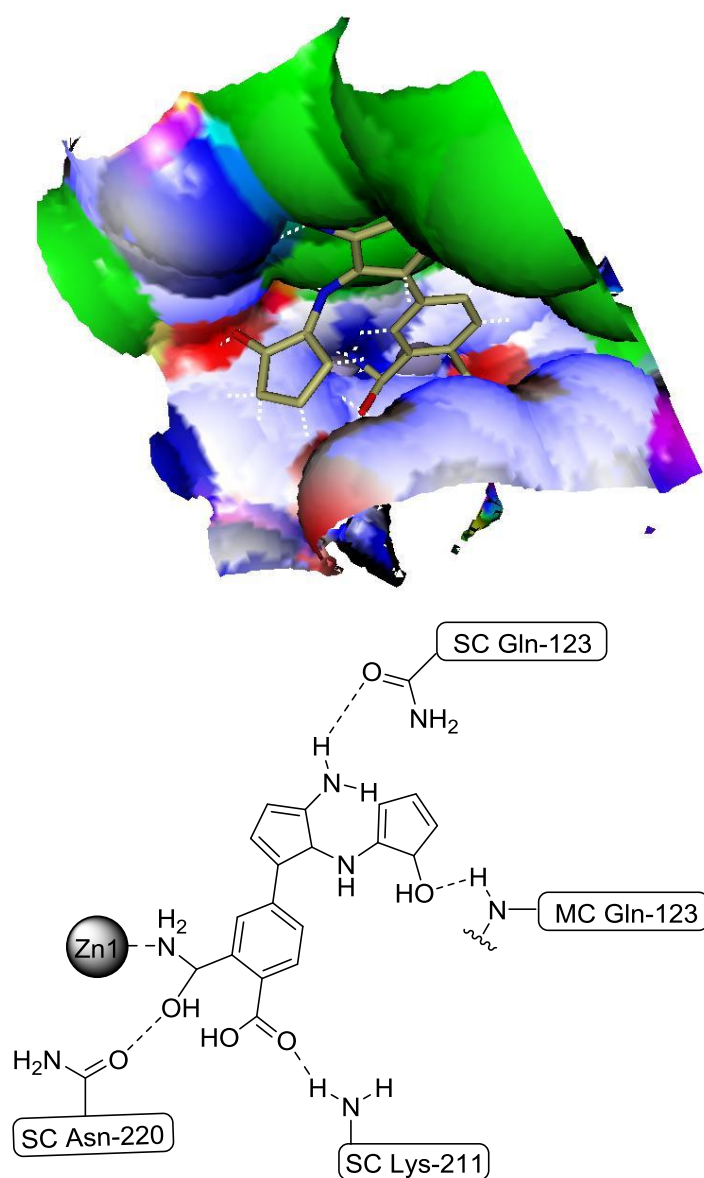
Figure 75: Designed compound (**7.1**) docking into the NDM-1 active site (PDB ID: 3Q6X): Visualised in SPROUT and 2D representation

Compound **7.1** was predicted to bind *via* the carboxylic acid to the side chain amine of the Lys-211 residue. The amine on the amine / hydroxyl containing carbon was predicted to bind to Zn1 and the hydroxyl was bound to the side chain carbonyl of the Asn-220 residue. Further interactions predicted involving with the amine attached to the 5-membered ring binding to the side chain carbonyl of the Gln-123 residue and the hydroxyl on the five membered ring being bound to the main chain amide of the Gln-123 residue respectively (**Figure 75**).

The identified structure (**7.1**) was quite complex so it was decided to scale the fragment down to the 'war head' which would bind directly to the zinc (**7.2**). Direct binding to the zinc atoms blocks them off from the β-lactam antibiotic. The β-lactam antibiotic should therefore not be hydrolysed by the enzyme and should be able to have its desired effect on its bacterial target. It was seen that SPROUT had placed an amine and a hydroxyl on the same carbon. This functionality is hydrolytically unstable therefore it was decided to focus on only one of these interactions (**7.3**). The alcohol was selected due to ease of the proposed synthetic route (**Scheme 22**). The molecule was then simplified to contain a phenyl ring rather than a cyclopentadiene ring as in (**7.4**) (**Scheme 21**).
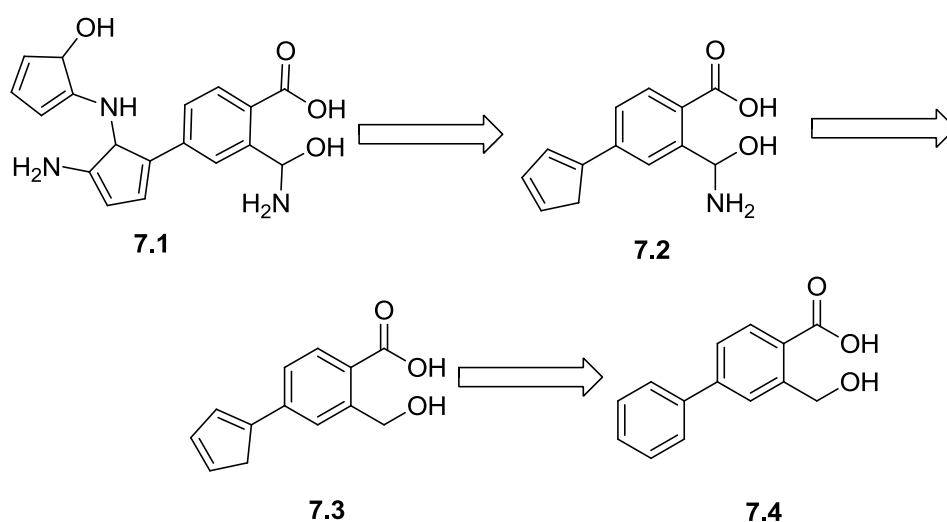
Scheme 21: Formation of the 'war head' fragment (**7.4**) from the SPROUT identified compound (**7.1**).

Compound **7.4** was predicted to bind from the carboxylic acid to the side chain amine of the Lys-211 residue and Zn2, from the hydroxyl to the Zn1 and Zn2 atoms and to form an edge to face π stacking interaction with the Trp-93 residue located in the hydrophobic wall of the NDM-1 active site. (**Figure 76**)
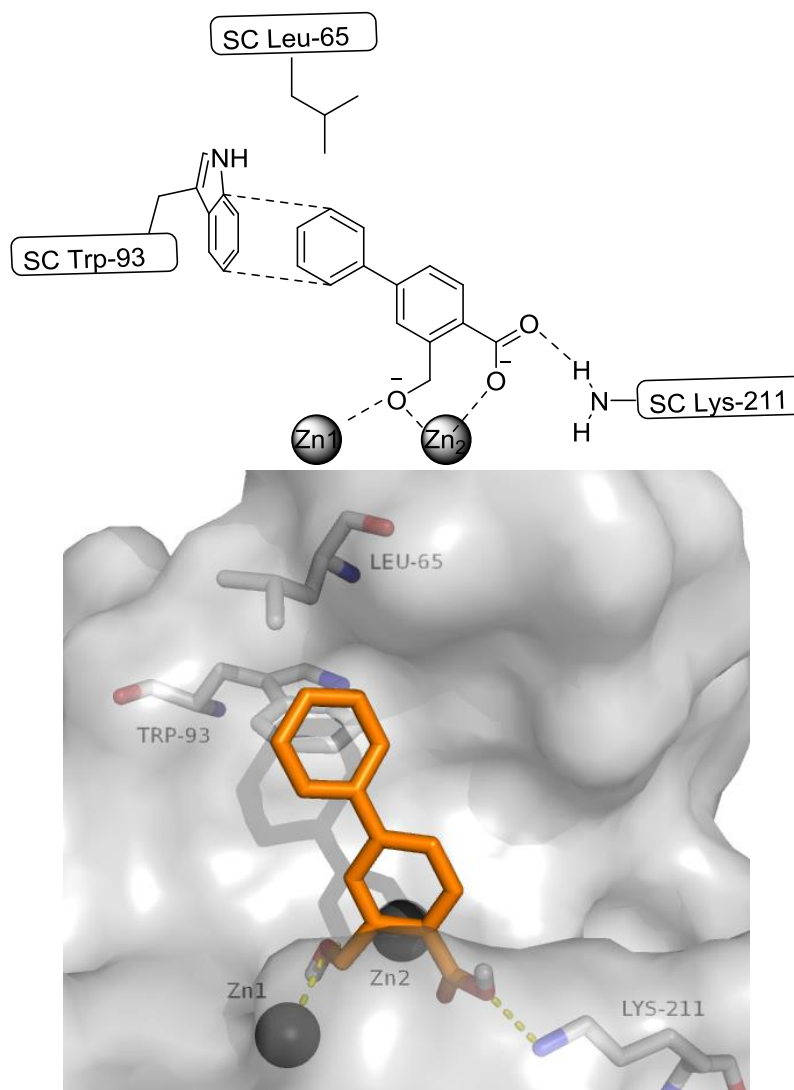
Figure 76: 'War head' fragment **7.4** docked into the active site of NDM-1 (PDB ID: 3Q6X)

7.3.1 Synthesis of SPROUT-generated compound

The synthesis of the SPROUT-derived alcohol compound **7.4** was conducted by use of a Suzuki cross coupling reaction[175] of **7.5** and phenyl boronic acid to form compound **7.6,** followed by lactone hydrolysis using base to afford compound **7.4** (**Scheme 22**). Both reactions proceeded in good yield (>65%).
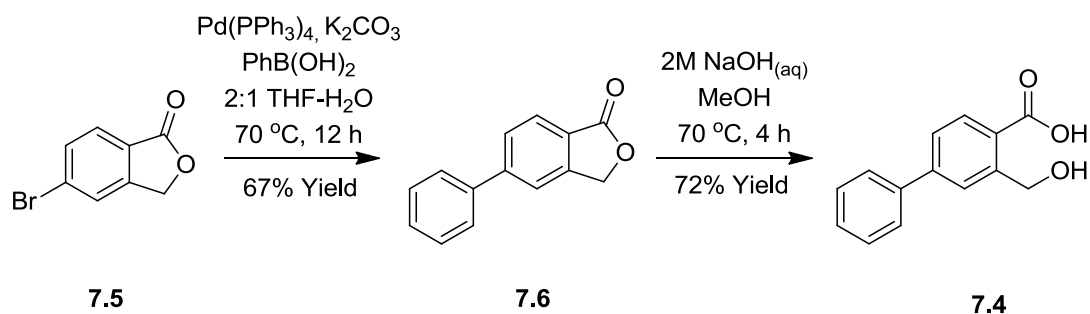
**Scheme 22:** Synthetic route to hydroxide compound (**7.4**)

7.3.2 First generation *de novo* designed inhibitors

A structure activity relationship investigation (SAR) was conducted on the phenyl ring attached to the 'war head' group to see if changing the sterics and electronics around this ring had an effect on the binding affinity (Position X, **Figure 77**). A further example (**7.11**) was included to investigate the role of variation in dihedral angle within the biphenyl unit introduced by the introduction of an ortho chloro group.
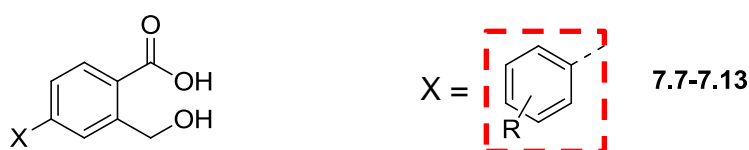
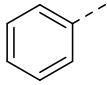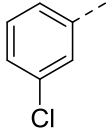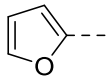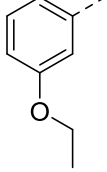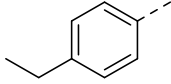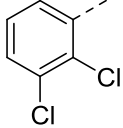**Figure 77:** Position of SAR investigation around compound **7.4**
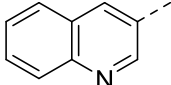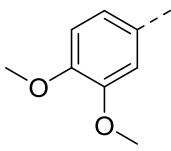
The compounds were synthesised by altering the phenyl boronic acid used in the Suzuki cross coupling step.(**Scheme 23**)
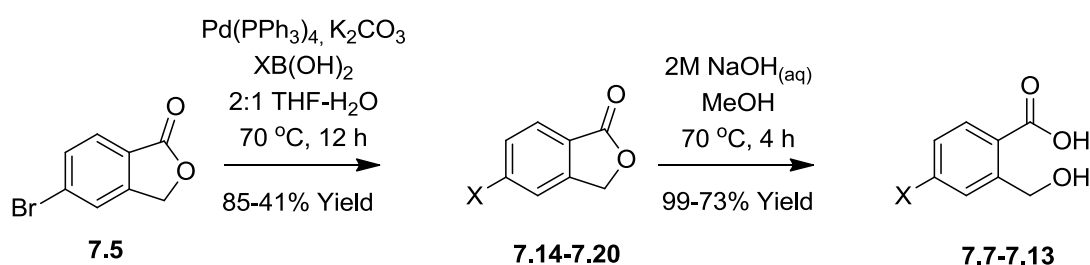
Scheme 23: Synthetic route to SAR compounds based upon lead compound **7.4**

The synthesised compounds were biologically evaluated against NDM-1 by Dr Jürgen Brem at the University of Oxford. The results of the biological evaluation are shown in **Table 12**.

Table 12: Biological screening results of hydroxide compounds against NDM-1

Compound Number	X	RA [%], 100 µM
7.4		93
7.7		56
7.8		98
7.9		95
7.10		70
7.11		74
7.12		49
7.13		97

None of the tested compounds gave a residual activity measurement of less than 30% at 100 µM therefore no IC_{50} measurements were determined. Overall there was no significant trend in the data. Increasing the hydrophobicity of the inhibitor is seen to weakly increase the inhibitory effect of the compound against the enzymes. This weak trend is observed in the SPROUT score however due to the low biological activity this effect was not investigated further.

7.3.3 Structure activity relationship investigation of the zinc binding group

Along with the investigation of substituents on the phenyl ring attached to the 'war head' group an investigation was conducted into the effects of changing the alcohol (**7.4**) into a thiol (**7.21**) (**Figure 78**).
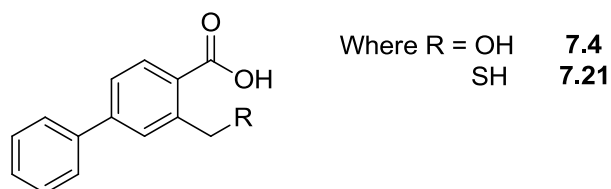

Where R = OH   **7.4**
SH   **7.21**

Figure 78: Site of heteroatom substitution on compound **7.4**

7.3.3.1 Thiol-based compound synthesis

In light of the known ability of sulfur to bind strongly to zinc, the thiol containing version of alcohol **7.4** was synthesised. It was predicted that the thiol containing compound (**7.21**) should provide a much stronger binding affinity to the MBL enzymes when compared to alcohol **7.4**. Compound **7.21** is predicted to retain the binding of the carboxylic acid to the Lys-211 residue and the edge to face π-stacking interactions with Trp-93 located within the hydrophobic wall of the active site as seen for compound **7.4** (**Figure 79 and Figure 80**).
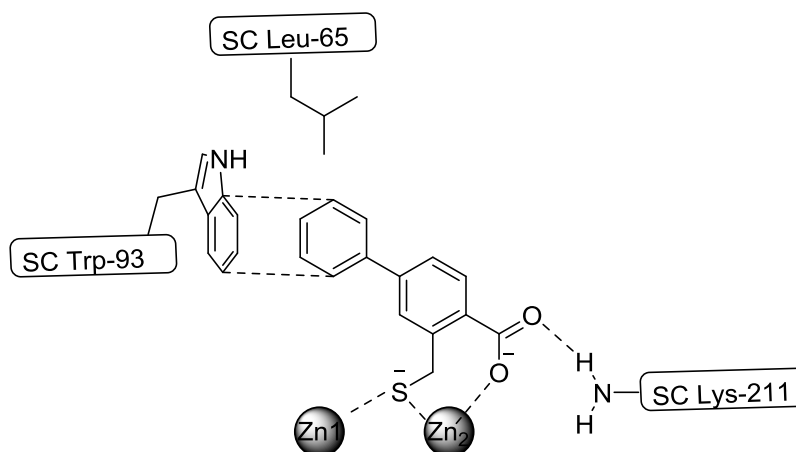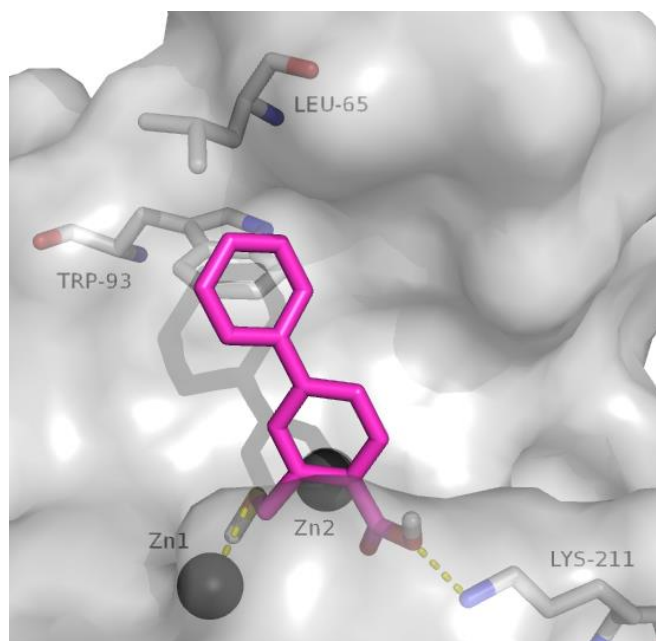

Figure 79: 2D representation of the docking pose of compound **7.21** into NDM-1 (PDB ID: 3Q6X) showing the predicted strong zinc sulfur bond

Figure 80: 3D representation of the docking pose of compound **7.21** into NDM-1 (PDB ID: 3Q6X) showing the predicted strong zinc sulfur bond

The thiol-based inhibitor (**7.21**) was synthesised as shown in **Scheme 24** by first conducting a Suzuki reaction between **7.5** and phenyl boronic acid which gave **7.6** in high yield (75%). The next step was a lactone opening of **7.6** using BBr$_3$ and NaI which gave ester **7.22** in low yield (31%). The final stage was the introduction of the thiol group by displacement of the iodine within **7.15** with thiourea and then the global hydrolysis to afford the product **7.21** (81%).
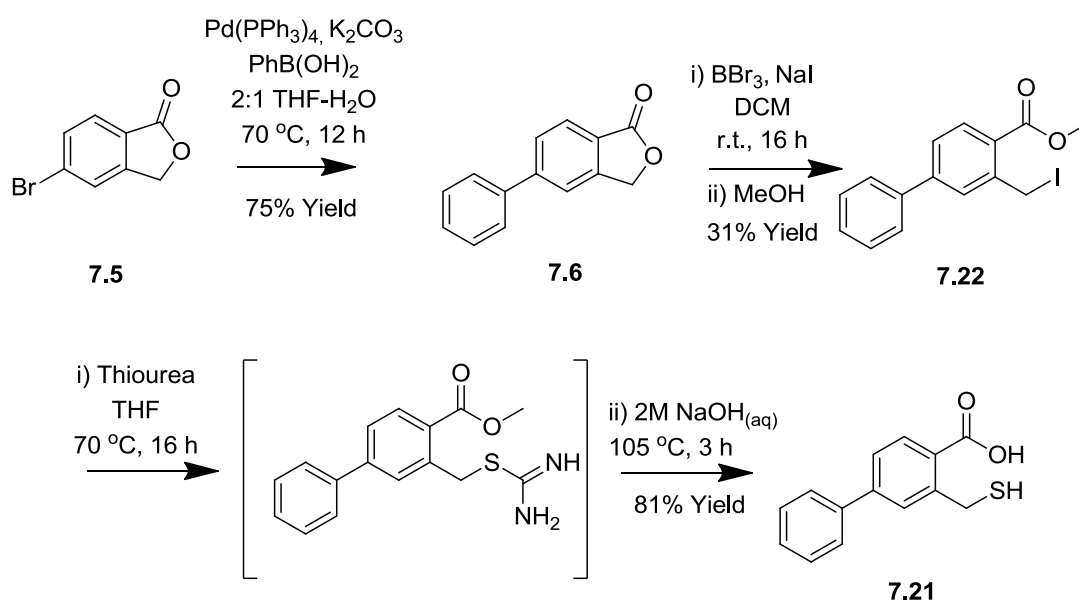
Scheme 24: Initial synthesis of compound **7.21**

Due to the use of a base hydrolysis in the final step, a portion of disulfide product was formed along with the desired mono thiol product. Purification to isolate pure mono thiol **7.21** proved unsuccessful. Column chromatography and recrystallisation attempts led to increased disulfide formation and the depletion of mono sulfide **7.21**. In order to gain an indication as to if the thiol was binding to the enzyme with better affinity than compound **7.4**, compound **7.21** was initially tested as part of a 4:1 ratio of mono to di sulfide.

7.3.3.3 Biological evaluation of thiol based compound 7.21

Compound **7.21** was biologically evaluated against NDM-1 by Dr Jürgen Brem at the University of Oxford. The result of the biological evaluation are shown in **Table 13**.
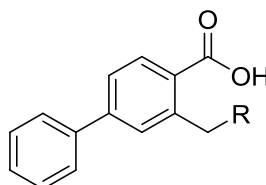
Table 13: SAR study of R group against NDM-1

Compound Number	R	RA [%], 100 μM
7.4	OH	93
7.21	SH	12

From **Table 13** we can see that the thiol-based inhibitor **7.21** was much a more potent inhibitor of NDM-1 than the alcohol **7.4**. An IC_{50} was then determined for the thiol compound **7.21** against IMP-1. **Figure 81** shows the IC_{50} curves for D-captopril and compound **7.21** against IMP-1. There is an observed IC_{50} of 12.2 ± 2 μM for captopril and 1.1 ± 0.2 μM for compound **7.21**.
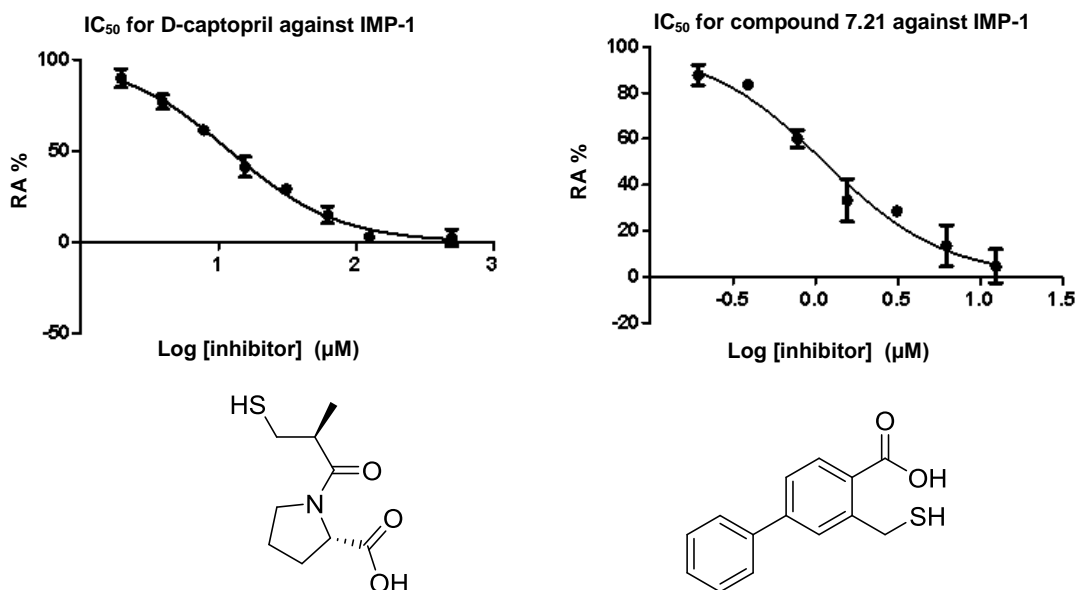
Figure 81: IC_{50} curves for D-captopril and compound **7.21** against IMP1

The inhibitory activity of compound **7.21** was also investigated in the presence of NDM-1 where it gave an IC_{50} of 24 ± 0.2 µM. D-captopril had an IC_{50} of 36 ± 0.4 µM against NDM-1. These results were very promising and therefore crystallisation of the inhibitor bound to VIM-2 was attempted along with further development of the synthetic route.

7.4 Crystallographic investigation of the binding of inhibitor 7.21 to VIM-2

In an attempt to confirm the binding mode of compound **7.21** a crystal structure was obtained of compound **7.21** co-crystallised in VIM-2 by Dr Michael MacDonough at the University of Oxford (**Figure 82**).

A strong zinc sulfur bond was observed in the active site as expected. Rather unexpectedly, there was a through-water interaction from the carboxylic acid to the Asp-117 residue. Originally this carboxyl group had been predicted to bind to Arg-205 in the active site which is similar to the Lys-211 residue in the NDM-1 enzyme (**Figure 80**). There is a face to face π-stacking interaction with the tyrosine residue Tyr-67 in the loop region. It is observed that the Arg-205 residue which is normally found located in the active site near to the zinc atoms has moved out away from the zinc atoms to accommodate the inhibitor in the active site. There was a significant

dihedral angle observed within the biphenyl unit which was not observed in the docking predictions (**Figure 83**).
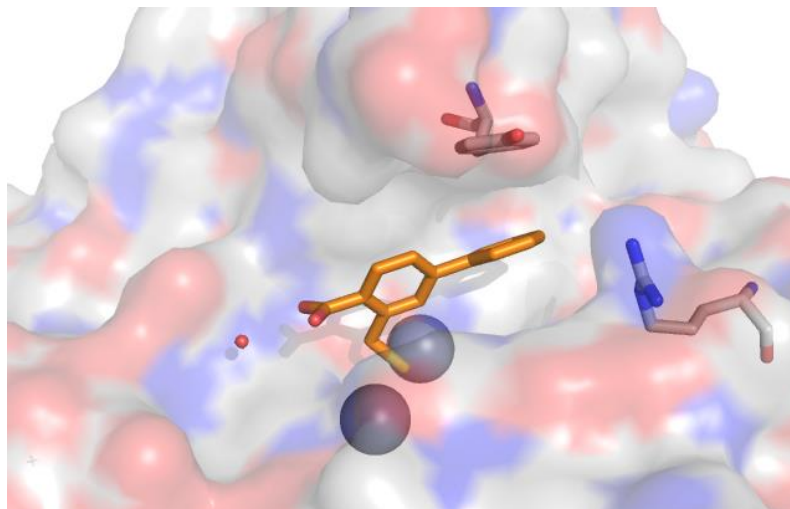
Figure 82: Crystal structure of small molecule inhibitor in the VIM-2 active site showing key interactions
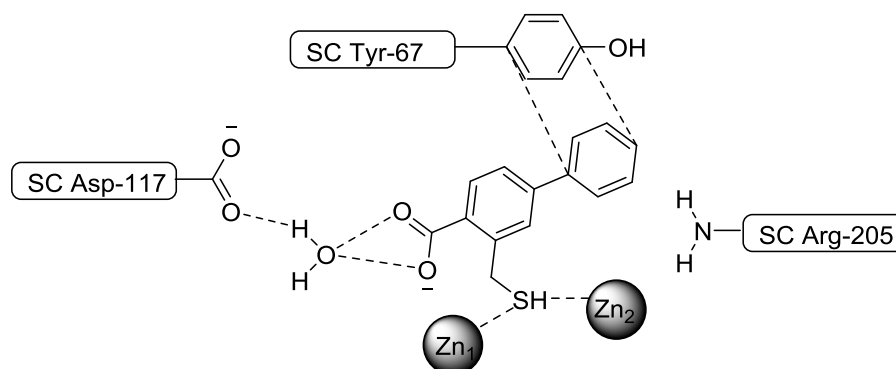
Figure 83: 2D Representation of the binding of compound **7.21** in the VIM-2 active site showing key interactions

7.5 Thiol-containing inhibitors: route development.

In order to attempt to reduce the formation of the disulfide and provide a sample of pure thiol compound **7.21**, a route development campaign was conducted. The first alteration to the route was to use aqueous 2M HCl for the final hydrolysis ensuring protonation of the thiol after the reaction and therefore preventing the disulfide formation (**Scheme 25**). However after 24 hours under reflux with dilute HCl no deprotection of the methyl ester was seen. This deprotection problem was seen as a key problem as the carboxylic acid was required for strong binding in the active site.
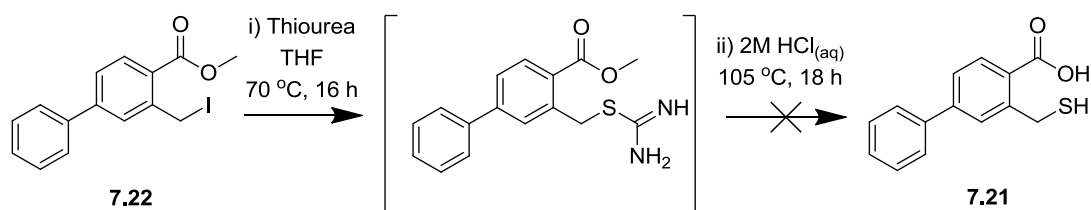
Scheme 25: The final steps of the synthesis of compound **7.21** using acid hydrolysis conditions

A second synthetic route was developed which would hopefully remove the problem of disulfide formation (**Scheme 26**). The route was also designed to move the diversification point to much later in the synthesis. The trityl protecting group was introduced after hydrolysis of the thiourea adduct and methyl ester to form compound **7.24** which could be easily separated from the disulfide *via* column chromatography. After this, the Suzuki reaction of compound **7.24** and phenyl boronic acid to form **7.25** could be conducted before removal of the trityl group using Reagent K (87% TFA, 3% ethanedithiol, 5% thioanisole, 5% H_2O) to afford compound **7.21**.
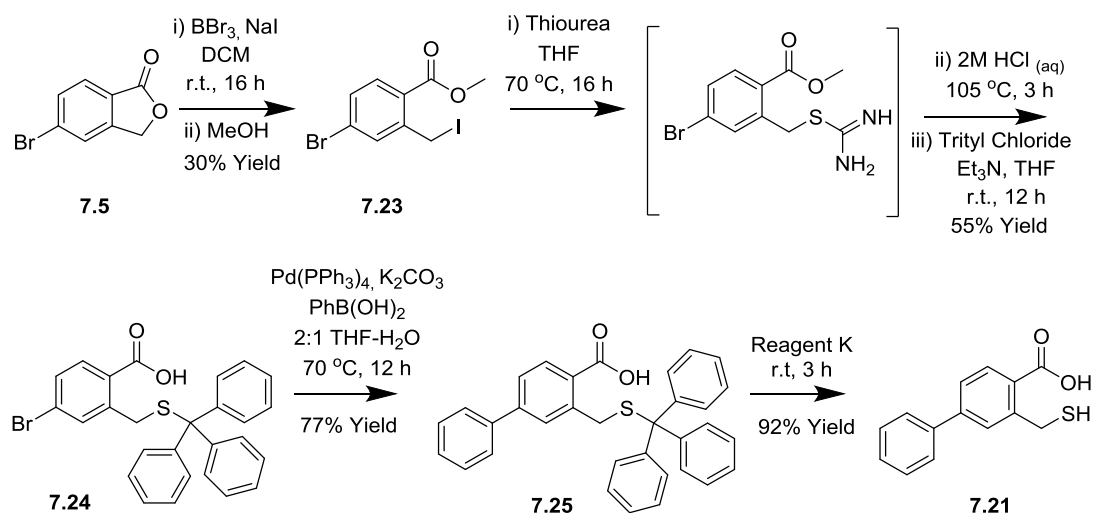
Scheme 26:Synthetic route to palladium contaminated palladium product

When thiol compound **7.21** was produced using the synthetic route set out in **Scheme 26** erroneous results were observed in the assay showing weak binding when compared to captopril and the previous mono/disulfide mixture. Most analytical techniques showed that the desired product **7.21** had been formed and isolated in high purity, However, microanalysis was

conducted on the product and it showed the presence of a metal due to a very large deviation to the expected percentage composition. The thiol-containing compound **7.21** was retaining the palladium from the Suzuki cross coupling reaction. A new synthetic route was therefore required avoiding the exposure of the thiol to metals.

The final route shown in **Scheme 27** which proved to be the most successful involves first a Suzuki cross coupling reaction between **7.5** and phenyl boronic acid which proceeds in good yield to give compound **7.6** (67%). Then a ring opening of the lactone **7.6** using TMSI which proceeded in high yield compared to the previous BBr$_3$ route to give iodide **7.26** (62%). The iodine containing intermediate was characterised by ^{1}H NMR, IR and MS. Full characterisation of **7.26** was not possible due to the degradation of the product by the loss of iodine in solution. The final two-part reaction was the introduction of the thiol group by nucleophilic displacement of the iodine within compound **7.26** by thiourea. The product of which was recrystallized before hydrolysis of the thiourea adduct with base to afford the desired product **7.21** in good yield (81%).
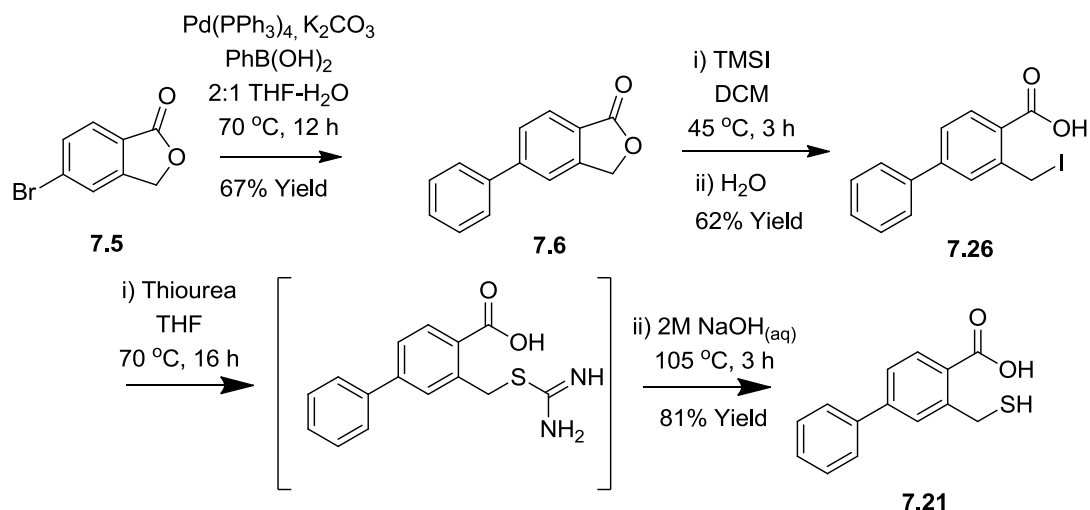

Scheme 27: Synthetic route to thiol based inhibitors featuring TMSI ring opening step.

Compound **7.21** was proved to be the thiol as opposed to disulfide (**7.27**) using NMR analysis. Conversion of the mono to disulfide can be monitored using the shift in the retention time within the HPLC and the change in the ^{1}H NMR spectrum of the reaction mixture (**Figure 85**).

Biological evaluation of pure **7.21**, produced by the route described in **Scheme 27**, gave a residual activity of < 1 % against IMP-1 at 100 μM. The IC_{50} of compound **7.21** against IMP-1 was calculated to be 232 nM.

The disulfide (**7.27**, **Figure 84**) was prepared using the conditions described by Niwa *et al.*[176] The disulphide (**7.27**) was biologically screened against IMP-1 and exhibited low inhibitory activity with a residual activity of 94% at 100 μM. The IC_{50} of disulfide **7.27** was therefore not determined as the residual activity was > 50%. The results of the biological evaluation confirm the mono thiol **7.21** to be the active inhibitor species.
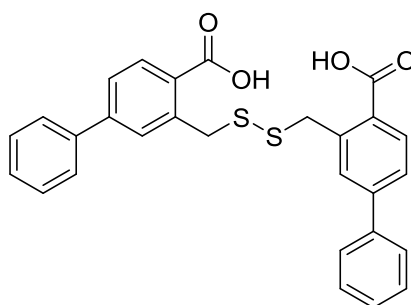
Figure 84: The structure of disulfide **7.27**

Before compound **7.21** could be considered for microbiological testing to see if it helped to recover the MIC of meropenem, the stability of the thiol in DMSO needed to be established. The stability of compound **7.21** needed to be established in DMSO because DMSO as the solvent used to dissolve compounds for the bacterial cell based assay. Compound **7.21** was found to be stable in DMSO up to 4 days by conducting NMR studies at relevant intervals. The NMR studies monitored the disappearance of the CH_2 and SH peaks, which show distinctive coupling to each other, and the appearance of the CH_2 singlet of the disulfide (**Figure 85**).

Thiol
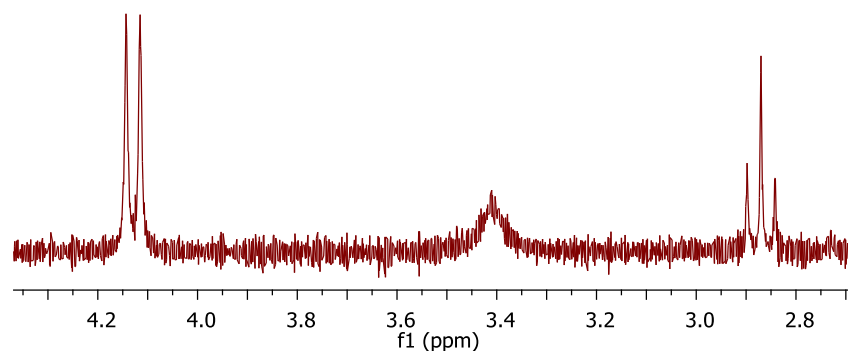
Disulfide
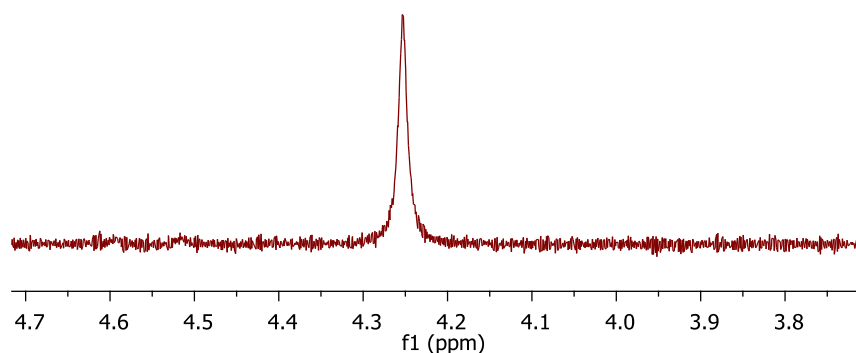
Figure 85: ^{1}H NMR spectra of key regions for determination of thiol or disulfide production.
Thiol: 4.13 (2H, d, J 7.4, C$\underline{H}_2$SH), 2.86 (1H, t, J 7.4, CH$_2$S$\underline{H}$).
Disulfide: 4.25 (4H, s, CH$_2$S)

7.6 Second generation *de novo* designed inhibitors

As observed in the crystal structure of **7.21** co-crystallised in VIM-2 (**Figure 82**), it is believed that adding an electron withdrawing group onto the phenyl ring attached to the 'war head' group would increase the binding affinity. This is due to increased face to face π-stacking interactions with the electron rich Tyr-67 residue. A structure activity relationship study was conducted to confirm this hypothesis (**Figure 86**).

X= **7.28-7.41**

7.21
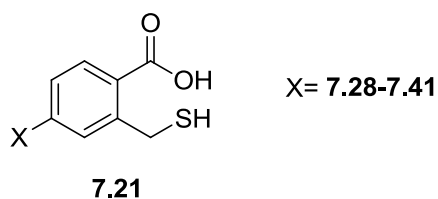
Figure 86: Location of SAR variation for thiol series

The phenyl group of compound **7.21** was also substituted for a bromine (**7.41**) to see if this had negative effects on the binding affinity due to the loss of the π-stacking interactions. Two examples were included which contained 5 membered rings (**7.36** and **7.38**) to see what effect changing from a 6 membered ring had on the binding affinity. **Scheme 28** shows the synthetic route to the thiol based compounds.
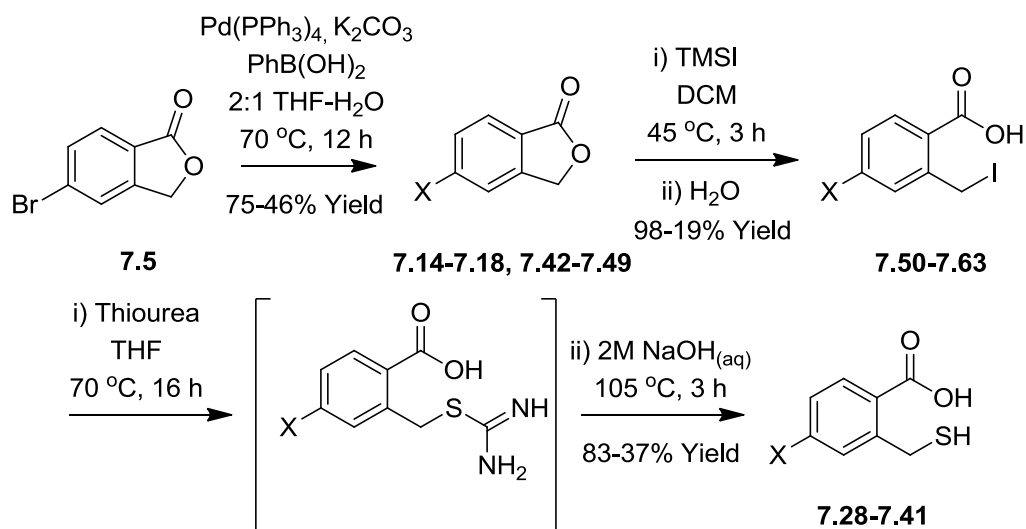
Scheme 28: Synthetic route to compounds **7.28-7.41** based around thiol compound **7.21**

Due to the observed dihedral angle in the crystal structure of compound **7.21** co-crystallised in VIM-2. Substituents were placed in the ortho position of the phenyl ring attached to the 'war head' group (Position X, **Figure 86**) to explore the role of the dihedral angle of the biphenyl ring system to investigate if changing the dihedral angle effects the binding affinity (**7.28** and **7.33**). Substituents were also placed in the meta and para positions of the phenyl group, attached to the 'war head' group (Position X, **Figure 86**), to investigate if placing substituents around the ring changed the binding affinity (**7.28**, **7.29** and **7.30**).

Compounds containing strong electron withdrawing groups, such as nitro groups and carboxylic acids, gave very poor yields for the Suzuki coupling reaction (<30%). The compounds also proved be very water soluble leading to problems with isolation of the iodine containing intermediate compounds following opening of the lactone with TMSI. A number of impurities from this step were then carried through the introduction of the thiol and hydrolysis steps lead to significantly impure final thiol compounds. Although purification

attempts through column chromatography and recrystallization were made, no compounds containing electron withdrawing groups could be obtained in high enough purity for biological testing. There was therefore no compounds containing electron withdrawing groups, such as nitro or carboxylic acids, that were tested against the MBL enzymes.
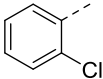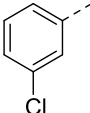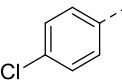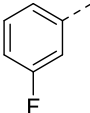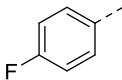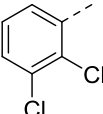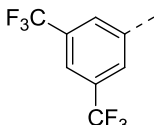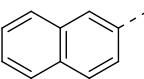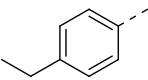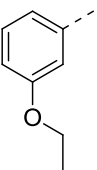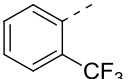
Generally, there is no clear trend from the SAR study, and it has been observed that changing the electron density on the phenyl ring of **7.21** has no real effect on the potency of the molecules (**Table 14**).

It is also observed that putting groups into the ortho position (**7.28, 7.33** and **7.40**) on the phenyl ring does not affect the binding affinity of the compounds to the IMP-1 enzyme implying the dihedral angle of the biphenyl unit does not have a large contribution to the binding affinity. However, In placing groups in the ortho position does lower the IC_{50} of the compounds against the VIM-2 enzyme. This result suggests that the increase in the dihedral angle of the biphenyl unit is favourable for binding to the VIM-2 enzyme.

Substitution of the phenyl ring for five membered rings (**7.36** and **7.38**) shows no significant change in the binding affinity of the inhibitors. This implies that the π-stacking interaction is not a major component of the binding affinity. Substitution of the phenyl ring for a bromine shows no change to the binding affinity for VIM-2. However, for IMP-1 there is a significant increase in the IC_{50} indicating that a bromine is not tolerated as well within this enzyme.

Placing groups onto the phenyl ring, attached to the 'war head' group, in the meta position lowers the IC_{50} of the inhibitor compounds towards the VIM-2 enzyme. In general increasing the hydrophobicity of the inhibitors causes them to exhibit stronger binding to the VIM-2 enzyme (**7.33** and **7.35**). The same effect is not observed for the IMP-1 enzyme where placing groups into the meta position weakens the binding affinity. Compound **7.30** exhibits the best IC50 against IMP-1 and contains a chloro group in the para position. This is potentially rationalised by the more enclosed active site seen in the IMP-1 enzyme compared to the VIM-2 enzyme (see Section 2.4.2.1)

Table 14: Biological evaluation results of thiol series SAR study

Compound Number	X	RA [%], 100 μM (VIM-2)	IC$_{50}$ VIM-2 (μM)	IC$_{50}$ IMP-1 (μM)
7.21		< 1	0.234 ± 0.044	0.232 ± 0.043
7.28		< 1	0.180 ± 0.098	0.309 ± 0.067
7.29		< 1	0.072 ± 0.059	0.147 ± 0.057
7.30		< 1	0.109 ± 0.039	0.069 ± 0.052
7.31		< 1	0.207 ± 0.069	0.397 ± 0.089
7.32		< 1	0.231 ± 0.030	0.307 ± 0.094
7.33		< 1	0.045 ± 0.031	0.378 ± 0.062
7.34		< 1	0.459 ± 0.073	1.723 ± 0.047
7.35		< 1	0.071 ± 0.031	0.220 ± 0.035
7.36		< 1	0.365 ± 0.023	0.393 ± 0.035
7.37		< 1	N.A.	N.A
7.38		1.25	0.174 ± 0.127	0.189 ± 0.049
7.39		< 1	0.184 ± 0.165	0.323 ± 0.037
7.40		< 1	0.158 ± 0.089	0.480 ± 0.045
7.41		< 1	0.170 ± 0.018	0.804 ± 0.030

N.A. = Not determined due to limited solubility

The thiolactone (**7.64**) was also synthesised and biologically evaluated. This could investigate if the thiolactone ring could be hydrolysed under the conditions of the assay to give inhibitor **7.21**. The idea being that this method could be used to produce a pro-drug to help with the administration of the compound with the thiol 'war head' masked until hydrolysed by the enzyme. To so synthesise **7.64**, compound **7.21** was refluxed in TFA to afford thiolactone **7.64** in good yield (99%) (**Scheme 29**).
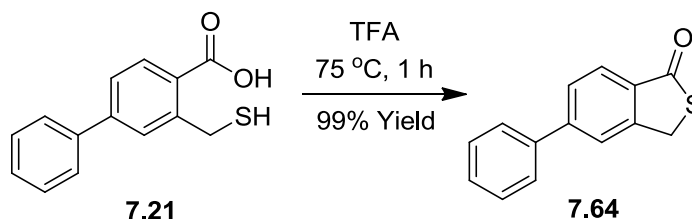
Scheme 29: Synthesis of thiolactone **7.64**

Additionally, compound (**7.67**) with the thiol group directly on the aromatic ring and a spacer to the carboxylic acid moiety, was also prepared and screened to probe the importance of the spatial arrangement of the groups. To synthesise **7.67**, boronic acid **7.65** was oxidised to thiolactone **7.66** with hydrogen peroxide in good yield (97%). Thiolactone **7.66** was then hydrolysed using base to yield compound **7.67** in good yield (93%) (**Scheme 30**).
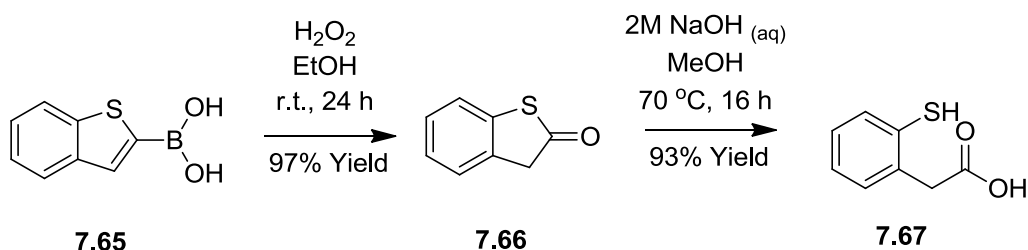
Scheme 30: Synthesis of compound **7.67**

Neither of these compounds (**7.64** and **7.67**) gave significant inhibitory activity in the presence of the NDM-1 enzyme. The thiolactone **7.64** gave a residual activity (RA) of 90% at 100 µM against NDM-1, which is significantly higher than the RA of **7.21** which is < 1% at 100 µM against NDM-1. No IC_{50} was determined for **7.64** against the MBLs as the RA was above 30%. The observed RA implies that **7.64** is not being hydrolysed rapidly by the NDM-1

enzyme. The results however do not confirm if hydrolysis is occurring slowly or not at all. Further biological evaluation would be required to establish this.

Compound **7.67** has a RA of 92% at 100 µM against NDM-1, which is significantly higher than the RA of **7.21** of < 1% at 100 µM against NDM-1. No IC_{50} was determined **7.67** against the MBLs as the RA was above 30%. This shows that the spatial arrangement of the thiol in relation to the benzene and carboxylic acid is important to the observed binding affinity of **7.21**.

7.6 Microbiology results

As the compounds (**7.21**, **7.28-7.41**) had shown significant activity against the enzyme in the enzymatic assay, a selection of these compounds was sent to Dr James Spencer, at the University of Bristol, to see if they had any effect on restoring the MIC of meropenem against MBL producing bacterial strains.

Microbiological screening was conducted by Dr James Spencer, at the University of Bristol, as described in Appendix A1.2 (**Table 15**).
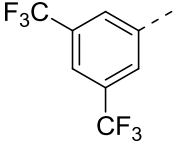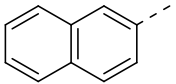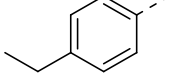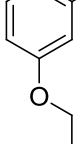
Initial tests of the MBL-producing bacteria with meropenem in the absence of inhibitor gave an MIC >128 µg/ml. Testing also showed that inhibitor **7.21** had no antibacterial effect on the enzyme alone. This confirmed that the inhibitor was suitable in terms of investigation into possible co-administered with a β-lactam antibiotic to achieve the desired effects.

Encouragingly, all the compounds, apart from **7.34**, showed restoration of the MIC of meropenem against the NDM-1-producing strains when using 100 µg/ml of inhibitor. Compound **7.38** was seen to be the best, showing restoration of the MIC of meropenem to 8 µg/ml against *K. pneumoniae.* Unfortunately when using a lower concentration (10 µg/mL) of inhibitor no significant change in the MIC of meropenem was observed.

There could be a number of reasons for no restoration of the MIC of meropenem being observed at lower concentrations (10 µg/ml). With compounds **7.21, 7.28-7.41** all displaying IC_{50}'s in the nanomolar region against both VIM-2 and IMP-1 enzymatic assays some restoration of the

meropenem MIC would be expected at this concentration. The first reason for no MIC restoration to be observed is that the thiol-containing compounds may have limited permeability through the outer membrane of the Gram Negative bacterial call wall. The second is that the compounds could be making it into the cell however are being effluxed out of the cell by efflux pumps. Further biological evaluation looking into efflux knockouts and membrane damaged bacteria will be required to be conducted to provide a conclusive answer to the lack of restoration of the MIC at lower concentrations.

Table 15: Determination of Meropenem MIC against bacterial strains when administered with designed inhibitors

Compound Number	Structure	Meropenem MIC (µg/mL) NDM-1 producing *K. pneumoniae* (ATCC 5055)	Meropenem MIC (µg/mL) NDM-1 producing *E. coli* (MG1655)
7.21		32	16
7.41	Br	64	32
7.34	F₃C CF₃	>128	>128
7.35		32	32
7.36	O	64	32
7.37		64	32
7.38	S	8	16
7.39	O	16	64

7.7 Drug Metabolism and PharmoKinetics studies (DMPK)

Before committing to full *in vivo* studies, compound **7.21** was sent to the DMPK group at Shanghai ChemPartner Co., Ltd for aqueous solubility and metabolic stability testing.[177]

ChemPartner state that aqueous solubility values less than 10 µM suggest compounds show low solubility, solubility values between 10 µM and 80 µM suggest compounds show moderate solubility and solubility values higher than 80 µM suggest compounds show high solubility. Compound **7.21** recorded an aqueous solubility of 88.45 µM in phosphate buffer solution (PBS, pH 7.4) with an RSD of 0.06. This indicates that compound **7.21** has high solubility at this pH.

For a metabolic study with human liver microsomes, ChemPartner state that $T_{1/2}$ values where $T_{1/2} > 120$ min suggest compounds are stable in human liver microsomes, where $T_{1/2} = 30\text{-}120$ min suggest compounds show moderate metabolism in human liver microsomes, and where $T_{1/2} < 30$ min suggest compounds are susceptible to metabolism in human liver microsomes. Compound **7.21** recorded a $T_{1/2} = 82.28$ mins which suggests that the compound is showing moderate metabolism in human liver microsomes. Compound **7.21** recorded an intrinsic predicted clearance rate of 21.13 (mL/min/kg). Ideally before progressing compound **7.21** into more *in vivo* studies, further modifications would be required to remove the metabolic susceptibility of the compound and increase the half-life.

7.8 Drug delivery

In order to overcome the potential limited permeability of the inhibitors through the outer membrane of Gram negative bacteria, the idea of 'co-drugging' was employed. The principle has been used in a number co-drugs, for example a quinolone drug attached to a cephalosporin through an ester linker has been investigated (**7.68**, **Figure 87**). Upon hydrolysis of the β-lactam, the resulting cascade results in the release of the carboxylic acid leaving the alkene containing hydrolysed cephalosporin (**Figure 88**).
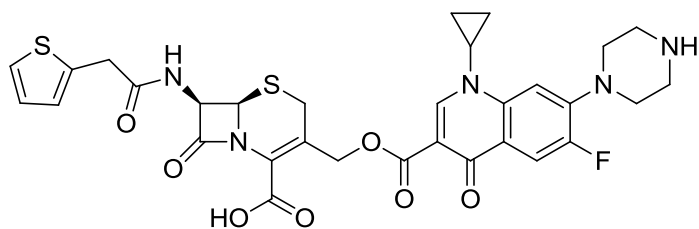
7.68

Figure 87: Structure of a cephalosporin-quinolone co-drug (**7.68**)

Beta-lactamase
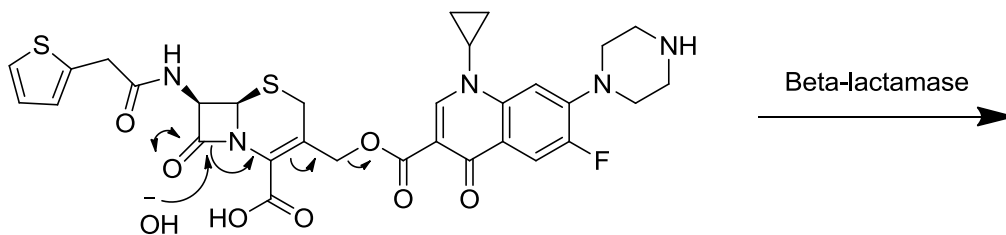
7.68
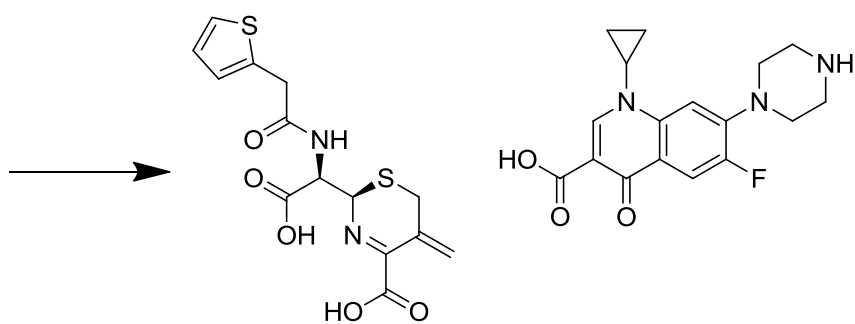
7.69   **7.70**

Figure 88: The hydrolysis cascade of a cephalosporin - quinalone co-drug (**7.68**) releasing the quinalone (**7.70**)

The aim in the present study was to couple compound **7.21** to a cephalosporin to help **7.21** permeate through the outer membrane of the Gram negative bacterial call wall. Once through, hydrolysis of the β-lactam in the co-drug will occur in the active site of the MBL which then releases the inhibitor following the cascade reaction. The inhibitor could then bind to the active site of the MBL preventing further β-lactam antibiotics administered with the co-drug from being hydrolysed. The inhibitor molecule **7.21** was coupled onto the cephalosporin cephlatin (**7.71**) using the S_N2 displacement of the acetate group by the thiol of the inhibitor (**Scheme 31**).
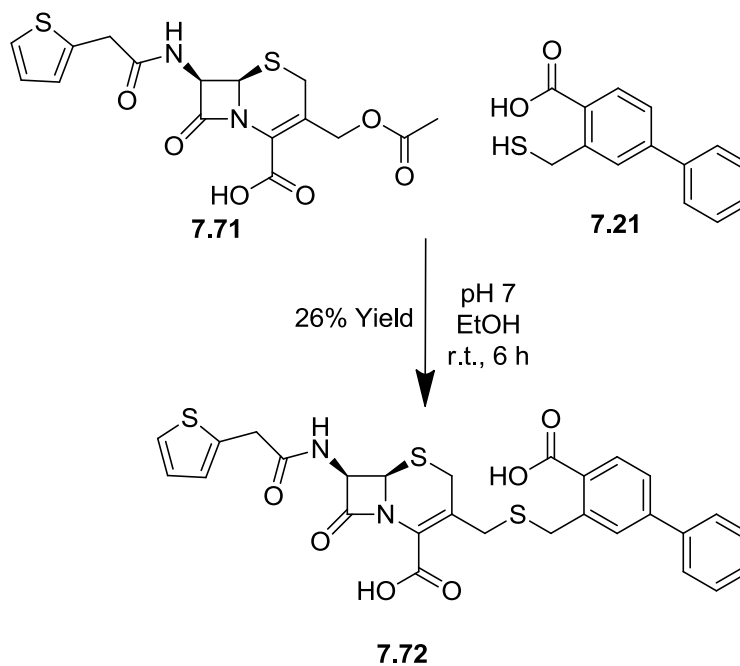
Scheme 31: Coupling of compound **7.21** onto ceflatin **7.71** to form compound **7.72**
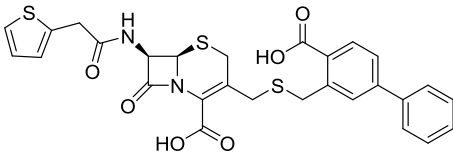
The product **7.72** was predicted to undergo fragmentation in a similar manner to the previously described co-drugs following hydrolysis of the β-lactam ring as shown in **Figure 89**.
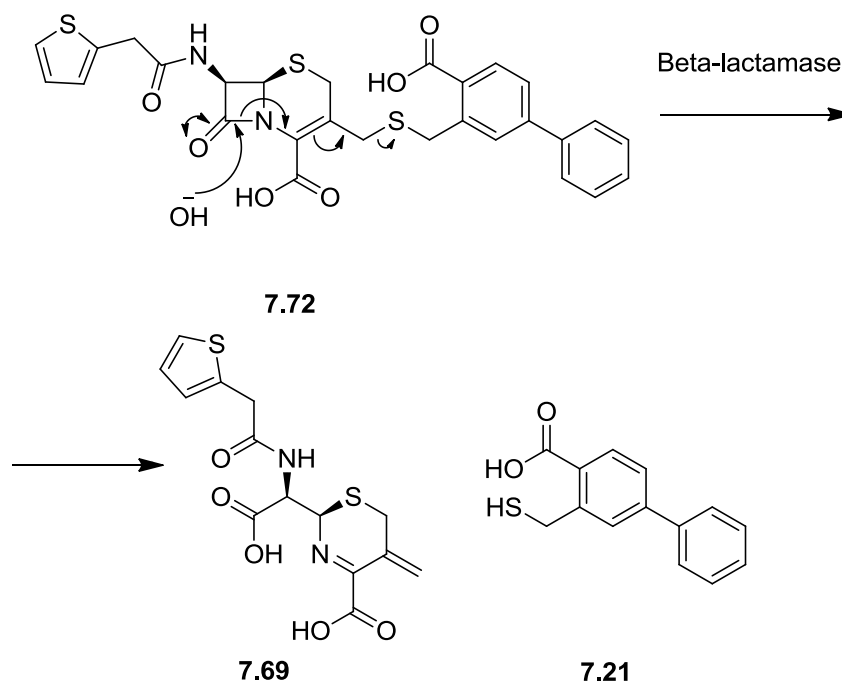
Figure 89: Hydrolysis cascade of cephalosporin containing compound **7.21** to release compound **7.21**.

The synthesis of **7.72** was conducted as described in **Scheme 31**. Compound **7.72** was then sent for testing in the enzymatic and microbiological assays (**Table 16**).

Table 16: Biological data for cephalosporin containing compound **7.72**

Compound Number	Structure	RA [%], 100 µM VIM-2	RA [%], 100 µM NDM-1
7.72		13.4	2.7

The initial biological screens at 100 µM against VIM-2 and NDM-1 show promising reduction in the activity. The residual activity is larger than for **7.21** alone. Further biological testing is required to establish the IC_{50} of the co-drug inhibitor and if the **7.72** can successfully restore the MIC of meropenem against NDM-1 producing bacteria to a greater extent than **7.21** alone. Further testing is also required to establish what is the active compound giving the reduction residual activity. It could be from **7.72** itself or from the release of **7.21** by hydrolysis.

7.9 Conclusions

A novel inhibitor class has been created using *de novo* structure based drug design which can be co-administered with current antibiotics restoring some of their activity against the bacteria. Results in tests with clinical isolates of MBL-producing bacteria have seen a restoration of the MIC of meropenem from >128 ug/mL to 8 ug/mL when administered with designed inhibitors. Additionally a number of these inhibitors have shown strong inhibition of the VIM-2 and IMP-1 enzymes in the enzymatic assays at around 200 nM.

In general, sulfur-containing drugs have often been avoided in medicinal chemistry due to side effect such as Stevens–Johnson syndrome,[178] a form of toxic epidermal necrolysis and a life-threatening skin condition. However we should not shy away from the use of sulfur containing compounds as a number have been seen to be successful in the clinic. An example of which is ticagrelor, which is marketed as Brilinta,[179] a platelet aggregator inhibitor. Further toxicity studies are required for the MBL inhibitors described in this thesis but initial testing against bacteria has been promising. Initial DMPK

studies show that one of the designed inhibitors is highly soluble in aqueous media but is susceptible to metabolic degradation by liver microsomes. Further development would be required to overcome this aspect.

Unlike a number of MBL inhibitors which have previously been discovered, this class of inhibitor is not a metal extractor and does not function by pulling the zincs out of the enzyme, but instead by chelating to them within the active site. This has been observed *via* crystallography and is consistent with the observations of Klingler *et al.*[68] who state that thiol compounds chelate and do not extract the zinc atoms out of the enzyme. There is still a question over the selectivity of the compounds over other metal-containing systems such as ACE which captopril is the known inhibitor. Due to limited access to an ACE assay and selectivity panel this has not been further investigated.

Further research should be conducted into overcoming the high loading required to rescue the activity. As suggested the high loading could be required due to poor permeability of the outer membrane or from efflux. A number of studies could be conducted looking at efflux knockouts and membrane permeating peptides to see what is causing the lower than optimally desired responses.

Chapter 8
In silico assay evaluation[82]

8.1 Introduction to MBL assays

A number of different screening methods for *in vitro* detection of β-lactamases have been reported in the literature.[180] Current assays in use for β-lactamase enzymes include the use of chromogenic cephalosporin-based substrates such as nitrocefin[181] and CENTA,[182] cephalosporin based fluorogenic substrates,[183] bioluminescent probes[184] and fluorescence resonance energy transfer (FRET)-based substrates.[185]

Widespread use of these types of compounds in HTS for MBL detection is often avoided due to their long and often difficult synthesis and the high costs associated with these substrates. These substrates often suffer from poor recognition by the MBLs due to the high diversity of the enzyme family. Additionally, the MBL family of enzymes vary in sequence, structure and substrate specificity therefore making it hard to use a single substrate for broad MBL activity screening.

Collaborators at the University of Oxford aimed to develop *in vitro* assay procedures suitable for a range of clinically relevant enzymes. The clinically relevant enzymes chosen were New Delhi metallo-β-lactamase (NDM-1),[38] Verona interon-encoded metallo-β-lactamase (VIM-2),[64] Imipenemase (IMP-1)[79] and Sao Paulo metallo-β-lactamase (SPM-1).[62] The substrates tested against the panel of MBLs were Nitrocefin[181] (**8.1**), CENTA[182] (**8.2**), Imipenem (**8.3**), and an in-house fluorogenic compound **8.4** (**Figure 90**). Each substrate was biologically evaluated against the panel of MBLs to identify the best substrate. (See Section 8.3.2 for NDM-1, IMP-1 and VIM-2 and see Section 8.3.3 for SPM-1)

To understand and rationalise the substrate binding constants of Nitrocefin (**8.1**), CENTA (**8.2**), Imipenem (**8.3**) and compound **8.4** for the different MBLs, *in silico* docking studies were performed to predict binding modes of the substrates to the enzymes. The *in silico* studies were conducted at the

University of Leeds and the results were compared against the *in vitro* biological evaluation data.

Nitrocefin (**8.1**)

CENTA (**8.2**)

Imipenem (**8.3**)

Fluorogenic compound **8.4**
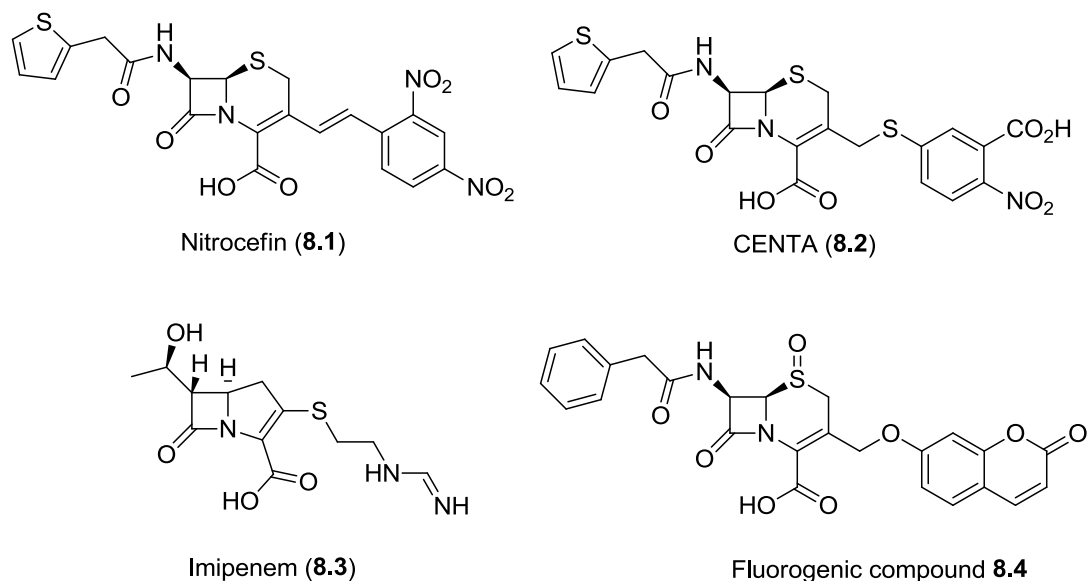
Figure 90: 2D Structures of Nitrocefin (**8.1**), CENTA (**8.2**), Imipenem (**8.3**) and fluorogenic compound **8.4**

8.2 Docking protocol

The *in silico* docking studies were conducted using AutoDock[88, 100] and SPROUT[125] as described below.

The following protocol was used:

1. Nitrocefin (**8.1**), CENTA (**8.2**), Imipenem (**8.3**), and compound **8.4**, in substrate form were constructed in maestro.[139] The resulting structures were then fully energy minimised using the multiple minimisation tool (MM).

2. Each compound was then imported into the SPROUT[125] programme and docked into the di-zinc containing active site of the crystal structure of NDM-1 (PDB ID: 3Q6X[38]).

3. SPROUT scores were taken of the resulting docking 'poses' (these are generated as negative log numbers such that a value of, say -6, corresponds- *very approximately-* to a predicted binding affinity of 1 x 10^{-6} M, i.e. μM).

4. These docking results were also independently assessed *via* repeating the docking procedure again using AutoDock[88, 100] which

utilises a different docking algorithm to that used within the SPROUT software. Again, the resulting docking 'poses' were scored, both within AutoDock and also using the SPROUT scoring function for comparison.

5. The procedure was repeated for IMP-1 (PDB ID: 1JJT[79]), SPM-1 (PDB ID: 2FHX[62]) and VIM-2 (PDB ID: 1KO3[64]).

8.3 *In silico* docking studies

8.3.1 Docking to IMP-1, NDM-1 and VIM-2

The predicted enzyme-substrate complex structures show some similarities in terms of orientation of the substrates within the binding cavity (**Figure 91a**). Both Nitrocefin (**8.1**) and CENTA (**8.2**) are predicted to bind in almost identical orientations having the C-4 carboxylic acid of the cephalosporin-derived thiazine ring positioned between the two zinc atoms of IMP-1 (**Figure 91b**). A similar situation can be seen in the NDM-1 and VIM-2 enzymes.
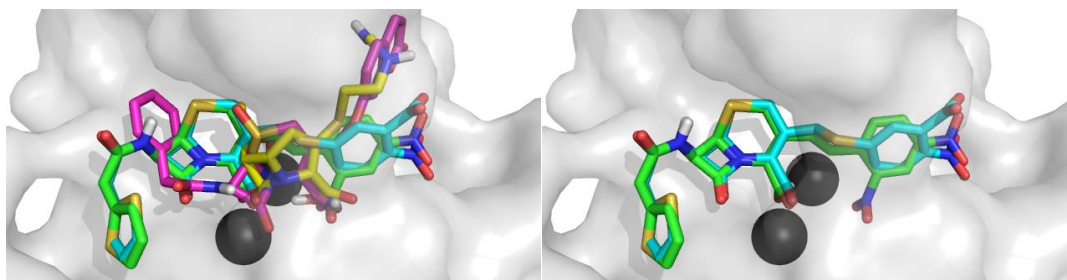
Figure 91: a) Overlay of Nitrocefin (**8.1**, green), Imipenem (**8.3**, yellow), CENTA (**8.2**, blue) and compound **8.4** (pink) structures modelled in the active site of IMP-1 (PDB ID: 1JJT); b) Overlay of Nitrocefin (**8.1**, green) and CENTA (**8.2**, blue).

Differences are found in the binding of the C-3' nitrophenyl ring systems (see **Figure 92** and **Figure 93**). In the case of Nitrocefin (**8.1**), the *ortho*-nitro group is positioned to form a hydrogen bond with Lys-161. This hydrogen bond does not occur in the case of CENTA (**8.2**). However, the carboxylic acid on the thiophenol ring of CENTA (**8.2**) is able to form a hydrogen bond with the indole nitrogen of Trp-28. (**Figure 91b**)
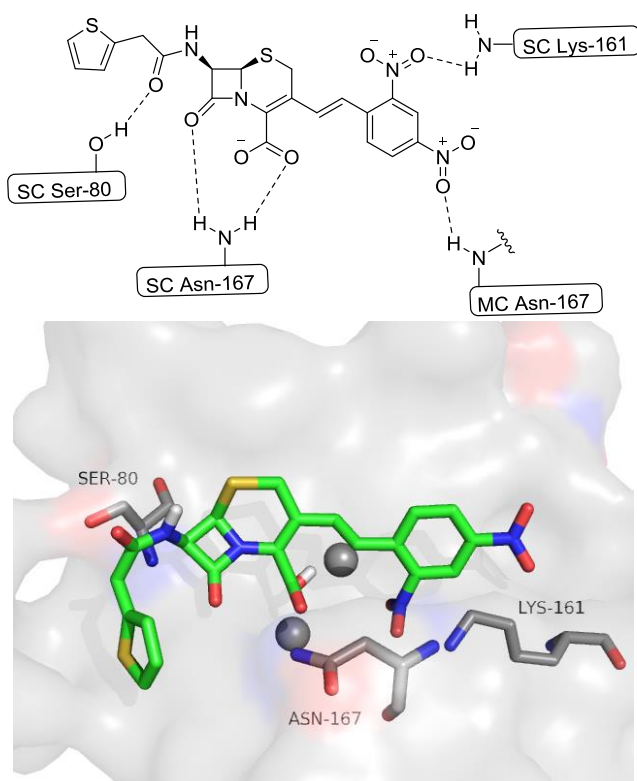
Figure 92: Binding of Nitrocefin (**8.1**) to IMP-1 (PDB ID: 1JJT): a) 2D Binding representation, b) 3D spatial representation
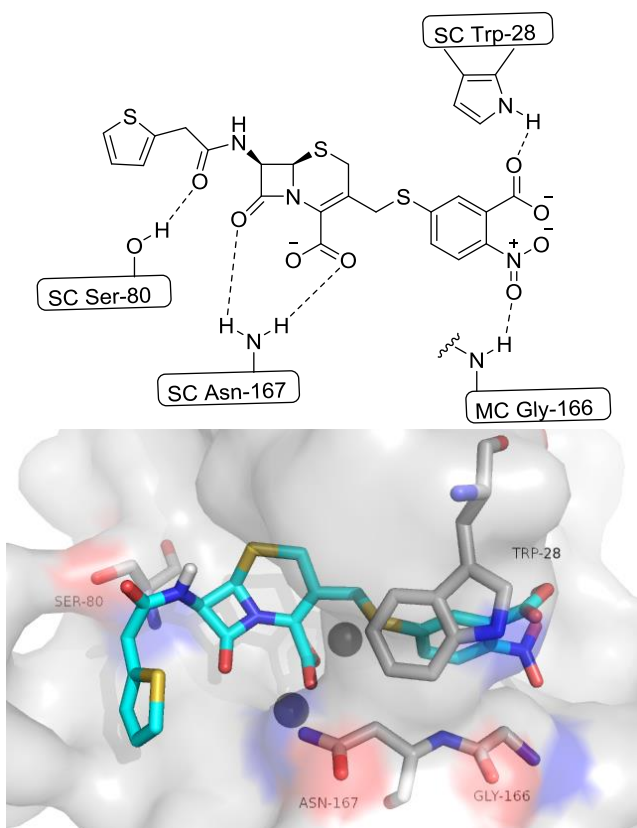
Figure 93: Binding of CENTA (**8.2**) to IMP-1 (PDB ID: 1JJT): a) 2D Binding representation, b) 3D spatial representation

Both Imipenem (**8.3**) and compound **8.4** have dissimilar zinc-binding orientations when compared to Nitrocefin (**8.1**) and CENTA (**8.2**). In the case of Imipenem (**8.3**), the β-lactam carbonyl is positioned between the two zinc atoms (**Figure 94**), whereas for compound **8.4,** coordination to the di-zinc atoms is predicted to occur *via* the C-4 carboxylic acid of the cephalosporin-derived thiazine ring and the β-lactam carbonyl respectively (**Figure 95**). Both Imipenem (**8.3**) and compound **8.4** are predicted to coordinate to Lys-161 through their C-3/C-4 carboxylic acids located on the thiazolidine and thiazine rings, respectively. This mode of binding, unlike the binding mode predicted for Nitrocefin (**8.1**) and CENTA (**8.2**) in which the C-4 carboxylate is positioned between the two zincs, is the predicted mode of productive substrate binding to MBLs.[186]

Fluorogenic compound **8.4** has the strongest predicted binding when compared to the other substrates. This is predicted to be due to an extra hydrogen bond between Glu-199 and the coumarin motif of the molecule. Nitrocefin (**8.1**) shows weak bonding to Glu-199 through its nitro groups. Imipenem (**8.3**) and CENTA do not bind to Glu-199 at all.
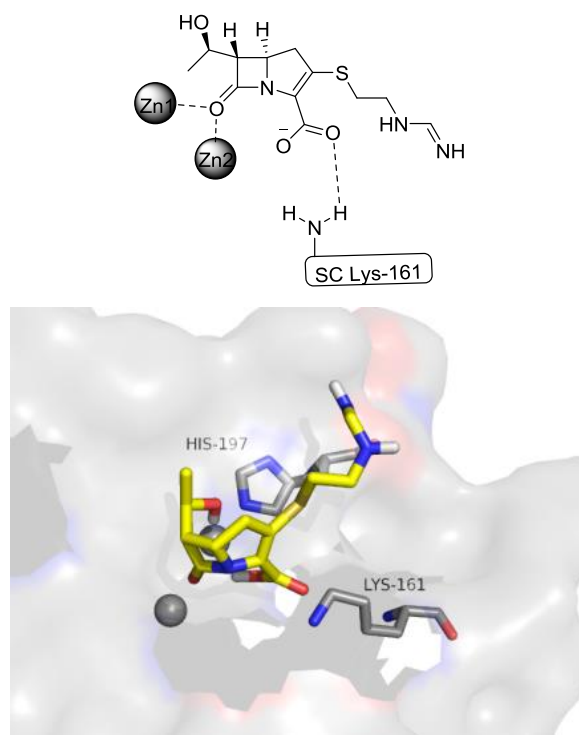
Figure 94: Binding of Imipenem (**8.3**) to IMP-1 (PDB ID: 1JJT): a) 2D Binding representation, b) 3D spatial representation
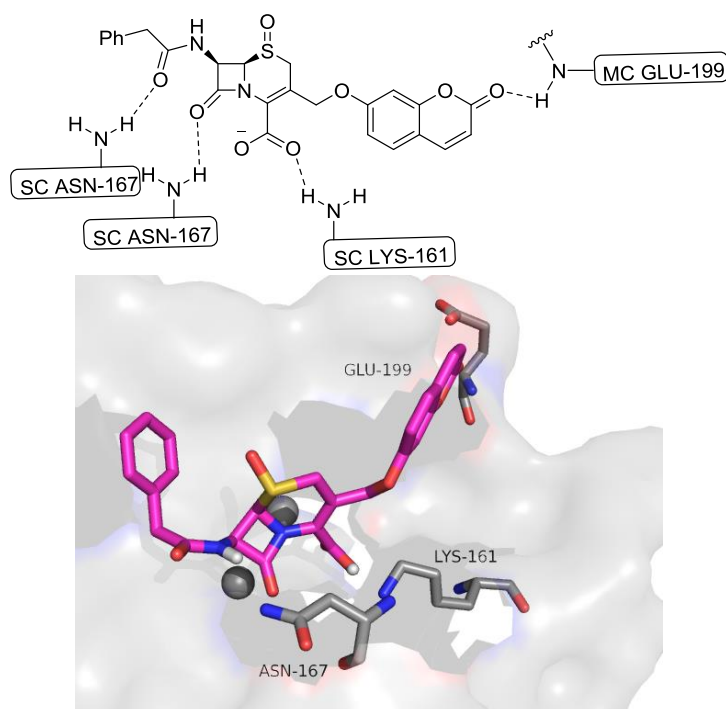
Figure 95: Binding of compound **8.4** to IMP-1 (PDB ID: 1JJT): a) 2D Binding representation, b) 3D spatial representation

Although in-depth structural analyses are required, the modelling results suggest that the cephalosporins may bind to the active site in more than one orientation, including non-catalytically productive ones. Overall, these results emphasize the importance of experimentally determining optimal MBL-substrate combinations, and the need for X-ray crystallography of MBL-substrate complexes.

8.3.2 Comparison to biological results

After analysis of the obtained substrate-enzyme models, the different docking poses, calculated using AutoDock 4 and SPROUT, were scored and compared to the substrate binding constants (K_M) (**Table 17**). Full docking analysis data can be found in Appendix A5.1.

From the biological evaluation of the substrates against the panel of MBL enzymes it was noticed that IMP-1 had much stronger binding interactions with all of the substrates than NDM-1 or VIM-2 which had similar binding scores to each other. IMP-1's much more closed active site, which includes a large hydrophobic region created by the closed L3 loop, is predicted to account for this increase in binding affinity. The *in silico* docking scores of

the substrates backs up this result predicting stronger binding for the IMP-1 enzyme compared to VIM-2 and NDM-1.

As seen in Section 2.4.2, the active sites of VIM-2 and NDM-1 have a calculated RMS similarity of 1.652 and as expected exhibit similar characteristics to each other in the *in vitro* and *in silico* studies.

Table 17: Docking scores for different substrates

Enzyme	Substrate	Normalized AutoDock Score	Normalized SPROUT Score[a]	K_M-values (μM)
IMP-1	CENTA	1.9	1.20	17.1
	Imipenem	1.25	1.23	42.7
	Nitrocefin	1.83	1.30	55.7
	8.4	1.92	1.35	15.2
NDM-1	Imipenem	1.03	0.95	111.2
	CENTA	1.18	1.01	34.6
	Nitrocefin	1.12	1.15	8.8
	8.4	1.33	1.34	4.0
VIM-2	Imipenem	1.23	0.76	37.8
	CENTA	1.15	0.81	26.1
	Nitrocefin	1.00	1.00	7.2
	8.4	1.33	1.14	6.3

[a] Note, higher normalised score equates to tighter predicted binding. Scores are ranked based on the normalized SPROUT scores going from the lowest score to the highest score.

Assessment of the AutoDock scoring data showed no clear correlations between the calculated pre-hydrolysis enzyme-substrate complexes and the experimentally obtained binding constants. In contrast to AutoDock, the SPROUT scoring data showed good correlation for NDM-1 and VIM-2; however less of a correlation was found for IMP-1. This is a clear example of where the use of a consensus scoring approach is advantageous when performing docking studies.[187]

For all three enzymes the highest ranking ligand in terms of SPROUT and AutoDock score is compound **8.4** which was also measured to have the highest binding affinity for all three enzymes. The broad correlation found, may reflect, in part, different Zn-binding modes as well as variation in the orientation of the side-chains of Imipenem (**8.3**), Nitrocefin (**8.1**), CENTA (**8.2**) and compound **8.4** (**Figure 91-Figure 95**).

8.3.3 Docking to SPM-1

Relatively poor K_M values were obtained for all substrates when biologically evaluated against SPM-1 (PDB ID: 2FHX) when compared to the other MBL enzymes. (**Table 18**, unpublished data). A similarly poor predicted binding affinity can be seen in the *in silico* studies where the AutoDock and SPROUT predicted binding scores are not comparable to the other MBL enzymes and are significantly lower. (Appendix A5.1)

The flexible loop region identified in Section 2.4.2.2 which has been seen to have an open and closed state is predicted to be the reason for the significant difference in binding affinity when compared to the other MBLs. In the closed form the flexible loop is predicted to be preventing access to the zinc atoms. (**Figure 96**)
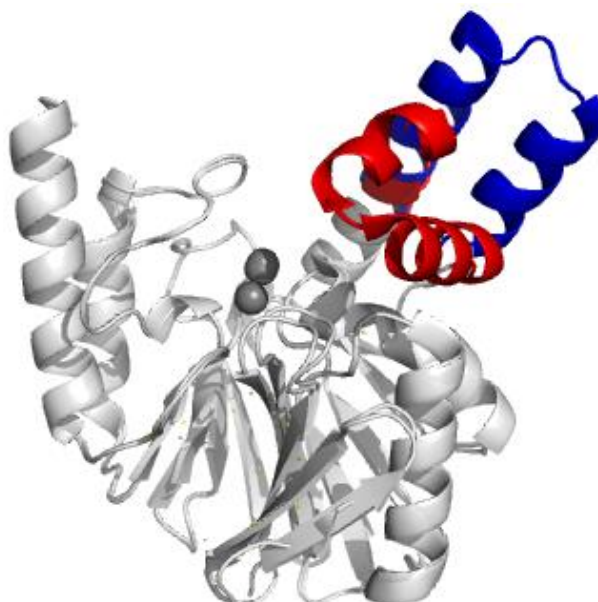
Figure 96: X-ray crystal structures of SPM-1 showing the flexible loop region in the open form (Blue, PDB ID: 2FHX) and closed form (Red, PDB ID: 4BP0[188]).

Table 18: Docking scores for different substrates against SPM-1

Enzyme	Substrate	Normalized AutoDock Score	Normalized SPROUT Score[a]	K_M-values (µM)
SPM-1	Imipenem	0.63	0.66	330.9
	CENTA	-0.42	0.88	25.3
	Nitrocefin	-0.33	0.90	16
	8.4	-1.25	1.02	2.5

[a] Note, higher normalised score equates to tighter predicted binding. Scores are ranked based on the normalized SPROUT scores going from the lowest score to the highest score.

Further studies on the SPM-1 enzyme should look at the identified flexible loop to see if molecular dynamics can explain the effects of this loop on the rate of hydrolysis when compared to the other enzymes.

8.4 Tetrahedral intermediates and hydrolysis products

8.4.1 NDM-1, IMP-1 and VIM-2

In an attempt to further understand the hydrolysis mechanism, the *in silico* docking of the tetrahedral hydrolysis intermediate and the hydrolysed product were conducted. (**Figure 97**) (Appendix A5.2 and A5.3)
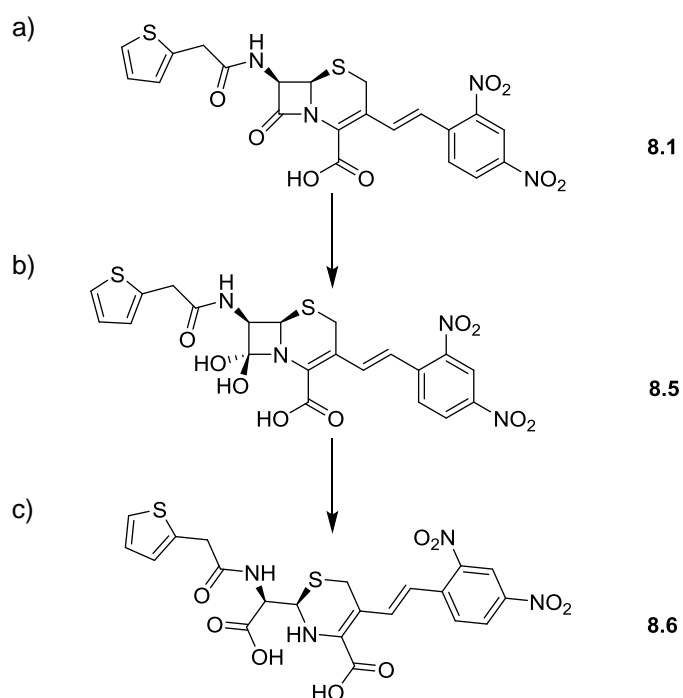
Figure 97: 2D structures of nitrocefin a) pre-hydrolysed substrate (**8.1**), b) tetrahedral intermediate (**8.5**) and c) hydrolysed substrate (**8.6**).

In general for NDM-1, IMP-1 and VIM-2 the best predicted binding scores come from the hydrolysed products of the substrates (**Figure 98**). In the hydrolysed form the newly formed carboxylic acid now binds to the side chain amine of the Asn-167 residue. The carboxylic acid that was bound to the Asn-167 residue is now bound to the Asn-167 residue and Zn1 atom. The extra interactions lead to a much stronger predicted binding energy for the hydrolysed product that the pre-hydrolysis substrate.

The pre-hydrolysis substrates give the next best predicted binding scores which shows that binding to the enzyme is favourable. In general the lowest scores are for the tetrahedral intermediate, which may be representative of the energy barrier for hydrolysis and also could be an indicator as to why the hydrolysis of the reaction is catalytic (**Figure 99**). The formation of the tetrahedral intermediate removes the binding interaction seen from the β-lactam carbonyl to the Asn-167 residue. The loss of this bond and the increase in space required to accommodate the tetrahedral intermediate reduces the binding energy.
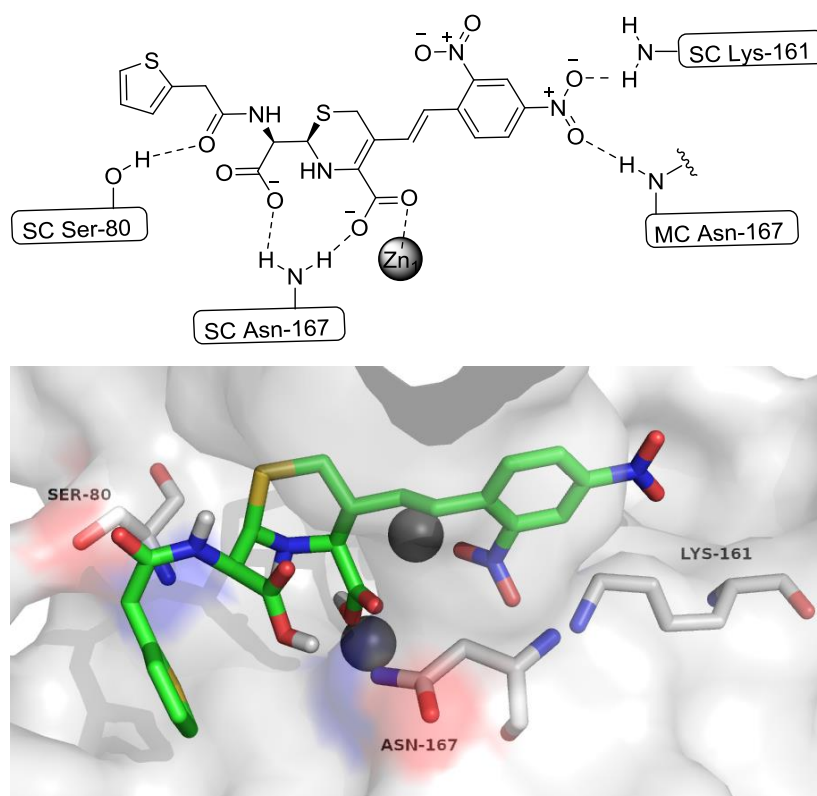
Figure 98: Hydrolysed nitrocefin docked into the active site of the IMP-1 (PDB ID: 1JJT): a) 2D binding representation, b) 3D spatial representation
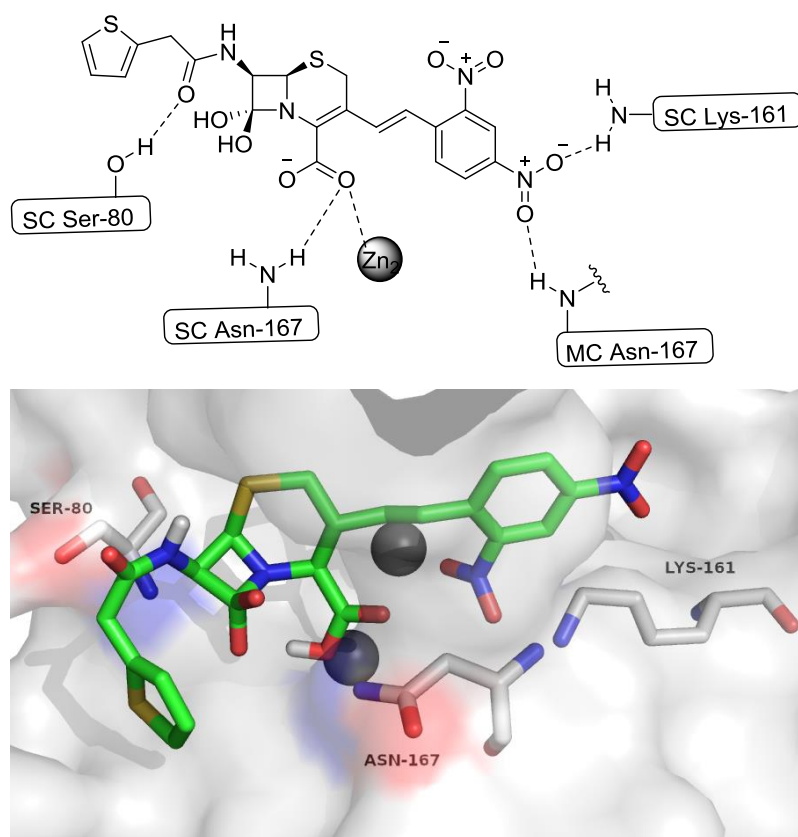
Figure 99: Tetrahedral intermediate in the hydrolysis of nitrocefin docked into IMP-1 (PDB ID: 1JJT).

Figure 100 shows the proposed energy profile for the hydrolysis of the substrates by the MBL enzymes showing the activation energy needed to pass through the tetrahedral intermediate and the lower energy hydrolysis product.

As seen with the pre-hydrolysis substrates, there is much stronger binding to the IMP-1 enzyme than to the other MBL enzymes. This is attributed to the more enclosed active site which gives stronger hydrophobic interactions between the active site wall and the substrates. There is a good correlation between the VIM-2 and NDM-1 results for all of the states and this is comparable to the results seen in the *in vitro* assays.
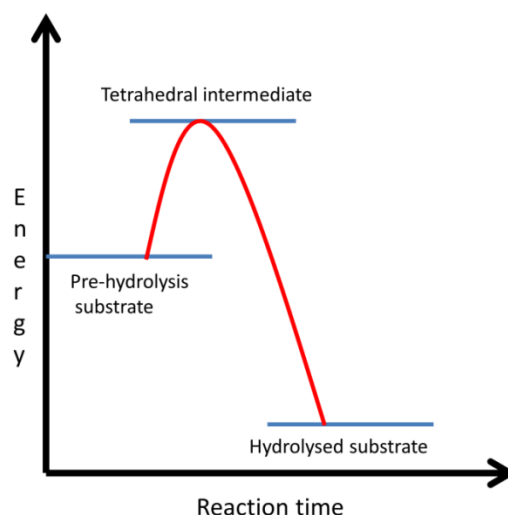
Figure 100: Proposed energy profile for the hydrolysis of substrates by MBL enzymes based upon *in silico* predicted binding scores

8.4.2 SPM-1

The predicted *in silico* binding scores of the substrates to the SPM-1 enzyme are significantly lower than to the other MBL enzymes.

The binding predictions from AutoDock give some unexpected results (Appendix A5.2 and A5.3). A number of positive binding energies were observed. This implies that energy is required to place the substrate into this position and would be highly disfavoured. An example of this is the positive score of 2.00 for the binding of pre-hydrolysed nitrocefin to SPM-1. All of the AutoDock scores for each substrate docked into the SMP-1 enzyme are much lower scoring then for any of the other enzymes which indicates poor binding. This was also observed in the biologically measured K_M values in **Table 18** however not to the extreme seen in the AutoDock scores.

The SPROUT predicted binding scores for each substrate are more consistent in value with the binding scores of the substrates to the other MBL enzymes. However they show the pre-hydrolysis substrate to give the tightest binding followed by the hydrolysed substrate and the most unfavored being the intermediate. This gives an indication that hydrolysis of the substrates may not be as favourable as with the other enzymes. The SPROUT scores also show stronger binding of imipenem to the SMP-1 enzyme rather than compound **8.4** as seen with all the other MBLs. This could be due to the flexible loop restricting the larger substrates from reaching the active site as easily.

A molecular dynamics studies of the flexible loop region of the SMP-1 enzyme would be required in order to fully understand why the scores are so different. However, as more crystal structures of SPM-1 enzyme become available researchers will gain a better understanding of the enzyme as a whole and especially the flexible loop region where it should be possible to establish whether the open or closed state is preferred.

8.5 Conclusions

The *in silico* SPROUT docking scores generally show a better correlation with the *in vitro* obtained kinetic parameters (specifically K_M values) compared to the docking scores obtained by AutoDock 4. It should however be noted that these studies are based upon a single crystal structure for each enzyme. This means that the docking does not take into account movement of any loops or changes in the inter atom distance between the zinc atoms which is widely reported in the literature especially with SPM-1. As more crystallographic data becomes available there will be an increase the accuracy of the docking predictions. Further studies on the SPM-1 enzyme should look at the identified flexible loop to see if molecular dynamics can explain the effects of this loop on the rate of hydrolysis when compared to the other enzymes.

Overall compound **8.4** provides the strongest binding to all of the enzymes in pre-hydrolysis substrate, tetrahedral intermediate and hydrolysed product forms. The stronger binding means that lower concentrations of substrate are required when conducting the assays which would save on the amount of substrate required for HTS screens and costs associated with producing substrate. Fluorogenic compound **8.4** provides good activity against all of the tested clinically relevant MBLs which shows it would be a good broad spectrum substrate to use in enzymatic assays.

Part 3

Conclusions and Experimental

Chapter 9
Conclusions and future work

This thesis reports on the molecular design, synthesis and biological evaluation of metallo-β-lactamase inhibitors which could be co-administered with current β-lactam antibiotics restoring the activity of the antibiotic against its bacterial target. The initial aim was to rationally identify novel inhibitors of the clinically relevant MBLs, VIM-2, IMP-1, NDM-1 and SPM-1, using a combination of structure-based drug design, chemical synthesis and biological evaluation.

Four classes of inhibitor compound were successfully identified using a range of *in silico* techniques.

9.1 vHTS identified inhibitors

An extensive vHTS campaign was carried out in an attempt to identify novel inhibitors of NDM-1. Using AutoDock running on an array of parallel processors, ten compounds were identified from the Peakdale Molecular screening library and, eight compounds were identified from the Chembridge chemical library compounds. A series of compounds investigating the effects of changing the sterics and electronics around one of the Peakdale hits was synthesised and assessed biologically at the University of Oxford. Some inhibition was seen against NDM-1. However the degree of inhibition was not considered sufficient to warrant a more detailed SAR investigation to be carried out around these compounds. To improve the study, more crystal structures of each enzyme should be used to provide a consensus of which identified inhibitors are the most likely to be active in the enzymatic assay.

9.2 Boronic acid inhibitors

A series of boronic acid-containing inhibitors were identified from a patent as potent inhibitors of MBLs. Five target compounds were identified through a combination of vHTS of the compounds contained in the patent, and a *de novo* design approach. The synthetic route described in the patent was modified to increase the yields with moderate success. When screened in

the biological assays, the boronic acid based inhibitors gave IC_{50}s in the region of 10 nM against VIM-2 and NDM-1 and 10 µM against IMP-1. The boronic acid-based inhibitors showed pan inhibition across the panel of MBL enzymes although much weaker binding was observed to the IMP-1 enzyme. A crystal structure of one of the compounds co-crystallised in one of the MBLs will help to elucidate how the boronic acid compounds bind to the active site of the MBLs. Although a crystal structure is not yet available the conducted docking studies gave a good insight into how the boronic acid-based inhibitors are predicted to bind.

9.3 Cysteine-containing peptides

A new method to identify strong-binding peptides *via* the docking of custom built virtual peptide libraries to MBLs has been developed which could be a great improvement on the current methods of inhibitor peptide identification. The method has been shown to work by identifying active peptides against NDM-1. Initially the study was carried out using only L-amino acids with the best L-amino acid trimer peptides giving moderate activity against the NDM-1 enzyme with an IC_{50} of 183 µM. Generally, improvements were seen when using peptides consisting of combinations of D and L amino acids however the best L-amino acid trimer was the most biologically active against NDM-1. Further testing is required to confirm this finding. A ROCs overlay screen was conducted with the zinc 'drug like' molecules screening library using the best scoring peptide as a template. Many of the compounds identified did not contain a strong zinc binding group and therefore would not make good peptide mimic drugs for this system. More screening libraries could be used or a better overlay based upon a crystal structure of the peptide bound into the active site.

9.4 *De novo* designed thiol-based inhibitors

De novo design successfully identified a novel small thiol-containing fragment. An investigation was conducted looking at the effects of changing the sterics and electronics of the lead molecule. This lead to the identification of a series of fragment molecules which are active against the MBLs. Evaluation in the enzymatic assays showed that the lead compound

had IC_{50}'s of 234 nM and 232 nM against VIM-2 and IMP-1 respectively, which is the most potent inhibitor discovered using a fragment based approach. The small thiol-containing fragment was successfully co-crystallised in VIM-2 leading to better understanding of the binding mode. In the bacterial cell assay, the thiol based inhibitor was seen to restore some of the activity of meropenem recovering the MIC of meropenem against NDM-1 producing isolates from >128 ug/mL to 8 ug/mL. There was moderately high loading of the inhibitor to see the restoration in the MIC which could be down to penetration of the outer membrane or from removal from the cell by efflux. Modifications to the molecule in future work may help to overcome this. DMPK studies also showed the thiol molecule to be highly soluble in aqueous media but does show susceptibility to metabolic degradation by human liver microsomes. Initial studies have been conducted with the idea of co-drugging the inhibitor attached to a β-lactam antibiotic. However, and perhaps not surprisingly, early studies with the co-drug described are not promising.

Studies are still required to investigate improving the drugability of all the identified inhibitor compounds. Getting the compounds into Gram negative bacteria still poses a considerable challenge, a challenge that has been the downfall to many antibacterial drug leads over the years. With the presence of elements such as sulfur and boron, full toxicity studies on these compounds will be required in order to ensure that they will have no adverse effects when administered *in vivo*.

9.5 The future direction of MBL research

The results described in this thesis provide a significant advancement of knowledge in the field as a whole. As yet no inhibitors of the MBLs have progressed to the clinic. This thesis reports a number of non-metal extracting compounds which have shown the ability to bind strongly to the MBLs and, in the case of the *de novo* fragments, potentiate the effect of meropenem on MBL producing bacteria. The successful identification of these novel tool compounds paves the way for other scientists to continue to develop

compounds which can be co-administered with our current β-lactam antibiotics prolonging their lifetime.

The *de novo* designed inhibitors offer the most promising lead. Given more time to expand on the research contained in this thesis, studies would focus on establishing a strong SAR. Efforts would also be concentrated on continuing to minimise the potential toxicity problems within the current leads by considering moving towards other zinc binding groups such as carboxylic acids and / or imidazole in place of the thiol moiety. Further microbiological studies would focus on how to ensure these inhibitors penetrate bacterial cells and rationalising why the current inhibitors only exhibit moderate potentiation in the cellular assay-despite their strong inhibition in the enzymatic assay. The principle of co-drugging to overcome penetration difficulties should be investigated further by coupling the inhibitors to different cephalosporins.

The boronic acid-containing inhibitors, which were found to exhibit strong binding to the MBLs, are some of the most potent MBL inhibitors known. Future research should focus on establishing the mode of binding of these compounds through crystallisation studies. Finding out more about how they bind will aid future development efforts to translate these systems to the clinic. Microbiological studies should be conducted taking the compounds into the cells with current β-lactam antibiotics to see if there is potentiation of the antibiotic against the MBL producing bacteria.

When used to identify peptide-based inhibitors for the MBLs the vHTS-derived peptide library approach ultimately proved to be unsuccessful. However, the principle of generation of such bespoke libraries should be further investigated using a number of different biological systems.

Further work should focus on the SPM-1 MBL which was briefly introduced in this thesis. The flexible loop area within this enzyme poses a particular challenge to designing a suitable inhibitor. As with the other clinically relevant MBLs spread of SPM-1 is expected to grow rapidly over the next few years. Future work on MBL inhibition should aim to design novel inhibitors which can specifically target the SPM-1 enzyme

9.6 The future of structure-based drug design and antibacterial resistance

As computational power increases, more accurate molecular screening will become available with hopefully, programs becoming capable to deal with the movement of the enzyme. This will allow for substantial increases in the accuracy of predictions and lower the need to synthesise large libraries of compounds which both reduces the cost and time of projects.

There is a major pressing need to either discover new antibiotics or to protect our current spectrum of antibacterial agents to avoid the return to a 'pre-antibiotic' era. The structure-based drug design approach outlined in this research offers rapid progression from target to lead compound at much reduced costs to the standard drug discovery approach. Progress is being made in identifying inhibitors of the MBLs but there are still some challenges nevertheless however challenging the fight against antibacterial resistance must go on.

Chapter 10
Experimental

10.1 General procedures and instrumentation.

All reactions were carried out under nitrogen unless otherwise specified. All reagents were obtained from commercial sources without further purification. All solvents were distilled before use or obtained dry from commercial suppliers; EtOAc refers to ethyl acetate and Petrol to Petroleum ether (bp. 40-60 °C). Analytical TLC was performed using silica gel pre-coated plates (Merck) and visualised by UV irradiation. Flash column chromatography was carried out on silica gel 60 (230-400 mesh, Merck). Solvents were removed under reduced pressure using a Buchi rotary evaporator at diaphragm pump pressure. Samples were freed of remaining traces of solvents under high vacuum.

^{1}H and ^{13}C NMR spectra were measured on a Bruker DPX300 Fourier transform spectrometer or a Bruker Avance 500 using an internal deuterium lock. Chemical shifts were reported in parts per million (ppm) downfield from TMS in δ units and coupling constants are given in hertz (Hz). TMS as defined as 0 ppm for ^{1}H NMR spectra and the centre line of the triplet CDCl$_3$ was also defined as 77.10 ppm for ^{13}C NMR spectra. When displaying the ^{1}H NMR data the following abbre*via*tions will be used; s= singlet, d= doublet, t= triplet, q= quartet, qi=quintet, m= multiplet, app= apparent.

High resolution mass spectra (HRMS) was recorded in house using a Micromass GCT Premier, using electron impact ionization (EI) or a Bruker MaXis Impact Time of Flight spectrometer, using electron spray ionization (ES). All quoted masses refer to the ^{79}Br isotope.

Infrared spectra were recorded as thin films using sodium chloride plates or solid samples on a Perkin Elmer Spectrum One FT-IR spectrophotometer or Bruker Alpha Platinum ATR FT-IR spectrophotometer. The vibrational frequencies are reported in wavenumbers (cm^{-1}).

Melting points were determined on a Reichert Hot Stage apparatus. Melting points obtained were unchanged.

Elemental analysis was carried out using a Carlo Erba 1108 Elemental Analyzer. Determination of chlorine, bromine, fluorine, iodine and sulfur were carried out using the Schoniger Oxygen Flask combustion method followed by the relevant titration for the particular halogen.

HPLC analyses were carried out on an Agilent 1290 Infinity system using a Supelco Ascentis Express C18, 50 x 2.1 mm, 2.7 micron column and diode array as a detector. A gradient of water and acetonitrile (5-95%) was used at a flow rate of 0.5 mL/min over 5 minutes.

Preparative HPLC was conducted on an Agilent mass directed prep. LCMS using a XBridge C18, 19 × 100 mm, 5 micron column and positive ion electrospray ioniozation. A gradient of water and acetonitrile (5-95%) was used at a flow rate of 20mL/min over 8 minutes.

LC-MS analysis was performed on a Bruker Daltronics instrument running on a gradient of increasing acetonitrile (5-95%) in water containing 0.1% formic acid at 1 mL min^{-1} on a 50 × 20 mm C_{18} reverse phase column and positive ion electrospray ionization.

Specific rotation measurements were recorded using a Schmidt and Haensch Polartronic H532 polarimeter, using a 100 mm cell and the Sodium D line (589 nm). $[\alpha]_D$ are reported in units of 10^{-1} deg dm^{2}g^{-1}.

10.2 General experimental methods

Method A: Suzuki couplings

The boronic acid (1.1 eq) was added to a stirred solution of 5-bromophthalide (1.0 eq), potassium carbonate (1.0 eq) and tetrakis (triphenylphosphine) palladium (0) (0.05 eq) in THF (4 mL) and water (2 mL). The reaction mixture was heated to reflux for 12 h. The reaction mixture was filtered through celite and concentrated *in vacuo*. The residue was diluted with water (20 mL) and extracted in DCM (3 × 20 mL). The combined organics were dried (MgSO$_4$) and concentrated *in vacuo* to give an off-white/yellow solid, which was purified using flash column chromatography to afford the coupled products which were used without further purification.

Method B: Lactone hydrolysis

2M NaOH $_{(aq)}$ (2.5 mL) was added to a stirred solution of the benzofuranone (1.0 eq) in methanol (5 mL). The reaction mixture was heated to reflux for 4 h. The reaction mixture was concentrated *in vacuo.* The residue was diluted with water (10 mL) and acidified with 2M HCl $_{(aq)}$ to ~pH 2. The precipitate was filtered and washed with cold water (5 mL) and cold ethyl acetate (5 mL). The collected solid was dried to afford the hydrolysed product as an off-white solid without further purification.

Method C: Lactone opening forming iodide

The desired benzofuranone (1.0 eq) was dissolved in DCM (4.5 mL). TMSI (1.5 eq) was added and the reaction was refluxed under nitrogen for 3 h. After this time the mixture was cooled to room temperature and quenched with water (3 mL). The precipitate was isolated by filtration and washed with water (2 × 10 mL) to give the desired product as an off-white solid which was used without further purification.

Method D: Introduction of Thiol[189]

A mixture of thiourea (1.1 eq) in THF (3 mL) was heated to reflux. To this was added the iodine containing open lactone product (1.0 eq). The reaction mixture was heated to reflux for 16 h under an atmosphere of nitrogen. The reaction mixture was cooled to room temperature. The mixture was then concentrated *in vacuo*. The residue was re-suspended in 2M NaOH $_{(aq)}$ (5 mL) and the solution refluxed for 3 h. The reaction mixture acidified with 2M HCl $_{(aq)}$ to ~pH2. The colourless precipitate was isolated by filtration.

Method E: TMS group deprotection and HATU Peptide coupling

The desired TMS protected amine (1.2-2.0 eq) was dissolved in THF (20 mL) and to this was added anhydrous MeOH (2 mL). The reaction mixture was stirred at room temperature for 2 h. The reaction mixture was concentrated *in vacuo* to afford a pale brown oil which was taken forward to the next step without further purification.

The desired carboxylic acid (1.0 eq) and HATU (1.1 eq) was dissolved in DCM (30 mL). The reaction mixture was cooled to 0 °C and Et$_3$N (1.5 eq) was added drop-wise. The reaction mixture was stirred at 0 °C for 30 mins and then at room temperature for 1 h. The solution was then cooled to −20 °C and the desired amine (1.2-2.0 eq) was added drop-wise. The reaction

was allowed to warm to room temperature overnight. After this time the reaction was quenched with water (50 mL). The aqueous layer was extracted with EtOAc (3 × 50 mL). The combined organics were dried (MgSO$_4$) and concentrated *in vacuo* to give the desired amide, which was purified using flash column chromatography to afford the coupled products.

Method F: S$_N$2 reaction in the synthesis of boronic acid-containing inhibitors

3-[(2R)-2-[4-(bromomethyl)-benzoylamino]-2-[(3aS,4S,6S,7aR)-3a,5,5-trimethylhexahydro-4,6-methano-1,3,2-benzodioxaborol-2-yl]-ethyl]-2-methoxy benzoic acid tert-butyl ester (1.0 eq) was dissolved in CH$_3$CN:DMF (1:1, 10 mL) and the desired amine (1.0 eq) was added. Na$_2$CO$_3$ (1.1 eq) was added and the solution heated to 70 °C for 3 h. The reaction was cooled to room temperature and extracted with EtOAc (3 × 20 mL). The organics were washed with water (3 × 20 mL) and brine (20 mL), dried (MgSO$_4$) and concentrated *in vacuo* to afford the crude product. The crude product was purified by mass directed HPLC to afford the desired product as an oil.

Method G: Boronic acid global deprotection.

Boron tribromide (1M in DCM, 7.0 eq) was added drop-wise to a solution of boronic acid species (1.0 eq) in DCM (10 mL) at −78 °C. The reaction mixture was stirred at −78 °C for 1 h before warming to room temperature and quenched with water (6 mL). The DCM layer was evaporated *in situ.* Water (75 mL) was added and the mixture was extracted with diethyl ether (3 × 50 mL). The aqueous layer was concentrated to ~5 mL and the pH adjusted to ~pH1 with 2M HCl $_{(aq)}$. The product was purified by biotage chromatography on a C$_{18}$ reverse phase cartridge eluting with 2:98 Isopropanol-water to afford the desired product as a colourless solid.

## 10.3 Synthesis of 'Peakdale screen hit molecule'

Synthesis of 2-oxo-2H-chromene-6-sulfonyl chloride (4.3)[190]
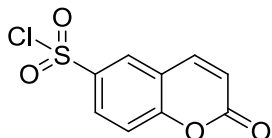
A solution of coumarin (1.00 g, 6.85 mmol) in chlorosulfonic acid (**4.2**) (20 mL) was refluxed for 15 mins. After cooling to room temperature the mixture was poured into ice and water (200 mL). The solution was extracted with chloroform (3 × 100 mL), dried over $MgSO_4$, and concentrated *in vacuo* to give the crude product as a colourless solid. The crude product was purified by flash column chromatography eluting with 3:1 DCM–Petrol. The title compound (**4.3**) was isolated after recrystallization from DCM as colourless plates. (0.68 g, 2.81 mmol, 41%) m.p.: 115.6-117.4 °C (from DCM) [lit.[190] m.p. 113-115 °C] ; R_f: 0.41 (3:1 DCM–Petrol); δ_H (300 MHz, $CDCl_3$): 8.24 (1H, d, J 2.1, 5-H), 8.20 (1H, dd, J 8.7 and 2.1, 7-H), 7.82 (1H, d, J 9.3, 4-H), 7.58 (1H, d, J 8.7, 8-H), 6.64 (1H, d, J 9.3, 3-H); δ_C (75 MHz, $CDCl_3$): 188.6 (C=O), 161.1 (C4a), 147.1 (C6), 141.8 (C4), 134.0 (C8a), 130.0 (C8), 127.6 (C5), 119.3 (C7), 118.7 (C3); v_{max}/ cm^{-1} (solid): 3458, 3084, 1734, 1370; HPLC: T_r= 2.77 (100% rel. area); *m/z* (EI): (Found: M^+, 243.9607. $C_9H_5ClO_4S$ requires *M*, 243.9597).

Synthesis of 2,3-dimethyl-7-nitroindole (4.5)[191]
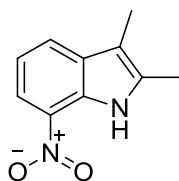
2-nitrophenyl hydrazine (**4.4**) (1.00 g, 6.54 mmol) and butan-2-one (0.58 mL, 6.54 mmol) were dissolved in methanol (10 mL) and to this was added ceric ammonium nitrate (0.72 g, 1.31 mmol). The solution was refluxed under an atmosphere of nitrogen for 16 h. The reaction was cooled to room temperature and poured into water (50 mL). The crude product was extracted with ethyl acetate (2 × 50 mL). The extracts were washed with water (20 mL), dried ($MgSO_4$) and concentrated *in vacuo.* The crude product was re-suspended in conc. HCl (10 mL) and refluxed for 12 h. The reaction mixture was concentrated *in vacuo.* The residue was re-suspended in DCM (20 mL) and water (20 mL). The aqueous layer was extracted with DCM (2 × 20 mL). The organics were concentrated *in vacuo* to yield a dark brown powder which was recrystallized from acetone to afford the title compound (**4.5**) as pale brown plates. (0.64 g, 3.38 mmol, 52%) m.p.: 94.4-96.2 °C (from acetone)

[lit.[191] m.p. 95-96 °C (from acetone)]; R_f: 0.38 (1:1 Petrol−EtOAc); δ_H (300 MHz, CDCl$_3$): 9.43 (1H, brs, NH), 8.00 (1H, d, J 7.7, 4-H), 7.71 (1H, d, J 7.7, 6-H), 7.10 (1H, app. t, J 7.7 5-H), 2.32 (3H, s, CH$_{3\text{-}3}$), 2.18 (3H, s, CH$_{3\text{-}2}$); δ_C (75 MHz, CDCl$_3$): 133.6 (C3a), 133.3 (C2), 128.9 (C3), 125.9 (C6), 118.3 (C4), 118.0 (C5), 108.5 (C7a), 11.6 (CH$_{3\text{-}3}$), 8.37 (CH$_{3\text{-}2}$); v_{max}/ cm^{-1} (solid): 3409, 2916, 1512, 1364; HPLC: T_r= 3.46 (92% rel. area); m/z (EI): (Found: M$^+$, 190.0741. C$_{10}$H$_{10}$N$_2$O$_2$ requires M, 190.0742).

Synthesis of 2,3-dimethyl-7-aminoindole (4.6)
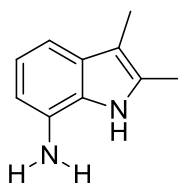
2,3-dimethyl-7-nitroindole (**4.5**) (0.50 g, 2.63 mmol) was dissolved in methanol (25 mL). To this was added (10%) palladium on carbon (0.14 g, 0.13 mmol). The reaction was placed under an atmosphere of hydrogen and stirred at room temperature for 12 h. The reaction mixture was filtred through celite and concentrated *in vacuo*. The product was re-suspended in DCM (20 mL) and washed with water (20 mL) and brine (20 mL). The organics were concentrated *in vacuo* to yield a pale brown powder which was recrystallized from chloroform to afford the title compound (**4.6**) as colourless needles. (0.35 g, 2.18 mmol, 83%). m.p.: 123.6-124.3 °C (decomp) [lit.[192] m.p. 126 °C (decomp)]; R_f: 0.52 (19:1 DCM–MeOH); δ_H (300 MHz, CDCl$_3$): 7.60 (1H, brs, NH), 7.00 (1H, d, J 7.1, 4-H), 6.90 (1H, app. t, J 7.1, 5-H), 6.51 (1H, d, J 7.1, 6-H), 3.50 (2H, brs, NH$_2$), 2.32 (3H, s, CH$_{3\text{-}3}$), 2.20 (3H, s, CH$_{3\text{-}2}$); δ_C (75 MHz, CDCl$_3$): 130.6 (C2), 130.0 (C7), 125.9 (C3a), 119.8 (C5), 110.2 (C4), 108.2 (C6), 108.0 (C7a), 11.5 (CH$_{3\text{-}3}$), 8.70 (CH$_{3\text{-}2}$); v_{max}/ cm^{-1} (solid): 3406, 2918, 1580; HPLC: T_r= 1.64 (100% rel. area); m/z (EI): (Found: M$^+$, 160.0997. C$_{10}$H$_{12}$N$_2$ requires M, 160.1000).

Synthesis of 7-aminoindole (4.7)
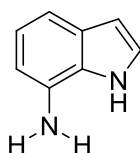
7-Nitroindole (0.50 g, 3.09 mmol) was dissolved in methanol (25 mL). To this was added (10%) palladium on carbon (0.15 g, 0.15 mmol). The reaction was placed under an atmosphere of hydrogen and stirred at room temperature for 12h. The reaction mixture was filtered through celite and concentrated *in vacuo*. The product was re-suspended in DCM (20 mL) and washed with water (20 mL) and brine (20 mL). The organics were concentrated *in vacuo* to yield an off-white

powder which was recrystallized in chloroform to afford the title compound (**4.7**) as colourless needles. (0.36 g, 2.72 mmol, 88%). m.p.: 95.2-96.6 °C (CHCl$_3$) [lit.[193] m.p.94-95 °C (CHCl$_3$)]; R_f: 0.55 (19:1 DCM–MeOH); δ$_H$ (300 MHz, CDCl$_3$): 8.10 (1H, brs, NH), 7.19 (1H, d, J 7.1, 4-H), 7.04 (1H, d, J 2.7, 2-H), 6.94 (1H, app. t, J 7.1, 5-H), 6.57 (1H, d, J 7.1, 6-H), 6.50 (1H, d, J 2.7, 3-H), 3.6 (2H, brs, NH$_2$); δ$_C$ (75 MHz, CDCl$_3$): 130.9 (C7), 128.9 (C3a), 126.9 (C7a), 124.1 (C2), 120.6 (C5), 112.8 (C4), 108.7 (C6), 103.4 (C3); ν$_{max}$/ cm^{-1} (solid): 3375, 3216, 2735; HPLC: T$_r$= 1.11 (100% rel. area); *m/z* (EI): (Found: M$^+$, 132.0690. C$_8$H$_8$N$_2$ requires *M*, 132.0687).

## Synthesis of N-(2,3-dimethyl-1H-indol-7-yl)-2-oxo-chromene-6-sulfonamide (4.1)
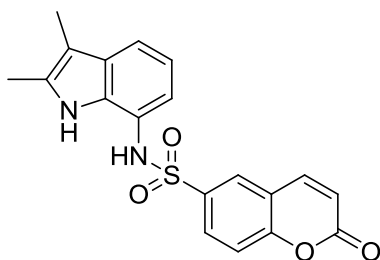
2-oxo-2H-chromene-6-sulfonyl chloride (**4.3**) (0.10 g, 0.41 mmol), 2,3-dimethyl-7-aminoindole (**4.6**) (66 mg, 0.41 mmol) and pyridine (0.03 mL, 0.41 mmol) were stirred in DCM (5 mL) under and atmosphere of nitrogen for 16 h. The reaction mixture was washed with water (10 mL), dried (MgSO$_4$) and concentrated *in vacuo* to yield the crude product as a pale brown powder. The crude product was purified using flash column chromatography, eluting with 1:1 Petrol–EtOAc. The title compound (**4.1**) was isolated by recrystallization from toluene as pale brown microcrystals. (0.11 g, 0.29 mmol, 70%) m.p.: 198.4-199.5 °C (from toluene); R_f: 0.36 (1:1 Petrol–EtOAc); δ$_H$ (300 MHz, CDCl$_3$): 8.70 (1H, brs, indole-NH), 7.89 (1H, d, J 2.1, 5-H), 7.88 (1H, d, J 9.3, 8-H), 7.60 (1H, d, J 9.3, 4-H), 7.27 (1H,d, J 7.6, 4'-H), 7.26 (1H, dd, J 9.3 and 2.1, 7-H), 6.79 (1H, app. t, J 7.6 5'-H), 6.62 (1H, brs, NH), 6.48 (1H, d, J 9.3, 3-H), 6.23 (1H, d, J 7.6, 6'-H), 2.40 (3H, s, CH$_{3-3}$), 2.21 (3H, s, CH$_{3-2}$); δ$_C$ (75 MHz, CDCl$_3$): 159.4 (C=O), 156.5 (C8a), 142.4 (C4), 134.2 (C6), 132.4 (C4a), 131.8 (C3'a), 131.5 (C7'a), 130.3 (C5), 127.9 (C8), 118.9 (C5'), 118.6 (C7), 118.2 (C3), 118.0 (C6'), 117.8 (C4' and C7), 117.6 (C2'), 107.5 (C3'), 11.7 (CH$_{3-3}$), 8.52 (CH$_{3-2}$); ν$_{max}$/ cm^{-1} (solid): 3422, 3220, 2915, 1731, 1324, 1148; HPLC: T$_r$= 3.17 (100% rel. area); *m/z* (ES): (Found: [M-H]$^-$, 367.0758. C$_{19}$H$_{16}$N$_2$O$_4$S requires *[M-H]*, 367.0770).

Synthesis of N-(1H-indol-7-yl)-2-oxo-chromene-6-sulfonamide (4.13)
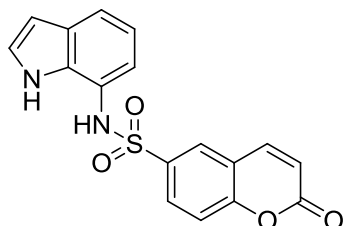
2-oxo-2H-chromene-6-sulfonyl chloride (**4.3**) (0.10 g, 0.41 mmol), 1H-indol-7-amine (**4.7**) (54 mg, 0.41 mmol) and pyridine (0.03 mL, 0.41 mmol) were stirred in DCM (5 mL) under and atmosphere of nitrogen for 16 h. The reaction mixture was washed with water (10 mL), dried (MgSO$_4$) and concentrated *in vacuo* to yield the crude product as a pale brown powder. The crude product was purified using flash column chromatography eluting with 1:1 Petrol–EtOAc. The title compound (**4.13**) was isolated by recrystallization from toluene as pale brown microcrystals. (0.12 g, 0.34 mmol, 83%) m.p.: 160.3-161.8 °C (from toluene); R_f: 0.48 (1:1 Petrol–EtOAc); (Found: C, 60.1; H, 3.55; N, 8.0; S, 9.2; C$_{17}$H$_{12}$N$_2$O$_4$S requires C, 59.9; H, 3.55; N, 8.2; S, 9.4%); δ$_H$ (300 MHz, CDCl$_3$): 9.20 (1H, brs, NH indol), 7.74 (1H, d, J 8.2, 8-H), 7.73 (1H, s, NH), 7.58 (1H, d, J 9.9, 4-H), 7.55 (1H, d, J 7.7, 4'-H), 7.36 (1H, dd, J 8.2 and 2.1, 7-H), 7.35 (1H, d, J 2.1, 2'-H), 6.84 (1H, app. t, J 7.7, 5'-H), 6.59 (1H, d, J 2.1, 5-H), 6.48 (1H, d, J 9.9, 3-H), 6.46 (1H, d, J 2.1, 3'-H), 6.30 (1H, d, J 7.7, 6-H'); δ$_C$ (75 MHz, CDCl$_3$): 188.8 (C=O), 160.9 (C8a), 142.3 (C4), 136.5 (C6), 131.1 (C4a) 130.3 (C8), 127.9 (C7), 125.5 (C7'a and C3'a), 125.4 (C4'), 120.6 (C5'), 119.7 (C6'), 118.5 (C3), 118.4 (C2'), 117.9 (C3'), 122.1 (C7'), 102.9 (C5); v$_{max}$/ cm^{-1} (solid): 3432, 3173, 1717, 1599, 1321, 1110; HPLC: T$_r$= 2.75 (100% rel. area); *m/z* (ES): (Found: [M-H]$^-$, 339.0450. C$_{17}$H$_{12}$N$_2$O$_4$S requires *[M-H]*, 339.0445).

Synthesis of 2-oxo-N-phenyl-2H-chromene-6-sulfonamide (4.14)
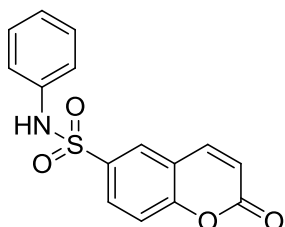
2-oxo-2H-chromene-6-sulfonyl chloride (**4.3**) (0.10 g, 0.41 mmol), aniline (**4.8**) (0.05 mL, 0.41 mmol) and pyridine (0.03 mL, 0.41 mmol) were stirred in DCM (5 mL) under and atmosphere of nitrogen for 16 h. The reaction mixture was washed with water (10 mL), dried (MgSO$_4$) and concentrated *in vacuo* to yield the crude product as a brown powder. The crude product was purified using flash column chromatography eluting with 1:1 Petrol–EtOAc. The title compound (**4.14**) was isolated by recrystallized from toluene as yellow microcrystals. (98 mg, 0.33 mmol, 79%) m.p.: 131.7-133.4 °C (from toluene) [lit.[194] m.p.132 °C

(from benzene)]; R_f: 0.74 (1:1 Petrol–EtOAc); (Found: C, 59.3; H, 3.75; N, 4.6; S, 10.6; $C_{15}H_{11}NO_4S$ requires C, 59.8; H, 3.68; N, 4.7; S, 10.6%); δ_H (300 MHz, CDCl$_3$): 7.96 (1H, d, J 2.2, 5-H), 7.88 (1H, dd, J 8.8 and 2.2, 7-H), 7.68 (1H, d, J 9.3, 4-H), 7.38 (1H, d, J 8.8, 8-H), 7.26 (2H, t, J 7.1, 5'-H and 3'-H), 7.18 (1H, t, J 7.1, 4'-H), 7.08 (2H, d, J 7.1, 6'-H and 2'-H), 6.94 (1H, brs, NH), 6.51 (1H, d, J 9.3, 3-H); δ_C (75 MHz, CDCl$_3$): 159.4 (C=O), 156.4 (C8a), 142.5 (C4), 135.8 (C6), 135.2 (C1'), 130.2 (C7), 129.6 (C6' and C2'), 127.8 (C5), 126.1 (C4'), 122.0 (C5' and C3'), 118.8 (C4a), 118.3 (C3), 117.0 (C8); v_{max}/ cm^{-1} (solid): 3408, 3160, 2872, 2818, 1714, 1621, 1344, 1160; HPLC: T_r= 2.53 (100% rel. area); m/z (ES): (Found: [M-H]$^-$, 300.0343 $C_{15}H_{11}NO_4S$ requires $[M-H]$, 300.0336).
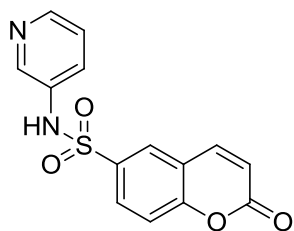
Synthesis of 2-oxo-N-(pyridine-3-yl)-2H-chromene-6-sulfonamide (4.15)
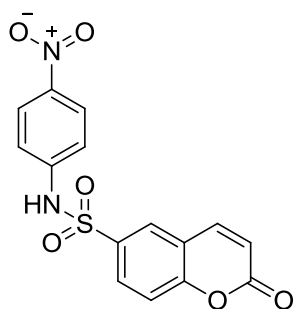

2-oxo-2H-chromene-6-sulfonyl chloride (**4.3**) (0.10 g, 0.41 mmol), 3-aminopyridine (**4.9**) (39 mg, 0.41 mmol) and pyridine (0.03 mL, 0.41 mmol) were stirred in DCM (5 mL) under and atmosphere of nitrogen for 16 h. The reaction mixture was washed with water (10 mL), dried (MgSO$_4$) and concentrated *in vacuo* to yield the crude product as a yellow solid. The crude product was purified using flash column chromatography eluting with 1:1 Petrol–EtOAc. The title compound (**4.15**) was isolated by recrystallized from toluene as off-white microcrystals. (0.10 g, 0.33 mmol, 82%) m.p.: 183.6-185.3 °C (from toluene); R_f: 0.45 (1:1 Petrol–EtOAc); (Found: C, 55.5; H, 3.40; N, 8.9; S, 10.3; $C_{14}H_{10}N_2O_4S$ requires C, 55.6; H, 3.33; N, 9.3; S, 10.6%); δ_H (300 MHz, DMSO-d6): 10.72 (1H, brs, NH), 8.32 (1H, d, J 2.7, 2'-H), 8.29 (1H, d, J 4.4, 6'-H), 8.21 (1H, d, J 2.5, 5-H), 8.17 (1H, d, J 9.3, 4-H), 7.92 (1H, dd, J 8.8 and 2.5, 7-H), 7.59 (1H, d, J 8.8, 8-H), 7.52 (1H, dd, J 8.2 and 2.7, 4'-H), 7.29 (1H, dd, J 8.2 and 4.4, 5'-H), 6.61 (1H, d, J 9.3, 3-H); δ_C (75 MHz, DMSO-d6): 159.0 (C=O), 155.9 (C8a), 145.4 (C6'), 143.3 (C4), 141.9 (C2'), 134.8 (C6), 134.0 (C3'), 129.4 (C7), 127.7 (C5 and C4), 124.1 (C5'), 119.0 (C4a), 117.9 (C8 and C3); v_{max}/ cm^{-1} (solid): 3462, 3061, 2856, 2774, 1737, 1603, 1471, 1164, 826; HPLC: T_r= 1.32 (100% rel. area); m/z (ES): (Found: [M-H]$^-$, 301.0284. $C_{14}H_{10}N_2O_4S$ requires $[M-H]$, 301.0289).

Synthesis of 2-oxo-N-(2,4,6-trimethylphenyl)-2H-chromene-6-sulfonamide (4.16)
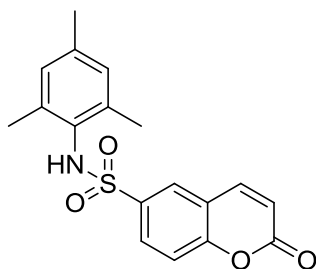
2-oxo-2H-chromene-6-sulfonyl chloride (**4.3**) (0.10 g, 0.41 mmol), 2,4,6 trimethyl aniline (**4.10**) (0.06 mL, 0.41 mmol) and pyridine (0.03 mL, 0.41 mmol) were stirred in DCM (5 mL) under an atmosphere of nitrogen for 16 h. The reaction mixture was washed with water (10 mL), dried ($MgSO_4$) and concentrated *in vacuo* to yield the crude product as a yellow powder. The crude product was purified using flash column chromatography eluting with 1:1 Petrol–EtOAc. The title compound (**4.16**) was isolated by recrystallized from toluene as off-white microcrystals. (96 mg, 0.28 mmol, 68%) m.p.: 170.4-171.9 °C (from toluene); R_f: 0.68 (1:1 Petrol–EtOAc); (Found: C, 63.2; H, 5.10; N, 4.1; S, 9.2; $C_{18}H_{17}NO_4S$ requires C, 63.0; H, 4.99; N, 4.1; S, 9.3%); δ_H (300 MHz, $CDCl_3$): 7.91 (1H, d, *J* 2.2, 5-H), 7.88 (1H, dd, *J* 8.8 and 2.2, 7-H), 7.68 (1H, d, *J* 9.3, 4-H), 7.40 (1H, d, *J* 8.8, 8-H), 6.84 (2H, s, 5'-H and 3'-H), 6.53 (1H, d, *J* 9.3, 3-H), 6.25 (1H, brs, NH), 2.25 (3H, s, $CH_{3-4'}$), 2.00 (6H, s, $CH_{3-6'}$ and $CH_{3-2'}$); δ_C (75 MHz, $CDCl_3$): 159.4 (C=O), 156.3 (C8a), 142.5 (C4), 138.1 (C6), 137.4 (C6' and C2'), 137.1 (C4'), 130.3 (C7), 129.7 (C5' and C3'), 129.3 (C1'), 127.4 (C5), 118.7 (C4a), 118.3 (C3), 117.8 (C8), 20.9 ($CH_{3-4'}$), 18.7 ($CH_{3-6'}$ and $CH_{3-2'}$); v_{max}/ cm^{-1} (solid): 3244, 1744, 1600, 1309, 1153; HPLC: T_r= 3.05 (100% rel. area); *m/z* (ES): (Found: [M-H]$^-$, 342.0798. $C_{18}H_{17}NO_4S$ requires *[M-H]*, 342.0806).

Synthesis of N-(4-nitrophenyl)-2-oxo-2H-chromene-6-sulfonamide (4.17)

2-oxo-2H-chromene-6-sulfonyl chloride (**4.3**) (0.10 g, 0.41 mmol), 4 nitro aniline (**4.11**) (57 mg, 0.41 mmol) and pyridine (0.03 mL, 0.41 mmol) were stirred in DCM (5 mL) under and atmosphere of nitrogen for 16 h. The reaction mixture was washed with water (10 mL), dried ($MgSO_4$) and concentrated *in vacuo* to yield the crude product as a yellow powder. The crude product was purified using flash column chromatography eluting with 1:1 Petrol–EtOAc. The title compound (**4.17**) was isolated by recrystallization from toluene as yellow microcrystals. (0.11 g, 0.30 mmol, 74%) m.p.: 221.7-

222.9 °C (from toluene) [lit.[194] m.p.220 °C (from benzene)]; R_f: 0.35 (1:1 Petrol–EtOAc); (Found: C, 52.1; H, 3.00; N, 7.8; S, 9.0; $C_{15}H_{10}N_2O_6S$ requires C, 52.0; H, 2.91; N, 8.1; S, 9.3%); δ_H (300 MHz, DMSO-d6): 8.36 (1H, d, J 2.2, 5-H), 8.16 (1H, d, J 9.8, 4-H), 8.12 (2H, d, J 9.3, 5'-H and 3'-H), 8.00 (1H, dd, J 8.8 and 2.2, 7-H), 7.60 (1H, d, J 8.8, 8-H), 7.33 (2H, d, J 9.3, 6'-H and 2'-H), 6.63 (1H, d, J 9.8, 3-H); δ_C (75 MHz, DMSO-d6): 159.0 (C=O), 156.2 (C8a), 143.7 (C4'), 143.3 (C4), 142.6 (C1'), 134.7 (C6), 129.5 (C7), 127.8 (C5), 125.4 (C5' and C3'), 119.1 C4a), 118.1 (C8, C6' and C2'), 117.9 (C3); v_{max}/ cm^{-1} (solid): 3423, 3159, 2448, 1736, 1724, 1595, 1521, 1347, 1226, 1162; HPLC: T_r= 2.65 (100% rel. area); m/z (ES): (Found: [M-H]⁻, 345.0198. $C_{15}H_{10}N_2O_6S$ requires $[M-H]$, 345.0187).
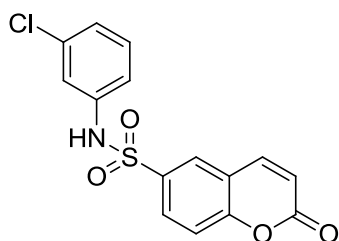
Synthesis of N-(3-chlorophenyl)-2-oxo-2H-chromene-6-sulfonamide (4.18)
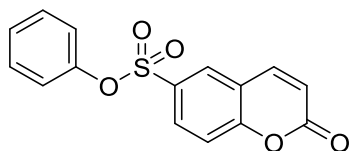

2-oxo-2H-chromene-6-sulfonyl chloride (**4.3**) (0.10 g, 0.41 mmol), 3-chloro aniline (**4.12**) (0.04 mL, 0.41 mmol) and pyridine (0.03 mL, 0.41 mmol) were stirred in DCM (5 mL) under and atmosphere of nitrogen for 16 h. The reaction mixture was washed with water (10 mL), dried (MgSO₄) and concentrated *in vacuo* to yield the crude product as a pale yellow powder. The crude product was purified using flash column chromatography eluting with 1:1 Petrol–EtOAc. The title compound (**4.18**) was isolated by recrystallization from toluene as colourless microcrystals. (0.12 g, 0.37 mmol, 90%) m.p.: 167.1-168.8 °C (from toluene); R_f: 0.72 (1:1 Petrol–EtOAc); (Found: C, 53.5; H, 3.10; Cl, 10.7; N, 4.2; S, 9.4; $C_{15}H_{10}ClNO_4S$ requires C, 53.7; H, 3.00; Cl, 10.6; N, 4.2; S, 9.6%); δ_H (300 MHz, DMSO-d6): 10.75 (1H, brs, NH), 8.25 (1H, d, J 2.2, 5-H), 8.17 (1H, d, J 9.9, 4-H), 7.92 (1H, dd, J 8.8, and J 2.2, 7-H), 7.57 (1H, d, J 8.8, 8-H), 7.25 (1H, app. t, J 8.2, 5'-H), 7.14 (1H, t, J 1.6, 2'-H), 7.09 (2H, m, 6'-H and 4'-H), 6.61 (1H, d, J 9.9, 3-H); δ_C (75 MHz, DMSO-d6): 159.0 (C=O), 155.9 (C8a), 143.3 (C4), 138.9 (C6), 134.9 (C1'), 133.4 (C3'), 131.0 (C5'), 129.4 (C7), 127.7 (C5), 124.0 (C4'), 119.3 (C2'), 119.0 (C4a), 118.1 (C6'), 117.8 (C3); v_{max}/ cm^{-1} (solid): 3185, 2970, 1738, 1723, 1373, 1217; HPLC: T_r= 2.93 (100% rel. area); m/z (ES): (Found: [M-H]⁻, 333.9938 $C_{15}H_{10}ClNO_4S$ requires $[M-H]$, 333.9946).

Synthesis of 6-benzylsulfonyl-2H-chromen-2-one (4.20)
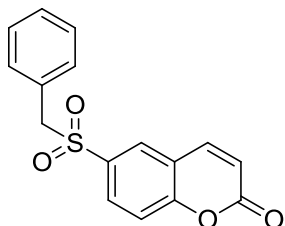
A stirred mixture of 2-oxo-2H-chromene-6-sulfonyl chloride (**4.3**) (0.10 g, 0.41 mmol), sodium bicarbonate (69 mg, 0.82 mmol) and sodium sulfite (0.10 g, 0.82 mmol) in water (2 mL) was heated at 100 °C under an atmosphere of nitrogen for 1 h. The reaction was cooled to 50 °C, treated with tetra-n-butyl ammonium iodide (10 mg) and benzyl bromide (**4.19**) (0.05 mL, 0.45 mmol) and re-heated to 70 °C for 18 h. The reaction was cooled, treated with water (5 mL) and extracted with DCM (3 × 10 mL). The extracts were dried (MgSO₄) and concentrated *in vacuo* to yield the crude product as a colourless solid. The crude product was purified using flash column chromatography eluting with 2:1 Petrol–EtOAc. The title compound (**4.20**) was isolated without further purification as a colourless powder. (36 mg, 0.12 mmol, 29%) m.p.: 182.3-184.0 °C; R_f: 0.73 (2:1 Petrol–EtOAc); δ_H (300 MHz, CDCl₃): 7.70 (1H, app s, 5-H), 7.64 (1H, dd, *J* 8.7 and 2.2, 7-H), 7.63 (1H, d, *J* 9.8, 4-H), 7.36 (1H, d, *J* 8.7, 8-H), 7.32-7.30 (1H, m, 4'-H), 7.28 (2H, t, *J* 7.1, 5'-H and 3'-H), 7.10 (2H, d, *J* 7.1, 6'-H and 2'-H), 6.52 (1H, d, *J* 9.8, 3-H), 4.36 (2H, s, CH₂); δ_C (75 MHz, CDCl₃): 159.1 (C=O), 157.0 (C8a), 142.2 (C4), 133.8 (C6), 131.6 (C7), 130.8 (C6' and C2'), 129.2 (C5), 129.1 (C4'), 128.8 (C5' and C3'), 127.8 (C1'), 118.7 (C4a), 118.5 (C3), 117.7 (C8); v_{max}/ cm⁻¹ (solid): 3446, 3084, 2928, 2455, 1979, 1732, 1601, 1313; HPLC: T_r= 2.59 (100% rel. area); *m/z* (ES): (Found: [M-H]⁻, 299.0377. C₁₆H₁₂O₄S requires *[M-H]*, 299.0384).

Synthesis of phenyl 2-oxo-2H-chromene-6-sulfonate (4.22)

2-oxo-2H-chromene-6-sulfonyl chloride (**4.3**) (0.48 g, 1.96 mmol), phenol (**4.21**) (0.19 g, 1.96 mmol) and pyridine (0.16 mL, 1.96 mmol) were stirred in DCM (10 mL) under and atmosphere of nitrogen for 16 h. The reaction mixture was washed with water (20 mL), dried (MgSO₄) and concentrated *in vacuo* to yield the crude product as a yellow powder. The crude product was purified using flash column chromatography eluting with 1:1 Petrol–EtOAc. The title compound (**4.22**) was isolated by recrystallization from toluene as pale pink needles. (0.43 g, 1.43 mmol, 73%) m.p.: 148.6-149.9 °C (from toluene); R_f: 0.80 (1:1 Petrol–EtOAc); δ_H (300

MHz, DMSO-d6): 8.39 (1H, d, J 2.3, 5-H), 8.19 (1H, d, J 7.9, 4-H), 8.00 (1H, dd, J 8.8 and 2.3, 7-H), 7.64 (1H, d, J 8.8, 8-H), 7.45-7.30 (3H, m, 5'-H, 4'-H and 3'-H), 7.06 (2H, d, J 7.7, 6'-H and 2'-H), 6.68 (1H, d, J 7.9, 3-H); δ_C (75 MHz, DMSO-d6): 158.9 (C=O), 157.1 (C8a), 148.9 (C7), 143.2 (C4), 131.0 (C6), 130.1 (C5' and C3'), 129.4 (C5), 127.6 (C6'), 122.1 (C6' and C2'), 119.5 (C4a), 118.4 (C8), 118.1 (C3); v_{max}/ cm^{-1} (solid): 1700, 1353, 1231, 1079; HPLC: T_r= 2.15 (100% rel. area); m/z (ES): (Found: MH$^+$, 303.0310. $C_{15}H_{10}O_5S$ requires MH, 303.0322).

Synthesis of 2-oxo-1,2-dihydroquinoline-6-sulfonyl chloride (4.24)
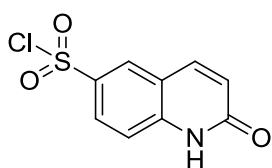
A solution of 1,2-dihydroquinolin-2-one (**4.23**) (0.20 g, 1.38 mmol) in chlorosulfonic acid (5 mL) was refluxed for 15 mins. After cooling to room temperature the mixture was poured into ice and water (50 mL). The solution was extracted with chloroform (3 × 50 mL), dried (MgSO$_4$), and concentrated *in vacuo* to yield the crude product as a pale yellow powder. The crude product was purified using flash column chromatography eluting with 1% MeOH:CHCl$_3$. The title compound (**4.24**) was isolated by recrystallization from DCM as colourless plates. (0.13 g, 0.54 mmol, 39%) m.p.: >250 °C (from DCM); R_f: 0.52 (1:99 MeOH–CHCl$_3$); δ_H (300 MHz, DMSO-d6): 7.97 (1H, d, J 9.3, 4-H), 7.91 (1H, d, J 1.6, 5-H), 7.70 (1H, dd, J 8.2 and J 1.6, 7-H), 7.26 (1H, d, J 8.2, 8-H), 6.49 (1H, d, J 9.3, 3-H); δ_C (75 MHz, DMSO-d6): 162.0 (C=O), 141.8 (C6), 140.7 (C4), 138.7 (C8a), 128.1 (C7), 124.8 (C5), 121.8 (C4a), 114.6 (C8); v_{max}/ cm^{-1} (solid): 3156, 2921, 1815, 1660, 1371, 1166; HPLC: T_r= 0.49 (100% rel. area); m/z (EI): (Found: M$^+$, 242.9761 $C_9H_6ClO_3S$ requires M, 242.9757).

## Synthesis of N-(2,3-dimethyl-1H-indol-7-yl)-2-oxo-1,2-dihydroquinoline-6-sulfonamide (4.25)
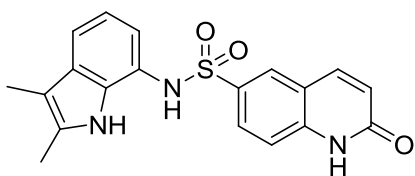
2-Oxo-1,2-dihydroquinoline-6-sulfonyl chloride (**4.24**) (0.10 g, 0.42 mmol), 2,3-dimethyl-7-aminoindole (**4.6**) (67 mg, 0.42 mmol) and pyridine (0.03 mL, 0.42 mmol) were stirred in DCM (5 mL) under and atmosphere of nitrogen for 16 h. The reaction mixture was washed with water (10 mL), dried (MgSO$_4$) and

concentrated *in vacuo* to yield the crude product as a yellow powder. The crude product was purified using flash column chromatography eluting with 1:1 Petrol–EtOAc. The title compound (**4.25**) was isolated by recrystallization from toluene as yellow microcrystals. (50 mg, 0.13 mmol, 31%) m.p.: > 250 °C (from toluene); R_f: 0.09 (1:1 Petrol–EtOAc); δ_H (300 MHz, DMSO-d6): 12.08 (1H, brs, quinolone-NH), 10.35 (1H, brs, indole-NH), 9.70 (1H, brs, sulphonamide-NH), 8.07 (1H, d, *J* 1.8, 5-H), 7.98 (1H, d, *J* 9.7, 4-H), 7.80 (1H, dd, *J* 8.3 and 1.8, 7-H), 7.34 (1H, d, *J* 8.3, 8-H), 7.10 (1H, d, *J* 7.3, 4'-H), 6.73 (1H, app. t, *J* 7.3 5'-H), 6.65-6.58 (2H, m, 6'-H and 3-H), 2.28 (3H, s, CH$_3$-C3'), 2.08 (3H, s, CH$_3$-C2'); δ_C (125 MHz, DMSO-d6): 161.8 (C=O), 141.5 (C7'), 139.9 (C4), 132.8 (C8a), 131.6 (C6), 130.6 (C7'a), 129.1 (C2'), 128.1 (C7), 127.5 (C5), 123.3 (C5'), 120.4 (C3'a), 118.3 (C4a), 118.2 (C8), 115.7 (C4'), 114.8 (C6'), 113.8 (C3), 105.8 (C3'), 11.1 (CH$_3$-C3'), 8.16 (CH$_3$-C2'); v_{max}/ cm^{-1} (solid): 3395, 1677, 1353, 1231, 1079; HPLC: T_r= 2.40 (91% rel. area); *m/z* (ES): (Found, MH$^+$, 368.1069. C$_{19}$H$_{17}$N$_3$O$_3$S requires *MH*, 368.1063).

### Synthesis of N-(2,3-dimethyl-1H-indol-7-yl)benzenesulfonamide (4.16)
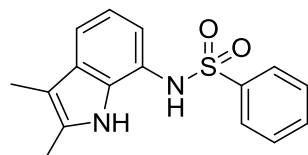
Benzenesulfonylchloride (0.07 mL, 0.56 mmol), 2,3-dimethyl-7-aminoindole (90 mg, 0.56 mmol) and pyridine (**4.6**) (0.05 mL, 0.56 mmol) were stirred in DCM (5 mL) under and atmosphere of nitrogen for 16 h. The reaction mixture was washed with water (10 mL), dried (MgSO$_4$) and concentrated *in vacuo* to yield the crude product as a pale yellow powder. The crude product was purified using flash column chromatography eluting with 1:1 Petrol–EtOAc. The title compound (**4.16**) was isolated by recrystallization from toluene as colourless microcrystals. (12 mg, 0.04 mmol, 2%) m.p.: 169.8-171.6 °C (from toluene); R_f: 0.86 (1:1 Petrol–EtOAc); δ_H (300 MHz, CDCl$_3$): 8.71 (1H, brs, indole NH), 7.64 (2H, d, *J* 7.1, 6-H and 2-H), 7.49 (1H, t, *J* 7.1, 4-H), 7.40 (2H, t, *J* 7.1, 5-H and 3-H), 7.32 (1H, d, *J* 7.7, 4'-H), 6.80 (1H, app. t, *J* 7.7, 5'-H), 6.48 (1H, brs, NH), 6.24 (1H, d, *J* 7.7, 6'-H), 2.39 (3H, s, CH$_3$-C3'), 2.20 (3H, s, CH$_3$-C2'); δ_C (75 MHz, CDCl$_3$): 137.8 (C1), 133.1 (C4), 132.2 (C2'), 131.7 (C7'a), 131.6 (C3'a), 128.9 (C5 and C3), 127.4 (C6 and C2), 118.8 (C5'), 118.5 (C3'), 117.6 (C6'), 117.4 (C4'), 107.4 (C7'), 11.7 (CH$_3$-C3'), 8.56 (CH$_3$-C2'); v_{max}/ cm^{-1} (solid): 3371, 3269, 1229, 1160, 1093;

HPLC: T_r= 3.27 (100% rel. area); *m/z* (ES): (Found: MNa$^+$, 323.0824. C$_{16}$H$_{16}$N$_2$O$_2$S requires *MNa*, 323.0825).

10.4 Synthesis of boronic acid based inhibitors

Synthesis of *tert*-butyl 3-bromo-2-methoxybenzoate (5.20)
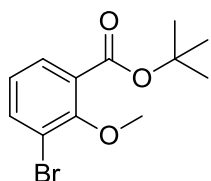
3-Bromo-2-methoxybenzoate (**5.19**) (0.50 g, 2.17 mmol) was dissolved in DCM (10 mL). To this was added oxalyl chloride (0.37 mL, 4.34 mmol) and cat. DMF (2 drops) and the reaction mixture was stirred for 1 h. The reaction mixture was concentrated *in vacuo*. The residue was dissolved in *tert*-butanol and refluxed for 16 h. The solvent was removed *in vacuo*. The crude product was purified by flash column chromatography eluting with 3:1 Petrol–EtOAc. The appropriate fractions were collected, combined and concentrated to afford the title compound (**5.20**) as a colourless oil which was used without further purification (0.29 g, 1.02 mmol, 47%) R_f: 0.84 (3:1 Petrol–EtOAc); δ_H (300 MHz, CDCl$_3$): 7.68 (2H, app. d, *J* 7.7, 6-H and 4-H), 7.02 (1H, app. t, *J* 7.7, 5-H), 3.93 (3H, s, OCH$_3$), 1.59 (9H, s, CH$_3$); δ_C (75 MHz, CDCl$_3$): 164.8 (C=O), 156.2 (C2), 136.5 (C4), 130.4 (C6), 128.9 (C1), 124.9 (C5), 118.9 (C3), 82.1 (C(CH$_3$)), 62.0 (OCH$_3$), 28.2 ((CH$_3$)$_3$); v_{max}/ cm^{-1} (oil): 2978, 1721, 1590, 1463, 1302; *m/z* (ES): (Found: MNa$^+$, 309.0098. C$_{12}$H$_{15}$BrO$_3$ requires *MNa*, 309.0097).
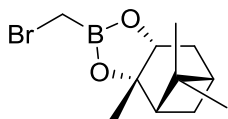
Synthesis of 2-(bromomethyl)-4,4,5,5-tetramethyl-1,3,2-dioxaborolane[140] (5.21)
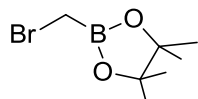
To a mixture of triisopropyl borate (20.0 g, 110 mmol), dibromomethane (8.60 mL, 120 mmol) and THF (150 mL) was added *n*-butyllithium (1.6M *n*-hexane solution, 63.6 mL, 100 mmol) at −100 °C (external temperature) over 1.5 h. The reaction mixture was stirred at the same temperature for 1.5 h, and then the reaction mixture was stirred at room temperature for 2 h. After the mixture was cooled at 0 °C (external temperature), to the reaction mixture was added methanesulfonic acid (6.50 mL, 100 mmol), and then the reaction mixture was stirred at room temperature for 1 h. After the mixture was cooled to 0 °C (external temperature), to the reaction mixture was added pinacol (12.0 g,

100 mmol), and then the reaction mixture was stirred at room temperature for 1 h. After the solvent was concentrated, the resulting residue was distilled under reduced pressure (80-82 °C, 40 mmHg), to obtain <u>the title compound</u> (**5.21**) as a colourless oil. (16.0g, 72.4 mmol, 72%) R_f: 0.37 (19:1 Petrol−EtOAc); δ_H (300 MHz, CDCl$_3$): 2.57 (2H, s, CH$_2$), 1.27 (12H, s, CH$_3$); δ_C (75 MHz, CDCl$_3$): 84.6 (CH$_2$), 24.7 (CH$_3$); v_{max}/ cm^{-1} (oil): 2922, 1415, 1338, 1286, 1144, 1029; *m/z* (ES): (Found: [M-Br]$^+$, 141.0833. C$_7$H$_{14}$BBrO$_2$ requires *[M-Br]*, 141.0837).

Synthesis of (3aS,4S,6S,7aR)-2-(bromomethyl)-3a,5,5-trimethylhexahydro-4,6-methano-1,3,2-benzodioxaborole[141] (5.22)


A mixture of 2-(bromomethyl)-4,4,5,5-tetramethyl-1,3,2 dioxaborolane (**5.21**) (0.40 g, 1.18 mmol) and (+)-Pinanediol (0.62 g, 3.62 mmol) in THF (10 mL) was stirred at room temperature for 18 h. The reaction mixture was concentrated *in vacuo*. The residue was partitioned between EtOAc (10 mL) and water (10 mL). The organics were separated and the aqueous extracted with further EtOAc (2 × 10 mL). The combined organics were dried (MgSO$_4$) and concentrated *in vacuo* to yield the crude product as a pale brown oil. The crude product was by flash column chromatography eluting with 3:1 Petrol–EtOAc. The appropriate fractions were collected, combined and concentrated to afford <u>the title compound</u> (**5.22**) as a colourless oil which was used without further purification (0.29 g, 1.02 mmol, 47%) R_f: 0.50 (19:1 Petrol−EtOAc); δ_H (300 MHz, CDCl$_3$): 4.37 (1H, dd, *J* 9.0 and 2.0, 7a-H), 2.63 (2H, s, CH$_2$Br), 2.36 (1H, ddt, *J* 14.5, 9.0 and 2.0, 7*-H), 2.22-2.29 (1H, m, 8-H), 2.08 (1H, app. t, *J* 5.5, 4-H), 1.87-1.96 (2H, m, 7*-H and 6-H), 1.42 (3H, s, CH$_3$-C3a), 1.30 (3H, s, CH$_3$-5b), 1.20 (1H, d, *J* 11.0, 8-H), 0.85 (3H, s, CH$_3$-5a) ; δ_C (75 MHz, CDCl$_3$): 86.7 (C3a), 78.6 (C7), 51.2 (C4), 39.3 (C6) 38.2 (C5), 35.2 (C7), 28.7 (C3a-CH$_3$), 27.2 (C5b-CH$_3$), 26.5 (C8), 23.9 (C5b-CH$_3$), 10.1 (CH$_2$Br); v_{max}/ cm^{-1} (oil): 2922, 1725, 1415, 1338; *m/z* (ES): (Found: [M-Br]$^+$, 193.1198. C$_{11}$H$_{18}$BBrO$_2$ requires *[M-Br]*, 193.1120). [α]$_D$ = + 35.2° (c 0.50, CHCl$_3$).

Synthesis of 2-methoxy-3-([(3aS,4S,6S,7aR)-3a,5,5-trimethylhexahydro-4,6-methano-1,3,2-benzodioxaborol-2-yl]methyl) benzoic acid tert-butly ester (5.9)
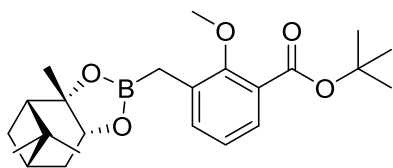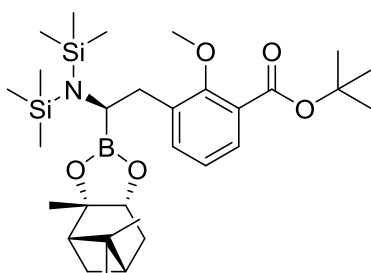
To a stirred solution of tert-butyl 3-bromo-2-methoxybenzoate (**5.20**) (2.63 g, 9.19 mmol) in THF (50 mL) was added *n*-butyllithium (1.6M *n*-hexane solution, 5.77 mL, 9.19 mmol) drop wise at -100 °C. The solution was stirred at −100 °C for 1 h. (3aS,4S,6S,7aR)-2-(bromomethyl)-3a,5,5-trimethylhexahydro-4,6-methano-1,3,2-benzodioxaborole (**5.22**) (3.00 g, 11.0 mmol) was added and the reaction mixture was stirred at −100 °C for 2 h. The mixture was then allowed to warm to room temperature with stirring overnight. The mixture was concentrated *in vacuo*. The residue was diluted with water (50 mL) and extracted in DCM (3 × 50 mL). The combined organics were dried (MgSO$_4$) and concentrated *in vacuo* to yield the crude product as a pale yellow oil. The crude product was by flash column chromatography eluting with 19:1 Petrol–EtOAc. The appropriate fractions were collected, combined and concentrated to afford the title compound (**5.9**) as a colourless oil which was used without further purification (2.79 g, 6.98 mmol, 76%). R$_f$: 0.85 (19:1 Petrol−EtOAc); δ$_H$ (300 MHz, CDCl$_3$): 7.52 (1H, dd, *J* 7.6 and 1.8, 6-HAr), 7.33 (1H, dd, *J* 7.6 and 1.8, 4-HAr), 7.02 (1H, app. t, *J* 7.6, 5-HAr), 4.27 (1H, dd, *J* 8.7 and 2.0, 7a-H), 3.81 (3H, s, OCH$_3$), 2.32 (2H, s, CH$_2$B), 2.32-2.24 (1H, m, 7*-H), 2.22-2.14 (1H, m, 8-H), 2.03 (1H, app. t, *J* 5.1, 4-H), 1.91-1.87 (1H, m, 6-H), 1.82 (1H, dd, *J* 14.2 and 2.1, 7*-H), 1.59 (9H, s, C(CH$_3$)$_3$), 1.38 (3H, s, CH$_3$-C3a), 1.27 (3H, s, CH$_3$-5b), 1.19 (1H, d, *J* 10.8, 8-H), 0.83 (3H, s, CH$_3$-5a); δ$_C$ (75 MHz, CDCl$_3$): 166.0 (C=O), 157.4 (C2-Ar), 134.2 (C6-Ar), 134.0 (C3-Ar), 128.4 (C5-Ar), 126.4 (C1-Ar), 123.3 (C4-Ar), 85.8 (C3a), 81.0 (C(CH$_3$)$_3$), 77.9 (C7), 61.5 (OCH$_3$), 51.3 (C4), 41.3 (C6), 39.5 (C5), 38.2 (C7), 28.6 (C3a-CH$_3$), 28.2 (C(CH$_3$)$_3$), 27.1 (C5b-CH$_3$), 24.0 (C8), 22.6 (C5a-CH$_3$), 11.4 (br, CH$_2$B); ν$_{max}$/ cm^{-1} (oil): 2977, 2925, 2869, 1700, 1278, 1135; HPLC: T$_r$= 2.79 (93% rel. area); *m/z* (ES): (Found: MH$^+$, 401.2505. C$_{24}$H$_{34}$BClO$_5$ requires *MH*, 401.2498). [α]$_D$ = + 12.4° (c 0.50, CHCl$_3$).

Synthesis of 2-methoxy-3-((2S)-2-chloro-2-[(3aS,4S,6S,7aR)-3a,5,5-trimethylhexahydro-4,6-methano-1,3,2-benzodioxaborol-2-yl]ethyl) benzoic acid tert-butly ester (5.23)
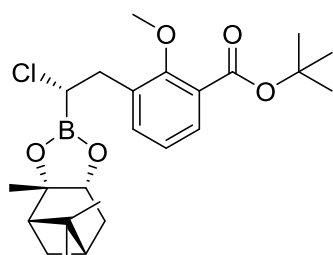
Lithium diisopropylamide (LDA) was prepared fresh by addition of *n*-butyllithium (1.6M *n*-hexane solution, 0.98 mL, 1.50 mmol) to a solution of diisopropylamine (0.21 mL, 1.50 mmol) in THF (3.5 mL) at -100 °C under a nitrogen atmosphere. The mixture was stirred at −100 °C for 10 mins before warming to ca. −20 °C. In a separate flask a mixture of 2-methoxy-3-([(3aS,4S,6S,7aR)-3a,5,5-trimethylhexahydro-4,6-methano-1,3,2-benzodioxaborol-2-yl]methyl) benzoic acid tert-butly ester (**5.9**) (0.50 g, 1.25 mmol), DCM (0.32 mL, 5.00 mmol) in THF (22.5 mL) was stirred at −100 °C under nitrogen. To this was added the LDA solution over 30 mins. Stirring was continued at −100 °C for 30 mins before addition of 1M $ZnCl_2$ solution in ether (2.00 mL, 2.00 mmol). The resulting mixture was left to warm to room temperature overnight. The mixture was concentrated *in vacuo* and sat. NH_4Cl solution (50 mL) was added and the resulting mixture stirred for 10 mins. The mixture was extracted with hexane (3 × 25 mL). The organics were combined, dried (MgSO₄) and concentrated *in vacuo* to afford <u>the title compound</u> (**5.23**) as a pale yellow oil (0.51 g, 1.14 mmol, 91%) R_f: 0.52 (19:1 Petrol−EtOAc); δ_H (300 MHz, CDCl₃): 7.63 (1H, dd, *J* 7.7 and 1.8 6-HAr), 7.39 (1H, dd, *J* 7.7 and 1.8, 4-HAr), 7.06 (1H, app. t, *J* 7.7, 5-HAr), 4.36 (1H, dd, *J* 8.5 and 2.1, 7a-H), 3.86 (3H, s, OCH₃), 3.74 (1H, t, *J* 8.2, ClC<u>H</u>), 3.20 (2H, dd, *J* 14.1 and 8.2 CH2Ar), 2.45-2.27 (1H, m, 7*-H), 2.25-2.18 (1H, m, 8-H), 2.06 (1H, app. t, *J* 5.5, 6-H), 1.95-1.83 (2H, m, 7*-H and 4-H), 1.59 (9H, s, <u>(CH₃)₃</u>), 1.38 (3H, s, C3a-CH₃), 1.28 (3H, s, C5b-CH₃), 1.10 (1H, d, *J* 11.2, 8-H), 0.83 (3H, s, C5a-CH₃); δ_C (75 MHz, CDCl₃): 165.7 (C=O), 158.3 (C2-Ar), 134.4 (C6-Ar), 132.7 (C3-Ar), 130.3 (C5-Ar), 126.4 (C1-Ar), 123.2 (C4-Ar), 86.8 (C3a), 81.3 (<u>C</u>(CH₃)₃), 78.5 (C7), 62.3 (OCH₃), 51.2 (C4), 41.2 (br, Cl<u>C</u>H), 39.4 (C6), 38.2 (C5), 35.1 (C7), 35.0 (CH₂Ar), 28.3 (C3a-<u>C</u>H₃), 28.2 (C(<u>CH₃</u>)₃), 27.0 (C5b-CH₃), 26.8 (C8), 24.0 (C5a-CH₃); v_{max}/ cm⁻¹ (oil): 2971, 2921, 2871, 1700, 1466, 1369, 1239, 1135; *m/z* (ES): (Found: MH⁺, 449.2233. C₂₄H₃₄BClO₅ requires *MH*, 449.2268). [α]$_D$ = + 52.1° (c 0.50, CHCl₃).
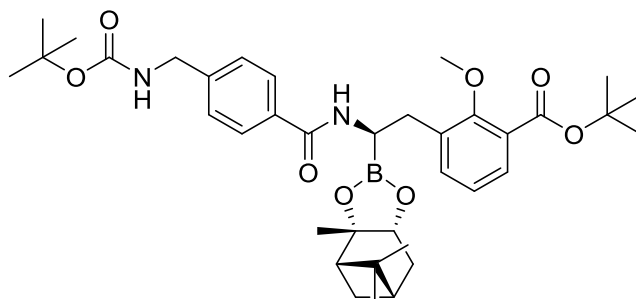
Synthesis of 2-methoxy-3-((2R)-2-[bis(trimethylsilyl)amino]-2-[(3aS,4S,6S,7aR)-3a,5,5-trimethylhexahydro-4,6-methano-1,3,2-benzodioxaborol-2-yl]ethyl) benzoic acid tert-butly ester (5.10)

To a stirred solution of 2-methoxy-3-((2S)-2-chloro-2-[(3aS,4S,6S,7aR)-3a,5,5-trimethylhexahydro-4,6-methano-1,3,2-benzodioxaborol-2-yl]ethyl) benzoic acid tert-butly ester (**5.23**) (0.45 g, 1.00 mmol) in THF (17.5 mL) at −100 °C was added a solution of LiHMDS (1M in THF, 1.1 mL) in THF (7 mL) over 30 mins. The resulting mixture was left to warm to room temperature with stirring overnight. The mixture was concentrated *in vacuo* and re-suspended in hexane (50 mL) with stirring for 1 h. The suspension was filtered through celite and the celite was washed with further hexane (2 × 25 mL). The filtrate was concentrated *in vacuo* to afford the title compound (**5.10**) as dense pale yellow oil which was used without further purification. (0.33 g, 0.58 mmol, 58%) R_f: 0.71 (19:1 Petrol−EtOAc); δ_H (300 MHz, CDCl$_3$): 7.48 (1H, dd, *J* 7.6 and 1.8, 6-HAr), 7.27 (1H, dd, *J* 7.6 and 1.8, 4-HAr), 6.94 (1H, app. t, *J* 7.6, 5-HAr), 4.18 (1H dd, *J* 8.7 and 1.9, 7a-H), 3.77 (3H, s, OC$\underline{H}_3$), 3.15 (1H, dd, *J* 13.2 and 6.6, CH$_2$Ara), 2.89 (1H, dd, *J* 8.4 and 6.6, NC$\underline{H}$), 2.49 (1H, dd, *J* 13.2 and 8.4, CH$_2$Arb), 2.28-2.13 (1H, m, 7*-H), 2.10-2.03 (1H, m, 8-H), 1.93 (1H, app. t, *J* 5.6, 4-H), 1.83-1.75 (1H, m, 6-H), 1.70-1.62 (1H, m, 7*-H), 1.54 (9H, s, C($\underline{CH_3})_3$), 1.30 (3H, s, C3a-CH$_3$), 1.20 (3H, s, C5b-CH$_3$), 0.94 (1H, d, *J* 10.8, 8-H), 0.76 (3H, s, C5a-CH$_3$), -0.01 (18H, s, TMS); δ_C (75 MHz, CDCl$_3$): 165.3 (C=O), 157.5 (C2-Ar), 134.9 (C6-Ar), 134.0 (C3-Ar), 128.2 (C5-Ar), 125.6 (C1-Ar), 121.8 (C4-Ar), 84.7 (C3a), 80.1 ($\underline{C}$(CH$_3$)$_3$), 77.3 (C7), 61.0 (O$\underline{C}$H$_3$), 50.5 (C4), 41.2 (N$\underline{C}$H), 35.1 (C7), 35.0 (CH$_2$Ar), 27.7 (C3a-$\underline{C}$H$_3$), 27.3 (C($\underline{CH_3})_3$), 26.2 (C5b-$\underline{C}$H$_3$), 25.4 (C8), 23.1 (C5b-CH$_3$); v_{max}/ cm^{-1} (oil): 2977, 2925, 2869, 1700, 1287, 1135; *m/z* (ES): (Found: [M-2TMS]$^+$, 430.2783. C$_{30}$H$_{52}$BNO$_5$Si$_2$ requires *[M-2TMS]*, 430.2760). [α]$_D$ = + 20.1° (c 0.50, CHCl$_3$).
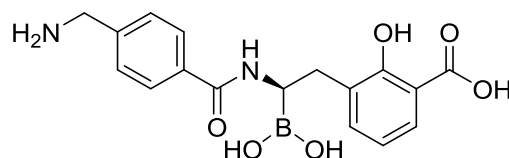
Synthesis of 3-[(2R)-2-[4-(tert-Butoxycarbonylamino-methyl)-benzoylamino]-2-[(3aS,4S,6S,7aR)-3a,5,5-trimethylhexahydro-4,6-methano-1,3,2-benzodioxaborol-2-yl]-ethyl]-2-methoxy-benzoic acid tert-butyl ester. (5.24)

Preparation was *via* general method E using 4-Boc (aminomethyl)benzoic acid (0.50 g, 1.99 mmol) and 2-methoxy-3-((2R)-2-[bis(trimethylsilyl)amino]-2-[(3aS,4S,6S,7aR)-3a,5,5-trimethylhexahydro-4,6-methano-1,3,2-benzodioxaborol-2-yl]ethyl) benzoic acid tert-butly ester (**5.10**) (1.70 g, 3.98 mmol) to afford the title compound (**5.24**) as a yellow glassy solid which was used without further purification (0.55 g, 0.84 mmol, 42%). m.p.: 73.8-75.5 °C; R_f: 0.21 (3:1 Hexane−EtOAc); δ_H (500 MHz, CDCl$_3$): 7.73 (2H, d, *J* 8.2 2'-HAr and 6'-HAr), 7.61 (1H, dd, *J* 7.7 and 1.7, 6-HAr), 7.48 (1H, brs, CONH), 7.38 (1H, dd, *J* 7.7 and 1.7, 4-HAr), 7.34 (2H, d, *J* 8.2, 3'-HAr and 6'-HAr), 7.09 (1H, t, *J* 7.7, 5-HAr), 4.94 (1H, brs, BOC-NH), 4.36 (2H, app. s, CH$_2$N), 4.31 (1H, d, J 7.6, 7a-H), 3.83 (3H, s, OCH$_3$), 3.09 (1H, t, *J* 5.4, NCH), 2.99 (2H, d, *J* 5.4, CH$_2$Ar), 2.44-2.30 (1H, m, 7*-H), 2.29-2.12 (1H, m, 8-H), 2.06 (1H, app. t, *J* 10.9, 6-H), 1.98-1.86 (2H, m, 7*-H and 4-H), 1.61 (9H, s, C(CH$_3$)$_3$), 1.58 (1H, d, *J* 10.9, 8-H), 1.48 (9H, s, BOC-CH$_3$), 1.46 (3H, s, C3-CH$_3$), 1.30 (3H, s, C5b-CH$_3$), 0.90 (3H, s, C5a-CH$_3$); δC(75 MHz, CDCl$_3$): 170.1 (CONH), 165.8 (C=O), 157.6 (C=O BOC), 135.8 (C4'-Ar), 134.8 (C6-Ar and C1'-Ar), 129.8 (C4-Ar), 128.0 (C5'-Ar, C3'-Ar and C3-Ar), 127.5 (C6'-Ar and C2'-Ar), 124.2 (C5-Ar and C1-Ar), 83.7 (C3a), 81.5 (C(CH$_3$)$_3$), 76.7 (C7a), 62.3 (OCH$_3$), 52.4 (C4), 45.0 (CH2CB), 40.2 (C6), 38.2 (C5), 36.7 (CH2N), 32.8 (C7), 28.3 (C3-CH3), 28.2 ((CH$_3$)$_3$), 27.4 (C5a-CH$_3$), 26.7 (C8), 24.3 (C5b-CH$_3$); v_{max}/ cm^{-1} (solid): 3272, 2971, 2870, 1700, 1502, 1388, 1228; *m/z* (ES): (Found: MH$^+$, 663.4033. C$_{37}$H$_{51}$BN$_2$O$_8$ requires MH, 663.3811). [α]$_D$ = − 22.3° (c 0.50, CHCl$_3$).

Synthesis of 3-[(2R)-2-(4-(Aminomethyl)benzoylamino)-2-borono-ethyl]-2-hydroxy-benzoic acid hydrochloride. (5.13)
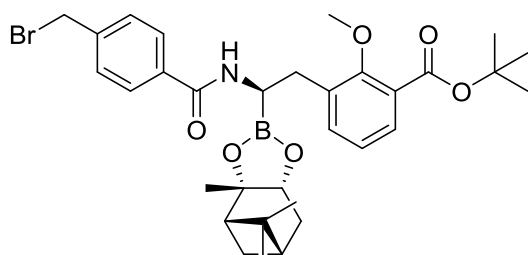

Preparation was *via* general method G using 3-[(2R)-2-[4-(tert-Butoxycarbonylamino-methyl)-benzoylamino]-2-[(3aS,4S,6S,7aR)-3a,5,5-trimethylhexahydro-4,6-methano-1,3,2-benzodioxaborol-2-yl]-ethyl]-2-methoxy-benzoic acid tert-butyl ester (**5.24**) (50 mg, 0.08 mmol) to afford the title compound (**5.13**) as a colourless solid which was used without further purification (3.8 mg, 0.01 mmol, 13%). m.p.: > 250 °C; R_f: 0.05 (9:1 DCM−MeOH); δ_H (500 MHz, MeOD-d4): 8.39 (1H, brs, CONH), 8.0-7.85 (2H, app. m, 6'-H and 2'-H), 7.82 (1H, d, *J* 7.8, 6-H), 7.62-7.50 (2H, app. m, 5'-H and 3'-H), 7.38-7.28 (1H, app. m, 4-H), 6.97-6.78 (1H, app. m, 5-H), 4.20 (2H, s, CH$_2$NH$_2$), 3.52 (1H, app. s, NCH), 3.09 (2H, app. s, CH$_2$); v_{max}/ cm^{-1} (solid): 3388, 2913, 1597, 1481, 1337; *m/z* (ES): (Found: [M-H$_2$O+H]$^+$, 341.1312. C$_{17}$H$_{19}$BN$_2$O$_6$ requires *[M-H$_2$O+H]*, 341.1306. [α]$_D$ = − 75.4° (c 0.10, MeOH).

Synthesis of 3-[(2R)-2-[4-(bromomethyl)-benzoylamino]-2-[(3aS,4S,6S,7aR)-3a,5,5-trimethylhexahydro-4,6-methano-1,3,2-benzodioxaborol-2-yl]-ethyl]-2-methoxy benzoic acid tert-butyl ester. (5.25)
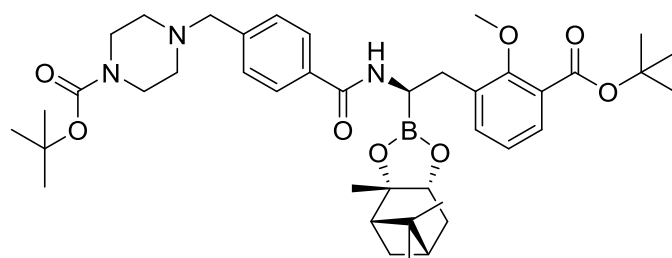

Preparation was *via* general method E using 4-bromomethylbenzoic acid (0.99 g, 4.64 mmol) and 2-methoxy-3-((2R)-2-[bis(trimethylsilyl)amino]-2-[(3aS,4S,6S,7aR)-3a,5,5-trimethylhexahydro-4,6-methano-1,3,2-benzodioxaborol-2-yl]ethyl) benzoic acid tert-butly ester (3.19 g, 5.57 mmol) to afford the title compound (**5.25**) as a yellow glassy solid which was used without further purification (0.50 g, 0.80 mmol, 14%). m.p.: 93.7-95.2 °C; R_f: 0.32 (3:1 Hexane−EtOAc); δ_H (500 MHz, CDCl$_3$): 7.72 (2H, d, *J* 7.8, 2'-HAr and 6'-HAr), 7.61 (1H, d, *J* 6.9, 6-HAr), 7.44 (3H, app. d, *J* 7.8, CONH, 3'-HAr and 5'-HAr), 7.36 (1H, d, *J* 6.9, 4-HAr), 7.10 (1H, t, *J* 6.9, 5-HAr), 4.48 (2H, s, CH$_2$Br), 4.32 (1H, d, *J* 9.0, 7a-H), 3.84 (3H, s, OCH$_3$), 3.15 (1H, t, *J* 6.9, NCH), 3.00 (2H, d, *J* 6.9, CH$_2$Ar), 2.48-2.29 (1H, m, 7*-H), 2.25-2.16 (1H, m, 8-H), 2.07-1.99 (1H, m, 6-H),

1.97-1.83 (2H, m, 7*-H and 4-H), 1.62 (9H, s, C(C<u>H$_3$</u>)$_3$), 1.52 (1H, d, *J* 7.4, 8-H), 1.74 (3H, s, C3-CH$_3$), 1.28 (3H, C5b-CH$_3$), 0.89 (3H, s, C5a-CH$_3$); δ$_C$ (125 MHz, CDCl$_3$): 169.5 (HNC=O), 165.8 (C=O), 157.6 (C2-Ar), 142.5 (C4'-Ar), 135.5 (C1'-Ar), 134.7 (C6-Ar), 129.9 (C4-Ar), 129.4 (C3-Ar), 129.3 (C6'-Ar and C2'-Ar), 128.1 (C5'-Ar and C3'-Ar), 124.2 (C5-Ar), 84.1 (C3a), 81.5 (C7a), 77.0 (<u>C</u>(CH$_3$)$_3$), 62.3 (OCH$_3$), 52.5 (C4), 45.0 (brs, NCH), 38.2 (C5), 36.5 (CH$_2$C), 32.6 (C7), 32.0 (CH$_2$Br), 29.1 (C3-CH$_3$), 27.4 (C5a-CH$_3$), 26.6 (C8), 24.2 (C5b-CH$_3$); ν$_{max}$/ cm^{-1} (solid): 2720, 1700, 1367, 1039, 1003; *m/z* (ES): (Found: MH$^+$, 626.2780. C$_{32}$H$_{41}$BBrNO$_6$ requires *MH*, 626.2283. [α]$_D$ = + 14.3° (c 0.50, CHCl$_3$).

Synthesis of 2-methoxy-3-[(2R)-2-((4-Boc-piperazinylmethyl)-benzoylamino)-2-[(3aS,4S,6S,7aR)-3a,5,5-trimethylhexahydro-4,6-methano-1,3,2-benzodioxaborol-2-yl]-ethyl] benzoic acid tert-butyl ester. (5.28)
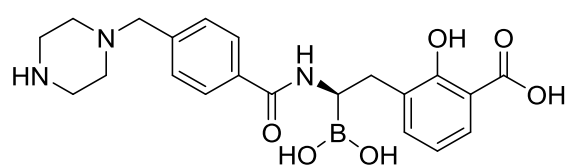

Preparation was *via* general method F using 3-3-[(2R)-2-[4-(bromomethyl)-benzoylamino]-2-[(3aS,4S,6S,7aR)-3a,5,5-trimethylhexahydro-4,6-methano-1,3,2-benzodioxaborol-2-yl]-ethyl]-2-methoxy benzoic acid tert-butyl ester (**5.25**) (0.41 g, 0.65 mmol) and 1-Boc-piperazine (0.12 g, 0.65 mmol) to afford <u>the title compound</u> (**5.28**) as a red oil which was used without further purification (80 mg, 0.11 mmol, 17%). *R$_f$*: 0.14 (3:1 Hexane−EtOAc); δ$_H$ (500 MHz, CDCl$_3$): 7.72 (2H, d, *J* 8.1, 6'-HAr and 2'-HAr), 7.61 (1H, dd, *J* 7.3 and 1.3, 6-HAr), 7.45 (1H, brs, CON<u>H</u>), 7.39 (2H, d, *J* 8.1, 5'-HAr and 3'-HAr), 7.38 (1H, dd, *J* 7.3 and 1.3, 4-HAr), 7.10 (1H, app.t, *J* 7.3, 5-HAr), 4.31 (1H, d, *J* 9.0, 7a-H), 3.83 (3H, s, OCH$_3$), 3.54 (2H, s, CH$_2$), 3.46-3.39 (4H, m, 5-HPip and 3-HPip), 3.09 (1H, t, *J* 6.3, NHC), 3.00 (2H, d, *J* 6.3, CH$_2$C), 2.43-2.31 (5H, m, 6-HPip, 2-HPip and 7*-H), 2.24-2.14 (1H, m, 8-H), 2.08-2.00 (1H, m, 6-H), 1.95-1.86 (2H, m, 7*-H and 4-H), 1.61 (9H, s, C(CH$_3$)$_3$), 1.48 (3H, s, C3-CH$_3$), 1.46 (9H, s, BOC), 1.30 (C5a-CH$_3$), 1.26 (1H, d, *J* 7.4, 8-H), 0.89 (3H, s, C5b-CH$_3$); δ$_C$ (125 MHz, CDCl$_3$): 170.3 (NHC=O), 165.8 (C=O), 154.8 (BOC C=O), 143.8 (C4'-Ar), 135.9 (C1'-Ar), 134.8 (C6-Ar), 129.8 (C4-Ar),

129.9 (C6'-Ar, C2'-Ar and C3-Ar), 127.8 (C5'-Ar and C3'-Ar), 127.7 (C1-Ar), 124.1 (C5-Ar), 83.7 (C3a), 81.5 ($\underline{C}$(CH$_3$)$_3$), 79.6 (BOC C), 77.0 (C7a), 62.5 (CH$_2$), 62.3 (OCH$_3$) 52.9 (C6-Pip, C5-Pip, C3-Pip and C2-Pip), 52.4 (C4), 45.0 (brs, NCH), 40.2 (C6), 38.2 (CH$_2$C), 36.8 (C5), 32.8 (C7), 29.2 (C3-CH$_3$), 28.3 (C($\underline{C}$H$_3$)$_3$ × 2), 27.3 (C5a-CH$_3$) 26.7 (C8), 24.2 (C5b-CH$_3$); ν$_{max}$/ cm^{-1} (oil): 2850, 1700, 1390, 1252, 1030; m/z (ES): (Found: MH$^+$, 732.4394. C$_{41}$H$_{58}$BN$_3$O$_8$ requires MH, 732.4397). [α]$_D$ = − 65.6° (c 0.50, CHCl$_3$).

Synthesis of 3-[(2R)-2-borono-2-(4-(1-piperazinylmethyl)benzoylamino)-ethyl]-2-hydroxy-benzoic acid hydrochloride. (5.14)

Preparation was via general method G using 2-methoxy-3-[(2R)-2-((4-Boc-piperazinylmethyl)-benzoylamino)-2-[(3aS,4S,6S,7aR)-3a,5,5-trimethylhexahydro-4,6-methano-1,3,2-benzodioxaborol-2-yl]-ethyl] benzoic acid tert-butyl ester (**5.28**) (50 mg, 0.07 mmol) to afford the title compound (**5.14**) as an off-white glassy solid which was used without further purification (0.7 mg, 2.00 µmol, 2%). m.p.: 36.3-37.6 °C; R$_f$: 0.08 (9:1 DCM−MeOH); δ$_H$ (500 MHz, MeOD-d4): 8.28 (1H, brs, CONH), 7.75-7.70 (2H, app. m, 6'-H and 2'-H), 7.61 (1H, d, J 7.6, 6-H), 7.44-7.36 (2H, app. m, 5'-H and 3'-H), 7.23-7.18 (1H, app. m, 4-H), 6.84-6.78 (1H, app. m, 5-H), 4.47 (2H, brs, B(OH)$_2$), 3.55 (2H, s, CH$_2$N), 3.36 (1H, brs, CHN), 3.13-3.04 (4H, m, 5''-H and 3''-H), 2.96 (2H, app. s, CH$_2$), 2.58-2.50 (4H, m, 6''-H and 2''-H); ν$_{max}$/ cm^{-1} (solid): 3358, 1670, 1610, 1478, 1018; m/z (ES): (Found: [M-H$_2$O+H]$^+$, 410.1891. C$_{21}$H$_{26}$BN$_3$O$_6$ requires [M-H$_2$O+H], 410.1895. [α]$_D$ = − 46.0° (c 0.05, MeOH).
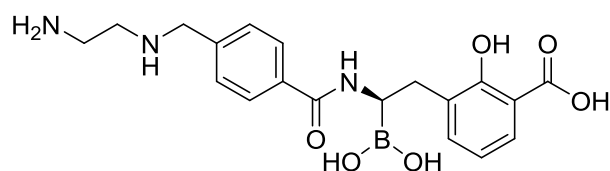
Synthesis of 3-[(2R)-2-[((Boc-ethylamine)methyl)-benzoylamino]-2-[(3aS,4S,6S,7aR)-3a,5,5-trimethylhexahydro-4,6-methano-1,3,2-benzodioxaborol-2-yl]-ethyl]-2-methoxy benzoic acid tert-butyl ester. (5.29)
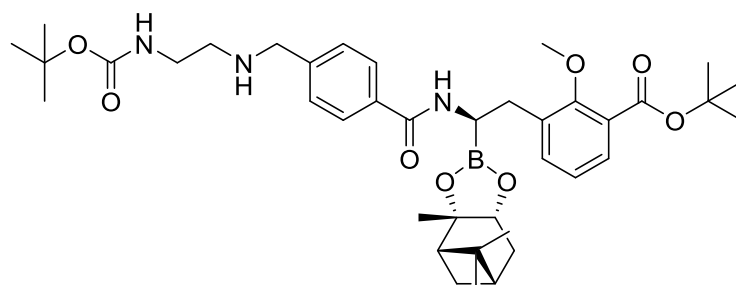
Preparation was via general method F using 3-[(2R)-2-[4-(bromomethyl)-benzoylamino]-2-[(3aS,4S,6S,7aR)-

3a,5,5-trimethylhexahydro-4,6-methano-1,3,2-benzodioxaborol-2-yl]-ethyl]-2-methoxy benzoic acid tert-butyl ester (**5.25**) (0.60 g, 0.96 mmol) and N-Boc-ethylenediamine (0.15 g, 0.96 mmol) to afford <u>the title compound</u> (**5.29**) as a pale brown oil which was used without further purification (0.12 g, 0.17 mmol, 18%). R_f: 0.18 (3:1 Hexane−EtOAc); δ_H (500MHz, CDCl$_3$): 7.67 (2H, d, J 7.6, 6'-HAr and 2'-HAr), 7.51 (1H, dd, J 6.5 and 1.3, 6-HAr), 7.36 (2H, d, J 7.6, 5'-HAr and 3'-HAr), 7.29 (1H, dd, J 6.5 and 1.3, 4-HAr), 7.01 (1H, app. t, J 6.5, 5-HAr), 5.86 (1H, brs, BOCNH), 4.20 (1H, d, J 7.7, 7a-H), 3.99 (2H, s, ArC<u>H$_2$</u>NH), 3.76 (3H, s, OCH$_3$), 3.26 (2H, d, J 5.5, CH$_2$C), 3.10 (1H, brs, NH), 2.95-2.85 (4H, m, HNC<u>H$_2$</u> and <u>CH$_2$</u>NH), 2.31-2.24 (1H, m, 7*-H), 2.13-2.06 (1H, m, 8-H), 1.96-1.91 (1H, m, 6-H), 1.85-1.77 (2H, m, 7*-H and 4-H), 1.54 (9H, s, C(CH$_3$)$_3$), 1.41 (1H, d, J 7.4, 8-H), 1.34 (3H, s, C3-CH$_3$), 1.30 (9H, s, BOC C(CH$_3$)$_3$), 1.20 (3H, s, C5a-CH$_3$), 0.78 (3H, s, C5b-CH$_3$); δ_C (100MHz, CDCl$_3$): 169.8 (NHC=O), 166.3 (BOC C=O), 165.9 (C=O), 157.8 (C2-Ar), 135.3 (C1'-Ar), 134.6 (C6-Ar), 130.0 (C6'-Ar and C2'-Ar), 129.9 (C3-Ar), 129.7 (C4-Ar), 128.5 (C5'-Ar and C3'-Ar), 126.8 (C1-Ar), 124.0 (C5-Ar), 84.0 (C3a), 81.5 (C(CH$_3$)$_3$ × 2), 76.7 (C7a), 62.2(OCH$_3$), 52.2 (C4), 50.6 (CH$_2$NH), 47.4 (CH$_2$NH), 45.0 (brs HCN), 40.1 (C6), 38.2 (C5), 36.4 (CH$_2$C), 32.4 (ArCH$_2$NH), 29.1 (C3-CH$_3$), 28.3 (C(CH$_3$)$_3$ × 2), 27.3 (C5a-CH$_3$), 24.2 (C5b-CH$_3$); v_{max}/ cm^{-1} (oil): 2920, 2914, 1700, 1652, 1080, 730 m/z (ES): (Found: MH$^+$, 706.4222. C$_{39}$H$_{56}$BN$_3$O$_8$ requires MH, 706.4240). [α]$_D$ = − 147.0° (c 0.50, CHCl$_3$).

Synthesis of 3-[(2R)- 2-[(4-(2-amino-ethylamino)-methyl)benzoylamino]-2-borono-ethyl]-2-hydroxy-benzoic acid hydrochloride. (5.15)
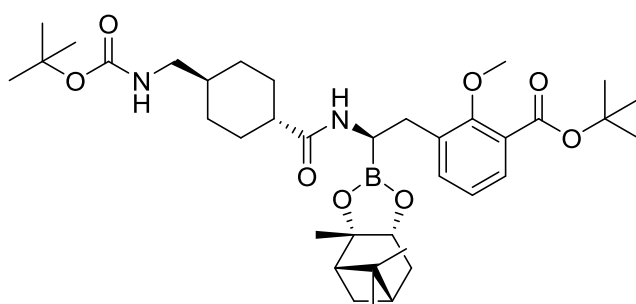

Preparation was *via* general method G using 3-[(2R)-2-((Boc-ethylamine)-benzoylamino)-2-[(3aS,4S,6S,7aR)-3a,5,5-trimethylhexahydro-4,6-methano-1,3,2-benzodioxaborol-2-yl]-ethyl]-2-methoxy benzoic acid tert-butyl ester (**5.29**) (0.10 g, 0.14 mmol) to afford <u>the title compound</u> (**5.15**) as a yellow glassy solid which was used without further purification (0.5 mg, 1.00 μmol, 1%). m.p.: 44.7-45.9 °C; R_f: 0.12 (9:1 DCM−MeOH); δ_H (500 MHz, MeOD-d4): 8.28 (1H, brs, CONH), 7.75-7.71 (2H, app. m, 6'-H and 2'-H), 7.70 (1H, d, J

7.6, 6-H), 7.44-7.41 (2H, m, 5'-H and 3'-H), 7.24-7.18 (1H, app. m, 4-H), 6.84-6.78 (1H, app. m, 5-H), 4.47 (2H, brs, B(OH)$_2$), 3.75 (2H, s, CH$_2$N), 3.39 (1H, app. s, NCH), 2.96 (2H, app. s, CH$_2$Ar), 2.86 (2H, app. t, J 5.7, Ethyl CH$_2$), 2.68 (2H, app. t, J 5.7, Ethyl-CH$_2$); v_{max}/ cm^{-1} (solid): 2892, 1717, 1662, 1530, 1389, 921; m/z (ES): (Found: [M-H$_2$O+H]$^+$, 384.1725. C$_{19}$H$_{24}$BN$_3$O$_6$ requires $[M-H_2O+H]$, 384.1729. $[α]_D$ = − 15.4 ° (c 0.10, MeOH).

Synthesis of 3-[(2R)-2-[4-(tert-Butoxycarbonylamino-methyl)-cyclohexyl formamido]-2-[(3aS,4S,6S,7aR)-3a,5,5-trimethylhexahydro-4,6-methano-1,3,2-benzodioxaborol-2-yl]-ethyl]-2-methoxy-benzoic acid tert-butyl ester. (5.26)
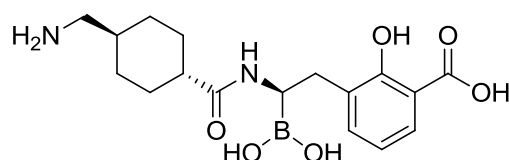

Preparation was *via* general method E using 4-BOC aminomethylcyclohexyl carboxylic acid (0.36 g, 1.40 mmol) and 2-methoxy-3-((2R)-2-[bis(trimethylsilyl)amino]-2-[(3aS,4S,6S,7aR)-3a,5,5-trimethylhexahydro-4,6-methano-1,3,2-benzodioxaborol-2-yl]ethyl) benzoic acid tert-butly ester (**5.10**) (0.80 g, 1.40 mmol) to afford the title compound (**5.26**) as a colourless oil which was used without further purification (0.15 g, 0.22 mmol, 16%). R_f: 0.18 (3:1 Hexane−EtOAc); $δ_H$ (500 MHz, CDCl$_3$): 7.58 (1H, dd, J 7.9 and 1.4, 6-HAr), 7.32 (1H, dd, J 7.9 and 1.4, 4-HAr), 7.08 (1H, app. t, J 7.9, 5-HAr), 6.85 (1H, brs, CONH), 4.56 (1H, brs, BOC NH), 4.23 (1H, d, J 6.0, 7a-H), 3.81 (3H, s, OCH$_3$), 2.97 (2H, t, J 7.1, CH$_2$NH), 2.84 (2H, d, J 8.9, CH$_2$C), 2.39-2.32 (1H, m, 7*-H), 2.20-2.11 (2H, m, 8-H and 1'-H), 2.03-1.99 (1H, m, 6-H), 1.97-1.80 (6H, m, 7*-H, 4-H, 6'-H and 2'-H), 1.65-1.63 (1H, m, 4'-H), 1.61 (9H, s, C(CH$_3$)$_3$) 1.50 (1H, d, J 7.7, 8-H), 1.46 (9H, s, CH$_3$ BOC), 1.48-1.37 (4H, m, 5'-H and 3'-H), 1.40 (3H, s, C3-CH$_3$), 1.28 (3H, s, C5a-CH$_3$), 0.89 (3H, s, C5b-CH$_3$); $δ_C$ (100MHz, CDCl$_3$): 179.3 (HNC=O), 165.8 (^{t}BuOC=O), 157.7 (C2-Ar), 156.0 (BOC C=O), 135.6 (C1-Ar), 134.5 (C6-Ar), 129.5 (C4-Ar), 127.1 (C3-Ar), 123.8 (C5-Ar), 83.5 (C3), 81.3 (C(CH$_3$)$_3$ × 2), 76.4 (C7a), 62.0 (OCH$_3$), 52.6 (C4), 46.4 (CH$_2$N), 45.0 (NCH), 41.4 (C1'), 40.3 (C6), 38.2 (C5), 37.8 (C4'), 36.8 (CH$_2$C), 32.5 (C7), 29.6 (C6' and C2'), 29.4 (C3-CH$_3$), 28.4 (BOC C(CH$_3$)$_3$), 28.3 (C5' and C3'), 28.2 (C(CH$_3$)$_3$), 27.4

(C5a-CH$_3$), 26.6 (C8), 24.1 (C5b-CH$_3$); v$_{max}$/ cm^{-1} (oil): 2973, 2925, 1698, 1365, 1228; HPLC: T$_r$= 3.11 (100% rel. area); *m/z* (ES): (Found: MH$^+$, 669.4285. C$_{37}$H$_{57}$BN$_2$O$_8$ requires *MH*, 669.4287). [α]$_D$ = − 9.04° (c 0.50, CHCl$_3$).

Synthesis of 3-[(2R)-2-[4-(aminomethyl)-cyclohexylformido]-2-borono-ethyl]-2-hydroxy-benzoic acid hydrochloride. (5.17)

Preparation was *via* general method G using 3-[(2R)-2-[4-(tert-Butoxycarbonylamino-methyl)-cyclohexyl formamido]-2-[(3aS,4S,6S,7aR)-3a,5,5-trimethylhexahydro-4,6-methano-1,3,2-benzodioxaborol-2-yl]-ethyl]-2-methoxy-benzoic acid tert-butyl ester (**5.26**) (50 mg, 0.07 mmol) to afford the title compound (**5.17**) as a colourless solid which was used without further purification (2.2 mg, 0.01 mmol, 8%). m.p.: 49.2-50.1 °C; R$_f$: 0.05 (9:1 DCM−MeOH); δ$_H$ (500 MHz, MeOD-d4): 8.36 (1H, brs, HNC=O), 7.71 (1H, app. s, 6-HAr), 7.20 (1H, app. s, 4-HAr), 6.86 (1H, app. s, 5-HAr), 4.47 (2H, brs, B(OH)$_2$), 3.16 (1H, brs, HCN), 2.83 (2H, s, CH$_2$), 2.67 (2H, dd, *J* 7.0 and 1.8, CH$_2$NH$_2$), 2.19 (1H, app. s, 1'-H), 1.74-1.63 (4H, m, 6'-H and 2'-H), 1.50-1.43 (1H, m, 4'-H), 1.35-1.20 (2H, m, 5a'-H and 3a'-H), 0.95-0.87 (2H, m, 5b'-H and 3b'-H); v$_{max}$/ cm^{-1} (solid): 2928, 2858, 1718, 1595, 1427, 1227; *m/z* (ES): (Found: [M-H$_2$O+H]$^+$, 347.1782. C$_{17}$H$_{25}$BN$_2$O$_6$ requires *[M-H$_2$O+H]*, 347.1776. [α]$_D$ = − 46.0 ° (c 0.10, MeOH).

Synthesis of 3-[(2R)-2-[cyclohexylformamido]-2-[(3aS,4S,6S,7aR)-3a,5,5-trimethylhexahydro-4,6-methano-1,3,2-benzodioxaborol-2-yl]-ethyl]-2-methoxy-benzoic acid tert-butyl ester. (5.27)
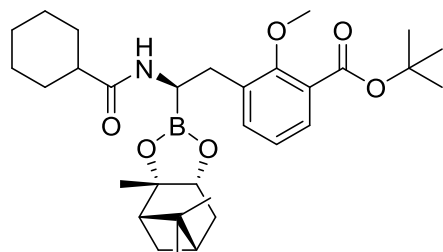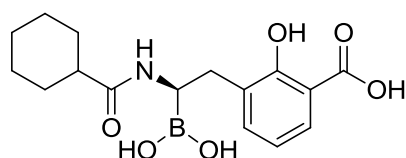

Preparation was *via* general method E using cyclohexane carboxylic acid (0.24 g, 1.80 mmol) and 2-methoxy-3-((2R)-2-[bis(trimethylsilyl)amino]-2-[(3aS,4S,6S,7aR)-3a,5,5-trimethylhexahydro-4,6-methano-1,3,2-benzodioxaborol-2-yl]ethyl) benzoic acid tert-butly ester (**5.10**) (1.25 g, 2.20 mmol) to yield the title compound (**5.27**) as a yellow glassy solid (0.14 g, 0.26 mmol, 14%); m.p.: 135-138 °C; R$_f$: 0.16 (3:1 Hexane–EtOAc); δ$_H$ (500 MHz, CDCl$_3$): 8.04 (1H, s, NH), 7.63

(1H, dd, *J* 7.7, 1.6, 6-HAr), 7.37 (1H, dd, *J* 7.7, 1.6, 4-HAr), 7.12 (1H, app. t, *J* 7.7, 5-HAr), 4.30 (1H, d, *J* 6.5, 7a-H), 3.85 (3H, s, OCH$_3$), 2.92-2.87 (3H, m, CH$_2$C and NCH), 2.39 (1H, t, *J* 2.5, 1`-H), 2.32-2.30 (1H, m, 7*-H), 2.21-2.18 (2H, m, 2`-H, 6`-H), 2.07 (1H, t, *J* 3.3, 16-H), 1.94-1.90 (4H, m, 2`-H, 3`H, 5`-H, 6`H), 1.81 (2H, d, *J* 12.5, 6-H, 8-H), 1.72-1.69 (1H, m, 7*-H), 1.64 (9H, s, C(CH$_3$)$_3$), 1.56 (1H, d, *J* 10.1, 4`-H), 1.46 (3H, s, C3-CH$_3$), 1.40 (1H, d, *J* 6.8, 8-H), 1.32 (3H, s, C5a-CH$_3$), 1.30-1.25 (2H, m, 5'-H and 3'-H), 1.25-1.20 (1H, m, 4`H), 0.91 (3H, s, C5b-CH$_3$); δ$_C$ (125 MHz, CDCl$_3$): 180.5 (NHC=O), 165.0 (C=O), 158.0 (C2-Ar), 136.0 (C1-Ar), 134.7 (C6-Ar), 129.7 (C4-Ar), 127.5 (C3-Ar), 124.1 (C5-Ar), 83.1 (C3a), 81.5 (C(CH$_3$)), 77.3 (C4), 76.3 (C7a), 62.2 (OCH$_3$), 52.6 (C4), 45.0 (brs, NCH), 40.5 (C1`), 40.3 (C6), 38.2 (C5), 37.0 (CH$_2$), 32.8 (C7*), 29.2 (C3-CH$_3$), 28.8 (C6` and C2`), 28.2 (C(CH$_3$)$_3$), 27.4 (C5a-CH$_3$), 26.7 (C4), 25.5 (C5`, C4' and C3`), 24.2 (C5b-CH$_3$); ν$_{max}$/ cm^{-1} (solid): 3197, 3072, 2975, 2929. 2896, 2856, 1717, 1590; *m/z* (ES): (Found: MH$^+$, 540.3513. C$_{31}$H$_{46}$BNO$_6$ requires *MH*, 540.3513). [α]$_D$ = + 10.2° (c 0.50, CHCl$_3$).

Synthesis of 3-[(2R)-2-borono-2-[cyclohexylformido]-ethyl]-2-hydroxy-benzoic acid hydrochloride. (5.18)

Preparation was *via* general method G using 3-[(2R)-2-[cyclohexylformamido]-2-[(3aS,4S,6S,7aR)-3a,5,5-trimethylhexahydro-4,6-methano-1,3,2-benzodioxaborol-2-yl]-ethyl]-2-methoxy-benzoic acid tert-butyl ester (**5.27**) (50 mg, 0.08 mmol) to afford the title compound (**5.18**) as a colourless solid which was used without further purification (1.9 mg, 0.01 mmol, 7%). m.p.: > 250 °C; *R*$_f$: 0.08 (9:1 DCM−MeOH); δ$_H$ (500 MHz, MeOD-d4): 7.64 (1H, d, *J* 7.6, 6-HAr), 7.12 (1H, d, *J* 7.6, 4-HAr), 6.78 (1H, app. t, *J* 7.6, 5-HAr), 3.07 (1H, app. s, NCH), 2.73 (2H, dd, *J* 15.5 and 7.1, CH$_2$), 2.16-2.08 (1H, m, 1-H), 1.45-1.30 (4H, m, 6-H and 2-H), 1.23-1.15 (2H, m, 4-H), 1.11-0.92 (4H, m, 5-H and 3-H); δ$_C$ (125 MHz, MeOD-d4): 185.0 (NHC=O), 169.1 (COOH), 157.2 (C2-Ar), 136.4 (C4-Ar), 131.1 (C6-Ar), 129.1 (C3-Ar), 122.2 (C5-Ar), 118.6 (C1-Ar), 45.0 (br, NCH), 40.1 (C1), 32.3 (CH$_2$), 29.5 (C6 and C2), 26.2 (C4), 25.6 (C5 and C3); ν$_{max}$/ cm^{-1} (solid): 2929, 2855, 1713, 1596, 1185; HPLC: T$_r$= 1.78 (90% rel. area); *m/z* (ES):

(Found: $[M-H_2O+H]^+$, 318.1516. $C_{16}H_{22}BNO_6$ requires *[M-H$_2$O+H]*, 318.1510. $[\alpha]_D = -32.0°$ (c 0.10, MeOH).

10.5 Peptide synthesis

### 10.5.1 General procedure for oligomer formation-single coupling

Fmoc-protected pre-loaded Wang resin was loaded onto a CEM microwave peptide synthesizer after being swelled for a total of 30 min in DMF. A series of washes (3 × DMF), deprotection (2 × 20% Piperidine/DMF, total of 10 min at rt) and further washes (5 × DMF) prepared the resin for coupling. Fmoc protected amino acids were dissolved in DMF, delivered to the reaction vessel and reacted with HCTU and DIPEA at room temperature for 90 min.

Each trimer peptide was then deprotected (5 × 20% Piperidine/DMF, total 10 min at room temperature), washed (5 × DMF, total 10 min at rt, 5 × DCM, total 10 min at room temperature and 3 × MeOH, total 6 min at rt) and cleaved from the resin (2 × Reagent K (87% TFA, 3% 1,2-ethanedithiol, 5% thioanisol, and 5% H_2O), 3 h total at room temperature). The resulting solution was concentrated *in vacuo* and triturated with ether to afford the desired crude peptide.

Peptides were purified by mass directed HPLC eluting with 5-95% MeOH in water.

10.5.2 (L)-Amino acid trimers

Pro-Ile-Cys (6.5)
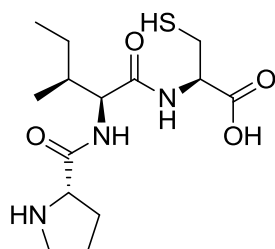
Preparation was *via* the general method outlined in Section 10.5.1. The title compound (**6.5**) was formed as colourless microcrystals (6.5 mg, 0.02 mmol, 13%). m.p.: 210.2 °C (depcomp); R_f: 0.05 (19:1 DCM−MeOH); δ_H (500 MHz, D_2O): 4.38 (1H, t, *J* 7.4, PRO-CH), 4.32 (1H, t, *J* 6.1, CYS-CH), 4.18 (1H, d, *J* 7.8, ILE-CH), 3.42-3.38 (1H, m, PRO-5a-H), 3.38-3.31 (1H, m, PRO-5b-H), 2.86 (2H, dd, *J* 14.0 and 5.4, CH$_2$SH), 2.48-2.36 (1H, m, PRO-3a-H), 2.19-1.95 (3H, m, PRO-4-H and PRO-3b-H), 1.85 (1H, m, CH-CH$_3$), 1.45-1.40 (1H, m, CH$_2$-CH$_3$), 1.24-1.12 (1H, m, CH$_2$-CH$_3$), 0.90 (3H, d, *J* 6.8, CH$_3$), 0.83 (3H, t, *J* 7.4, CH$_3$-CH$_2$); δ_C (75 MHz, D_2O): 175.7 (PRO C=O), 172.5 (ILE C=O), 169.7 (CYS

C=O), 59.6 (PRO-<u>CH</u>), 59.2 (ILE-<u>CH</u>), 56.5 (CYS-CH) 46.6 (C5), 35.8 (<u>CH</u>-CH$_3$), 29.9 (C3), 26.3 (<u>CH$_2$</u>SH), 24.6 (C4) 23.7 (<u>CH$_2$</u>-CH$_3$), 14.8 (<u>CH$_3$</u>-CH), 10.2 (<u>CH$_3$</u>-CH$_2$); v_{max}/ cm^{-1} (solid): 3093, 2968, 2875, 1750, 1640, 1420; *m/z* (ES): (Found: MH$^+$, 332.1639. C$_{14}$H$_{25}$N$_3$O$_4$S requires *MH*, 332.1639). [α]$_D$ = − 41.1° (c 0.10, H$_2$O).

Asn-Pro-Cys (6.6)
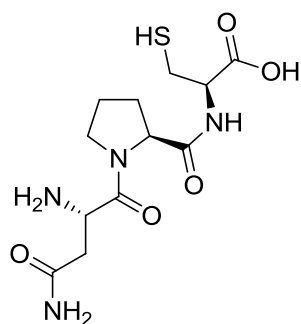
Preparation was *via* the general method outlined in Section 10.5.1. <u>The title compound</u> (**6.6**) was formed as a pale yellow oil (14 mg, 0.04 mmol, 27%). *R*$_f$: 0.04 (19:1 DCM−MeOH); δ$_H$ (500 MHz, D$_2$O): 4.65 (1H, dd, J 6.8 and 4.3, ASN-CH), 4.58 (1H, dd, J 6.8 and 4.8, CYS-CH), 4.55-4.44 (1H, m, PRO-CH), 3.72-3.60 (2H, m, PRO-5-H), 3.38 (1H, dd, *J* 14.1 and 4.3, ASN-<u>CH$_2$</u>-C=Oa), 3.05 (1H, m, <u>CH$_2$</u>-SHa), 3.00 (1H, dd, J 14.1 and 4.3, ASN-<u>CH$_2$</u>-C=Ob) 2.80 (1H, dd, *J* 14.1 and 6.8, <u>CH$_2$</u>-SHb), 2.29 (1H, t, *J* 19.1 PRO-3a-H), 2.19-1.93 (3H, m, PRO-4-H and PRO-3b-H); δ$_C$ (125 MHz, D$_2$O): 174.0 (ASN C=O), 173.7 (C=O-NH$_2$), 172.8 (CYS C=O), 167.7 (PRO C=O), 60.8 (PRO-CH), 52.2 (CYS-CH), 48.8 (ASN-CH), 48.0 (C5), 38.5 (CH$_2$-C=O), 34.3 (<u>CH$_2$</u>SH), 29.4 (C3), 24.6 (C4); v_{max}/ cm^{-1} (oil): 3200, 2950, 1630, 1240; *m/z* (ES): (Found: MH$^+$, 333.1229. C$_{12}$H$_{20}$N$_4$O$_5$S requires *MH*, 333.1227). [α]$_D$ = + 200.8° (c 0.10, H$_2$O).
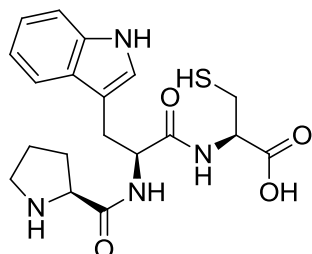
Pro-Pro-Cys (6.7)
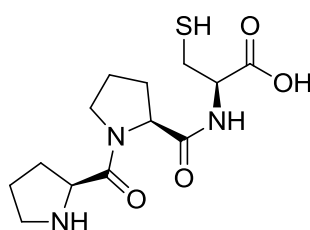
Preparation was *via* the general method outlined in Section 10.5.1. <u>The title compound</u> (**6.7**) was formed as a dark yellow oil (6.2 mg, 0.02 mmol, 12%). *R*$_f$: 0.07 (19:1 DCM−MeOH). δ$_H$ (500 MHz, D$_2$O): 4.65-4.55 (1H, m, PRO-CH) 4.55-4.45 (1H, m, PRO-CH'), 4.45-4.35 (1H, m, CYS-CH), 4.10 (1H, m, PRO-5a'-H), 3.70-3.00 (5H, m, PRO-5b'-H, PRO-5-H and <u>CH$_2$</u>SH) 2.58-2.47 (1H, m, PRO-3a-H), 2.35-2.15 (2H, m, PRO-3b-H and PRO-3a'-H), 2.12-1.80 (5H, m, PRO-4-H, PRO-4'-H and PRO-3b'-H); δ$_C$ (125 MHz, D$_2$O): 168.5 (PRO C=O and CYS C=O), 60.8 (PRO-CH), 59.3 (CYS-CH), 45.6 (C5), 27.3 (CH$_2$SH and C3), 22.8 (C4); v_{max}/ cm^{-1} (oil): 3400, 2950, 2900, 1675, 1490; *m/z* (ES): (Found: MH$^+$,
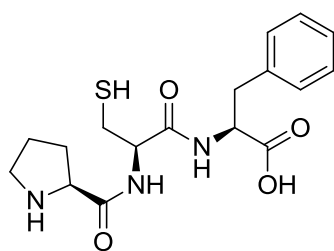
316.1327. $C_{13}H_{21}N_3O_4S$ requires *MH*, 316.1326). $[α]_D$ = + 187.6° (c 0.10, H_2O).

Pro-Trp-Cys (6.8)

Preparation was *via* the general method outlined in Section 10.5.1. <u>The title compound</u> (**6.8**) was formed as a pale brown oil (26 mg, 0.07 mmol, 14%). R_f: 0.07 (19:1 DCM−MeOH). $δ_H$ (500 MHz, D_2O): 7.39 (1H, d, *J* 7.8, 4'-H), 7.23 (1H, d, *J* 8.7, 7'-H), 7.18-6.95 (3H, m, 6'-H, 5'-H and 2'-H), 4.68-4.53 (1H, m, TRP-CH), 4.54-4.39 (1H, m, CYS-CH), 4.19 (1H, dd, *J* 20.1 and 14.1, PRO-CH), 3.26-2.68 (6H, m, <u>CH</u>$_2$Ar, <u>CH</u>$_2$SH and PRO-5-H), 2.41-2.17 (1H, m, PRO-3a-H), 2.10-1.71 (3H, m, PRO-4-H and PRO-3b-H); $δ_C$ (75 MHz, D_2O): 172.6 (PRO-C=O), 168.9 (TRP-C=O), 163.0 (CYS-C=O), 136.2 (C8'), 129.8 (C2'), 126.7 (C9'), 124.5 (C6'), 121.9 (C5'), 118.2 (C4'), 111.9 (C7'), 108.5 (C3'), 59.5 (TRP-CH and PRO-CH), 55.0 (CYS-CH), 46.8 (C5), 37.9 (C3), 29.8 (<u>CH</u>$_2$SH), 27.0 (C4), 23.6 (<u>CH</u>$_2$Ar); v_{max}/ cm^{-1} (oil): 3330, 2950, 1675, 1210; LCMS: (Tr = 1.32, *m/z* (ES): (Found: MH$^+$, 404.6. $C_{19}H_{24}N_4O_4S$ requires *MH*, 404.6)). $[α]_D$ = + 220.1° (c 0.10, H_2O).
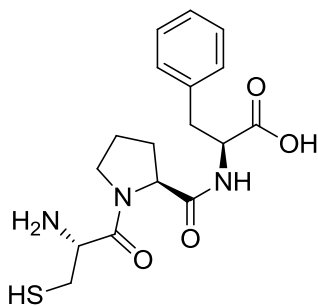
Pro-Cys-Phe (6.9)

Preparation was *via* the general method outlined in Section 10.5.1. <u>The title compound</u> (**6.9**) was formed as colourless microcrystals (2.7 mg, 0.01 mmol, 5%). m.p.: 219.3 °C (decomp.); R_f: 0.05 (19:1 DCM−MeOH). $δ_H$ (500 MHz, D_2O): 7.30 (2H, app. t, *J* 6.4, 5'-H and 3'-H), 7.25 (1H, t, *J* 6.4, 4'-H), 7.20 (2H, d, *J* 6.4, 6'-H and 2'-H), 4.75-4.66 (1H, m, CYS-CH), 4.59-4.45 (1H, m, PHE-CH), 4.35-4.28 (1H, m, PRO-CH), 3.42-3.26 (2H, m, PRO-5-H), 3.25-3.09 (2H, m, <u>CH</u>$_2$Ar), 2.98-2.76 (1H, m, <u>CH</u>$_2$SHa), 2.74-2.69 (1H, m, <u>CH</u>$_2$SHb), 2.35-2.25 (1H, m, PRO-3a-H), 1.98-1.87 (2H, m, PRO-4-H), 1.82 (1H, dd, *J* 13.3 and 6.7, PRO-3-Hb); $δ_C$ (125 MHz, D_2O): 170.5 (PRO-C=O), 170.3 (PHE-C=O), 169.3 (CYS-C=O), 137.1 (C1'), 129.4 (C6' and C2'), 128.7 (C5' and C3'), 127.0 (C4'), 59.8 (PRO-CH), 59.7 (CYS-CH), 51.0 (PHE-CH), 46.6 (C5), 38.9 (<u>CH</u>$_2$Ar), 29.9 (C3), 25.3 (<u>CH</u>$_2$SH), 23.9 (C4); v_{max}/ cm^{-1} (solid): 3350,

3100, 2995, 2495, 1650, 1590, 1470; *m/z* (ES): (Found: MH+, 366.1490. $C_{17}H_{23}N_3O_4S$ requires *MH*, 366.1482. $[\alpha]_D$ = + 180.8° (c 0.10, H_2O).
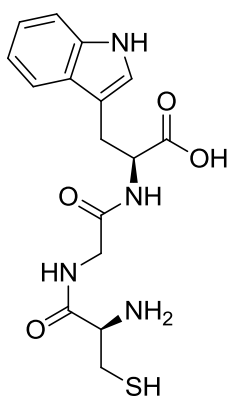
Cys-Pro-Phe (6.10)

Preparation was *via* the general method outlined in Section 10.5.1. The title compound (**6.10**) was formed as colourless microcrystals (1.2 mg, 3.29 μmol, 2%). m.p: 145.4-146.9 °C R_f: 0.05 (19:1 DCM−MeOH). δ_H (500 MHz, D_2O): 7.36 (2H, t, *J* 7.4, 3'-H and 5'-H), 7.30 (1H, t, *J* 7.4, 4'-H), 7.26 (2H, app. t, *J* 7.4, 6'-H and 2'-H), 4.59 (1H, s, PHE-CH), 4.33-4.24 (1H, m, PRO-CH), 4.00-3.86 (1H, m, CYS-CH), 3.50 (2H, dd, *J* 18.0 and 8.5 PRO-5-H), 3.58-3.42 (3H, m, CH₂Ar and CH₂SHa), 3.06 (1H, dd, *J* 14.0 and 8.0, CH₂HSb), 2.33-2.27 (1H, m, PRO-3a-H), 2.05-1.98 (1H, m, PRO-3b-H), 1.88 (2H, dd, *J* 20.9 and 8.5, PRO-4-H); δ_C (75 MHz, D_2O): 170.0 (PRO-C=O), 171.7 (PHE-C=O), 165.7 (CYS-C=O), 135.2 (C1'), 129.5 (C6' and C2'), 129.2 (C5' and C3'), 127.8 (C4'), 59.2 (PRO-CH), 56.2 (CYS-CH), 55.0 (PHE-CH), 45.7 (C5), 39.6 (CH₂Ar), 36.4 (C3), 28.3 (CH₂SH), 21.8 (C4); v_{max}/ cm⁻¹ (solid): 3420, 3250, 3110, 1620, 1430; *m/z* (ES): (Found: MH⁺, 366.1484. $C_{17}H_{23}N_3O_4S$ requires *MH*, 366.1482). $[\alpha]_D$ = + 476.8° (c 0.10, H_2O).
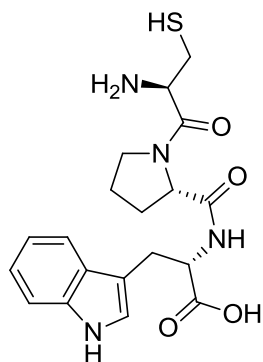
Cys-Gly-Trp (6.11)

Preparation was *via* the general method outlined in Section 10.5.1. The title compound (**6.11**) was formed as colourless microcrystals (8.0 mg, 0.02 mmol, 16%). R_f: 0.13 (19:1 DCM−MeOH). δ_H (500 MHz, D_2O): 7.57 (1H, dd, *J* 20.2 and 7.7, 4-H), 7.41 (1H, d, *J* 24.7 and 8.1, 7-H) 7.23-7.02 (3H, m, 6-H, 5-H and 2-H), 4.78-4.70 (1H, m, GLY-CH₂), 4.54 (1H, dd, *J* 7.2 and 5.5, TRP-CH), 4.20 (1H, dd, J 7.5 and 5.8, CYS-CH), 3.35-3.24 (1H, m CH₂Ara), 3.22-3.08 (2H, m, CH₂Arb and CH₂SHa), 2.98 (1H, d, *J* 5.8 CH₂SHb); δ_C (125 MHz, D_2O): 176.5 (CYS-C=O), 169.8 (GLY-C=O), 168.4 (TRP-C=O), 136.2 (C8), 127.2 (C9), 124.5 (C2), 121.9 (C6), 119.4 (C5), 118.5 (C4), 112.0 (C7), 109.5 (C3), 54.8 (CYS-CH), 54.4 (TRP-CH), 42.4

(GLY-CH$_2$), 27.1 (<u>CH$_2$</u>Ar) 24.8 (<u>CH$_2$</u>SH); v$_{max}$/ cm^{-1} (solid): 3255, 3000, 2500, 1600, 1530, 1500, 1420; *m/z* (ES): (Found: MH$^+$, 365.1275. C$_{16}$H$_{20}$N$_4$O$_4$S requires *MH*, 365.1239). [α]$_D$ = + 604.7° (c 0.10, H$_2$O).

Cys-Pro-Trp (6.12)

Preparation was *via* the general method outlined in Section 10.5.1. <u>The title compound</u> (**6.12**) was formed as a purple oil (13 mg, 0.03 mmol, 26%). *R*$_f$: 0.10 (19:1 DCM−MeOH). δ$_H$ (500 MHz, D$_2$O): 7.58 (1H, dd, *J* 20.8 and 7.6, 4'-H), 7.40 (1H, dd, *J* 16.4 and 7.4, 7'-H), 7.24-6.98 (3H, m, 5'-H, 6'-H and 2'-H), 4.70-4.59 (1H, m, CYS-CH), 4.58-4.49 (1H, m, TRP-CH), 4.48-4.36 (1H, m, PRO-CH), 3.64-3.57 (1H, m, 5-Ha), 3.45-3.05 (4H, m. 5-Hb, <u>CH$_2$</u>Ar and <u>CH$_2$</u>SHa), 2.95-2.86 (1H, m, <u>CH$_2$</u>SHb), 2.23-2.04 (1H, m, 3-Ha), 1.98-1.77 (2H, m, 4-H), 1.77-1.72 (1H, m, 3-Hb); δ$_C$ (75 MHz, D$_2$O): 175.2 (TRP-C=O), 174.3 (PRO-C=O), 166.6 (CYS-CH), 136.2 (C8'), 129.8 (C2'), 126.9 (C9'), 121.9 (C6'), 119.3 (C5'), 111.9 (C7'), 108.9 (C3'), 60.7 (CYS-CH and PRO-CH), 50.8 (TRP-CH), 47.9 (C5), 38.0 (<u>CH$_2$</u>Ar), 29.0 (C3), 26.6 (<u>CH$_2$</u>SH), 24.5 (C4); v$_{max}$/ cm^{-1} (oil): 3400, 2890, 1670, 1500, 1220; LCMS: (Tr = 1.40, *m/z* (ES): (Found: MH$^+$, 404.1. C$_{19}$H$_{24}$N$_4$O$_4$S requires *MH*, 404.1)). [α]$_D$ = + 194.4° (c 0.10, H$_2$O).
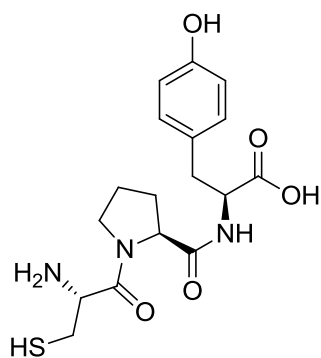
Cys-Phe-Tyr (6.13)
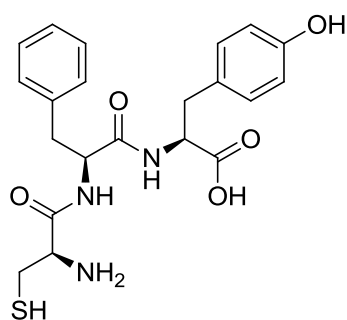
Preparation was *via* the general method outlined in Section 10.5.1. <u>The title compound</u> (**6.13**) was formed as colourless microcrystals (12 mg, 0.03 mmol, 23%). *R*$_f$: 0.12 (19:1 DCM−MeOH). δ$_H$ (500 MHz, D$_2$O): 8.24 (1H, brs, COOH), 7.26 (2H, app. t, *J* 7.4, 5-H and 3-H), 7.25 (1H, t, *J* 7.4, 4-H), 7.20 (2H, d, *J* 7.4, 6-H and 2-H), 7.01 (2H, d, *J* 8.3, 6'-H and 2'-H), 6.72 (2H, d, *J* 8.3, 5'-H and 3'-H), 4.87 (1H, t, *J* 7.6, PHE-CH), 4.40 (1H, dd, *J* 8.9 and 4.8, CYS-CH), 4.00 (1H, t, *J* 5.7, TYR-CH), 2.92-2.71 (6H, m, PHE-<u>CH$_2$</u>, TYR-<u>CH$_2$</u> and CYS-<u>CH$_2$</u>), 2.65 (1H, s, SH); δ$_C$ (75 MHz, D$_2$O): 175.7 (PHE C=O), 171.6 (TYR C=O), 167.3 (CYS C=O),154.2 (C4'), 136.2 (C1), 130.6 (C6' and C2'), 129.1 (C6 and C2), 128.8 (C1'), 128.8 (C5 and C3), 127.2 (C4), 115.3

(C3' and C5'), 55.2 (PHE-CH), 55.0 (CYS-CH), 54.1 (TYR-CH), 37.0 (PHE-CH$_2$), 36.5 (TYR-CH$_2$), 25.0 (CH$_2$SH); v_{max}/ cm^{-1} (solid): 3280, 3050, 2500, 1600, 1510, 1220; *m/z* (ES): (Found: MH+, 432.1584. C$_{21}$H$_{25}$N$_3$O$_5$S requires *MH*, 432.1587). [α]$_D$ = + 310.0° (c 0.10, H$_2$O).

Cys-Pro-Tyr (6.14)

Preparation was *via* the general method outlined in Section 10.5.1. The title compound (**6.14**) was formed as colourless microcrystals (16 mg, 0.04 mmol, 33%). m.p.: 157.3-154.2 °C R_f: 0.09 (19:1 DCM−MeOH). δ$_H$ (500 MHz, D$_2$O): 7.07 (2H, dd, *J* 7.4 and 2.1, 5'-H and 3'-H), 6.79 (2H, dd, *J* 7.4 and 2.1, 6'-H and 2'-H), 4.63 (1H, d, *J* 6.5, CYS-CH), 4.47 (1H, t, *J* 6.8, TYR-CH), 4.45-4.40 (1H, m, PRO-CH), 3.75-3.63 (1H, m, PRO-5a-H), 3.63-3.49 (1H, m, PRO-5b-H), 3.38 (1H, dd, *J* 14.9 and 3.4, CH$_2$SHa), 3.10-2.81 (3H, m, CH$_2$Ar and CH$_2$SHb), 2.18 (1H, dt, *J* 12.4 and 6.1, PRO-3a-H), 1.98-1.84 (2H, m, PRO-4-H), 1.78 (1H, dt, *J* 12.4 and 6.1, PRO-3b-H); δ$_C$ (75 MHz, D$_2$O): 175.2 (TYR-C=O), 172.8 (PRO-C=O), 166.7 (CYS-C=O), 154.4 (C4'), 130.6 (C6' and C2'), 128.3 (C1'), 115.4 (C5' and C3'), 60.8 (PRO-CH), 54.6 (CYS-CH), 50.8 (TYR-CH), 47.9 (C5), 38.7 (C3), 35.8 (CH$_2$), 29.2 (C4), 24.5 (CH$_2$SH); v_{max}/ cm^{-1} (solid): 3420, 3050, 2500, 1670, 1500, 1250; *m/z* (ES): (Found: MH+, 382.1432. C$_{17}$H$_{23}$N$_3$O$_5$S requires *MH*, 382.1431). [α]$_D$ = + 238.8° (c 0.10, H$_2$O).
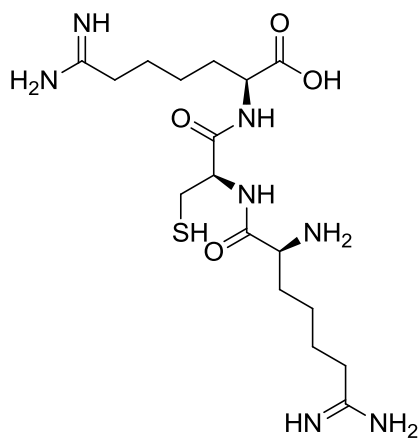
Cys-Arg-Arg (6.15)
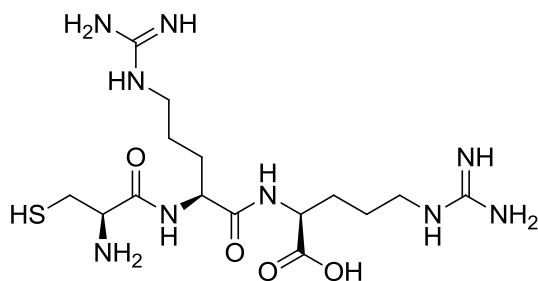
Preparation was *via* the general method outlined in Section 10.5.1. The title compound (**6.15**) was formed as a colourless oil (6.1 mg, 0.02 mmol, 12%). R_f: 0.02 (19:1 DCM−MeOH). δ$_H$ (500 MHz, D$_2$O): 4.40-4.31 (2H, m, CYS-CH and ARG-CH), 4.29-4.19 (1H, m, ARG-CH), 3.35 (1H, dd, *J* 14.0 and 6.4, CH$_2$SHa), 3.21-3.17 (4H, m, CH$_2$NH × 2), 3.17-3.09 (1H, m, CH$_2$SHb), 1.91-1.78 (2H, m, ARG-CH-CH$_2$), 1.78-1.66 (2H, m, ARG-CH-CH$_2$), 1.66-1.54 (4H, m, CH$_2$CH$_2$CH$_2$ × 2); δ$_C$ (75 MHz, D$_2$O): 173.0

(ARG C=O), 172.4 (ARG C=O), 167.9 (CYS C=O), 156.9 (ARG-CN$_3$ × 2), 53.6 (CYS-CH), 53.0 (ARG-CH), 51.8 (ARG-CH), 40.6 (C$\underline{H_2}$NH ×2), 28.5 (CHC$\underline{H_2}$), 27.9 (CHC$\underline{H_2}$), 24.7 (C$\underline{H_2}$SH), 24.4 (CH$_2$C$\underline{H_2}$CH$_2$ × 2); v_{max}/ cm^{-1} (oil): 3500-3000, 1670, 1440, 1190, 1100; *m/z* (ES): (Found: MH$^+$, 433.2221. C$_{15}$H$_{31}$N$_9$O$_4$S requires *MH*, 433.2220). [α]$_D$ = + 430.8° (c 0.10, H$_2$O).

Arg-Cys-Arg (6.16)

Preparation was *via* the general method outlined in Section 10.5.1. <u>The title compound</u> (**6.16**) was formed as a colourless oil (37 mg, 0.09 mmol, 74%). *R*$_f$: 0.03 (19:1 DCM−MeOH). δ$_H$ (500 MHz, D$_2$O): 4.73-4.69 (1H, m, CYS-CH), 4.40-4.28 (1H, m, ARG-CH), 4.10-3.96 (1H, m, ARG-CH), 3.26-3.05 (5H, m, C$\underline{H_2}$SHa and CH$_2$NH × 2), 2.99 (1H, dd, *J* 14.3 and 8.6, CH$_2$SHb), 1.98-1.83 (3H, m, ARG-CH-C$\underline{H_2}$ and ARG-CH-C$\underline{H_2}$b) 1.82-1.69 (1H, m, ARG-CH-C$\underline{H_2}$a), 1.69-1.51 (4H, m, CH$_2$C$\underline{H_2}$CH$_2$ × 2); δ$_C$ (125 MHz, D$_2$O): 175.0 (ARG-C=O), 171.4 (ARG-C=O), 169.6 (CYS-C=O), 156.9 (ARG-CN$_3$ × 2), 52.7 (ARG-CH and CYS-CH), 40.6 (CH$_2$NH × 2), 27.9 (CH$_2$C$\underline{H_2}$CH × 2), 24.6 (CH$_2$SH) 23.6 (CH$_2$C$\underline{H_2}$CH$_2$ × 2); v_{max}/ cm^{-1} (oil): 3500-3000, 2495, 1650, 1480, 1200, 1110; LCMS: (Tr = 0.13, *m/z* (ES): (Found: MH$^+$, 434.2. C$_{15}$H$_{31}$N$_9$O$_4$S requires *MH*, 434.2)). [α]$_D$ = + 50.0° (c 0.10, H$_2$O).

Gln-Cys-Arg (6.17)
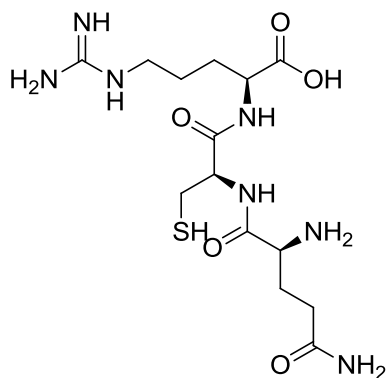
Preparation was *via* the general method outlined in Section 10.5.1. <u>The title compound</u> (**6.17**) was formed as a pale yellow oil (34 mg, 0.08 mmol, 69%). *R*$_f$: 0.03 (19:1 DCM−MeOH). δ$_H$ (500 MHz, D$_2$O): 4.73-4.65 (1H, m, CYS-CH), 4.45-4.28 (1H, m, ARG-CH), 4.12-4.00 (1H, m, GLN-CH), 3.28-3.06 (3H, m, C$\underline{H_2}$NH and C$\underline{H_2}$SHa), 3.05-2.91 (1H, m, C$\underline{H_2}$SHb), 2.37 (1H, dt, *J* 10.2 and 6.9, C$\underline{H_2}$CONH$_2$), 2.12 (1H, t, *J* 7.7, GLN-CH-C$\underline{H_2}$a), 2.07-1.96 (1H, m, GLN-CH-C$\underline{H_2}$b), 1.96-1.84 (1H, m, ARG-CH-C$\underline{H_2}$a), 1.79-1.68 (1H, m, ARG-CH-

C$\underline{H_2}$b), 1.68-1.50 2H, m, CH$_2$C$\underline{H_2}$CH$_2$); δ$_C$ (75 MHz, D$_2$O): 182.2 (CONH$_2$), 176.7 (GLN-C=O), 174.9 (ARG-C=O), 171.2 (CYS-C=O), 156.7 (ARG-CN$_3$), 56.7 (GLN-CH), 52.7 (CYS-CH), 52.3 (ARG-CH), 40.3 ($\underline{CH_2}$NH), 29.2 ($\underline{CH_2}$CONH$_2$), 27.2 (GLU-$\underline{CH_2}$CH), 26.6 (ARG-CH-$\underline{CH_2}$), 25.3 ($\underline{CH_2}$SH), 24.4 (CH$_2$C$\underline{H_2}$CH$_2$); ν$_{max}$/ cm^{-1} (oil): 3250, 3020, 2500, 1600, 1220, 1200; *m/z* (ES): (mass not found). [α]$_D$ = + 40.1° (c 0.10, H$_2$O).
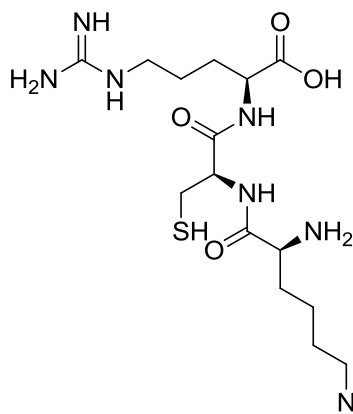
Lys-Cys-Arg (6.18)

Preparation was *via* the general method outlined in Section 10.5.1. The title compound (**6.18**) was formed as a pale yellow oil (35 mg, 70%). R_f: 0.02 (19:1 DCM−MeOH). δ$_H$ (500 MHz, D$_2$O): 4.71-4.54 (1H, m, CYS-CH), 4.45-4.24 (1H, m, ARG-CH), 4.11-3.93 (1H, m, LYS-CH), 3.20-3.11 (3H, m, $\underline{CH_2}$SHa and $\underline{CH_2}$NH), 3.05-2.85 (3H, m, $\underline{CH_2}$SHb and $\underline{CH_2}$NH$_2$), 1.92-1.81 (3H, m, LYS-$\underline{CH_2}$CH and ARG-CH-$\underline{CH_2}$a), 1.80-1.69 (1H, m, ARG-CH-C$\underline{H_2}$b), 1.68-1.58 (4H, m, $\underline{CH_2}$CH$_2$NH$_2$ and $\underline{CH_2}$CH$_2$NH), 1.47-1.30 (2H, m, LYS-CHCH$_2$C$\underline{H_2}$); δ$_C$ (75 MHz, D$_2$O): 174.7(LYS-C=O), 171.3 (ARG-C=O), 169.7 (CYS-C=O), 156.7 (ARG-CN$_3$), 58.2-58.6 (ARG-CH, LYS-CH, CYS-CH), 40.5 (CH$_2$NH$_2$), 39.0 (CH$_2$NH), 30.4 (LYS-CH-$\underline{CH_2}$), 27.6 (ARG-CH$_2$-CH), 23.7 (ARG-CH$_2$$\underline{CH_2}CH_2$), 20.9 (LYS-CH$_2$$\underline{CH_2}CH_2$); ν$_{max}$/ cm^{-1} (oil): 3420, 3005, 1670, 1220, 1190; LCMS: (Tr = 0.25, *m/z* (ES): (Found: MH$^+$, 406.2. C$_{15}$H$_{31}$N$_7$O$_4$S requires *MH*, 406.2)). [α]$_D$ = + 73.4° (c 0.10, H$_2$O).

Asp-Cys-Asp (6.19)
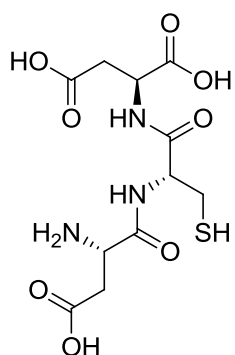
Preparation was *via* the general method outlined in Section 10.5.1. The title compound (**6.19**) was formed as a colourless oil (36 mg, 0.10, mmol, 73%). R_f: 0.01 (19:1 DCM−MeOH). δ$_H$ (500 MHz, D$_2$O): 4.71 (1H, d, *J* 7.5, ASP-CH), 4.67 (1H, dd, *J* 8.7 and 5.1, ASP-CH), 4.31 (1H, dd, *J* 12.1 and 7.2, CYS-CH), 3.17 (1H, dd, *J* 14.3 and 5.1, $\underline{CH_2}$COOHa), 3.11-2.99 (2H, m, CH$_2$SH) 2.99-2.84 (3H, m, $\underline{CH_2}$COOHb and $\underline{CH_2}$COOH'); δ$_C$ (75 MHz, D$_2$O): 174.2 (ASP-C=O), 173.5 (CYS-C=O), 171.5 (ASP-C=O), 170.9 (COOH), 170.8 (COOH), 52.5

(CYS-CH), 49.4 (ASP-CH), 49.2 (ASP-CH), 38.6 (CH$_2$COOH), 34.1 (CH$_2$COOH), 33.7 (CH$_2$SH); v_{max}/ cm^{-1} (oil): 3400-2700, 1670, 1220, 1190, 1000; m/z (ES): (Found: MH+, 352.0810. C$_{11}$H$_{17}$N$_3$O$_8$S requires MH, 352.0809). $[\alpha]_D$ = + 21.6° (c 0.10, H$_2$O).

Arg-Arg-Cys (6.20)

Preparation was *via* the general method outlined in Section 10.5.1. The title compound (**6.20**) was formed as a pale brown oil (21 mg, 0.05 mmol, 41%). R_f: 0.01 (19:1 DCM−MeOH). δ_H (500 MHz, D$_2$O): 4.71-4.63 (1H, m, CYS-CH), 4.37 (1H, t, J 7.0, ARG-CH), 4.00 (1H, t, J 6.4 ARG-CH), 3.25 (1H, dt, J 19.6 and 9.9, CH$_2$SHa), 3.21-3.09 (4H, m, CH$_2$NH × 2) 3.07-2.89 (1H, m, CH$_2$SHb), 1.89-1.77 (3H, m, ARG-CH$_2$CH and ARG-CH-CH$_2$a), 1.77-1.68 (1H, m, ARG-CH-CH$_2$b), 1.68-1.51 (4H, m, CH$_2$CH$_2$CH$_2$ × 2); δ_C (75 MHz, D$_2$O): 173.7 (ARG-C=O), 173.1 (ARG-C=O), 169.4 (CYS-C=O), 156.9 (ARG CN$_3$ × 2), 53.6 (CYS-CH), 52.6 (ARG-CH), 52.2 (ARG-CH), 40.7 (CH$_2$NH × 2), 28.3 (CH$_2$CH × 2), 24.5 (CH$_2$SH), 23.6 (CH$_2$CH$_2$CH$_2$ × 2); v_{max}/ cm^{-1} (oil): 3400-2700, 1675, 1550, 1200; m/z (ES): (Found: [M+2H]$^{2+}$, 217.6187. C$_{15}$H$_{31}$N$_9$O$_4$S requires $[M+2H]^{2+}$, 217.6182). $[\alpha]_D$ = + 139.5° (c 0.10, H$_2$O).
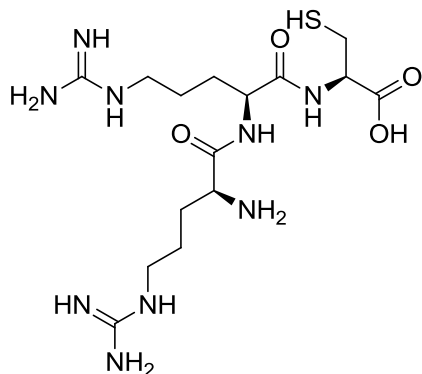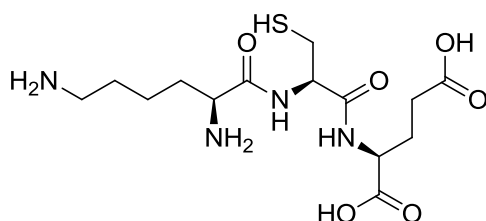
Cys-Lys-Glu (6.21)

Preparation was *via* the general method outlined in Section 10.5.1. The title compound (**6.21**) was formed as a colourless oil (16 mg, 0.04 mmol, 32%). R_f: 0.06 (19:1 DCM−MeOH). δ_H (500 MHz D$_2$O): 4.43-4.29 (3H, m, CYS-CH, LYS-CH and GLU-CH), 3.31 (1H, dd, J 14.9 and 5.1, CH$_2$SHa), 3.11 (1H, dd, J 14.9 and 7.9, CH$_2$SHb), 2.92 (2H, t, J 7.6, CH$_2$NH$_2$), 2.43 (2H, dt, J 13.9 and 8.5, CH$_2$COOH), 2.15 (1H, td, J 15.1 and 7.4, GLU-CH-CH$_2$a), 1.94 (1H, dt, J 15.1 and 7.4, GLU-CH-CH$_2$b), 1.80-1.67 (2H, m, LYS-CH$_2$CH), 1.63 (2H, app. t, J 7.4, CH$_2$CH$_2$NH$_2$), 1.42-1.36 (2H, m, CH$_2$CH$_2$CH); δ_C (75 MHz, D$_2$O): 176.9 (GLU-C=O), 174.8 (LYS-

C=O), 173.0 (COOH), 167.7 (CYS-C=O), 53.7 (LYS-CH), 52.0 (CYS-CH), 51.5 (GLU-CH), 39.2 (CH$_2$NH$_2$), 37.4 (CH$_2$COOH), 30.6 (LYS-CH-CH$_2$), 29.8 (NH$_2$CH$_2$CH$_2$) 26.3 (GLU-CH-CH$_2$), 25.7 (CH$_2$SH), 21.8 (CH$_2$CH$_2$CH$_2$); ν_{max}/ cm^{-1} (oil): 3000, 1650, 1230, 1150; *m/z* (ES): (Found: MH$^+$, 379.1649. C$_{14}$H$_{26}$N$_4$O$_6$S requires *MH*, 379.1646). [α]$_D$ = + 296.6° (c 0.10, H$_2$O).
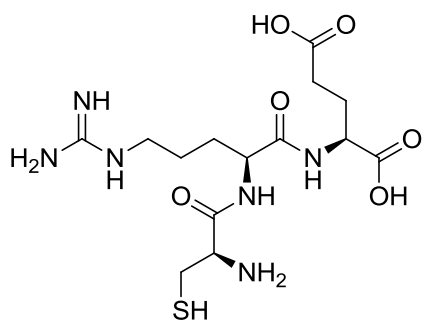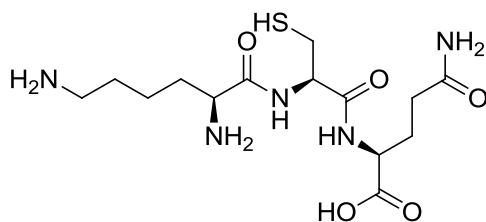
Cys-Arg-Glu (6.22)

Preparation was *via* the general method outlined in Section 10.5.1. The title compound (**6.22**) was formed as a colourless oil (23 mg, 0.06 mmol, 45%). R_f: 0.04 (19:1 DCM−MeOH). δ$_H$ (500 MHz D$_2$O): 4.44-4.31 (3H, m, CYS-CH, ARG-CH and GLU-CH), 3.32 (1H, dd, *J* 14.9 and 5.2, CH$_2$SHa), 3.22-3.04 (3H, m, CH$_2$SHb and CH$_2$NH), 2.44 (2H, t, *J* 7.1, CH$_2$COOH), 2.23-2.09 (1H, m, GLU-CH-CH$_2$a), 2.05-1.86 (1H, m, GLU-CH-CH$_2$b), 1.84-1.67 (2H, m, ARG-CH-CH$_2$), 1.661.55 (2H, m, CH$_2$CH$_2$NH); δ$_C$ (75 MHz, D$_2$O): 177.0 (GLU-C=O), 175.0 (ARG-C=O), 172.7 (COOH), 167.7 (CYS-C=O), 156.7 (ARG-CN$_3$), 53.5 (ARG-CH), 52.2 (CYS-CH), 51.5 (GLU-CH), 40.5 (CH$_2$NH), 37.4 (CH$_2$COOH), 30.0 (LYS-CH$_2$-CH), 28.3 (NHCH$_2$CH$_2$) 25.8 (CH$_2$SH), 24.2 (GLU-CH$_2$-CH); ν_{max}/ cm^{-1} (oil): 3300, 3050, 2600, 2480, 1670, 1460; *m/z* (ES): (Found: MH$^+$, 407.1711. C$_{14}$H$_{26}$N$_6$O$_6$S requires *MH*, 407.1707). [α]$_D$ = + 402.9° (c 0.10, H$_2$O).

Lys-Cys-Gln (6.23)

Preparation was *via* the general method outlined in Section 10.5.1. The title compound (**6.23**) was formed as colourless microcrystals (1.3 mg, 3.45 μmol, 3%). m.p.: 165.6-167.2 °C; R_f: 0.14 (19:1 DCM−MeOH). δ$_H$ (500 MHz, D$_2$O): 4.77-4.63 (1H, m, CYS-CH), 4.45-4.28 (1H, m, GLN-CH), 4.08-3.95 (1H, m, LYS-CH), 3.20 (1H, dd, *J* 14.2 and 5.4, CH$_2$SHa), 3.00 (1H, dd, *J* 14.2 and 5.4, CH$_2$SHb), 2.95-2.86 (2H, m, CH$_2$NH$_2$), 2.40-2.27 (2H, m, CH$_2$CONH$_2$), 2.21-2.12 (1H, m, GLN-CH$_2$CHa), 2.06-1.80 (1H, m, GLN-CH-CH$_2$b), 1.87 (2H, dd, *J* 15.1 and 6.9,

LYS-CH-<u>CH$_2$</u>), 1.72-1.57 (2H, m, <u>CH$_2$</u>CH$_2$NH$_2$), 1.49-1.31 (2H, m, <u>CH$_2$</u>CH$_2$CH); δ$_C$ (75 MHz, D$_2$O): 177.9 (<u>C</u>ON$_2$), 174.4 (GLN-C=O), 171.2 (LYS-C=O), 169.7 (CYS-C=O), 52.8 (LYS-CH and CYS-CH), 52.5 (GLN-CH), 38.9 (<u>C</u>H$_2$NH$_2$), 38.8 (<u>C</u>H$_2$CONH$_2$) 31.1 (LYS-<u>C</u>H$_2$CH), 30.3 (GLN-<u>C</u>H$_2$CH), 26.5 (<u>C</u>H$_2$CH$_2$NH$_2$) 26.3 (CH$_2$SH), 20.9 (<u>C</u>H$_2$CH$_2$CH); v$_{max}$/ cm^{-1} (solid): 3250, 3220, 3090, 2940, 1680, 1510; LCMS: (Tr = 0.13, *m/z* (ES): (Found: MH$^+$, 377.6. C$_{14}$H$_{27}$N$_5$O$_4$S requires *MH*, 377.5)). [α]$_D$ = + 277.0° (c 0.10, H$_2$O).

Arg-Cys-Tyr (6.24)
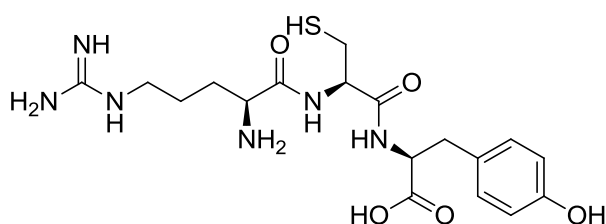

Preparation was *via* the general method outlined in Section 10.5.1. <u>The title compound</u> (**6.24**) was formed as a glassy solid (9.2 mg, 0.02 mmol, 18%).

m.p.: 84.2-85.4 °C; *R*$_f$: 0.11 (19:1 DCM−MeOH). δ$_H$ (500 MHz D$_2$O): 7.06 (2H, dd, *J* 16.4 and 8.4, 2-H and 6-H), 6.72 (2H, dd, *J* 16.4 and 8.4, 3-H and 5-H), 4.82 (1H, dd, *J* 9.3 and 5.0, CYS-CH), 4.56-4.39 (1H, m, TYR-CH), 3.99 (1H, t, *J* 6.3, ARG-CH), 3.29-2.97 (4H, m, CH$_2$SH and CH$_2$NH), 2.97-2.71 (2H, m, CH$_2$Ar), 1.81 (2H, d, J 6.8, ARG-CH-<u>CH$_2$</u>) 1.42 (1H, d, *J* 6.6, CH$_2$<u>CH$_2$</u>CH$_2$); δ$_C$ (125 MHz, D$_2$O): 176.0 (ARG-C=O), 170.5 (TYR-C=O), 169.2 (CYS-C=O), 156.8 (ARG-CN$_3$), 154.4 (C4), 130.8 (C6 and C2), 128.8 (C1), 115.4 (C5 and C3), 55.7 (ARG-CH), 52.8 (CYS-CH), 52.7 (TYR-CH), 40.4 (CH$_2$NH), 36.6 (CH$_2$Ar), 28.2 (<u>CH$_2$</u>CH), 25.5 (CH$_2$SH), 23.4 (CH$_2$<u>CH$_2$</u>CH$_2$); v$_{max}$/ cm^{-1} (solid): 3500-2700, 1670, 1500, 1260; *m/z* (ES): (Found: MH$^+$, 441.1917. C$_{18}$H$_{28}$N$_6$O$_5$S requires *MH*, 441.1915). [α]$_D$ = + 42.4° (c 0.10, H$_2$O).

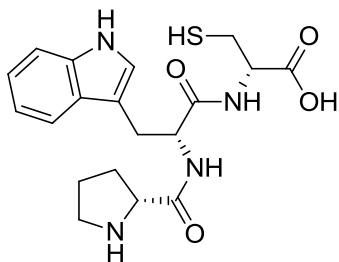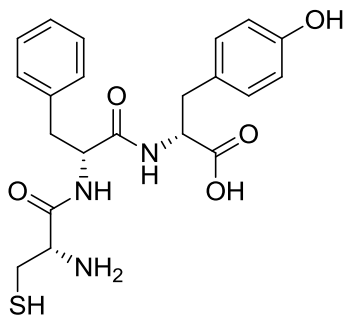### 10.5.3 (DL)-Combination amino acid trimers

D-Pro-D-Trp-D-Cys (6.25)

Preparation was *via* the general method outlined in Section 10.5.1. The title compound (**6.25**) was formed as a purple oil (40 mg, 0.10 mmol, 80%). R_f: 0.08 (19:1 DCM-MeOH). δ_H (500 MHz, D2O): 7.53 (1H, d, *J* 7.7, 4'-H), 7.39 (1H, d, *J* 7.9, 7'-H), 7.23-6.96 (3H, m, 5'-H, 6'-H and 2'-H), 4.63 (1H, t, *J* 7.6, TRP-CH), 4.46-4.38 (1H, m, CYS-CH), 4.26-4.18 (1H, m, PRO-CH), 3.30-2.82 (6H, m, CH$_2$SH, 5-CH$_2$ and CH$_2$Ar), 2.34-2.30 (1H, m, 3-CH$_2$a), 2.08-1.75 (3H, m, 4-CH$_2$ and 3-CH$_2$b); δ_C (75 MHz, D$_2$O): 174.1 (PRO-C=O), 172.9 (TRP-C=O), 169.3 (CYS-C=O), 136.3 (C8'), 129.9 (C2'), 126.9 (C9'), 122.2 (C6'), 119.4 (C5'), 118.1 (C4'), 112.1 (C7'), 108.7 (C1'), 59.6 (PRO-CH), 55.0 (TRP-CH), 52.6 (CYS-CH), 46.7 (C5), 31.9 (C3), 29.9 (CH2SH), 23.7 (C4), 22.3 (CH$_2$Ar); v_{max}/ cm^{-1} (oil): 3262, 3011, 2921, 1660, 1515, 1174, 1012; *m/z* (ES): (Found: [M-H]$^-$, 403.1433. C$_{19}$H$_{24}$N$_4$O$_4$S requires *[M-H]*, 403.1445). [α]$_D$ = + 15.2° (c 0.10, H$_2$O).

D-Cys-D-Phe-D-Tyr (6.26)

Preparation was *via* the general method outlined in Section 10.5.1. The title compound (**6.26**) was formed as colourless microcrystals (37 mg, 0.09 mmol, 74%). m.p.: 183.4 °C (decomp); R_f: 0.10 (19:1 DCM−MeOH). δ_H (500 MHz, D$_2$O): 7.33-7.18 (3H, m, 3-H, 5-H and 4-H), 7.12 (2H, d, *J* 6.5, 2-H and 6-H), 6.97 (2H, d, *J* 7.9, 6'-H and 2'-H), 6.70 (2H, d, *J* 7.9, 5'-H and 3'-H), 4.66 (1H, t, *J* 7.4 PHE-CH), 4.47 (1H, dd, *J* 8.9 and 5.1, CYS-CH), 4.16 (1H, s, TYR-CH), 3.16-2.70 (6H, m, CH$_2$SH, PHE-CH$_2$Ar and TYR-CH$_2$Ar); δ_H (125 MHz, D$_2$O): 174.3 (PHE-C=O), 171.8 (CYS-C=O), 167.4 (TYR-C=O), 154.4 (C4'), 136.1 (C1), 130.6 (C5 and C3), 129.3 (C6' and C2'), 128.9 (C6 and C2), 128.4 (C1'), 127.4 (C4), 115.6 (C5' and C3'), 55.0 (PHE-CH), 54.2 (CYS-CH), 51.4 (TYR-CH), 37.7 (PHE-CH$_2$), 36.1 (TYR-CH$_2$), 14.2 (CH$_2$SH); v_{max}/ cm^{-1} (solid): 3241, 3013, 2912, 1660, 1515, 1174;

LCMS: (Tr = 1.55, *m/z* (ES): (Found: MH⁺, 431.1. C₂₁H₂₅N₃O₅S requires *MH*, 431.2)). [α]$_D$ = − 69.2° (c 0.10, H₂O).

D-Cys-D-Pro-D-Tyr (6.27)

Preparation was *via* the general method outlined in Section 10.5.1. The title compound (**6.27**) was formed as colourless microcrystals (44 mg, 0.12 mmol, 88%). m.p.: 164.2-165.7 °C; R_f: 0.14 (19:1 DCM−MeOH). δ$_H$ (500 MHz D₂O): 7.07 (2H, t, *J* 8.6 2'-H and 6'-H), 6.77 (2H, t, *J* 8.6 3'-H and 5'-H), 4.60-4.45 (2H, m, TYR-CH and CYS-CH), 4.47-4.36 (1H, m, PRO-CH), 3.69 (1H, t, *J* 5.5, PRO-5a-H), 3.54 (1H, t, *J* 5.5 PRO-5b-H), 3.40 (1H, dd, *J* 16.1 and 5.5, CH₂Ara), 3.15-2.83 (3H, m, CH₂Arb and CH₂SH), 2.21-2.14 (1H, m, PRO-3a-H), 1.93 (2H, d, *J* 5.5, PRO-4-H), 1.86-1.70 (1H, m, PRO-3b-H); δ$_C$ (75 MHz, D₂O): 174.7 (TYR-C=O), 173.1 (PRO-C=O), 166.7 (CYS-C=O), 154.6 (C4'), 130.7 (C6' and C2'), 128.3 (C1'), 115.5 (C5' and C3'), 60.7 (PRO-CH), 54.3 (CYS-CH), 50.9 (TYR-CH), 48.0 (C5), 35.7 (CH₂Ar), 29.2 (C3), 24.7 (CH₂SH), 23.7 (C4); v$_{max}$/ cm⁻¹ (solid): 3241, 3013, 2921, 1723, 1660, 1515, 1174, 1131; LCMS: (Tr = 1.27, *m/z* (ES): (Found: MH⁺, 381.1. C₁₇H₂₃N₃O₅S requires *MH*, 381.1)). [α]$_D$ = + 47.8° (c 0.10, H₂O).
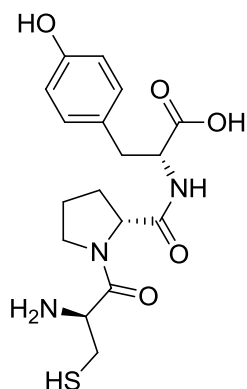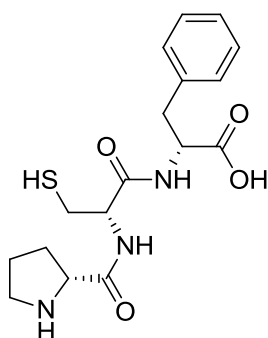
D-Pro-D-Cys-Phe (6.28)

Preparation was *via* the general method outlined in Section 10.5.1. The title compound (**6.28**) was formed as colourless microcrystals (39 mg, 0.11 mmol, 78%). m.p.: 202.1-203.4 °C; R_f: 0.15 (19:1 DCM−MeOH). δ$_H$ (500 MHz, D₂O): 7.41-7.11 (5H, m, 2'-H, 3'-H, 4'-H, 5'-H, and 6'-H), 4.72-4.65 (1H, m, PHE-CH), 4.63 (1H, dd, *J* 8.9 and 5.4 CYS-CH), 4.30 (1H, t, *J* 7.7, PRO-CH), 3.31 (2H, t, *J* 7.3 PRO-5-H), 3.21 (1H, dd, *J* 14.2 and 5.4, CH₂Ara), 2.99 (2H, dt, *J* 12.9 and 6.3, CH₂Arb and CH₂SHa), 2.83 (1H, dd, *J* 18.1 and 6.4 CH₂SHb), 2.30 (1H, dt, *J* 20.6 and 7.7, PRO-3a-H), 1.93 (2H, dt, *J* 20.5 and 7.7, PRO-4-H), 1.78 (1H, dd, *J* 20.6 and 7.7 PRO-3b-H); δ$_C$ (125 MHz, D₂O): 174.5 (PRO-C=O), 170.9 (PHE-C=O), 169.5 (CYS-C=O), 136.6 (C1'), 129.3 (C6' and C2'), 128.8 (C5' and C3'), 127.2 (C4'), 59.6 (PRO-CH), 54.1 (CYS-

CH), 52.9 (PHE-CH), 46.7 (C5), 39.0 ($\underline{CH_2}$Ar), 36.8 (C4), 29.9 ($\underline{CH_2}$SH), 23.8 (C3); v_{max}/ cm^{-1} (solid): 3326, 3255, 3096, 2958, 1671, 1539, 1175; LCMS: (Tr = 1.50, *m/z* (ES): (Found: MH$^+$, 365.0. $C_{17}H_{23}N_3O_4S$ requires *MH*, 365.1)). [α]$_D$ = + 51.0° (c 0.10, H_2O).

10.6 Synthesis of *de novo* designed inhibitors

10.6.1 Synthesis of 'first generation' *de novo* designed inhibitors of NDM-1

Synthesis of 5-phenyl-1,3-dihydo-2-benzofuranone (7.6)
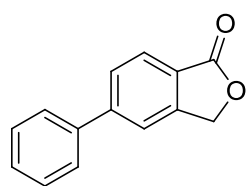
Preparation was *via* general method A using 5-bromophthalide (**7.5**) (0.50 g, 2.35 mmol) and phenyl boronic acid (0.32 g, 2.58 mmol) to afford the title compound (**7.6**) as a cream coloured powder which was used without further purification (0.33 g, 1.58 mmol, 67%) m.p.: 124.4-125.8 °C; R_f: 0.5 (2:1 Petrol–EtOAc); δ$_H$ (300 MHz, CDCl$_3$): 7.98 (1H, d, *J* 7.6, 3-H), 7.75 (1H, d, *J* 7.6, 4-H), 7.68 (1H, s, 6-H), 7.62 (2H, d, *J* 7.1, 2'-H and 6'-H), 7.47 (2H, app. t, *J* 7.1, 3'-H and 5'-H) 7.45 (1H, t, *J* 7.1, 4'-H), 5.38 (2H, s, CH$_2$O); δ$_C$ (75 MHz, CDCl$_3$): 147.5 (C=O), 147.3 (C1), 139.6 (C3), 129.1 (C3' and C5'), 128.6 (C2), 128.5 (C5),127.5 (C2' and C6') 126.1 (C4'), 124.5 (C1'), 120.6 (C6), 69.9 (CH$_2$O); v_{max}/ cm^{-1} (solid): 3473, 3070, 2924, 1747, 1615, 1452; HPLC: T$_r$= 3.00 (100% rel. area); *m/z* (ES): (Found: MNa+, 233.0573. $C_{14}H_{10}O_2$ requires *MNa*, 223.0570).

Synthesis of 2-hydroxymethyl-4-phenylbenzoic acid (7.4)
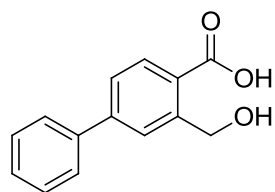
Preparation was *via* general method B using 5-phenyl-1,3-dihydo-2-benzofuranone (**7.6**) (0.30 g, 1.43 mmol) to afford the title compound (**7.4**) as an off-white solid which was used without further purification (0.26 g, 1.04 mmol, 73%) m.p.: 121.3-121.8 °C; R_f: 0.95 (19:1 DCM–MeOH); δ$_H$ (300 MHz, DMSO-d6): 8.11 (1H, d, *J* 1.6, 3-H), 7.96 (1H, d, *J* 8.2, 6-H), 7.72 (2H, d, *J* 7.1, 6'-H and 2'-H), 7.64 (1H, dd, *J* 8.2 and *J* 1.6, 5-H), 7.52 (2H, app. t, *J* 7.1, 5'-H and 3'-H), 7.42 (1H, t, *J* 7.1, 4'-H), 4.90 (2H, s, CH$_2$OH); δ$_C$ (75 MHz, DMSO-d6): 168.0 (C=O), 145.2 (C2), 143.4 (C4), 139.4 (C1'), 124.8 (C3), 124.4 (C5), 131.0 (C6), 129.0 (C3' and C5'), 128.1 (C4'), 126.8 (C2'

and C6'), 61.2 (CH$_2$OH); v_{max}/ cm^{-1} (solid): 3472, 3063, 1753, 1681, 1356; HPLC: T$_r$= 2.42 (96% rel. area); *m/z* (ES): (Found: [M-H]$^-$, 227.0714. C$_{14}$H$_{12}$O$_3$ requires *[M-H]*, 227.0717).

Synthesis of 5-(3-chlorophenyl)-1,3-dihydo-2-benzofuranone (7.14)
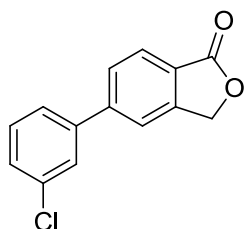
Preparation was *via* general method A using 5-bromophthalide (**7.5**) (0.20 g, 0.94 mmol) and 3-chlorophenyl boronic acid (0.16 g, 1.03 mmol) to afford the title compound (**7.14**) as yellow plates which was used without further purification (0.14 g, 0.58 mmol, 62%) m.p.: 150.7-151.2 °C; R_f: 0.47 (2:1 Petrol–EtOAc); δ_H (300 MHz, CDCl$_3$): 7.94 (1H, d, *J* 8.2, 3-H), 7.72 (1H, d, *J* 8.2, 4-H), 7.66 (1H, s, 6-H), 7.61 (1H, s, 2'-H), 7.50 (1H, app. t, *J* 7.7, 5'-H), 7.43 (2H, m, 4'-H and 6'-H), 5.39 (2H, s, CH$_2$O); δ_C (75 MHZ, CDCl$_3$): 180.7 (C=O), 147.4 (C1), 145.9 (C1'), 141.5 (C5), 135.1 (C3'), 130.3 (C5'), 128.6 (C3'), 127.7 (C6'), 126.3 (C3), 125.7 (C4), 125.1 (C2), 120.7 (C6), 69.6 (CH$_2$O); v_{max}/ cm^{-1} (solid): 3490, 3069, 1747, 1350; HPLC: T$_r$= 3.37 (95% rel. area); *m/z* (ES): (Found: MNa$^+$, 267.0183. C$_{14}$H$_9$ClO$_2$ requires *MNa*, 267.0162).
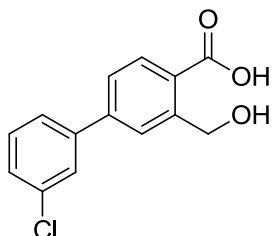
Synthesis of 4-(3-chlorophenyl)-2-(hydroxymethyl) benzoic acid (7.7)

Preparation was *via* general method B using 5-(3-chlorophenyl)-1,3-dihydo-2-benzofuranone (**7.14**) (0.15 g, 0.75 mmol) to afford the title compound (**7.7**) as an off-white solid which was used without further purification (0.16 g, 0.74 mmol, 99%) m.p.: 134.5-135.6 °C; R_f: 0.12 (19:1 DCM–MeOH); δ_H (300 MHz, DMSO-d6): 8.00 (1H, d, *J* 1.1, 3-H), 7.96 (1H, d, *J* 7.7, 6-H), 7.78 (1H, d, *J* 1.6, 2'-H), 7.67 (2H, m, 5-H and 4'-H), 7.58 (1H, app. t, *J* 8.2, 5'-H), 7.50 (1H, dd, *J* 8.2 and 1.6 6'-H), 4.91 (2H, s, CH$_2$OH); δ_C (75 MHz, DMSO-d6): 167.9 (C=O), 145.2 (C2), 141.7 (C4), 141.5 (C1'), 133.8 (C3'), 131.0 (C5'), 130.9 (C6), 127.9 (C3), 127.6 (C1), 126.5 (C2'), 125.6 (C4'), 124.9 (C6'), 124.7 (C5), 61.2 (CH$_2$OH); v_{max}/ cm^{-1} (solid): 3456, 3015, 1738, 1716, 1221; HPLC: T$_r$= 2.77 (100% rel. area); *m/z* (ES): (Found: [M-H]$^-$, 261.0330. C$_{14}$H$_{11}$ClO$_3$ requires *[M-H]*, 261.0324).

Synthesis of 5-(furan-2-yl)-1,3-dihydo-2-benzofuranone (7.15)
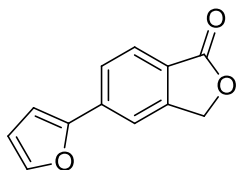
Preparation was *via* general method A using 5-bromophthalide (**7.5**) (0.50 g, 2.35 mmol) and 2-furanboronic acid (0.29 g, 2.58 mmol) to afford the title compound (**7.15**) as yellow plates which was used without further purification (0.19 g, 0.97 mmol, 41%) m.p.: 153.8-154.3 °C; R_f: 0.51 (2:1 Petrol–EtOAc); δ_H (300 MHz, CDCl$_3$): 7.96 (1H, d, *J* 8.2, 3-H), 7.82 (1H, d, *J* 8.2, 4-H), 7.73 (1H, s, 6-H), 7.53 (1H, d, *J* 2.2, 5'-H), 6.91 (1H, d, *J* 3.3, 3'-H), 6.55 (1H, dd, *J* 3.3 and 2.2, 4'-H), 5.37 (2H, s, CH$_2$O); δ_C (75 MHz, CDCl$_3$): 180.3 (C=O), 147.4 (C2'), 143.7 (C1), 135.0 (C5), 133.8 (C2), 126.1 (C5'), 124.7 (C3), 116.6 (C4), 112.3 (C6), 108.3 (C3' and C4'), 69.6 (CH$_2$O); v_{max}/ cm^{-1} (solid): 3472, 3110, 1740, 1602, 1446, 1352; HPLC: T_r= 2.65 (92% rel. area); *m/z* (ES): (Found: MNa$^+$, 223.0366. C$_{12}$H$_8$O$_3$ requires *MNa*, 223.0350).

Synthesis of 4-(furan-2-yl)-2-(hydroxymethyl) benzoic acid (7.8)
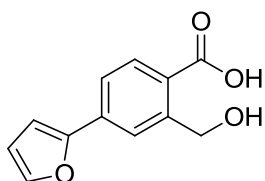
Preparation was *via* general method B using 5-(furan-2-yl)-1,3-dihydo-2-benzofuranone (**7.15**) (0.15 g, 0.75 mmol) to afford the title compound (**7.8**) as an off-white solid which was used without further purification (0.16 g, 0.74 mmol, 99%) m.p.: 137.7-138.3 °C; R_f: 0.96 (19:1 DCM–MeOH); δ_H (300MHz, DMSO-d6): 8.16 (1H, d, *J* 1.6, 3-H), 7.92 (1H, d, *J* 7.7, 6-H), 7.83 (1H, d, *J* 1.6, 5'-H), 7.66 (1H, dd, *J* 7.7 and 1.6, 5-H), 7.18 (1H, d, *J* 3.3, 3'-H), 6.62 (1H, dd, *J* 3.3 and 1.6, 4'-H), 4.88 (2H, s, CH$_2$OH); δ_C (75 MHz, DMSO-d6): 167.8 (C=O), 152.3 (C1'), 145.6 (C2) 143.8 (C5'), 133.2 (C4), 131.1 (C6), 126.4 (C1), 121.1 (C3 and C5), 107.8 (C3'), 61.1 (CH$_2$OH); v_{max}/ cm^{-1} (solid): 3379, 2970, 1738, 1607, 1377, 1217; HPLC: T_r= 2.13 (94% rel. area) *m/z* (ES): (Found: [M-H]$^-$, 217.0506. C$_{14}$H$_{10}$O$_4$ requires *[M-H]*, 217.0514).

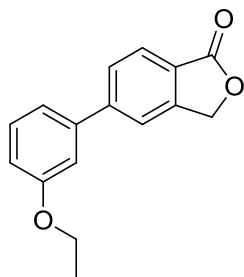## Synthesis of 5-(3-ethoxyphenyl)-1,3-dihydo-2-benzofuranone (7.16)

Preparation was *via* general method A using 5-bromophthalide (**7.5**) (0.20 g, 0.94 mmol) and 3-ethoxyphenyl boronic acid (0.17 g, 1.03 mmol) to afford the title compound (**7.16**) as an off-white solid which was used without further purification (0.20 g, 0.80 mmol, 85%) m.p.: 89.7-91.5 °C; R_f: 0.43 (2:1 Petrol–EtOAc); δ_H (300 MHz, CDCl$_3$): 7.89 (1H, d, J 8.2, 3-H), 7.66 (1H, d, J 8.2, 4-H), 7.58 (1H, s, 6-H), 7.32 (1H, app. t, J 7.7, 5'-H), 7.10 (1H, dd, J 7.7 and 2.2, 4'-H), 7.05 (1H, app. t, J 2.2, 2'-H), 6.87 (1H, dd, J 7.7 and J 2.2, 6'-H), 5.29 (2H, s, CH$_2$O), 4.02 (2H, q, J 7.1, CH$_2$), 1.35 (3H, t, J 7.1, CH$_3$); δ_C (75 MHz, CDCl$_3$): 159.5 (C=O), 147.4 (C3'), 147.3 (C1 or C1'), 141.1 (C5), 130.2 (C5'), 128.5 (C4), 126.1 (C3), 124.5 (C2), 120.6 (C6), 119.8 (C4'), 114.4 (C2'), 114.0 (C6'), 69.7 (CH$_2$O), 63.6 (CH$_2$), 14.9 (CH$_3$); v_{max}/ cm^{-1} (solid): 3482, 2970, 1730, 1598, 1352, 1217; HPLC: T$_r$= 3.34 (96% rel. area); *m/z* (EI): (Found: M$^+$, 254.0947. C$_{16}$H$_{14}$O$_3$ requires *M*, 254.0943).

Synthesis of 4-(3-ethoxyphenyl)-2-(hydroxymethyl) benzoic acid (7.9)
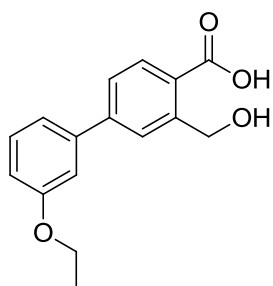
Preparation was *via* general method B using 5-(3-ethoxyphenyl)-1,3-dihydo-2-benzofuranone (**7.16**) (0.10 g, 0.34 mmol) to afford the title compound (**7.9**) as an off-white solid which was used without further purification (83 mg, 0.31 mmol, 77%) m.p.: 145.3-146.4 °C; R_f: 0.12 (19:1 DCM–MeOH); (Found: C, 70.4; H, 5.85; C$_{16}$H$_{16}$O$_4$ requires C, 70.5; H, 5.92%); δ_H (300 MHz, DMSO-d6): 7.98 (1H, s, 3-H), 7.95 (1H, d, J 8.2, 6-H), 7.64 (1H, d, J 8.2, 5-H), 7.40 (1H, t, J 7.7, 5'-H), 7.26 (1H, d, J 7.7, 6'-H), 7.20 (1H, s, 2'-H), 6.97 (1H, dd, J 7.7 and 2.7, 4'-H), 4.90 (2H, s, CH$_2$OH), 4.11 (2H, q, J 7.1, CH$_2$), 1.34 (3H, t, J 7.1, CH$_3$); δ_C (75 MHz, DMSO-d6): 168.0 (C=O), 159.0 (C2), 145.1 (C3'), 143.2 (C1'), 140.9 (C4), 131.0 (C6), 130.2 (C5'), 127.0 (C1), 124.9 (C3), 124.5 (C5), 119.0 (C6'), 114.1 (C2'), 112.8 (C4') 63.1 (CH$_2$), 61.2 (CH$_2$OH), 14.6 (CH$_3$); v_{max}/ cm^{-1} (solid): 3213, 2520, 2030, 1976, 1688, 1230; HPLC: T$_r$= 2.71 (100% rel. area); *m/z* (ES): (Found: [M-H]$^-$, 271.0976. C$_{16}$H$_{16}$O$_4$ requires *[M-H]*, 271.0798).

Synthesis of 5-(4-ethylphenyl)-1,3-dihydo-2-benzofuranone (7.17)
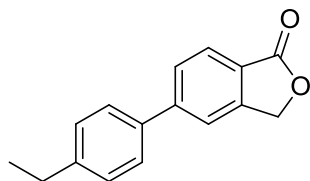
Preparation was *via* general method A using 5-bromophthalide (**7.5**) (0.20 g, 0.94 mmol) and 4-ethylphenyl boronic acid (0.16 g, 1.03 mmol) to afford the title compound (**7.17**) as yellow plates which were used without further purification (0.14 g, 0.57 mmol, 61%) m.p.: 114.3-115.7 °C; R_f: 0.58 (2:1 Petrol–EtOAc); δ_H (300 MHz, CDCl$_3$): 7.98 (1H, d, *J* 8.2, 3-H), 7.74 (1H, dd, *J* 8.2 and 1.6, 4-H), 7.66 (1H, d, *J* 1.6, 6-H), 7.55 (2H, d, *J* 8.2, 6'-H and 2'-H), 7.33 (2H, d, *J* 8.2, 5'-H and 3'-H), 5.35 (2H, s, CH$_2$O), 2.72 (2H, q, *J* 7.7, ethyl CH$_2$), 1.28 (3H, t, *J* 7.7, ethyl CH$_3$); δ_C (75 MHz, CDCl$_3$): 180.5 (C=O), 147.4 (C5), 147.3 (C1'), 145.1 (C4'), 141.1 (C1), 132.2 (C2), 128.7 (C3' and C5'), 128.3 (C4), 127.4 (C2' and C6'), 126.1 (C3), 120.1 (C6), 69.7 (CH$_2$O), 28.6 (CH$_2$), 15.5 (CH$_3$); v_{max}/ cm^{-1} (solid): 3489, 2968, 1746, 1618, 1347, 1282; HPLC: T_r= 3.51 (100% rel. area); *m/z* (ES): (Found: MNa$^+$, 261.0882. C$_{16}$H$_{14}$O$_2$ requires *MNa*, 261.0886).

Synthesis of 4-(4-ethylphenyl)-2-(hydroxymethyl) benzoic acid (7.10)
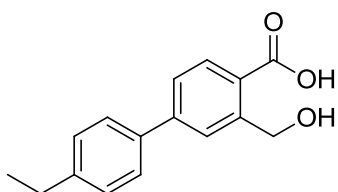
Preparation was *via* general method B using 5-(4-ethylphenyl)-1,3-dihydo-2-benzofuranone (**7.17**) (0.14 g, 0.57 mmol) to afford the title compound (**7.10**) as an off-white solid which was used without further purification (0.16 g, 0.74 mmol, 99%) m.p.: 143.4-145.2 °C; R_f: 0.15 (19:1 DCM–MeOH); δ_H (300MHz, DMSO-d6): 7.98 (1H, d, *J* 2.2, 3-H), 7.96 (1H, d, *J* 8.2, 6-H), 7.68 (2H, d, *J* 8.2, 6'-H and 2'-H), 7.63 (1H, dd, *J* 8.2 and 2.2, 5-H), 7.35 (2H, d, *J* 8.2, 5'-H and 3'-H), 4.90 (2H, s, CH$_2$OH), 2.66 (2H, q, *J* 7.7, ethyl CH$_2$), 1.22 (3H, t, *J* 7.7, CH$_3$); δ_C (75 MHz, DMSO-d6): 168.1 (C=O), 145.2 (C2), 143.9 (C4'), 143.3 (C4), 136.7 (C1'), 131.0 (C6), 128.4 (C3' and C5'), 126.7 (C2' and C6'), 126.6 (C1), 124.5 (C3), 124.2 (C5), 61.2 (CH$_2$OH), 27.8 (CH$_2$), 15.5 (CH$_3$); v_{max}/ cm^{-1} (solid): 3365, 3296, 2968, 2551, 1690, 1608, 1301; HPLC: T_r= 2.88 (100% rel. area); *m/z* (ES): (Found: MNa$^+$, 279.0984. C$_{16}$H$_{16}$O$_3$ requires *MNa*, 279.0992).

Synthesis of 5-(2,3-dichlorophenyl)-1,3-dihydo-2-benzofuranone (7.18)
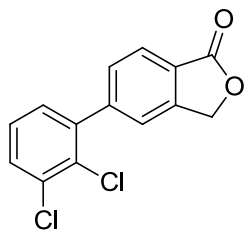
Preparation was *via* general method A using 5-bromophthalide (**7.5**) (0.50 g, 2.35 mmol) and 2,3-dichlorophenyl boronic acid (0.49 g, 2.58 mmol) to afford the title compound (**7.18**) as an off-white solid which was used without further purification (0.46 g, 1.64 mmol, 74%)

m.p.: 144.6-145.3 °C; R_f: 0.48 (2:1 Petrol–EtOAc); δ_H (300 MHz, CDCl$_3$): 7.93 (1H, d, J 8.2, 3-H), 7.51 (1H, s, 6-H), 7.48 (1H, dd, J= 8.2 and 2.2, 4-H), 7.46 (1H, dd, J 7.7 and 1.6, 4'-H), 7.24 (1H, t, J 7.7, 5-H), 7.19 (1H, dd, J 7.7 and 1.6, 6'-H), 5.33 (2H, s, CH$_2$O); δ_C (75 MHz, CDCl$_3$): 181.0 (C=O), 146.6 (C1), 145.2 (C1'), 141.3 (C5), 134.0 (C3'), 130.7 (C2'), 130.5 (C6 and C4), 129.3 (C6'), 127.5 (C5'), 125.6 (C3), 125.3 (C2), 123.1 (C4'), 69.6 (CH$_2$O); v_{max}/ cm^{-1} (solid): 3506, 3072, 2970, 2325, 1750, 1620, 1365, 1216; HPLC: T$_r$= 3.51 (100% rel. area); *m/z* (EI): (Found: M$^+$, 277.9903. C$_{14}$H$_8$Cl$_2$O$_2$ requires *M*, 227.9901).
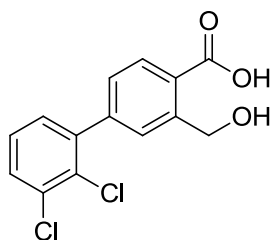
Synthesis of 4-(2,3-dichlorophenyl)-2-(hydroxymethyl)benzoic acid (7.11)

Preparation was *via* general method B using 5-(2,3-dichlorophenyl)-1,3-dihydro-2-benzofuranone (**7.18**) (0.10 g, 0.36 mmol) to afford the title compound (**7.11**) as an off-white solid which was used without further purification (83 mg, 0.31 mmol, 77%) m.p.: 151.2-151.8

°C; R_f: 0.11 (19:1 DCM–MeOH); δ_H (300 MHz, DMSO-d6): 7.96 (1H, d, J 8.2, 6-H), 7.74 (1H, d, J 1.6, 3-H), 7.73 (1H, dd, J 8.2 and 1.6, 5-H), 7.48 (1H, app. t, J 7.7, 5'-H), 7.40 (2H, m, 4'-H and 6'-H), 5.30 (1H, brs, OH), 4.89 (2H, s, CH$_2$OH); δ_C (75 MHz, DMSO-d6): 167.9 (C=O), 144.5 (C2), 141.8 (C4), 141.7 (C1'), 132.4 (C1), 130.1 (C6), 129.9 (C5), 129.4 (C3'), 128.4 (C5'), 127.8 (C2'), 127.3 (C3) 127.0 (C6' and C4'), 60.1 (CH$_2$OH); v_{max}/ cm^{-1} (solid): 3470, 3017, 1717, 1203; HPLC: T$_r$= 2.90 (100% rel. area); *m/z* (ES): (Found: MNa$^+$, 318.9879 C$_{14}$H$_{10}$Cl$_2$O$_3$ requires *MNa*, 318.9899).

Synthesis of 5-(quinolin-3-yl)-1,3-dihydo-2-benzofuranone (7.19)
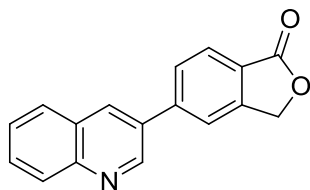
Preparation was *via* general method A using 5-bromophthalide (**7.5**) (0.50 g, 2.35 mmol) and 3-quinoline boronic acid (0.45 g, 2.58 mmol) to afford the title compound (**7.19**) as an off-white solid which was used without further purification (0.27 g, 1.04 mmol, 44%) m.p.: >250 °C; R_f: 0.05 (2:1 Petrol–EtOAc); δ_H (300MHz, CDCl$_3$): 9.25 (1H, d, *J* 2.2, 2'-H), 8.40 (1H, d, *J* 2.2, 4'-H), 8.18 (1H, d, *J* 8.2, 3-H), 8.06 (1H, d, *J* 8.2, 4-H), 7.93 (1H, d, *J* 8.2, 8'-H), 7.89 (1H, d, *J* 8.2, 5'-H), 7.83 (1H, s, 6-H), 7.80 (1H, app. dd, *J* 8.2 and 1.6, 6'-H), 7.64 (1H, app. dd, *J* 8.2 and 1.6, 7'-H), 5.45 (2H, s, CH$_2$O); δ_C (75 MHz, CDCl$_3$): 170.0 (C=O), 149.4 (C2'), 147.8 (C9'), 147.6 (C1), 144.0 (C5), 134.3 (C4'), 132.4 (C10'), 132.1 (C5'), 132.0 (C2), 130.5 (C6'), 129.4 (C4), 128.7 (C7'), 128.2 (C5'), 127.5 (C3), 126.1 (C6), 69.6 (CH$_2$O); v_{max}/ cm^{-1} (solid): 3478, 3059, 2970, 1741, 1348; HPLC: T_r= 1.61 (100% rel. area); *m/z* (EI): (Found: M$^+$, 261.0765. C$_{17}$H$_{11}$NO$_2$ requires *M*, 261.0790).

Synthesis of 2-(hydroxymethyl)-4-(quinolone-3-yl) benzoic acid (7.12)

Preparation was *via* general method B using 5-(quinolin-3-yl)-1,3-dihydo-2-benzofuranone (**7.19**) (0.15 g, 0.57 mmol) to afford the title compound (**7.12**) as an off-white solid which was used wi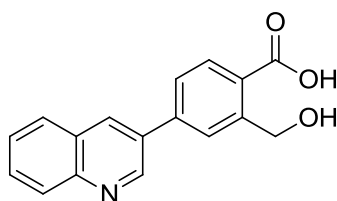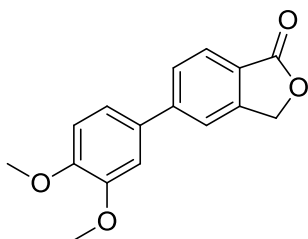thout further purification (84 mg, 0.30 mmol, 78%) m.p.: >250 °C; R_f: 0.15 (19:1 DCM–MeOH); δ_H (300MHz, DMSO-d6): 9.36 (1H, d, *J* 2.2, 2'-H), 8.89 (1H, d, *J* 2.2, 4'-H), 8.23 (1H, s, 3-H), 8.19 (1H, d, *J* 7.7, 8'-H), 8.16 (1H, d, *J* 7.7, 5'-H), 8.02 (1H, d, *J* 7.7, 6-H), 7.88 (1H, d, *J* 7.7, 5-H), 7.86 (1H, app. t, *J* 7.7, 6'-H), 7.72 (1H, app. t, *J* 7.7, 7'-H), 5.18 (2H, s, CH$_2$OH); δ_C (75 MHz, DMSO-d6): 167.9 (C=O), 153.9 (C9'), 150.0 (C2), 148.3 (C2'), 145.5 (C4), 139.6 (C4'), 137.2 (C10'), 137.1 (C3'), 132.2 (C6'), 131.1 (C6), 130.7 (C1), 128.7 (C7'), 127.9 (C5), 127.7 (C4'), 127.4 (C5'), 125.4 (C8'), 125.0 (C3), 61.1 (CH$_2$OH); v_{max}/ cm^{-1} (solid): 3448, 2970, 1739, 1365, 1232; HPLC: T_r= 1.39 (100% rel. area); *m/z* (ES): (Found: [M-H]$^-$, 278.0819. C$_{17}$H$_{13}$NO$_3$ requires *[M-H]*, 278.0823).

Synthesis of 5-(3,4-dimethoxyphenyl)-1,3-dihydo-2-benzofuranone (7.20)

Preparation was *via* general method A using 5-bromophthalide (**7.5**) (0.20 g, 0.94 mmol) and 3,4-dimethoxyphenyl boronic acid (0.19 g, 1.03 mmol) to afford <u>the title compound</u> (**7.20**) as yellow plates which was used without further purification (0.18 g, 0.67 mmol, 72%) m.p.: 172.8-174.1 °C; R_f: 0.32 (2:1 Petrol–EtOAc); δ_H (300MHz, CDCl$_3$): 7.98 (1H, d, J 8.2, 3-H), 7.74 (1H, d, J 8.2, 4-H), 7.64 (1H, s, 6-H), 7.20 (1H, dd, J 8.2 and 2.2, 6'-H), 7.12 (1H, d, J 2.2, 2'-H), 6.98 (1H, d, J 8.2, 5'-H), 5.38 (2H, s, CH$_2$O), 3.98 (3H, s, CH$_3$-3'), 3.96 (3H, s, CH$_3$-4'); δ_C (75 MHz, CDCl$_3$): 181.1 (C=O), 149.7 (C3'), 149.3 (C4'), 147.4 (C5), 147.3 (C1'), 132.4 (C2), 128.1 (C4), 126.1 (C3), 124.0 (C1), 120.1 (C6' and C6), 111.5 (C5'), 110.5 (C2'), 69.6 (CH$_2$O), 56.0 (CH$_3$-3' and CH$_3$-4'); v_{max}/ cm^{-1} (solid): 3481, 2944, 1751, 1605, 1226; HPLC: T$_r$= 2.50 (95% rel. area); *m/z* (ES): (Found: MNa$^+$, 293.0777. C$_{16}$H$_{14}$O$_4$ requires *MNa*, 293.0784).

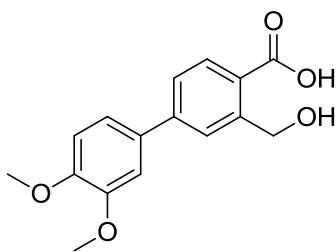## Synthesis of 4-(3,4-dimethoxyphenyl)-2-(hydroxymethyl)benzoic acid (7.13)

Preparation was *via* general method B using 5-(3,4-dimethoxyphenyl)-1,3-dihydro-2-benzofuranone (**7.20**) (0.15 g, 0.75 mmol) to afford <u>the title compound</u> (**7.13**) as an off-white solid which was used without further purification (0.16 g, 0.74 mmol, 99%) m.p.: 159.1-159.8 °C; R_f: 0.15 (19:1 DCM–MeOH); δ_H (300MHz, DMSO-d6): 7.97 (1H, d, J 1.1, 3-H), 7.91 (1H, d, J 8.2, 6-H), 7.63 (1H, dd, J 8.2 and 1.1, 5-H), 7.32 (2H, m, 5'-H and 2'-H), 7.27 (1H, d, J 9.3, 6'-H), 4.89 (2H, s, CH$_2$OH), 3.85 (3H, s, CH$_3$-3'), 3.81 (3H, s, CH$_3$-4'); δ_C (75 MHz, DMSO-d6): 168.1 (C=O), 149.0 (C4' and C3'), 145.1 (C4), 143.4 (C1'), 131.9 (C2), 131.0 (C6), 126.2 (C1), 124.4 (C3), 124.1 (C5), 119.2 (C6'), 112.1 (C5'), 110.3 (C2'), 61.3 (CH$_2$OH), 55.5 (CH$_3$-3' and CH$_3$-4'); v_{max}/ cm^{-1} (solid): 3513, 2940, 2652, 1687, 1605, 1322, 1255; HPLC: T$_r$= 2.05 (89% rel. area); *m/z* (ES): (Found: MNa$^+$, 311.0877. C$_{16}$H$_{16}$O$_5$ requires *MNa*, 311.0890).

## 10.6.2 Thiol-containing inhibitors: route development

Synthesis of methyl-2-(iodomethyl)-4-phenyl-benzoate (7.22)
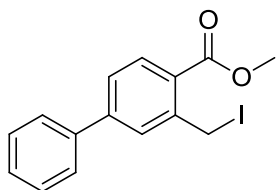
A solution of 5-phenyl-1,3-dihydo-2-benzofuranone (**7.6**) (1.00 g, 4.76 mmol) in DCM (40 ml) was added to a stirred solution of 1M boron tribromide in DCM (4.76 mL, 4.76 mmol), sodium iodide (1.07 g, 7.14 mmol) and cat. tetra-n-butly ammonium iodide (20 mg, 0.04 mmol). The mixture was stirred at room temperature for 16 h under an atmosphere of nitrogen. The reaction mixture was poured into methanol (20 ml) and concentrated *in vacuo*. The crude product was purified using flash column chromatography, eluting with chloroform, to afford the title compound (**7.22**) as an off-white solid which was used without further purification (0.52 g, 1.48 mmol, 31%). m.p.: 79.1-80.5 °C; R_f: 0.73 (CHCl$_3$); δ_H (300 MHz, CDCl$_3$): 8.05 (1H, d, *J* 8.2, 6-H), 7.62 (2H, d, *J* 7.1, 6'-H and 2'-H), 7.61 (1H, d, *J* 1.6, 3-H), 7.54 (1H, dd, *J* 8.2 and *J* 1.6, 5-H), 7.48 (2H, app. t, *J* 7.1, 5'-H and 3'-H), 7.40 (1H, t, *J* 7.1, 4'-H), 5.01 (2H, s, CH$_2$I), 3.96 (3H, s, CH$_3$); δ_C (75 MHz, CDCl$_3$): 166.9 (C=O), 145.3 (C2), 141.9 (C4), 139.2 (C1'), 132.2 (C6), 129.7 (C4'), 129.0 (C5' and C3'), 128.4 (C5), 127.2 (C6' and C2'), 126.7 (C1), 126.5 (C3), 52.3 (CH$_3$), 4.2 (CH$_2$I); v_{max}/ cm^{-1} (solid): 3419, 3060, 2977, 2584, 1712, 1605, 1293, 1104; HPLC: T_r= 4.10 (96% rel. area); *m/z* (EI): (Found: [M-I]$^+$, 225.0906. C$_{15}$H$_{13}$IO$_2$ requires [*M-I*], 225.0916).

Synthesis of methyl-4-bromo-2-(iodomethyl)-benzoate (7.23)
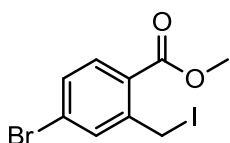
A solution of 5-bromophthalide (**7.5**) (3.00 g, 14.1 mmol) in DCM (50 ml) was added to a stirred solution of 1M boron tribromide in DCM (14.1 mL, 14.1 mmol), sodium iodide (3.17 g, 21.1 mmol) and cat. tetra-n-butly ammonium iodide (52 mg, 0.14 mmol). The mixture was stirred at room temperature for 16 h under an atmosphere of nitrogen. The reaction mixture was poured into methanol (20 ml) and concentrated *in vacuo*. The crude product was purified using flash column chromatography, eluting with chloroform, to afford the title compound (**7.23**) (1.50 g, 4.23 mmol, 30%) was obtained as pale brown plates, m.p: 92.2-93.5 °C; R_f 0.85 (CHCl$_3$); δ_H (300 MHz, CDCl$_3$): 7.85 (1H, d, *J* 8.2, 6-H), 7.59 (1H, s, 3-H), 7.48 (1H, d, *J* 8.2,

5-H), 4.88 (2H, s, CH_2), 3.96 (3H, s, CH_3); δ_C (75 MHz, $CDCl_3$): 164.2 (C=O), 141.2 (C2), 131.9 (C6), 130.9 (C5), 129.0 (C3), 124.9 (C1), 124.9 (C4), 50.3 (CH_3); v_{max}/ cm^{-1} (solid): 3423, 3078, 3055, 2952, 2311, 1939, 1745, 1585, 1558; HPLC: T_r = 2.05 (100% rel.area); m/z (ES): (Found: MNa^+, 377.8615. $C_9H_8IO_2$ requires *MNa*, 377.8645).

Synthesis of 4-bromo-2-([(triphenylmethyl)sulfanyl]methyl)benzoic acid (7.24)
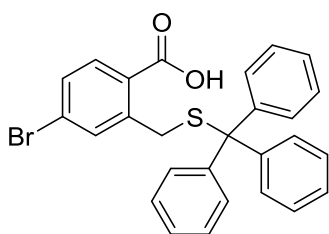
Preparation was *via* general method D using 4-bromo-2-(iodomethyl) benzoic acid (**7.23**) (1.50 g, 4.24 mmol) to afford the crude compound 4-bromo-2-(sulfanylmethyl) benzoic acid as colourless microcrystals which were re-suspended in THF (30 mL). Trityl chloride (1.18 g, 4.24 mmol) and Et_3N (1.77 mL, 12.7 mmol) were added and the reaction stirred at room temperature for 18 h. The reaction mixture was concentrated *in vacuo*. The residue was re-suspended in DCM (30 mL), washed with water (3 × 30 mL), dried ($MgSO_4$) and concentrated *in vacuo*. The crude product was purified by flash column chromatography eluting with 3:1 Petrol−EtOAc to afford the title compound (**7.24**) as an off white solid (0.65 g, 1.33 mmol, 31%). m.p: 106.2-107.9 °C; R_f 0.31 (DCM); δ_H (300 MHz, $CDCl_3$): 7.92 (1H, d, *J* 8.2, 6-H), 7.57 (1H, dd, *J* 8.2 and 1.6, 5-H), 7.41 (1H, d, *J* 1.6, 3-H), 7.39 (6H, d, *J* 7.6, 6-Htrt and 2-Htrt), 7.26 (6H, app. t, *J* 7.6, 5-Htrt and 3-Htrt), 7.20 (3H, t, *J* 7.6, 4H-trt), 3.74 (2H, s, CH_2); δ_C (75 MHz, $CDCl_3$): 169.2 (C=O), 144.3 (C1trt), 138.6 (C2), 133.7 (C5), 130.9 (C3), 130.2 (C6), 129.4 (C6trt and C2trt), 128.5 (C1), 128.0 (C5trt and C3trt), 126.7 (C4trt), 122.6 (C4), 68.3 ($\underline{C}(Ph)_3$), 35.7 (CH_2); v_{max}/ cm^{-1} (solid): 3078, 2972, 1723, 1521, 1458; HPLC: T_r = 4.21 (100% rel.area); m/z (ES): (Found: $[M-H]^-$, 487.0367. $C_{27}H_{21}BrO_2S$ requires *[M-H]*, 487.0373).

Synthesis of 4-phenyl-2-([(triphenylmethyl)sulfanyl]methyl)benzoic acid (7.25)
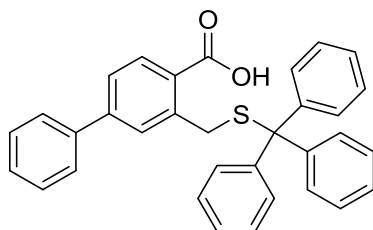
Preparation was *via* general method A using 4-bromo-2-([(triphenylmethyl)sulfanyl]methyl) benzoic acid **(7.24)** (0.10 g, 0.20 mmol) and phenyl boronic acid (27 mg, 0.22 mmol) to afford the title compound (**7.25**) as an off-white solid which was used without further purification (82 mg, 0.17 mmol, 77%). m.p: 115.4-117.2 °C; R_f 0.37 (DCM); δ_H (300 MHz, CDCl$_3$): 8.21 (1H, d, *J* 8.3, 6-H), 7.71 (1H, dd, *J* 8.3 and 1.9, 5-H), 7.62-7.53 (3H, m, 6'-H, 2'-H and 3-H), 7.46 (2H, app. t, *J* 7.5, 5'-H and 3'-H), 7.41 (6H, d, *J* 7.5, 6-Htrt and 2-Htrt), 7.39 (1H, t, *J* 7.5, 4'-H), 7.27 (6H, app. t, *J* 7.2, 5-Htrt and 3-Htrt), 7.20 (3H, t, *J* 7.2, 4-Htrt), 3.75 (2H, s, CH$_2$); δ_C (75 MHz, CDCl$_3$):; v_{max}/ cm^{-1} (solid): 3065, 2984, 1704, 1521, 1458; HPLC: T_r = 4.03 (100% rel.area); *m/z* (ES): (Found: [M-H]$^-$, 485.1562. C$_{33}$H$_{26}$O$_2$S requires *[M-H]*, 485.1581).

Synthesis of 2-iodomethyl-4-phenyl-benzoic acid (7.26)
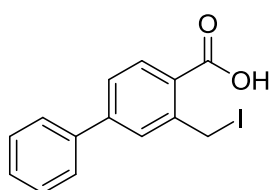
Preparation was *via* general method C using 5-phenyl-1,3 dihydro-2-benzofuranone (**7.6**) (0.20 g, 0.95 mmol) to afford the title compound (**7.26**) as an off-white solid which was used without further purification (0.20 g, 0.59 mmol, 62%) m.p.: 81.3-82.4 °C; R_f: 0.75 (CHCl$_3$); δ_H (300MHz, DMSO-d6): 7.94 (1H, d, J 8.3, 6-H), 7.88 (1h, d, J 1.8, 3-H), 7.73 (2H, d, J 7.3, 6'-H and 2'-H), 7.68 (1H, dd, J 8.3 and 1.8, 5-H), 7.51 (2H, app. t, J 7.3, 5'-H and 3'-H), 7.44 (1H, t, J 7.3, 4'-H), 5.09 (2H, s, CH$_2$); v_{max}/ cm^{-1} (solid): 2806, 2630, 1750, 1603, 1257, 909; *m/z* (ES): (Found: [M+2Na-H]$^+$, 382.9516. C$_{14}$H$_{11}$IO$_2$ requires *[M+2Na-H]*, 382.9515).

Synthesis of 4-phenyl-2-sulfonylmethylbenzoic acid (7.21)
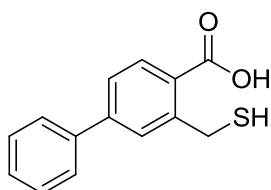
Preparation was *via* general method D using (2-iodomethyl)-4-phenyl benzoic acid (**7.26**) (0.65 g, 1.92 mmol) to afford the crude title compound. The title compound (**7.21**) was isolated as colourless microcrystals (0.25 g, 1.01 mmol, 53%). m.p.: 168.2-169.9 °C; R_f: 0.18 (19:1 DCM−MeOH); δ_H (300 MHz, DMSO-d6): 7.95 (1H, d, *J* 8.2, 6-H), 7.77 (1H,

d, J 2.0, 3-H), 7.73 (2H, d, J 7.4, 6'-H and 2'-H), 7.65 (1H, dd, J 8.2 and 2.0, 5-H), 7.52 (2H, app. t, J 7.4, 5'-H and 3'-H), 7.44 (1H, t, J 7.4, 4'-H), 4.13 (2H, d, J 8.5, CH$_2$), 2.87 (1H, t, J 8.5, SH); δ_C (75 MHz, DMSO-d6): 168.0 (C=O), 144.3 (C4), 143.6 (C1'), 138.7 (C2), 131.5 (C6), 129.0 (C5' and C3'), 128.9 (C4'), 128.2 (C5), 127.8 (C1), 126.9 (C6' and C2'), 124.9 (C3), 26.4 (CH$_2$); v_{max}/ cm^{-1} (solid): 2976, 1681, 1350, 1278, 756; HPLC: T$_r$= 2.88 (95% rel. area); m/z (ES): (Found: [M-H]$^-$, 243.0477 C$_{14}$H$_{12}$O$_2$S requires *[M-H]*, 243.0485).

10.6.3 Second generation *de novo* designed inhibitors

Synthesis of 5-(2-chlorophenyl)-1,3-dihydo-2-benzofuranone (7.42)
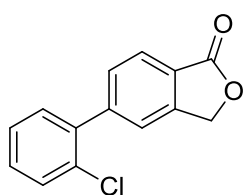
Preparation was *via* general method A using 5-bromophthalide (**7.5**) (0.50 g, 2.35 mmol) and 2-chlorophenyl boronic acid (0.40 g, 2.59 mmol) to afford the title compound (**7.42**) as yellow plates which was used without further purification (0.43 g, 1.76 mmol, 75%) m.p.: 80.4-81.7 °C; R_f: 0.40 (4:1 Petrol−EtOAc); δ_H (300 MHz, CDCl$_3$): 8.01 (1H, d, J 7.9, 3-H), 7.62 (1H, dd, J 7.9 and 2.2, 4-H), 7.58 (1H, d, J 2.2, 6-H), 7.57-7.50 (1H, m, 3'-H), 7.42-7.30 (3H, m, 4'-H, 5'-H and 6'-H), 5.41 (2H, s, CH$_2$); δ_C (75 MHz, CDCl$_3$): 170.8 (C=O), 146.5 (C1), 145.4 (C1'), 139.0 (C5), 132.3 (C2'), 131.1 (C3'), 130.7 (C6'), 130.3 (C6), 129.6 (C4'), 127.1 (C3), 125.5 (C4), 125.0 (C2), 123.5 (C5'), 69.6 (CH$_2$); v_{max}/ cm^{-1} (solid): 1752, 1351, 1072; HPLC: T$_r$= 2.95 (100% rel. area); m/z (ES): (Found: MNa$^+$, 267.0186. C$_{14}$H$_9$ClO$_2$ requires *MNa*, 267.0183).

Synthesis of 4-(2-chlorophenyl)-2-iodomethyl-benzoic acid (7.50)
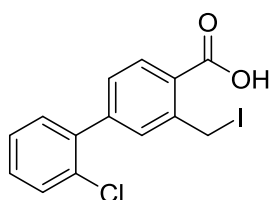
Preparation was *via* general method C using 5-(2-chlorophenyl)-1,3 dihydro-2-benzofuranone (**7.42**) (0.30 g, 1.23 mmol) to afford the title compound (**7.50**) as an off-white solid which was used without further purification (0.24 g, 0.64 mmol, 52%) m.p.: 152.4-153.2 °C; R_f: 0.29 (CHCl$_3$); δ_H (300 MHz, DMSO-d6): 7.91 (1H, d, J 7.9, 6-H), 7.59 (1H, d, J 2.0, 3-H), 7.54 (1H, dd, J 7.9 and 2.0, 5-H), 7.47-7.37 (4H, m, 6'-H, 5'-H, 4'-H and 3'-H), 5.03 (2H, s, CH$_2$); v_{max}/ cm^{-1} (solid): 3052, 2197, 1672, 1605, 1439, 1260; m/z (ES): (Found: [M-I]$^+$, 245.0365. C$_{14}$H$_{10}$ClO$_2$ requires *[M-I]*, 245.0364).

Synthesis of 4-(2-chlorophenyl)-2-(sulfonylmethyl) benzoic acid (7.28)
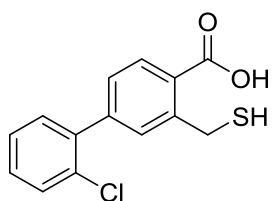
Preparation was *via* general method D using 4-(2-chlorophenyl)-2-(iodomethyl) benzoic acid (**7.50**) (0.15 g, 0.40 mmol) to afford the title compound (**7.28**) as colourless needles. (66 mg, 0.24 mmol, 59%). m.p.: 129.3-130.7 °C; R_f: 0.22 (19:1 DCM−MeOH); δ_H (300MHz, DMSO-d6): 7.93 (1H, d, *J* 8.2, 6-H), 7.62-7.57 (1H, m, 3'-H), 7.52(1H, d, *J* 1.8, 3-H), 7.46-7.43 (3H, m, 6'-H, 5'-H and 4'-H), 7.42 (1H, dd, *J* 8.2 and 1.8, 5-H), 4.11 (2H, d, *J* 8.3, CH₂), 2.84 (1H, t, *J* 8.3, SH); δ_C (75 MHz, DMSO-d6): 168.0 (C=O), 143.4 (C1'), 142.2 (C2), 38.6 (C4), 131.4 (C6' and C3'), 131.1 (C2'), 130.6 (C6), 129.9 (C5), 129.7 (C4'), 128.4 (C1), 127.8 (C5'), 127.6 (C3), 26.2 (CH₂); v_{max}/ cm⁻¹ (solid): 2912, 1676, 1438, 1296, 1068; HPLC: T_r= 3.04 (95% rel. area); *m/z* (ES): (Found: [M-H]⁻, 277.0090. $C_{14}H_{11}ClO_2S$ requires *[M-H]*, 277.0096).

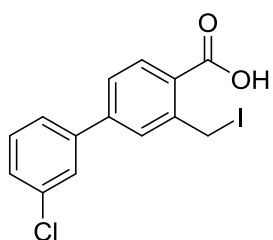## Synthesis of 4-(3-chlorophenyl)-2-iodomethyl-benzoic acid (7.51)

Preparation was *via* general method C using 5-(3-chlorophenyl-1,3 dihydro-2-benzofuranone (**7.14**) (0.30 g, 1.22 mmol) to afford the title compound (**7.51**) as an off-white solid which was used without further purification (0.38 g, 1.03 mmol, 84%) m.p.: 167.8-169.9 °C; R_f: 0.26 (CHCl₃); δ_H (300 MHz, DMSO-d6): 7.90 (1H, d, *J* 1.8, 3-H), 7.89 (1H, d, *J* 8.1, 6-H), 7.77 (1H, t, *J* 1.4, 2'-H), 7.69-7.63 (2H, app. d, *J* 8.0, 5-H and 4'-H), 7.49 (1H, t, *J* 8.0, 5'-H), 7.46 (1H, d, *J* 8.0, 6'-H), 5.03 (2H, s, CH₂); v_{max}/ cm⁻¹ (solid): 3067, 2815, 2521, 1678, 1412, 1253.

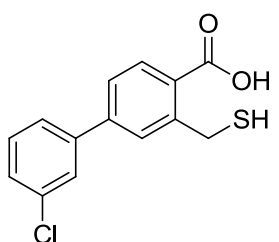## Synthesis of 4-(3-chlorophenyl)-2-(sulfonylmethyl) benzoic acid (7.29)

Preparation was *via* general method D using 4-(3-dichlorophenyl)-2-(iodomethyl) benzoic acid (**7.51**) (0.19 g, 0.50 mmol) to afford the title compound (**7.29**) as pale yellow microcrystals. (0.11 g, 0.38 mmol, 77%) m.p.: 144.2-145.9 °C; R_f: 0.16 (19:1 DCM-MeOH); δ_H (300 MHz, DMSO-d6): 7.95 (1H, d, *J* 8.2, 6-H), 7.83 (1H, d, *J* 1.7, 2'-H), 7.82 (1H, d, *J* 1.9, 3-H), 7.72 (1H, dd, *J* 8.9 and 1.7, 4'-H), 7.69 (1H, dd, *J* 8.2 and 1.9, 5-H), 7.53 (1H, app t, *J* 8.9, 5'-H), 7.49 (1H, dd, *J* 8.9 and 1.7, 6'-H),

4.13 (2H, d, J 8.4, CH$_2$SH), 2.87 (1H, t, J 8.4, SH); δ_C (75 MHz, DMSO-d6): 167.9 (C=O), 144.5 (C4), 141.8 (C1'), 140.8 (C2), 133.8 (C3'), 131.6 (C5'), 130.8 (C6), 129.0 (C2'), 128.4 (C1), 128.1 (C4'), 126.7 (C5) 125.6 (C3), 125.2 (C6'), 26.3 (CH$_2$); v_{max}/ cm^{-1} (solid): 2962, 2643, 1762, 1261, 772; HPLC: T$_r$= 2.33 (90% rel. area); m/z (ES): (Found: [M-H]$^-$, 277.0088 C$_{14}$H$_{11}$ClO$_2$S requires *[M-H]*, 277.0096.

Synthesis of 5-(4-chlorophenyl)-1,3-dihydo-2-benzofuranone (7.43)
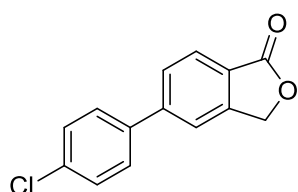
Preparation was *via* general method A using 5-bromophthalide (**7.5**) (0.50 g, 2.35 mmol) and 3-thienyl boronic acid (0.40 g, 2.59 mmol) to afford the title compound (**7.43**) as yellow plates which was used without further purification (0.43 g, 1.76 mmol, 75%) m.p.: 186.6-187.4 °C; R_f: 0.32 (4:1 Petrol−EtOAc); δ_H (300 MHz, CDCl$_3$): 7.91 (1H, d, J 8.0, 6-H), 7.63 (1H, dd, J 8.0 and 1.5, 5-H), 7.57 (1H, d, J 1.5, 3-H), 7.48 (2H, d, J 8.4, 6'-H and 2'-H), 7.39 (2H, d, J 8.4, 5'-H and 3'-H), 5.30 (2H, s, CH$_2$); δ_C (75 MHz, CDCl$_3$): 170.7 (C=O), 147.5 (C1), 146.2 (C1'), 138.2 (C5), 135.0 (C4'), 129.3 (C5' and C3'), 128.8 (C6' and C2'), 128.3 (C6), 126.3 (C3), 124.9 (C2), 120.5 (C4), 69.6 (CH$_2$); v_{max}/ cm^{-1} (solid): 1747, 1614, 1321, 1112; HPLC: T$_r$= 3.07 (100% rel. area); m/z (ES): (Found: MH$^+$, 245.0356. C$_{14}$H$_{10}$ClO$_2$ requires *MH*, 245.0364).

Synthesis of 4-(4-chlorophenyl)-2-iodomethyl-benzoic acid (7.52)

Preparation was *via* general method C using 5-(4-chlorophenyl)-1,3 dihydro-2-benzofuranone (**7.43**) (0.30 g, 1.23 mmol) to afford the title compound (**7.52**) as an off-white solid which was used without further purification (0.33 g, 0.87 mmol, 71%) m.p.: 181.5-187.1 °C; R_f: 0.21 (CHCl$_3$); δ_H (300 MHz, DMSO-d6): 7.91 (1H, d, J 8.1, 6-H), 7.86 (1H, d, J 1.8, 3-H), 7.74 (2H, d, J 8.5, 6'-H and 2'-H), 7.66 (1H, dd, J 8.3 and 1.8, 5-H), 7.53 (2H, d, J 8.7, 5'-H and 3'-H), 5.04 (2H, s, CH$_2$); v_{max}/ cm^{-1} (solid): 3065, 2649, 1676, 1318, 1190.

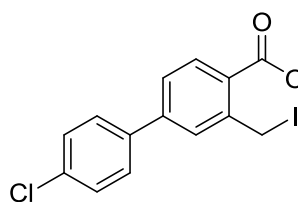## Synthesis of 4-(4-chlorophenyl)-2-(sulfonylmethyl) benzoic acid (7.30)
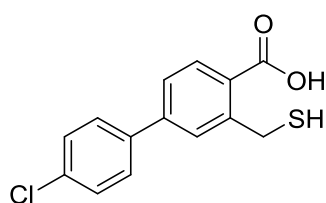
Preparation was *via* general method D using 4-(4-chlorophenyl)-2-(iodomethyl) benzoic acid (**7.52**) (0.30 g, 0.81 mmol) to afford the title compound (**7.30**) as pale yellow microcrystals. (0.17 g, 0.59 mmol, 73%). m.p.: 215.0-216.6 °C; R_f: 0.05 (19:1 DCM−MeOH); δ_H (300 MHz, DMSO-d6): 7.95 (1H, d, *J* 8.2, 6-H), 7.78 (1H, d, *J* 2.0, 3-H), 7.77 (2H, d, *J* 8.6, 6'-H and 2'-H), 7.66 (1H, dd, *J* 8.2 and 2.0, 5-H), 7.57 (2H, d, *J* 8.6, 5'-H and 3'-H), 4.13 (2H, d, *J* 8.4, CH$_2$), 2.87 (1H, t, *J* 8.4, SH); δ_C (75 MHz, DMSO-d6): 167.9 (C=O), 144.4 (C4), 142.1 (C1'), 137.5 (C2), 133.1 (C4'), 131.6 (C6), 129.0 (C5' and C3'), 128.8 (C5), 128.6 (C6' and C2'), 128.1 (C1), 124.9 (C3), 26.3 (CH$_2$) v_{max}/ cm^{-1} (solid): 3225, 1698, 1650, 1302, 1008; HPLC: T_r= 3.23 (90% rel. area); *m/z* (ES): (Found: [M-H]$^-$, 277.0089. C$_{14}$H$_{11}$ClO$_2$S requires *[M-H]*, 277.0096).

## Synthesis of 5-(3-fluorophenyl)-1,3-dihydo-2-benzofuranone (7.44)

Preparation was *via* general method A using 5-bromophthalide (**7.5**) (0.50 g, 2.35 mmol) and 3-flurorophenyl boronic acid (0.36 g, 2.59 mmol) to afford the title compound (**7.44**) as yellow plates which was used without further purification (0.32 g, 1.42 mmol, 60%) m.p.: 126.6-127.6 °C; R_f: 0.33 (4:1 Petrol−EtOAc); δ_H (300 MHz, CDCl$_3$): 8.00 (1H, d, *J* 8.7, 3-H), 7.73 (1H, d, *J* 8.7, 4-H), 7.66 (1H, s, 6-H), 7.46 (1H, dd, *J* 7.8 and 1.6, 2'-H), 7.40 (1H, dt, *J* 7.8 and 1.6, 6'-H), 7.32 (1H, dt, *J* 7.8 and 1.6, 5'-H), 7.14 (1H, dd, *J* 7.8 and 1.6, 4'-H), 5.39 (2H, s, CH$_2$); δ_C (75 MHz, CDCl$_3$): 170.7 (C=O), 164.8 (C3'), 147.4 (C1), 146.1 (C1'), 141.8 (C5), 130.6 (C5'), 128.4 (C6), 126.3 (C3), 125.1 (C2), 123.2 (C4), 120.7 (C6'), 115.5 (C4'), 114.5 (C2'), 69.6 (CH$_2$); v_{max}/ cm^{-1} (solid): 3077, 1748, 1506, 1079; HPLC: T_r= 2.75 (98% rel. area); *m/z* (ES): (Found: MH$^+$, 229.0708. C$_{14}$H$_9$FO$_2$ requires *MH*, 229.0659).

Synthesis of 4-(3-fluorophenyl)-2-iodomethyl-benzoic acid (7.53)
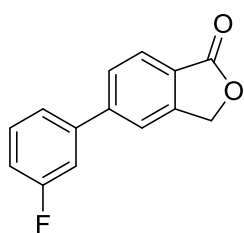

Preparation was *via* general method C using 5-(3-fluorophenyl)-1,3 dihydro-2-benzofuranone (**7.44**) (0.25 g, 1.10 mmol) to afford the title compound (**7.53**) as an off-white solid which was used without further purification (0.31 g, 0.87 mmol, 79%) m.p.: 176.1-177.9 °C; R_f: 0.24 (CHCl$_3$); δ$_H$ (300 MHz, DMSO-d6): 7.90 (1H, d, *J* 8.1, 6-H), 7.89 (1H, d, *J* 2.0, 3-H), 7.68 (1H, dd, *J* 8.1 and 1.9, 5-H), 7.58 (1H, app. s, 2'-H), 7.58 (1H, d, *J* 1.8, 6'-H), 7.49 (1H, app. q, *J* 6.5, 5'-H), 7.22 (1H, app. t, *J* 8.1, 4'-H), 5.02 (2H, s, CH$_2$); ν$_{max}$/ cm^{-1} (solid): 3063, 2632, 1687, 1557, 1205, 792.

Synthesis of 4-(3-fluorophenyl)-2-(sulfonylmethyl) benzoic acid (7.31)
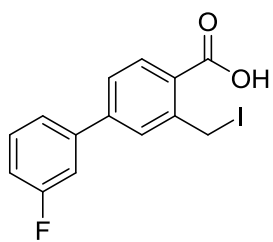

Preparation was *via* general method D using 4-(3-fluorophenyl)-2-(iodomethyl) benzoic acid (**7.53**) (0.25 g, 0.70 mmol) to afford the title compound (**7.31**) as pale yellow microcrystals. (73 mg, 0.28 mmol, 40%). m.p.: 167.0-168.9 °C; R_f: 0.16 (19:1 DCM−MeOH); δ$_H$ (300 MHz, DMSO-d6): 7.94 (1H, d, *J* 8.2, 6-H), 7.82-7.76 (2H, m, 6'-H and 2'-H), 7.75 (1H, d, *J* 1.6, 3-H), 7.64 (1H, dd, *J* 8.2 and 1.6, 5-H), 7.34 (2H, app.t, *J* 8.9, 5'-H and 4'-H), 4.12 (2H, d, *J* 8.3, CH$_2$), 2.87 (1H, t, *J* 8.3, SH); δ$_C$ (75 MHz, DMSO-d6): 167.9 (C=O), 163.1 (C3'), 144.4 (C4), 142.4 (C1'), 138.5 (C2), 131.6 (C5'), 128.9 (C6' and C6), 128.8 (C5), 128.3 (C1), 127.7 (C3), 115.8 (C4'), 111.5 (C2'), 26.3 (CH$_2$); ν$_{max}$/ cm^{-1} (solid): 3415, 1681, 1490, 1295; HPLC: T$_r$= 2.93 (81% rel. area); *m/z* (ES): (Found: [M-H]$^-$, 261.0389 C$_{14}$H$_{11}$FO$_2$S requires [M-H], 261.0391).

Synthesis of 5-(4-fluorophenyl)-1,3-dihydo-2-benzofuranone (7.45)
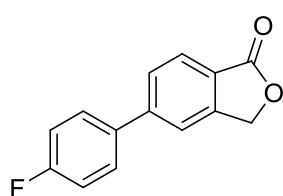
Preparation was *via* general method A using 5-bromophthalide (**7.5**) (0.50 g, 2.35 mmol) and 4-fluorophenyl boronic acid (0.36 g, 2.59 mmol) to afford the title compound (**7.45**) as yellow plates which was used without further purification (0.21 g, 0.94 mmol, 40%) m.p.: 172.4-173.8 °C; R_f: 0.32 (4:1 Petrol−EtOAc); δ$_H$ (300 MHz, CDCl$_3$): 7.98 (1H, d, *J* 8.2, 3-H), 7.70 (1H, d, *J* 8.2, 4-H), 7.63 (1H, s, 6-H), 7.59 (2H, dd, *J* 8.7 and 1.2, 2'-

H and 6'-H), 7.19 (2H, t, J 8.7, 3'-H and 5'-H), 5.38 (2H, s, CH$_2$); δ$_C$ (75 MHz, CDCl$_3$):170.8 (C=O), 165.3 (C4'), 147.4 (C1),146.5 (C5), 139.8 (C1'), 131.3 (C60, 129.3 (C2' and C6'), 128.5 (C3), 126.2 (C4), 124.9 (C2), 120.7 (C3' and C5'), 69.6 (CH$_2$); v$_{max}$/ cm^{-1} (solid): 3064, 2977, 1746, 1438, 1295; HPLC: T$_r$= 2.73 (98% rel. area); m/z (ES): (Found: MH$^+$, 229.0706. C$_{14}$H$_9$FO$_2$ requires MH, 229.0659).
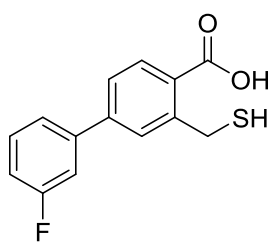
Synthesis of 4-(4-fluorophenyl)-2-iodomethyl-benzoic acid (7.54)

Preparation was via general method C using 5-(4-fluorophenyl)-1,3 dihydro-2-benzofuranone (**7.45**) (0.15 g, 0.66 mmol) to afford the title compound (**7.54**) as an off-white solid which was used without further purification (0.19 g, 0.52 mmol, 79%) m.p.: 177.4-178.5 °C; R_f: 0.21 (CHCl$_3$); δ$_H$ (300 MHz, DMSO-d6): 7.95 (1H, d, J 8.3, 6-H), 7.88 (1h, d, J 1.8, 3-H), 7.80 (2H, dd, J 8.8 and 5.4, 6'-H and 2'-H), 7.62 (1H, dd, J 8.1 and 1.8, 5-H), 7.35 (2H, app. t, J 8.9, 5'-H and 3'-H), 5.09 (2H, s, CH$_2$); v$_{max}$/ cm^{-1} (solid): 3068, 2639, 1678, 1235, 1168.

Synthesis of 4-(4-fluorophenyl)-2-(sulfonylmethyl) benzoic acid (7.32)
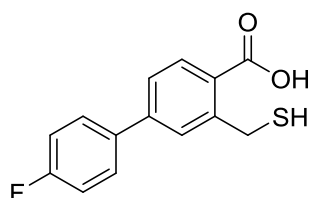
Preparation was via general method D using 4-(4-fluorophenyl)-2-(iodomethyl) benzoic acid (**7.54**) (0.30 g, 0.84 mmol) to afford the title compound (**7.32**) as pale yellow microcrystals. (92 mg, 0.35 mmol, 42%) m.p.: 156.4-157.8 °C; R_f: 0.14 (19:1 DCM−MeOH); δ$_H$ (300 MHz, DMSO-d6): 7.94 (1H, d, J 8.1, 6-H), 7.79 (2H, dd, J 8.9 and 5.6, 6'-H and 2'-H), 7.75 (1H, d, J 1.8, 3-H), 7.63 (1H, dd, J 8.1 and 1.8, 5-H), 7.34 (2H, app. t, J 8.9, 5'-H and 3'-H), 4.13 (1H, d, J 8.4, CH$_2$), 2.85 (1H, t, J 8.4, SH); δ$_C$ (75 MHz, DMSO-d6): 167.9 (C=O), 160.0 (C4'), 144.4 (C4), 142.5 (C1), 135.2 (C1'), 131.6 (C6), 128.9 (C6', C2' and C5), 127.7 (C1), 124.9 (C3), 115.8 (C5' and C3'); v$_{max}$/ cm^{-1} (solid): 2980, 1680, 1558, 1294, 1219; HPLC: T$_r$= 2.25 (90% rel. area); m/z (ES): (Found: [M-H]$^-$, 261.0390. C$_{14}$H$_{11}$FO$_2$S requires $[M-H]$, 261.0391).

Synthesis of 4-(2,3-dichlorophenyl)-2-iodomethyl-benzoic acid (7.55)
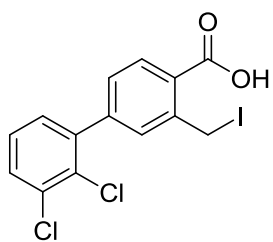
Preparation was *via* general method C using 5-(2,3-dichlorophenyl-1,3 dihydro-2-benzofuranone (**7.18**) (0.30 g, 1.08 mmol) to afford the title compound (**7.55**) as an pale brown solid which was used without further purification (0.44 g, 1.07 mmol, 99%) m.p.: 154.3-155.7 °C; R_f: 0.26 (CHCl$_3$); δ$_H$ (300 MHz, DMSO-d6): 7.92 (1H, d, *J* 8.1 6-H), 7.70 (1H, dd, *J* 7.7 and 2.1 5-H), 7.59 (1H, d, *J* 1.9 3-H), 7.45 (2H, d, *J* 7.8, 6'-H and 4'-H), 7.38 (1H, td, *J* 7.8 and 2.2 5'-H), 5.02 (2H, s, CH$_2$); v_{max}/ cm^{-1} (solid): 3363, 2973, 2653, 1771, 1378, 1268.

Synthesis of 4-(2,3-dichlorophenyl)-2-(sulfonylmethyl) benzoic acid (7.33)
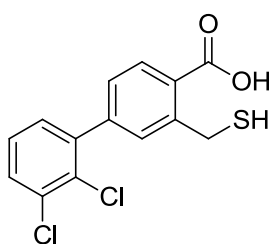
Preparation was *via* general method D using 4-(2,3-dichlorophenyl)-2-(iodomethyl) benzoic acid (**7.55**) (0.15 g, 0.57 mmol) to afford the title compound (**7.33**) as pale yellow microcrystals. (98 mg, 0.31 mmol, 55%). m.p.: 154.1-155.7 °C; R_f: 0.38 (19:1 DCM−MeOH) δ$_H$ (300 MHz, DMSO-d6): 7.94 (1H, d, *J* 8.0, 6-H), 7.71 (1H, dd, *J* 8.0 and 1.4, 5-H), 7.52 (1H, d, *J* 1.4, 3-H), 7.47(1h, d, *J* 7.7, 4'-H), 7.47-7.70 (2H, m, 6'-H and 5'-H), 4.10 (2H, d, *J* 7.5, CH2), 2.84 (1H, t, *J* 7.5, SH); δ$_C$ (75 MHz, DMSO-d6): 167.8 (C=O), 143.5 (C1'), 142.0 (C4), 141.5 (C2), 139.1 (C3'), 132.4 (C5'), 131.3 (C6), 130.9 (C5), 130.7 (C6'), 129.2 (C2'), 128.8 (C1), 128.4 (C4'), 127.6 (C3), 26.1 (CH$_2$); v_{max}/ cm^{-1} (solid): 2750, 1680, 1247, 1020, 759; HPLC: T$_r$= 2.57 (100% rel. area); *m/z* (ES): (Found: [M-H]⁻, 310.9707. C$_{14}$H$_{10}$Cl$_2$O$_2$S requires *[M-H]*, 310.9706)

Preparation of 5-[3,5-bis(trifluoromethyl)phenyl]-1,3-dihydro-2-benzofuran-1-one (7.46)
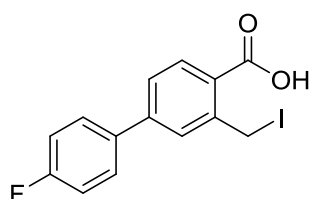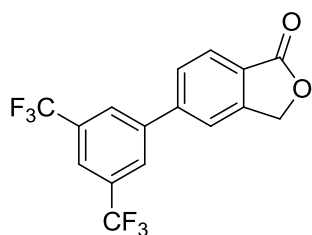
Preparation was *via* general method A using 5-bromophthalide (**7.5**) (0.50 g, 2.35 mmol) and 3,5-bis-(trifluoromethyl)phenyl boronic acid (0.49 g, 2.59 mmol) to yield the title compound (**7.46**) as a yellow solid (0.39 g, 1.13 mmol, 48%); m.p.: 167-171 °C; R_f: 0.51 (4:1 Petrol–EtOAc); δ$_H$ (300 MHz, DMSO-d6): 8.46 (2H, s, 6`-H and 2`-

H), 8.22 (2H, s, 6-H and 4`H), 8.12 (1H, d, $J$ 8.1, 3-H), 7.98 (1H, d, $J$ 8.1, 4-H), 5.50 (2H, s, CH$_2$); $\delta_C$ (75 MHz, DMSO-d6): 170.3 (C=O), 147.7 (C1), 144.2 (C1`), 141.9 (C5), 132.8 (C6`), 132.5 (C2`), 132.3 (C5`), 128.6 (C3`), 127.7 (C4), 126.8 (C6), 126.2 (C2), 124.2 (C3), 122.3 (CF$_3$ × 2), 121.1 (C4'), 69.5 (CH$_2$); v_{max}/ cm^{-1} (solid): 3071, 2922 1758, 1681; HPLC: T$_r$= 2.78 (100% rel. area); m/z (ES) (Found: MNa$^+$, 369.0312. C$_{16}$H$_8$F$_6$O$_2$ requires MNa, 369.0321).

Preparation of 4-[3,5-bis(trifluoromethyl)phenyl]-2-(iodomethyl)benzoic acid (7.56)

Preparation was *via* general method C using 5-[3,5-bis(trifluoromethyl)phenyl]-1,3-dihydro-2-benzofuranone (**7.46**) (0.30 g, 0.86 mmol) to yield the title compound (**7.56**) as a grey solid (0.39 g, 0.82 mmol, 95%); m.p.: 156.2-157.9 °C; R_f: 0.88 (19:1 DCM−MeOH); δ_H (300 MHz, DMSO-d6): 8.43 (2H, s, 6`-H and 2`-H), 8.22-8.13 (2H, m, 3-H and 4`H), 7.99 (1H, d, J 8.2, 6-H), 7.91 (1H, d, J 8.2, 5-H), 5.09 (2H, s, CH$_2$); v_{max}/ cm^{-1} (solid): 2818, 2635, 1763, 1688.

Preparation of 4-[3,5-bis(trifluoromethyl)phenyl]-2-(sulfanylmethyl)benzoic acid (7.34)
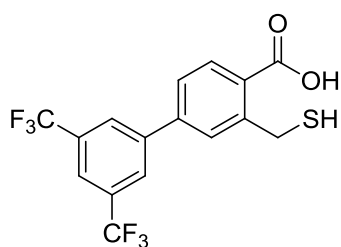
Preparation was *via* general method D using 4-[3,5-bis(trifluoromethyl)phenyl]-2-(iodomethyl) benzoic acid (**7.56**) (0.30 g, 0.81 mmol) to yield the title compound (**7.34**) as a colourless solid (0.15 g, 0.39 mmol, 55%); m.p.: 147-151 °C; R_f: 0.10 (19:1 DCM−MeOH); δ_H (300 MHz, DMSO-d6): 8.31 (2H, s, 6`-H and 2`-H), 8.07 (1H, s, 6-H), 7.88 (2H, d, J 7.8, 3-H and 4`-H), 7.78 (1H, d, $J$ 7.6, 5-H), 4.04 (2H, d, $J$ 8.5, CH$_2$), 2.82 (1H, $J$ 8.3, SH); $\delta_C$ (75 MHz, DMSO-d6): 168.0 (C=O), 144.6 (C1`), 141.0 (C2), 139.5 (C4), 132.3 (C5' and C3'), 131.6 (C6`), 129.5 (C2`), 127.6 (C6), 125.7 (C3), 125.4 (C5), 123.1 (CF$_3$ × 2), 121.6 (C4`), 26.2 (CH$_2$); v_{max}/ cm^{-1} (solid): 2965, 2651, 1763, 1690; m/z (ES) (Found: [M-H]$^+$, 379.0232. C$_{16}$H$_{10}$F$_6$O$_2$S requires $[M-H]$, 379.0306).

Preparation of 5-(naphthalen-2-yl)-1,3-dihydro-2-benzofuran-1-one (7.47)
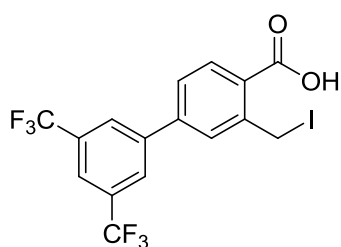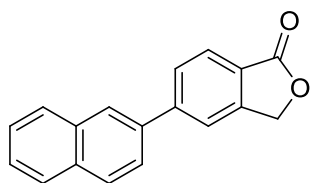

Preparation was *via* general method A using 5-bromophthalide (**7.5**) (0.50 g, 2.35 mmol) and 2-napthalene boronic acid (0.45 g, 2.59 mmol) to yield the title compound (**7.47**) as a colourless powder (0.34 g, 1.31 mmol, 56%); m.p.: 204-206 °C; R_f: 0.36 (3:1 Petrol–EtOAc); δ_H (300 MHz, CDCl$_3$): 8.10 (1H, s, 1`-H), 8.03 (1H, d, *J* 8.1, 3-H), 7.98 (1H, d, *J* 8.9, 5`-H), 7.94-7.86 (3H, m, 3'-H, 8`-H and 3-H), 7.83 (1H, s, 6-H), 7.75 (1H, dd, *J* 9.0 and 1.8, 3`-H), 7.61-7.52 (2H, m, 7`-H and 6`-H), 5.42 (2H, s, CH$_2$); δ_C (75 MHz, CDCl$_3$): 171.5 (C=O), 147.4 (C1), 137.0 (C5), 133.5 (C2`), 133.2 (C8`a and C4`a),129.0 (C4), 128.7 (C4`), 128.4 (C8`), 127.7 (C5`), 126.8 (C7`), 126.7 (C3`), 126.2 (C6` and C2), 125.2 (C6 and C3`), 120.8 (C1), 69.6 (CH$_2$); v_{max}/ cm^{-1} (solid): 3056, 2942, 2872, 1740, 1610; HPLC: T_r= 2.93 (100% rel. area); *m/z* (ES) (Found: MH$^+$, 261.0918. C$_{18}$H$_{12}$O$_2$ requires *MH*, 261.0871).

Preparation of 2-(iodomethyl)-4-(naphthalen-2-yl)benzoic acid (7.57)
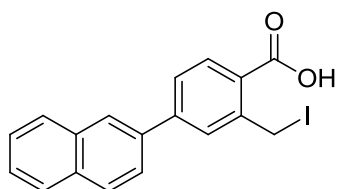
Preparation was *via* general method C using 5-(napthalen-2-yl)-1,3-dihydro-2-benzofuranone (**7.47**) (0.30 g, 1.15 mmol) to yield the title compound (**7.57**) as a brown solid (0.33 g, 0.85 mmol, 74%); m.p.: 174-178 °C; R_f: 0.50 (19:1 DCM−MeOH); δ_H (300 MHz, DMSO): 8.33 (1H, d, *J* 8.1, 6-H), 8.29–8.20 (1H, m, 8`-H), 8.14 (1H, d, *J* 7.5, 5`-H), 8.06-7.95 (2H, m, 3-H, 1`-H), 7.90 (1H, dd, *J* 8.7 and 1.9, 4`-H), 7.84 (1H, dd, *J* 8.1 and 2.0, 5-H), 7.55 (1H, d, *J* 8.7, 3`-H), 7.49–7.43 (2H, m, 7`-H and 6`H), 5.12 (2H, s, CH$_2$); v_{max}/ cm^{-1} (solid): 2957, 2646, 1679, 1600.

Preparation of 4-(naphthalen-2-yl)-2-(sulfanylmethyl)benzoic acid (7.35)
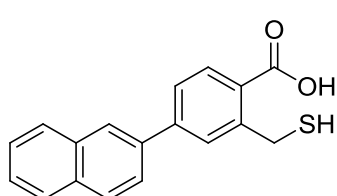
Preparation was *via* general method D using 2-(iodomethyl)-4-(naphthalene-2-yl) benzoic acid (**7.57**) (0.30 g, 0.81 mmol) to yield the title compound (**7.35**) as a colourless solid (0.13 g, 0.44 mmol, 63%); m.p.: 163-165 °C; R_f: 0.33 (19:1 DCM−MeOH); δ_H (300 MHz, DMSO): 13.30 (1H, s, OH), 8.32 (1H, s, 6-H), 8.04-8.04 (1H, m, 4`-H),

8.03-8.02 (1H, m, 7`H), 8.01-7.99 (2H, m, 3`-H and 3-H), 7.97 (1H, d, J 1.0, 8`-H), 7.80 (1H, dd, $J$ 7.8 and 2.6, 5-H), 7.57 (1H, d, $J$ 1.8, 1`-H), 7.56-7.54 (2H, m, 5`-H and 6`H), 4.15 (2H, d, J 8.6, CH$_2$), 2.88 (1H, t, J 8.4, SH); δ_C (75 MHz, DMSO): 168.0 (C=O), 144.5 (C2), 143.3 (C4), 136.0 (C2`), 133.20 (C8a`), 132.6 (C4a`), 131.7 (C6), 129.1 (C3), 128.6 (C5), 128.3 (C8`), 127.8 (C5`), 127.5 (C1), 126.6 (C7`), 125.8 (C1`), 125.2 (C6`), 124.8 (C3`), 26.5 (CH$_2$); ν_{max}/ cm^{-1} (solid): 3057, 2968, 2647, 2557, 1759, 1682, 1605; HPLC: T$_r$= 2.71 (100% rel. area); m/z (ES) (Found: [M-H]$^-$, 293.0647. C$_{18}$H$_{14}$O$_2$S requires $[M-H]$, 293.0715).

Preparation of 4-(furan-2-yl)-2-(iodomethyl)benzoic acid (7.58)
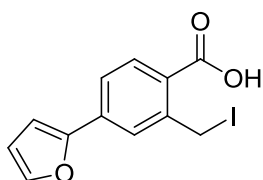
Preparation was *via* general method C using 5-(furan-2-yl)-1,3-dihydro-2-benzofuranone (**7.15**) (0.23 g, 1.15 mmol) to yield the title compound (**7.58**) as a brown solid which was used without further purification (0.37 g, 1.12 mmol, 98%); m.p.: 149.1-150.4 °C; R_f: 0.81 (19:1 DCM−MeOH); δ_H (300 MHZ, DMSO): 7.91 (1H, d, J 8.2, 6-H), 7.87 (1H, d, J 1.7, 5`-H), 7.85 (1H, d, $J$ 1.8, 3-H), 7.67 (1H, dd, $J$ 8.2 and 1.8, 5-H), 7.14 (1H, d, $J$ 3.4, 3`-H), 6.66 (1H, dd, J 3.2 and 1.7, 4`-H), 5.04 (2H, s, CH$_2$); ν_{max}/ cm^{-1} (solid): 2796, 2634, 1681, 1607.

Preparation of 4-(furan-2-yl)-2-(sulfanylmethyl)benzoic acid (7.36)
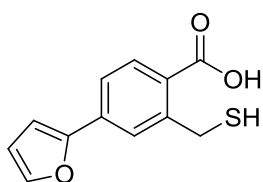
Preparation was *via* general method D using 4-(furan-2-yl)-2-(iodomethyl) benzoic acid (**7.58**) (0.30 g, 0.90 mmol) to yield the title compound (**7.36**) as a colourless solid (0.10 g, 0.43 mmol, 48%); m.p.: 154.9-157.3 °C; R_f: 0.22 (19:1 DCM−MeOH); δ_H (300 MHz, DMSO): 13.16 (1H, s, OH), 7.91 (1H, d, J 8.1, 6-H), 7.82 (1H, s, 5`-H), 7.76 (1H, s, 3-H), 7.64 (1H, d, $J$ 8.1, 5-H), 7.11 (1H, d, $J$ 5.1, 3`-H), 6.66 (1H, d, J 5.1, 6, 4`-H), 4.08 (2H, d, $J$ 8.4, CH$_2$), 2.83 (1H, t, $J$ 8.4, SH); $\delta_C$ (75 MHz, DMSO): 167.7 (C=O), 151.8 (C1`), 144.5 (C3`), 144.0 (C6), 133.4 (C2), 131.7 (C3), 127.4 (C4), 125.2 (C5), 121.6 (C1), 112.4 (C4`), 108.1 (C5`), 26.4 (CH$_2$); ν_{max}/ cm^{-1} (solid): 2941, 2809, 2634, 2540, 1762 and 1680; HPLC: T$_r$= 2.52 (91% rel. area); m/z (ES) (Found: [M-H]$^-$, 233.0277, C$_{12}$H$_{10}$O$_3$S requires $[M-H]$, 233.0351).

Synthesis of 4-(4-ethylphenyl)-2-iodomethyl-benzoic acid (7.59)
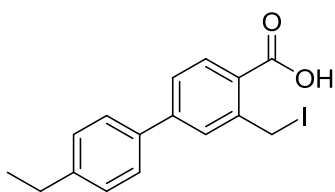
Preparation was *via* general method C using 5-(4-ethylphenyl-1,3 dihydro-2-benzofuranone (**7.16**) (0.30 g, 1.26 mmol) to afford the title compound (**7.59**) as an off-white solid which was used without further purification (0.19 g, 0.51 mmol, 41%) m.p.: 164.1-165.7 °C; R_f: 0.24 (CHCl$_3$); δ$_H$ (300 MHz, DMSO-d6): 7.85 (1H, d, *J* 8.4, 6-H), 7.78 (1H, d, *J* 1.8, 3-H), 7.57 (3H, app. d, *J* 8.3, 5-H, 2'-H and 6'-H), 7.26 (2H, d, *J* 8.3, 5'-H and 3'-H), 5.01 (2H, s, CH$_2$I), 2.58 (2H, q, *J* 7.8, CH$_2$), 1.13 (3H, t, *J* 7.6 CH$_3$); ν$_{max}$/ cm^{-1} (solid): 2970, 2631, 1669, 1572, 1252, 828; *m/z* (ES): (Found: [M-I]$^+$, 239.1068. C$_{16}$H$_{15}$IO$_2$ requires *[M-I]*, 239.1067).

Synthesis of 4-(4-ethylphenyl)-2-(sulfonylmethyl) benzoic acid (7.37)
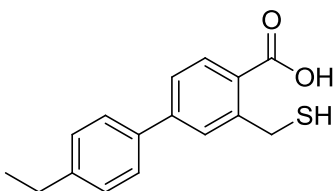
Preparation was *via* general method D using 4-(4-ethylphenyl)-2-(iodomethyl) benzoic acid (**7.59**) (0.15 g, 0.41 mmol) to afford the title compound (**7.37**) as pale yellow microcrystals. (65 mg, 0.22 mmol, 55%) m.p.: 139.2-140.5 °C; R_f: 0.20 (19:1 DCM−MeOH); δ$_H$ (300 MHz, DMSO-d6): 7.95 (1H, d, *J* 8.2, 6-H), 7.74 (1H, d, *J* 2.2, 3-H), 7.66 (2H, d, *J* 8.2, 6'-H and 2'-H), 7.62 (1H, dd, *J* 8.2 and 2.2, 5-H), .34 (2H, d, *J* 8.2, 5'-H and 3'-H), 4.12 (2H, d, *J* 8.5, CH$_2$SH), 2.85 (1H, t, *J* 8.5, SH), 2.66 (2H, q, *J* 7.4, CH2CH$_3$), 1.21 (3H, t, *J* 7.4, CH$_3$); δ$_C$ (75 MHz, DMSO-d6): 168.0 (C=O), 144.3 (C4), 144.0 (C4'), 143.5 (C2), 136.1 (C1'), 131.5 (C6), 128.5 (C5), 128.4 (C5' and C3'), 127.8 (C1), 126.7 (C6' and C2'), 124.7 (C3), 27.8 (CH$_2$CH$_3$), 26.4 (CH$_2$SH), 15.5 (CH$_3$); ν$_{max}$/ cm^{-1} (solid): 2942, 1673, 1274, 830; HPLC: T$_r$= 2.61 (91% rel. area); *m/z* (ES): (Found: [M-H]$^-$, 271.0790 C$_{16}$H$_{16}$O$_2$S requires *[M-H]*, 271.0798).

Synthesis of 5-(thiophen-3-yl)-1,3-dihydo-2-benzofuranone (7.48)
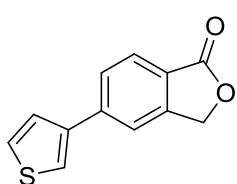
Preparation was *via* general method A using 5-bromophthalide (**7.5**) (0.50 g, 2.35 mmol) and 3-thienyl boronic acid (0.33 g, 2.59 mmol) to afford the title compound (**7.48**) as yellow plates which was used without further purification (0.23 g, 1.08 mmol, 46%) m.p.: 171.7-173.4 °C; R_f: 0.30 (4:1 Petrol−EtOAc); δ$_H$ (300 MHz, CDCl$_3$): 7.96 (1H, d, *J* 8.1, 3-H), 7.78 (1H,

dd, J 8.1 and 1.6, 4-H), 7.70 (1H, d, J 1.6, 6-H), 7.63 (1H, dd, J 2.9 and 1.5, 5'-H), 7.49 (1H, dd, J 5.0 and 2.9, 2'-H), 7.45 (1H, dd, J 5.0 and 1.5, 4'-H), 5.39 (2H, s, CH$_2$); δ$_C$ (75 MHz, CDCl$_3$):170.9 (C=O), 147.5 (C1), 141.6 (C3'), 140.8 (C5), 127.6 (C6), 127.2 (C4), 126.1 (C5' and C3), 124.2 (C2), 122.8 (C4'), 119.6 (C2'), 69.5 (CH$_2$); ν$_{max}$/ cm^{-1} (solid): 3095, 1768, 1747, 1366, 1046; HPLC: T$_r$= 2.54 (100% rel. area); m/z (ES): (Found: MNa$^+$, 239.0141. C$_{12}$H$_8$NaO$_2$S requires MNa, 239.0137).

Synthesis of 4-(thien-3-yl)-2-iodomethyl-benzoic acid (7.60)
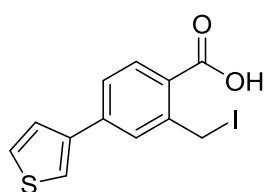
Preparation was *via* general method C using 5-(thien-3-yl)-1,3 dihydro-2-benzofuranone (**7.48**) (0.30 g, 1.39 mmol) to afford the title compound (**7.60**) as an off-white solid which was used without further purification (0.38 g, 1.10 mmol, 79%) m.p.: 168.9-170.7 °C; R_f: 0.18 (CHCl$_3$); δ$_H$ (300 MHz, DMSO-d6): 8.05 (1H, app. s, 4'-H), 7.93 (1H, d, J 1.8, 3-H), 7.90 (1H, d, J 8.1, 6-H), 7.74-7.68 (2H, m, 5-H and 2'-H), 7.64 (1H, dd, J 5.6 and 2.0, 4'-H), 5.04 (2H, s, CH$_2$); ν$_{max}$/ cm^{-1} (solid): 3405, 2505, 1665, 1600, 1248, 786; m/z (ES): (Found: [M-I+Na]$^+$, 239.0137. C$_{12}$H$_8$NaO$_2$S requires $[M-I+Na]$, 239.0137.

Synthesis of 4-(thiophen-3-yl)-2-(sulfonylmethyl) benzoic acid (7.38)
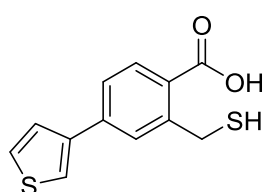
Preparation was *via* general method D using 4-(thiophen-3-yl)-2-(iodomethyl) benzoic acid (**7.60**) (0.30 g, 0.87 mmol) to afford the title compound (**7.38**) as colourless microcrystals. (0.12 g, 0.48 mmol, 54%). m.p.: 171.5-173.2 °C; R_f: 0.21 (19:1 DCM−MeOH); δ$_H$ (300 MHz, DMSO-d6): 8.04 (1H, dd, J 5.0 and 2.9, 5'-H), 7.90 (1H, d, J 8.2, 6-H), 7.82 (1H, d, J 1.4, 3-H), 7.72-7.68 (2H, m, 5-H and 2'-H), 7.64 (1H, dd, J 7.9 and 2.9, 4'-H), 4.10 (2H, d, J 8.4, CH$_2$), 2.84 (1H, t, J 8.4, SH); δ$_C$ (75 MHz, DMSO-d6): 167.9 (C=O), 144.4 (C1'), 140.1 (C2), 138.5 (C4), 131.6 (C6), 128.1 (C3), 127.4 (C4'), 127.1 (C1), 126.1 (C5), 124.3 (C3'), 122.7 (C5'), 26.4 (CH$_2$); ν$_{max}$/ cm^{-1} (solid): 1675, 1607, 1281, 772; HPLC: T$_r$= 2.74 (100% rel. area); m/z (ES): (Found: [M-H]$^-$, 248.9522. C$_{12}$H$_{10}$O$_2$S$_2$ requires $[M-H]$, 249.0049).

Synthesis of 4-(3-ethoxyphenyl)-2-iodomethyl-benzoic acid (7.61)
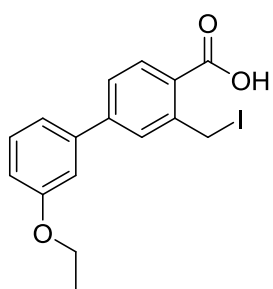
Preparation was *via* general method C using 5-(3-ethoxyphenyl)-1,3 dihydro-2-benzofuranone (**7.16**) (0.30 g, 1.18 mmol) to afford the title compound (**7.61**) as an off-white solid which was used without further purification (86 mg, 0.23 mmol, 19%) m.p.: 145.8-146.4 °C; R_f: 0.15 (CHCl$_3$); δ_H (300 MHz, DMSO-d6): 8.18 (1H, d, *J* 8.3, 6-H), 7.68 (1H, d, *J* 1.8, 3-H), 7.59 (1H, dd, *J* 8.3 and 1.8, 5-H), 7.39 (1H, t, *J* 8.1, 5'-H), 7.23 (1H, dd, *J* 8.1 and 1.9, 4'-H), 7.17 (1H, t, *J* 1.8, 2'-H), 6.96 (1H, dd, *J* 8.1 and 1.9, 6'-H), 5.08 (2H, s, CH$_2$I), 4.25 (2H, q, CH$_2$), 1.37 (3H, t, CH$_3$); v_{max}/ cm^{-1} (solid): 2980, 1676, 1597, 1305, 1262.

Synthesis of 4-(3-ethoxyphenyl)-2-(sulfonylmethyl) benzoic acid (7.39)
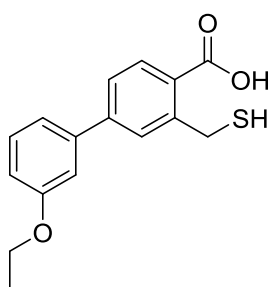
Preparation was *via* general method D using 4-(3-ethoxyphenyl)-2-(iodomethyl) benzoic acid (**7.61**) (0.30 g, 0.79 mmol) to afford the title compound (**7.39**) as colourless microcrystals. (84 mg, 0.29 mmol, 37%). m.p.: 128.0-129.8 °C; R_f: 0.21 (19:1 DCM−MeOH); (Found: C, 66.8; H, 5.60; C$_{16}$H$_{16}$O$_3$S requires C, 66.6; H, 5.59%); δ_H (300 MHz, DMSO-d6): 7.93 (1H, d, *J* 8.1, 6-H), 7.77 (1H, d, *J* 1.6, 3-H), 7.65 (1H, dd, *J* 8.1 and 1.6, 5-H), 7.40 (1H, app. t, *J* 7.9, 5'-H), 7.29 (1H, d, *J* 7.9, 6'-H), 7.26 (1H, d, *J* 1.4, 2'-H), 6.98 (1H, dd, *J* 7.9 and 1.4, 4'-H), 4.20-4.03 (4H, m, CH$_2$CH$_3$ and CH$_2$SH), 2.86 (1H, t, *J* 8.3, SH), 1.36 (3H, t, *J* 7.0, CH$_3$); δ_C (75 MHz, DMSO-d6): 168.0 (C=O), 159.1 (C3'), 144.3 (C1'), 143.4 (C2), 140.2 (C4), 131.5 (C5'), 130.1 (C6), 128.9 (C5), 127.8 (C1), 125.0 (C3), 119.0 (C6'), 114.2 (C4'), 112.9 (C2'), 63.1 (CH$_2$CH$_3$), 26.4 (CH$_2$S), 14.6 (CH$_3$); v_{max}/ cm^{-1} (solid): 3045, 1650, 1541, 1301, 952; HPLC: T$_r$= 3.11 (100% rel. area); *m/z* (ES): (Found: [M-H]$^-$, 287.0675. C$_{16}$H$_{16}$O$_3$S requires *[M-H]*, 287.0747).

## Synthesis of 5-(2-trifluoromethylphenyl)-1,3-dihydo-2-benzofuranone (7.49)
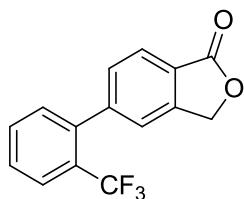
Preparation was *via* general method A using 5-bromophthalide (**7.5**) (0.50 g, 2.30 mmol) and 3-nitrophenyl boronic acid (0.49 g, 2.60 mmol) to afford the title compound (**7.49**) as an off-white solid which was used without further purification (0.45 g, 1.61 mmol, 70%); m.p.: 87-89 °C; R_f: 0.41 (4:1 Petrol–EtOAc); $\delta_H$ (300 MHz, CDCl$_3$): 7.87 (1H, d, *J* 7.9, 3-H), 7.71 (1H, dd, *J* 7.4 and 0.9, 4-H), 7.65-7.51 (2H, m, 5`-H and 4`-H), 7.42 (1H, d, *J* 7.6, 6`-H), 7.38 (1H, d, *J* 0.9, 6-H), 7.29 (1H, d, *J* 7.6, 3`-H), 5.30 (2H, s, CH$_2$); δ_C (75 MHz, CDCl$_3$): 170.7 (C=O), 146.2 (C5), 145.9 (C1`), 139.6 (C1), 131.6 (C4`), 131.5 (C5`), 130.3 (C6), 128.4 (C6`), 128.0 (C2`), 126.4 (C4), 125.2 (C3), 125.0 (C2), 125.0 (CF$_3$), 122.7 (C3`), 69.5 (CH$_2$); v_{max}/ cm^{-1} (solid): 2967, 1758, 1619; HPLC: T$_r$= 2.85 (100% rel. area); *m/z* (ES) (Found: MH$^+$, 279.0617. C$_{15}$H$_9$F$_3$O$_2$ requires *MH*, 279.0555).

## Synthesis of 4-(2-trifluoromethylphenyl)-2-iodomethyl-benzoic acid (7.62)
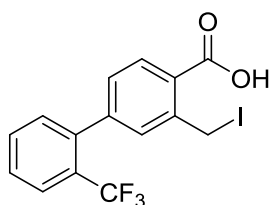
Preparation was *via* general method C using 5-(2-trifluoromethylphenyl)-1,3 dihydro-2-benzofuranone (**7.49**) (0.30 g, 1.08 mmol) to afford the title compound (**7.62**) as an off-white solid which was used without further purification (0.32 g, 0.78 mmol, 72%) m.p.: 149.5-151.0 °C; R_f: 0.27 (CHCl$_3$); δ_H (300 MHz, DMSO-d6): 7.86 (1H, d, *J* 8.0, 6-H), 7.81 (1H, d, *J* 7.3, 3'-H), 7.70 (1H, app. t, *J* 7.3, 5'-H), 7.61 (1H, app. t, *J* 7.3, 4'-H), 7.44 (1H, d, *J* 1.7, 3-H), 7.37 (1H, d, *J* 7.3, 6'-H), 7.27 (1H, dd, *J* 8.0 and 1.7, 5-H), 4.83 (2H, s, CH$_2$); v_{max}/ cm^{-1} (solid): 2855, 1690, 1678, 1254, 1085.

Synthesis of 4-(2-trifluoromethylphenyl)-2-(sulfonylmethyl) benzoic acid (7.40)
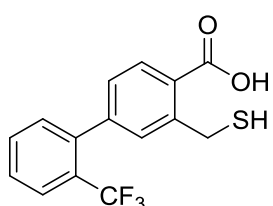
Preparation was *via* general method D using 4-(2-trifluoromethyl)-2-(iodomethyl) benzoic acid (**7.62**) (0.25 g, 0.61 mmol) to afford the title compound (**7.40**) as pale yellow microcrystals. (79 mg, 0.25 mmol, 42%). m.p.: 114.4-115.9 °C; R_f: 0.20 (19:1 DCM−MeOH); δ_H (300MHz, DMSO-d6): 7.91 (1H, d, *J* 8.0, 6-H), 7.86 (1H, d, *J* 7.4, 3'-H), 7.76 (1H, app. t, *J* 7.4, 5'-

H), 7.66 (1H, app. t, J 7.4, 4'-H), 7.45 (1H, app. d, J 7.4, 6'-H), 7.41 (1H, d, J 1.8, 3-H), 7.30 (1H, dd, J 8.0 and 1.8, 5-H), 4.09 (2H, d, J 8.5, CH$_2$), 2.80 (1H, t, J 8.5, SH); δ_C (75 MHz, DMSO-d6): 169.0 (C=O), 143.1 (C1'), 142.9 (C4), 139.4 (C2), 132.4 (C4' and C2'), 131.8 (C5'), 130.9 (C6' and C1), 130.3 (C3'), 128.5 (C6 and C5), 128.6 (CF$_3$), 127.3 (C3), 126.1 (C6'), 26.1 (CH$_2$); v_{max}/ cm^{-1} (solid): 3066, 1677, 1413, 1167, 1093; HPLC: T$_r$= 3.11 (100% rel. area); m/z (ES): (Found: [M-H]$^-$, 311.0207. C$_{15}$H$_{11}$F$_3$O$_2$S requires *[M-H]*, 311.0210).

Preparation of 4-bromo-2-(iodomethyl) benzoic acid (7.63)
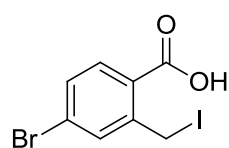
Preparation was *via* general method C using 5-bromophthalide (**7.5**) (0.30 g, 1.40 mmol) to yield the title compound (**7.63**) as a yellow solid (0.26 g, 0.76 mmol, 55%); m.p.: 154-157 °C; R_f: 0.79 (19:1 DCM−MeOH); δ_H (300 MHz, DMSO-d6): 7.81 (1H, d, J 2.0, 6-H), 7.71 (1H, d, J 8.4, 3-H), 7.58 (1H, dd, J 8.4 and 2.0, 5-H), 4.97 (2H, s, CH$_2$); v_{max}/ cm^{-1} (solid): 2797, 2632, 1675 and 1584.

## Preparation of 4-bromo-2-(sulfanylmethyl)benzoic acid (7.41)
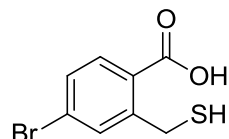
Preparation was *via* general method D using 4-bromo-2-(iodomethyl) benzoic acid (**7.63**) (0.23 g, 0.67 mmol) to yield the title compound (**7.41**) as a colourless solid (62 mg, 0.25, mmol, 37%); m.p.: 134-137 °C; R_f: 0.14 (5% MeOH–DCM); δ_H (300 MHz, DMSO-d6): 7.78 (1H, d, J 8.3, 6-H), 7.70 (1H, d, J 2.0, 3-H), 7.58 (1H, dd, J 8.3 and 2.0, 5-H), 4.02 (2H, d, J 8.5, CH$_2$), 2.90 (1H, t, J 8.5, SH); δ_C (75 MHz, DMSO-d6): 167.5 (C=O), 146.0 (C2), 133.1 (C3), 132.7 (C6), 129.9 (C5), 128.3 (C1), 125.6 (C4), 25.7 (CH$_2$); v_{max}/ cm^{-1} (solid): 2956, 2809, 2646, 2525, 1673 and 1585; HPLC: T$_r$= 2.12 (100% rel. area); m/z (ES) (Found: MH$^+$, 246.9250. C$_8$H$_7$BrO$_2$S requires 246.9350).

Synthesis of 5-phenyl-1,3-dihydro-2-benzothiophen-1-one (7.64)
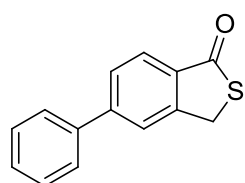
4-(phenyl)-2-(sulfanylmethyl) benzoic acid (**7.21**) (50 mg, 0.20 mmol) was dissolved in TFA (5 mL). The reaction was heated to reflux for 1 h. The reaction mixture was allowed to cool to room temperature before being concentrated *in vacuo* to afford the title compound (**7.64**) as off-white microcrystals. (45 mg, 0.20 mmol, 99%). m.p.: 114.3-115.7 °C; R_f: 0.48 (4:1

Petrol−EtOAc); δ_H (300 MHz, DMSO-d6): 7.95 (1H, s, 6-H), 7.78 (1H, d, J 7.4, 4-H), 7.75-7.30 (3H, m, 3-H, 6'-H and 2'-H), 7.46 (2H, app. t, J 7.3, 5'-H and 3'-H), 7.41 (1H, t, J 7.3, 4'-H), 4.67 (2H, s, CH$_2$); δ_C (75 MHz, DMSO-d6): 189.7 (C=O), 148.7 (C5), 145.3 (C1'), 138.6 (C1), 133.8 (C2), 129.2 (C6' and C2'), 128.7 (C4), 127.3 (C5' and C3'), 126.8 (C3), 125.1 (C4'), 123.4 (C6), 34.5 (CH$_2$); v_{max}/ cm^{-1} (solid): 3481, 1657, 1138, 870; HPLC: T_r= 2.57 (100% rel. area); m/z (ES): (Found: MH$^+$, 227.0518. C$_{14}$H$_{10}$OS requires MH, 227.0525).

Synthesis of 3H-benzo[b]thiophene-2-one (7.66)
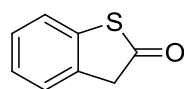
To a stirred solution of thianapthene-2-boronic acid (**7.65**) (0.25 g, 1.40 mmol) in ethanol (1 mL) was added dropwise hydrogen peroxide solution (0.46 mL, 1.74 mmol). The mixture was stirred at room temperature for 24 h. The solution was diluted with water (5 mL). The aqueous mixture was extracted with chloroform (3 × 5 mL). The combined organics were dried and concentrated *in vacuo*. The crude product was purified by flash column chromatography eluting with 19:1 Petrol−EtOAc to afford the title compound (**7.66**) as pale pink needles. (0.20 g, 1.36 mmol, 97%) R_f: 0.35 (19:1 Petrol–EtOAc); (Found: C, 64.1; H, 4.05; S, 21.2; C$_8$H$_6$OS requires C, 63.9; H, 4.03; S, 21.4%); δ_H (300 MHz, CDCl$_3$): 7.36-7.19 (4H, m, 5-H and 2-H); δ_C (75 MHz, CDCl$_3$): 203.1 (C=O), 137.1 (C6), 132.2 (C1), 128.4 (C3), 126.2 (C5), 124.8 (C4), 123.1, (C2), 47.3 (CH$_2$); v_{max}/ cm^{-1} (solid): 3410, 2926, 1714, 1466, 1387; HPLC: T_r= 2.64 (100% rel. area); m/z (EI): (Found: M$^+$, 150.0114 C$_8$H$_6$OS requires M, 150.0139).

Synthesis of 2-(2 sulfanylphenyl)acetic acid (7.67)
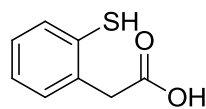
3H-benzo[b]thiophene-2-one (**7.66**) (0.10 g, 0.67 mmol) was dissolved in methanol (10 mL) and to this was added 2M NaOH $_{(aq)}$ (5 mL). The reaction was refluxed under nitrogen for 16 h. The reaction mixture was concentrated *in vacuo*. The residue was re-suspended in water (5 mL) and the mixture acidified to ~pH1 with 2M HCl $_{(aq)}$. The resulting precipitate was isolated to afford the title compound (**7.67**) as pale brown plates. (0.10 g, 0.62 mmol, 93%) m.p: 98.9-100.9 °C R_f: 0.38 (19:1 DCM−MeOH); δ_H (300 MHz, DMSO-d6): 7.42 (1H, t, J 7.7 4-H), 7.20

(3H , m, 6-H, 5-H and 3-H), 3.82 (2H, s, CH2), 3.50 (1H, s, SH); δ_C (75 MHz, DMSO-d6): 176.8 (C=O), 133.3 (C2), 132.3 (C4), 131.0 (C5), 130.8 (C1), 128.3 (C3), 127.0 (C6), 39.9 (CH$_2$); v_{max}/ cm^{-1} (solid): 3063-2637, 1696, 1467, 1232; HPLC: T$_r$= 2.48 (88% rel. area); *m/z* (ES): (Found: [M-H]$^-$, 167.0187 C$_8$H$_8$O$_2$S requires *[M-H]*, 167.0172).

Synthesis of 2-((([(2-carboxy-5-phenylphenyl)methyl]disulfanyl)methyl)-4-phenylbenzoic acid[176] (7.27)
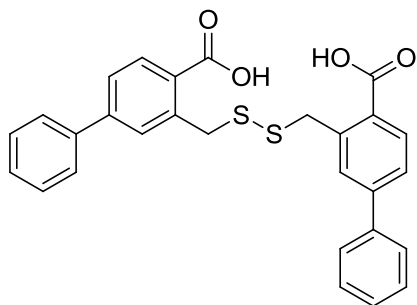
A solution of 4-(phenyl)-2-(sulfanylmethyl) benzoic acid (**7.21**) (50 mg, 0.20 mmol) in EtOH (2 mL) was cooled to 0 °C. To the mixture was added iodine (0.5 M in ethanol) until the colour of the solution turned red. The reaction was stirred at 0 °C for 1 h. Sodium thiosulfate (0.5M in H$_2$O) was added to the mixture until the colour changed from red to white. The EtOH was removed *in vacuo* and the resulting precipitate was isolated by filtration. The product was washed (H$_2$O) and dried to afford the title compound (**7.27**) as colourless microcrystals. (46 mg, 0.09 mmol, 95%). m.p.: 234.2-235.9 °C; *R*$_f$: 0.15 (19:1 DCM−MeOH); δ_H (300 MHZ, DMSO-d6): 8.00 (2H, d, *J* 8.2, 6-H), 7.70 (2H, dd, *J* 8.2 and 1.2, 5-H), 7.69 (4H, d, *J* 7.5, 6'-H and 2'-H), 7.56 (2H, d, *J* 1.2, 3-H), 7.52-7.39 (6H, m, 5'-H, 4'-H and 3'-H), 4.25 (4H, s, CH$_2$); δ_C (75 MHz, DMSO-d6): 167.9 (C=O), 143.1 (C4), 139.9 (C1'), 138.5 (C2), 131.9 (C6), 129.8 (C5), 129.1 (C5' and C3'), 128.3 (C4'), 128.2 (C1), 126.8 (C6' and C2'), 125.6 (C3), 40.6 (CH$_2$); v_{max}/ cm^{-1} (solid): 2931, 1681, 1450, 1166; HPLC: T$_r$= 2.70 (100% rel. area); *m/z* (ES): (Found: [M-H]$^-$, 485.0884. C$_{28}$H$_{22}$O$_4$S$_2$ requires *[M-H]*, 485.0887).

10.6.4 Synthesis of cephalosporin / inhibitor co-drug

Synthesis of (6R,7R)-3-((([(2-carboxy-5-phenylphenyl)methyl]sulfanyl)methyl)-8-oxo-7-[2-(thiophen-2-yl)acetamido]-5-thia-1-azabicyclo[4.2.0]oct-2-ene-2-carboxylic acid (7.72)
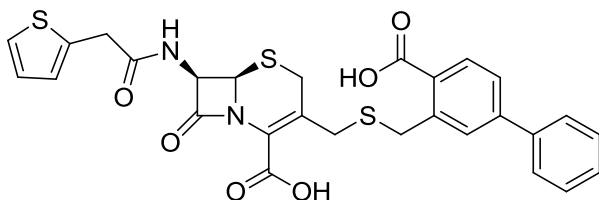
To a solution containing cephalotin sodium salt (**7.71**) (0.20 g, 0.48 mmol) in HPLC grade H_2O (10 mL) was added 4-(phenyl)-2-(sulfanylmethyl) benzoic acid (**7.21**) (0.12 g, 0.48 mmol). The pH was adjusted to pH 7.0 by the drop wise addition of 1M NaOH$_{(aq)}$ and the solution was stirred at 65 °C for 6 h. The pH was kept at pH 7.0 throughout the reaction. After cooling to room temperature the reaction was extracted with EtOAc (2 × 10 mL). The aqueous was then acidified to ~pH 4 using 1M HCl$_{(aq)}$ and extracted with EtOAC (3 × 10 mL). The organics were concentrated *in vacuo* and the residue re-dissolved in NaHCO$_3$ (10 mL). The aqueous was slowly acidified to pH 2 by the addition of 1M HCl$_{(aq)}$. The acidified aqueous was extracted with EtOAc (3 × 10 mL). The organics were dried (MgSO$_4$) and concentrated to give a crude brown powder. The crude product was purified by mass directed HPLC to afford the title compound (**7.72**) as off-white plates. (72 mg, 0.12 mmol, 26%). m.p.: 114.7-115.3 °C; R_f: 0.02 (19:1 DCM−MeOH); δ$_H$ (500 MHz, MeOD-d4): 7.92 (1H, d, *J* 8.1, 3-HAr), 7.62 (2H, d, *J* 7.4, 6'-HAr and 2'-HAr), 7.61 (1H, d, *J* 2.0, 6-HAr), 7.53 (1H, dd, *J* 8.1 and 2.0, 5-HAr), 7.38 (2H, app.t, *J* 7.4, 5'-HAr and 3'-HAr), 7.30 (1H, t, *J* 7.4, 4'-H), 7.16 (1H, dd, *J* 4.8 and 1.6, Thio-5-H), 6.86-6.82 (2H, m, Thio-4-H and Thio-3-H), 5.32 (1H, d, *J* 4.7, 7a-H), 4.68 (1H, d, *J* 4.7, 6a-H), 4.21 (1H, d, *J* 12.9, 3c-H), 3.98 (1H, d, *J* 12.9, 3c-H), 3.83 (1H, d, *J* 13.8, 3a-H), 3.68 (2H, dd, *J* 3.5 and 0.6, 7c-H), 3.50 (1H, d *J* 13.8, 3a-H), 3.41 (1H, d, *J* 17.7, 4-H), 3.28 (1H, d, *J* 17.7, 4-H); δ$_C$ (125 MHz, MeOD-d4): 172.7 (HNC=O), 170.1 (COOH), 165.7 (Lactam C=O, Lactam COOH), 145.8 (C4-Ar), 140.3 (C1'-Ar), 137.1 (C2-Ar), 133.3 (C2), 133.2 (C2-Thio), 133.1 (C3-Ar), 130.5 (C5-Ar), 130.0 (C5'-Ar and C3'-Ar), 129.3 (C4'-Ar), 129.1 (C1-Ar), 128.1 (C4-Thio and C3-Thio), 127.7 C6'-Ar and C2'-Ar), 126.7 (C3), 126.4 (C6-Ar), 125.7 (C5-Thio), 60.6 (C7a), 59.4 (C6a), 31.7 (C7c), 36.0

(C3c), 35.9 (C3a), 28.8 (C4); $v_{max}/$ cm^{-1} (solid): 3330, 1750, 1686, 1019; HPLC: T_r= 2.30 (100% rel. area); *m/z* (ES): (Found: MH$^+$, 581.0870. C$_{28}$H$_{24}$N$_2$O$_6$S$_3$ requires MH, 581.0869). [α]$_D$ = + 92.5 ° (c 0.10, MeOH).

10.7 General computational procedures

All computational dockings were conducted on a LINUX computer using the CentOS 6.6 operating system. Parallel docking was conducted on the Milin6 cluster housed at the University of Leeds.

10.7.1 PBD pre-processing

All PDBs were sourced from the RCSB PDB databank. Standard PDBs used for molecular docking are NDM-1: 3Q6X, VIM-2: 1KO3, IMP-1: 1JJT, SPM-1: 2FHX. Each PDB complex was first opened in Maestro Version 9.9.013 where they were visually inspected. If more than one protein molecule was present in the asymmetric unit, one was removed to generate a monomer and all water molecules were removed from the structure.

10.7.2 SPROUT *de novo* design

All SPROUT *de novo* design was conducted using SPROUT v6.4.10. Each pre-processed PDB complex was opened in the SPROUT Cangaroo module where the cavity was defined and receptor was defined as a 10Å cut around the cavity. The sites were explored by Hippo and Hydrophobic sites created. Fragments selected in the Elefant module came from the built in Fragment library. Fragments were joined in Spider using spacer templates restricted to carbon, nitrogen, oxygen, 5 and 6 membered aromatic rings. Suggested molecules were scored using Alligator. The top 1000 molecules were then analysed using the complexity analysis tool. The top 500 were then re scored and visually inspected. From this the top 10-20 were selected for re-docking with AutoDock.

10.7.3 AutoDock dockings

All AutoDock dockings were conducted using AutoDock 4.2 and the results were visualised with AutoDockTools v1.5.6. The receptor used for docking was the receptor previously defined in SPROUT. 10 or 20 dockings were conducted per ligand. The results were scored and ranked based upon the most populated cluster from the graphical output.

References

1.   Butler, M. S.; Buss, A. D., Natural products - The future scaffolds for novel antibiotics? *Biochem. Pharmacol.* **2006,** *71* (7), 919-929.

2.   O'Neill, A. J.; Chopra, I., Preclinical evaluation of novel antibacterial agents by microbiological and molecular techniques. *Expert Opin. Investig. Drugs* **2004,** *13* (8), 1045-1063.

3.   Waksman, S. A., What Is an Antibiotic or an Antibiotic Substance? *Mycologia* **1947,** *39* (5), 565-569.

4.   Bacterial cell shapes: https://www.studyblue.com/notes/note/n/bio-exam-1/deck/5524410. 15/01/2013.

5.   Glauert, A. M., Fine structure of bacteria. *Br. Med. Bull.* **1962,** *18* (3), 245-250.

6.   Nicklin, J.; Graeme-Cook, K.; Paget, T.; Killington, R., *Instant Notes in Microbiology.* BIOS Scientific Publishers Ltd: Oxford, 1999.

7.   Bartholomew, J. W.; Mittwer, T., The Gram stain. *Bacteriol. Rev.* **1952,** *16* (1), 1-29.

8.   Hughes, D.; Andersson, D., *Antibiotic development and resistance.* Taylor & Francis: London, 2001.

9.   Hamad, B., The antibiotics market. *Nat. Rev. Drug Discov.* **2010,** *9* (9), 675-675.

10.   Lloyd, N. C.; Morgan, H. W.; Nicholson, B. K.; Ronimus, R. S., The Composition of Ehrlich's Salvarsan: Resolution of a Century-Old Debate. *Angew. Chem. Int. Ed.* **2005,** *44* (6), 941-944.

11.   Fleming, A., On the Antibacterial Action of Cultures of a Penicillium, with Special Reference to Their Use in the Isolation of B. influenzae. *Rev. Infect. Dis.* **1980,** *2* (1), 129-139.

12.   Otten, H., Domagk and the development of the sulphonamides. *J. Antimicrob. Chemother.* **1986,** *17* (6), 689-690.

13.   Silver, L. L., Challenges of Antibacterial Discovery. *Clin. Microbiol. Rev.* **2011,** *24* (1), 71-109.

14.   Spellberg, B.; Powers, J. H.; Brass, E. P.; Miller, L. G.; Edwards, J. E., Trends in antimicrobial drug development: Implications for the future. *Clin. Infect. Dis.* **2004,** *38* (9), 1279-1286.

15.   Livermore, D. M.; British Soc, A., Discovery research: the scientific challenge of finding new antibiotics. *J. Antimicrob. Chemother.* **2011,** *66* (9), 1941-1944.

16.   Molstad, S.; Lundborg, C. S.; Karlsson, A. K.; Cars, O., Antibiotic prescription rates vary markedly between 13 European countries. *Scand. J. Infect. Dis.* **2002,** *34* (5), 366-371.

17.   Livermore, D. M., Has the era of untreatable infections arrived? *J. Antimicrob. Chemother.* **2009,** *64 Suppl 1*, i29-36.

18.   Chain, E.; Florey, H. W.; Gardner, A. D.; Heatley, N. G.; Jennings, M. A.; Orr-Ewing, J.; Sanders, A. G., Penicillin as a chemotherapeutic agent. *The Lancet* **1940,** *236* (6104), 226-228.

19.   Sheehan, J. C.; Henery-Logan, K. R., The total synthesis of penicillin v. *J. Am. Chem. Soc.* **1957,** *79* (5), 1262-1263.

20.   Partick, G. L., An Introduction to Medicinal Chemistry. 5 ed.; Oxford University Press: 2013.

21.   McFee, R. B., Nosocomial or Hospital-acquired Infections: An Overview. *Dm Disease-a-Month* **2009,** *55* (7), 422-438.

22.   Projan, S. J.; Bradford, P. A., Late stage antibacterial drugs in the clinical pipeline. *Curr. Opin. Microbiol.* **2007,** *10* (5), 441-446.

23.   Barker, K. F., Antibiotic resistance: a current perspective. *Br. J. Clin. Pharmacol.* **1999,** *48* (2), 109-124.

24.   Tenover, F. C., Mechanisms of antimicrobial resistance in bacteria. *Am. J. Med.* **2006,** *119* (6), S3-S10.

25.   Coates, A.; Hu, Y. M.; Bax, R.; Page, C., The future challenges facing the development of new antimicrobial drugs. *Nat. Rev. Drug Discov.* **2002,** *1* (11), 895-910.

26.   Mills, S. D., When will the genomics investment pay off for antibacterial discovery? *Biochem. Pharmacol.* **2006,** *71* (7), 1096-1102.

27.   Drawz, S. M.; Bonomo, R. A., Three Decades of beta-Lactamase Inhibitors. *Clin. Microbiol. Rev.* **2010,** *23* (1), 160-201.

28.   Ambler, R. P., The Structure of beta-Lactamases. *Philos. Trans. R. Soc. B* **1980,** *289* (1036), 321-331.

29.   Hall, B. G.; Barlow, M., Evolution of the serine beta-lactamases: past, present and future. *Drug Resistance Updates* **2004,** *7* (2), 111-123.

30.   Fenollar-Ferrer, C.; Frau, J.; Donoso, J.; Munoz, F., Evolution of class C beta-lactamases: factors influencing their hydrolysis and recognition mechanisms. *Theor. Chem. Acc.* **2008,** *121* (3-4), 209-218.

31.   Sun, T.; Nukaga, M.; Mayama, K.; Braswell, E. H.; Knox, J. R., Comparison of beta-lactamases of classes A and D: 1.5-angstrom crystallographic structure of the class D OXA-1 oxacillinase. *Protein Sci.* **2003,** *12* (1), 82-91.

32. Arulanantham, H.; Kershaw, N. J.; Hewitson, K. S.; Hughes, C. E.; Thirkettle, J. E.; Schofield, C. J., ORF17 from the clavulanic acid biosynthesis gene cluster catalyzes the ATP-dependent formation of N-glycyl-clavaminic acid. *J. Biol. Chem.* **2006,** *281* (1), 279-287.

33. Yang, Y.; Rasmussen, B. A.; Shlaes, D. M., Class A β-lactamases—enzyme-inhibitor interactions and resistance. *Pharmacol. Ther.* **1999,** *83* (2), 141-151.

34. Totir, M. A.; Helfand, M. S.; Carey, M. P.; Sheri, A.; Buynak, J. D.; Bonomo, R. A.; Carey, P. R., Sulbactam Forms Only Minimal Amounts of Irreversible Acrylate-Enzyme with SHV-1 β-Lactamase. *Biochemistry* **2007,** *46* (31), 8980-8987.

35. Li, H.; Estabrook, M.; Jacoby, G. A.; Nichols, W. W.; Testa, R. T.; Bush, K., In vitro susceptibility of characterized beta-lactamase-producing strains tested with avibactam combinations. *Antimicrob. Agents Chemother.* **2015,** *59* (3), 1789-93.

36. Cornaglia, G.; Giamarellou, H.; Rossolini, G. M., Metallo-beta-lactamases: a last frontier for beta-lactams? *Lancet Infect. Dis.* **2011,** *11* (5), 381-393.

37. Bebrone, C.; Delbrueck, H.; Kupper, M. B.; Schloemer, P.; Willmann, C.; Frere, J.-M.; Fischer, R.; Galleni, M.; Hoffmann, K. M. V., The Structure of the Dizinc Subclass B2 Metallo-beta-Lactamase CphA Reveals that the Second Inhibitory Zinc Ion Binds in the Histidine Site. *Antimicrob. Agents Chemother.* **2009,** *53* (10), 4464-4471.

38. Zhang, H.; Hao, Q., Crystal structure of NDM-1 reveals a common beta-lactam hydrolysis mechanism. *FASEB J.* **2011,** *25* (8), 2574-2582.

39. Cornaglia, G.; Akova, M.; Amicosante, G.; Canton, R.; Cauda, R.; Docquier, J.-D.; Edelstein, M.; Frere, J.-M.; Fuzi, M.; Galleni, M.; Giamarellou, H.; Gniadkowski, M.; Koncan, R.; Libisch, B.; Luzzaro, F.; Miriagou, V.; Navarro, F.; Nordmann, P.; Pagani, L.; Peixe, L.; Poirel, L.; Souli, M.; Tacconelli, E.; Vatopoulos, A.; Rossolini, G. M.; Grp, E., Metallo-beta-lactamases as emerging resistance determinants in Gram-negative pathogens: open issues. *Int. J. Antimicrob. Agents* **2007,** *29* (4), 380-388.

40. Sun, Q.; Law, A.; Crowder, M. W.; Geysen, H. M., Homo-cysteinyl peptide inhibitors of the L1 metallo-beta-lactamase, and SAR as determined by combinatorial library synthesis. *Bioorg. Med. Chem. Lett.* **2006,** *16* (19), 5169-5175.

41. Weide, T.; Saldanha, S. A.; Minond, D.; Spicer, T. P.; Fotsing, J. R.; Spaargaren, M.; Frere, J.-M.; Bebrone, C.; Sharpless, K. B.; Hodder, P. S.; Fokin, V. V., NH-1,2,3-Triazole Inhibitors of the VIM-2 Metallo-beta-Lactamase. *ACS Med. Chem. Lett.* **2010,** *1* (4), 150-154.

42.   Bounaga, S.; Galleni, M.; Laws, A. P.; Page, M. I., Cysteinyl peptide inhibitors of Bacillus cereus zinc beta-lactamase. *Biorg. Med. Chem.* **2001,** *9* (2), 503-510.

43.   Lienard, B. M. R.; Horsfall, L. E.; Galleni, M.; Frere, J.-M.; Schofield, C. J., Inhibitors of the FEZ-1 metallo-beta-lactamase. *Bioorg. Med. Chem. Lett.* **2007,** *17* (4), 964-968.

44.   King, D. T.; Worrall, L. J.; Gruninger, R.; Strynadka, N. C. J., New Delhi Metallo-beta-Lactamase: Structural Insights into beta-Lactam Recognition and Inhibition. *J. Am. Chem. Soc.* **2012,** *134* (28), 11362-11365.

45.   Liang, Z.; Li, L.; Wang, Y.; Chen, L.; Kong, X.; Hong, Y.; Lan, L.; Zheng, M.; Guang-Yang, C.; Liu, H.; Shen, X.; Luo, C.; Li, K. K.; Chen, K.; Jiang, H., Molecular basis of NDM-1, a new antibiotic resistance determinant. *Plos One* **2011,** *6* (8), e23606.

46.   Tripathi, R.; Nair, N. N., Mechanism of Meropenem Hydrolysis by New Delhi Metallo β-Lactamase. *ACS Catalysis* **2015,** *5* (4), 2577-2586.

47.   Walsh, T. R.; Toleman, M. A.; Poirel, L.; Nordmann, P., Metallo-beta-lactamases: the quiet before the storm? *Clin. Microbiol. Rev.* **2005,** *18* (2), 306-325.

48.   Yong, D.; Toleman, M. A.; Giske, C. G.; Cho, H. S.; Sundman, K.; Lee, K.; Walsh, T. R., Characterization of a New Metallo-beta-Lactamase Gene, bla(NDM-1), and a Novel Erythromycin Esterase Gene Carried on a Unique Genetic Structure in Klebsiella pneumoniae Sequence Type 14 from India. *Antimicrob. Agents Chemother.* **2009,** *53* (12), 5046-5054.

49.   Kumarasamy, K. K.; Toleman, M. A.; Walsh, T. R.; Bagaria, J.; Butt, F.; Balakrishnan, R.; Chaudhary, U.; Doumith, M.; Giske, C. G.; Irfan, S.; Krishnan, P.; Kumar, A. V.; Maharjan, S.; Mushtaq, S.; Noorie, T.; Paterson, D. L.; Pearson, A.; Perry, C.; Pike, R.; Rao, B.; Ray, U.; Sarma, J. B.; Sharma, M.; Sheridan, E.; Thirunarayan, M. A.; Turton, J.; Upadhyay, S.; Warner, M.; Welfare, W.; Livermore, D. M.; Woodford, N., Emergence of a new antibiotic resistance mechanism in India, Pakistan, and the UK: a molecular, biological, and epidemiological study. *Lancet Infect. Dis.* **2010,** *10* (9), 597-602.

50.   Lascols, C.; Hackel, M.; Marshall, S. H.; Hujer, A. M.; Bouchillon, S.; Badal, R.; Hoban, D.; Bonomo, R. A., Increasing prevalence and dissemination of NDM-1 metallo-beta-lactamase in India: data from the SMART study (2009). *J. Antimicrob. Chemother.* **2011,** *66* (9), 1992-1997.

51.   Nordmann, P.; Poirel, L.; Toleman, M. A.; Walsh, T. R., Does broad-spectrum beta-lactam resistance due to NDM-1 herald the end of the antibiotic era for treatment of infections caused by Gram-negative bacteria? *J. Antimicrob. Chemother.* **2011,** *66* (4), 689-692.

52.   Kus, J. V.; Tadros, M.; Simor, A.; Low, D. E.; McGeer, A. J.; Willey, B. M.; Larocque, C.; Pike, K.; Edwards, I.-A.; Dedier, H.; Melano, R.; Boyd, D.

A.; Mulvey, M. R.; Louie, L.; Okeahialam, C.; Bayley, M.; Whitehead, C.; Richardson, D.; Carr, L.; Jinnah, F.; Poutanen, S. M., New Delhi metallo-beta-lactamase-1: local acquisition in Ontario, Canada, and challenges in detection. *Can. Med. Assoc. J.* **2011,** *183* (11), 1257-1261.

53.   Karthikeyan, K.; Thirunarayan, M. A.; Krishnan, P., Coexistence of bla(OXA-23) with bla(NDM-1) and armA in clinical isolates of Acinetobacter baumannii from India. *J. Antimicrob. Chemother.* **2010,** *65* (10), 2253-2254.

54.   Guo, Y.; Wang, J.; Niu, G.; Shui, W.; Sun, Y.; Zhou, H.; Zhang, Y.; Yang, C.; Lou, Z.; Rao, Z., A structural view of the antibiotic degradation enzyme NDM-1 from a superbug. *Protein & cell* **2011,** *2* (5), 384-94.

55.   Moellering, R. C., Jr., NDM-1-A Cause for Worldwide Concern. *New Engl. J. Med.* **2010,** *363* (25), 2377-2379.

56.   King, D.; Strynadka, N., Crystal structure of New Delhi metallo-beta-lactamase reveals molecular basis for antibiotic resistance. *Protein Sci.* **2011,** *20* (9), 1484-1491.

57.   Kim, Y.; Tesar, C.; Mire, J.; Jedrzejczak, R.; Binkowski, A.; Babnigg, G.; Sacchettini, J.; Joachimiak, A., Structure of Apo- and Monometalated Forms of NDM-1-A Highly Potent Carbapenem-Hydrolyzing Metallo-beta-Lactamase. *Plos One* **2011,** *6* (9), e24621.

58.   Wang, J.-F.; Chou, K.-C., Insights from modeling the 3D structure of New Delhi metallo-beta-lactamse and its binding interactions with antibiotic drugs. *Plos One* **2011,** *6* (4), e18414.

59.   Yang, H.; Aitha, M.; Hetrick, A. M.; Richmond, T. K.; Tierney, D. L.; Crowder, M. W., Mechanistic and Spectroscopic Studies of Metallo-beta-lactamase NDM-1. *Biochemistry* **2012,** *51* (18), 3839-3847.

60.   Green, V. L.; Verma, A.; Owens, R. J.; Phillips, S. E. V.; Carr, S. B., Structure of New Delhi metallo-[beta]-lactamase 1 (NDM-1). *Acta Crystallographica Section F* **2011,** *67* (10), 1160-1164.

61.   Concha, N. O.; Janson, C. A.; Rowling, P.; Pearson, S.; Cheever, C. A.; Clarke, B. P.; Lewis, C.; Galleni, M.; Frere, J. M.; Payne, D. J.; Bateson, J. H.; Abdel-Meguid, S. S., Crystal structure of the IMP-1 metallo beta-lactamase from Pseudomonas aeruginosa and its complex with a mercaptocarboxylate inhibitor: Binding determinants of a potent, broad-spectrum inhibitor. *Biochemistry* **2000,** *39* (15), 4288-4298.

62.   Murphy, T. A.; Catto, L. E.; Halford, S. E.; Hadfield, A. T.; Minor, W.; Walsh, T. R.; Spencer, J., Crystal structure of Pseudomonas aeruginosa SPM-1 provides insights into variable zinc affinity of metallo-beta-lactamases. *J. Mol. Biol.* **2006,** *357* (3), 890-903.

63.   Yamaguchi, Y.; Jin, W.; Matsunaga, K.; Ikemizu, S.; Yamagata, Y.; Wachino, J. I.; Shibata, N.; Arakawa, Y.; Kurosaki, H., Crystallographic investigation of the inhibition mode of a VIM-2 metallo-beta-lactamase from

Pseudomonas aeruginosa by a mercaptocarboxylate inhibitor. *J. Med. Chem.* **2007,** *50* (26), 6647-6653.

64.   Garcia-Saez, I.; Docquier, J. D.; Rossolini, G. M.; Dideberg, O., The three-dimensional structure of VIM-2, a Zn-beta-lactamase from Pseudomonas aeruginosa in its reduced and oxidised form. *J. Mol. Biol.* **2008,** *375* (3), 604-611.

65.   Brem, J.; Struwe, W. B.; Rydzik, A. M.; Tarhonskaya, H.; Pfeffer, I.; Flashman, E.; van Berkel, S. S.; Spencer, J.; Claridge, T. D. W.; McDonough, M. A.; Benesch, J. L. P.; Schofield, C. J., Studying the active-site loop movement of the Sao Paolo metallo-beta-lactamase-1. *Chemical Science* **2015,** *6* (2), 956-963.

66.   King, A. M.; Reid-Yu, S. A.; Wang, W.; King, D. T.; De Pascale, G.; Strynadka, N. C.; Walsh, T. R.; Coombes, B. K.; Wright, G. D., Aspergillomarasmine A overcomes metallo-beta-lactamase antibiotic resistance. *Nature* **2014,** *510* (7506), 503-506.

67.   Wachino, J.-i.; Yamaguchi, Y.; Mori, S.; Kurosaki, H.; Arakawa, Y.; Shibayama, K., Structural Insights into the Subclass B3 Metallo-beta-Lactamase SMB-1 and the Mode of Inhibition by the Common Metallo-beta-Lactamase Inhibitor Mercaptoacetate. *Antimicrob. Agents Chemother.* **2013,** *57* (1), 101-109.

68.   Klingler, F.-M.; Wichelhaus, T. A.; Frank, D.; Cuesta-Bernal, J.; El-Delik, J.; Müller, H. F.; Sjuts, H.; Göttig, S.; Koenigs, A.; Pos, K. M.; Pogoryelov, D.; Proschak, E., Approved Drugs Containing Thiols as Inhibitors of Metallo-β-lactamases: Strategy To Combat Multidrug-Resistant Bacteria. *J. Med. Chem.* **2015,** *58* (8), 3626-3630.

69.   Zervosen, A.; Lu, W. P.; Chen, Z. L.; White, R. E.; Demuth, T. P.; Frere, J. M., Interactions between penicillin-binding proteins (PBPs) and two novel classes of PBP inhibitors, arylalkylidene rhodanines and arylalkylidene iminothiazolidin-4-ones. *Antimicrob. Agents Chemother.* **2004,** *48* (3), 961-969.

70.   Baell, J.; Walters, M. A., Chemical con artists foil drug discovery. *Nature* **2014,** *513* (7519), 481-483.

71.   Spicer, T., Probe Reports from the NIH Molecular Libraries Program (US National Centre for Biotechnology Information). **2010**.

72.   Brem, J.; van Berkel, S. S.; Aik, W.; Rydzik, A. M.; Avison, M. B.; Pettinati, I.; Umland, K.-D.; Kawamura, A.; Spencer, J.; Claridge, T. D. W.; McDonough, M. A.; Schofield, C. J., Rhodanine hydrolysis leads to potent thioenolate mediated metallo-beta-lactamase inhibition. *Nature Chemistry* **2014,** *6* (12), 1084-1090.

73.   Yang, K.-W.; Feng, L.; Yang, S.-K.; Aitha, M.; LaCuran, A. E.; Oelschlaeger, P.; Crowder, M. W., New beta-phospholactam as a carbapenem transition state analog: Synthesis of a broad-spectrum inhibitor

of metallo-beta-lactamases. *Bioorg. Med. Chem. Lett.* **2013,** *23* (21), 5855-5859.

74.   Winkler, M. L.; Rodkey, E. A.; Taracila, M. A.; Drawz, S. M.; Bethel, C. R.; Papp-Wallace, K. M.; Smith, K. M.; Xu, Y.; Dwulit-Smith, J. R.; Romagnoli, C.; Caselli, E.; Prati, F.; van den Akker, F.; Bonomo, R. A., Design and Exploration of Novel Boronic Acid Inhibitors Reveals Important Interactions with a Clavulanic Acid-Resistant Sulfhydryl-Variable (SHV) beta-Lactamase. *J. Med. Chem.* **2013,** *56* (3), 1084-1097.

75.   Hernandez, V.; Crepin, T.; Palencia, A.; Cusack, S.; Akama, T.; Baker, S. J.; Bu, W.; Feng, L.; Freund, Y. R.; Liu, L.; Meewan, M.; Mohan, M.; Mao, W.; Rock, F. L.; Sexton, H.; Sheoran, A.; Zhang, Y.; Zhang, Y.-K.; Zhou, Y.; Nieman, J. A.; Anugula, M. R.; Keramane, E. M.; Savariraj, K.; Reddy, D. S.; Sharma, R.; Subedi, R.; Singh, R.; O'Leary, A.; Simon, N. L.; De Marsh, P. L.; Mushtaq, S.; Warner, M.; Livermore, D. M.; Alley, M. R. K.; Plattner, J. J., Discovery of a Novel Class of Boron-Based Antibacterials with Activity against Gram-Negative Bacteria. *Antimicrob. Agents Chemother.* **2013,** *57* (3), 1394-1403.

76.   Worthington, R. J.; Bunders, C. A.; Reed, C. S.; Melander, C., Small Molecule Suppression of Carbapenem Resistance in NDM-1 Producing Klebsiella pneumoniae. *ACS Med. Chem. Lett.* **2012,** *3* (5), 357-361.

77.   Rogers, S. A.; Huigens, R. W., III; Cavanagh, J.; Melander, C., Synergistic Effects between Conventional Antibiotics and 2-Aminoimidazole-Derived Antibiofilm Agents. *Antimicrob. Agents Chemother.* **2010,** *54* (5), 2112-2118.

78.   Minond, D.; Saldanha, S. A.; Subramaniam, P.; Spaargaren, M.; Spicer, T.; Fotsing, J. R.; Weide, T.; Fokin, V. V.; Sharpless, K. B.; Galleni, M.; Bebrone, C.; Lassaux, P.; Hodder, P., Inhibitors of VIM-2 by screening pharmacologically active and click-chemistry compound libraries. *Biorg. Med. Chem.* **2009,** *17* (14), 5027-5037.

79.   Toney, J. H.; Hammond, G. G.; Fitzgerald, P. M. D.; Sharma, N.; Balkovec, J. M.; Rouen, G. P.; Olson, S. H.; Hammond, M. L.; Greenlee, M. L.; Gao, Y. D., Succinic acids as potent inhibitors of plasmid-borne IMP-1 metallo-beta-lactamase. *J. Biol. Chem.* **2001,** *276* (34), 31913-31918.

80.   Stone, N. R. H.; Woodford, N.; Livermore, D. M.; Howard, J.; Pike, R.; Mushtaq, S.; Perry, C.; Hopkins, S., Breakthrough bacteraemia due to tigecycline-resistant Escherichia coli with New Delhi metallo-beta-lactamase (NDM)-1 successfully treated with colistin in a patient with calciphylaxis. *J. Antimicrob. Chemother.* **2011,** *66* (11), 2677-2678.

81.   Albur, M.; Noel, A.; Bowker, K.; MacGowan, A., Bactericidal Activity of Multiple Combinations of Tigecycline and Colistin against NDM-1-Producing Enterobacteriaceae. *Antimicrob. Agents Chemother.* **2012,** *56* (6), 3441-3443.

82. van Berkel, S. S.; Brem, J.; Rydzik, A. M.; Salimraj, R.; Cain, R.; Verma, A.; Owens, R. J.; Fishwick, C. W. G.; Spencer, J.; Schofield, C. J., Assay Platform for Clinically Relevant Metallo-beta-lactamases. *J. Med. Chem.* **2013,** *56* (17), 6945-6953.

83. Methods for dilution antimicrobial susceptibility testing for bacteria that grow aerobically, approved standard - eighth edition. CLSI. **2009**.

84. Cain, R.; Narramore, S.; McPhillie, M. J.; Simmons, K. J.; Fishwick, C. W. G., Applications of structure-based design to antibacterial drug discovery. *Bioorg. Chem.* **2014,** *55* (1), 69-76.

85. Moro, S.; Bacilieri, M.; Deflorian, F., Combining ligand-based and structure-based drug design in the virtual screening arena. *Expert Opin. Drug Discovery* **2007,** *2* (1), 37-49.

86. Klebe, G., Virtual ligand screening: strategies, perspectives and limitations. *Drug Discov. Today* **2006,** *11* (13-14), 580-594.

87. Doman, T. N.; McGovern, S. L.; Witherbee, B. J.; Kasten, T. P.; Kurumbail, R.; Stallings, W. C.; Connolly, D. T.; Shoichet, B. K., Molecular docking and high-throughput screening for novel inhibitors of protein tyrosine phosphatase-1B. *J. Med. Chem.* **2002,** *45* (11), 2213-2221.

88. Morris, G. M.; Huey, R.; Lindstrom, W.; Sanner, M. F.; Belew, R. K.; Goodsell, D. S.; Olson, A. J., AutoDock4 and AutoDockTools4: Automated Docking with Selective Receptor Flexibility. *J. Comput. Chem.* **2009,** *30* (16), 2785-2791.

89. Zsoldos, Z.; Reid, D.; Simon, A.; Sadjad, B. S.; Johnson, A. P., eHITS: An innovative approach to the docking and scoring function problems. *Curr. Protein Peptide Sci.* **2006,** *7* (5), 421-435.

90. Irwin, J. J.; Shoichet, B. K., ZINC - A free database of commercially available compounds for virtual screening. *J. Chem. Inf. Model.* **2005,** *45* (1), 177-182.

91. ChemNavigator iResearch Library. www.chemnavigator.com, 28/2/2014.

92. ChemBridge Molecular Screening Library. www.Hit2Lead.com, 28/2/2014.

93. Friesner, R. A.; Banks, J. L.; Murphy, R. B.; Halgren, T. A.; Klicic, J. J.; Mainz, D. T.; Repasky, M. P.; Knoll, E. H.; Shelley, M.; Perry, J. K.; Shaw, D. E.; Francis, P.; Shenkin, P. S., Glide: A new approach for rapid, accurate docking and scoring. 1. Method and assessment of docking accuracy. *J. Med. Chem.* **2004,** *47* (7), 1739-1749.

94. Jones, G.; Willett, P.; Glen, R. C.; Leach, A. R.; Taylor, R., Development and validation of a genetic algorithm for flexible docking. *J. Mol. Biol.* **1997,** *267* (3), 727-748.

95.   Chen, Y.; Shoichet, B. K., Molecular docking and ligand specificity in fragment-based inhibitor discovery. *Nat. Chem. Biol.* **2009,** *5* (5), 358-364.

96.   McGann, M., FRED Pose Prediction and Virtual Screening Accuracy. *J. Chem. Inf. Model.* **2011,** *51* (3), 578-596.

97.   Warr, W., Scientific workflow systems: Pipeline Pilot and KNIME. *J. Comput.-Aided Mol. Des.* **2012,** *26* (7), 801-804.

98.   Lipinski, C. A.; Lombardo, F.; Dominy, B. W.; Feeney, P. J., Experimental and computational approaches to estimate solubility and permeability in drug discovery and development settings. *Adv. Drug Del. Rev.* **2001,** *46* (1-3), 3-26.

99.   Peakdale Molecular Screening Library. www.peakdale.co.uk, 28/2/2014.

100.   Goodsell, D. S.; Morris, G. M.; Olson, A. J., Automated docking of flexible ligands: Applications of AutoDock. *J. Mol. Recognit.* **1996,** *9* (1), 1-5.

101.   (a) Prasad, J. C.; Goldstone, J. V.; Camacho, C. J.; Vajda, S.; Stegeman, J. J., Ensemble modeling of substrate binding to cytochromes p450: Analysis of catalytic differences between CYP1A orthologs. *Biochemistry* **2007,** *46* (10), 2640-2654; (b) Kallblad, P.; Mancera, R. L.; Todorov, N. P., Assessment of multiple binding modes in ligand-protein docking. *J. Med. Chem.* **2004,** *47* (13), 3334-3337.

102.   Zsoldos, Z.; Reid, D.; Simon, A.; Sadjad, S. B.; Johnson, A. P., eHiTS: A new fast, exhaustive flexible ligand docking system. *J. Mol. Graphics Model.* **2007,** *26* (1), 198-212.

103.   Mok, N. Y.; Chadwick, J.; Kellett, K. A. B.; Hooper, N. M.; Johnson, A. P.; Fishwick, C. W. G., Discovery of novel non-peptide inhibitors of BACE-1 using virtual high-throughput screening. *Bioorg. Med. Chem. Lett.* **2009,** *19* (23), 6770-6774.

104.   Simmons, K. J.; Gotfryd, K.; Billesbolle, C. B.; Loland, C. J.; Gether, U.; Fishwick, C. W. G.; Johnson, A. P., A virtual high-throughput screening approach to the discovery of novel inhibitors of the bacterial leucine transporter, LeuT. *Mol. Membr. Biol.* **2013,** *30* (2), 184-194.

105.   Axerio-Cilies, P.; See, R. H.; Zoraghi, R.; Worral, L.; Lian, T.; Stoynov, N.; Jiang, J.; Kaur, S.; Jackson, L.; Gong, H.; Swayze, R.; Arnandoron, E.; Kumar, N. S.; Moreau, A.; Hsing, M.; Strynadka, N. C.; McMaster, W. R.; Finay, B. B.; Foster, L. J.; Young, R. N.; Reiner, N. E.; Cherkasov, A., Cheminformatics-Driven Discovery of Selective, Nanomolar Inhibitors for Staphylococcal Pyruvate Kinase. *ACS Chem. Biol.* **2012,** *7* (2), 349-358.

106.   Cherkasov, A., Can 'bacterial-metabolite-likeness' model improve odds of 'in silico' antibiotic discovery? *J. Chem. Inf. Model.* **2006,** *46* (3), 1214-1222.

107.   Halgren, T. A.; Murphy, R. B.; Friesner, R. A.; Beard, H. S.; Frye, L. L.; Pollard, W. T.; Banks, J. L., Glide: A new approach for rapid, accurate docking and scoring. 2. Enrichment factors in database screening. *J. Med. Chem.* **2004,** *47* (7), 1750-1759.

108.   Jorgensen, W. L.; Ruiz-Caro, J.; Tirado-Rives, J.; Basavapathruni, A.; Anderson, K. S.; Hamilton, A. D., Computer-aided design of non-nucleoside inhibitors of HIV-1 reverse transcriptase. *Bioorg. Med. Chem. Lett.* **2006,** *16* (3), 663-667.

109.   Coleman, W. A., Mathmatical verification of a certain Monte Carlo sampling technique and applications of technique to radiation transport problems. *Nucl. Sci. Eng.* **1968,** *32* (1), 76-81.

110.   Hu, X.; Compton, J. R.; AbdulHameed, M. D. M.; Marchand, C. L.; Robertson, K. L.; Leary, D. H.; Jadhav, A.; Hershfield, J. R.; Wallqvist, A.; Friedlander, A. M.; Legler, P. M., 3-Substituted Indole Inhibitors Against Francisella tularensis FabI Identified by Structure-Based Virtual Screening. *J. Med. Chem.* **2013,** *56* (13), 5275-5287.

111.   Berman, H. M.; Westbrook, J.; Feng, Z.; Gilliland, G.; Bhat, T. N.; Weissig, H.; Shindyalov, I. N.; Bourne, P. E., The Protein Data Bank. *Nucleic Acids Res.* **2000,** *28* (1), 235-242.

112.   Ingram, R. N.; Orth, P.; Strickland, C. L.; Le, H. V.; Madison, V.; Beyer, B. M., Stabilization of the autoproteolysis of TNF-alpha converting enzyme (TACE) results in a novel crystal form suitable for structure-based drug design studies. *Protein Eng., Des.Sel.* **2006,** *19* (4), 155-161.

113.   Menchise, V.; De Simone, G.; Di Fiore, A.; Scozzafava, A.; Supuran, C. T., Carbonic anhydrase inhibitors: X-ray crystallographic studies for the binding of 5-amino-1,3,4-thiadiazole-2-sulfonamide and 5-(4-amino-3-chloro-5-fluorophenylsulfonamido)1,3,4-thiadiazole-2-sulfon amide to human isoform II. *Bioorg. Med. Chem. Lett.* **2006,** *16* (24), 6204-6208.

114.   de Jongh, T. E.; van Roon, A.-M. M.; Prudencio, M.; Ubbink, M.; Canters, G. W., Click chemistry with an active site variant of azurin. *Eur. J. Inorg. Chem.* **2006,** (19), 3861-3868.

115.   Rao, B. G.; Bandarage, U. K.; Wang, T.; Come, J. H.; Perola, E.; Wei, Y.; Tian, S.-K.; Saunders, J. O., Novel thiol-based TACE inhibitors: Rational design, synthesis, and SAR of thiol-containing aryl sulfonamides. *Bioorg. Med. Chem. Lett.* **2007,** *17* (8), 2250-2253.

116.   Gui, Z.; Green, A. R.; Kasrai, M.; Bancroft, G. M.; Stillman, M. J., Sulfur K-Edge EXAFS Studies of Cadmium-, Zinc-, Copper-, and Silver-Rabbit Liver Metallothioneins. *Inorg. Chem.* **1996,** *35* (22), 6520-6529.

117.   Sadowski, J.; Gasteiger, J.; Klebe, G., Comparison of Automatic Three-Dimensional Model Builders Using 639 X-ray Structures. *J. Chem. Inf. Comput. Sci.* **1994,** *34* (4), 1000-1008.

118.   Maybridge Screening Collection. www.maybridge.com; 28/02/2014.

119.   KeyOrganics Screening Collection. www.keyorganics.net, 31/10/2014.

120.   ACD/Percepta, v., Advanced Chemistry Development, Inc.,Toronto, ON, Canada, www.acdlabs.com, 2014.

121.   Lanevskij, K.; Japertas, P.; Didziapetris, R.; Petrauskas, A., Ionization-specific prediction of blood–brain permeability. *J. Pharm. Sci.* **2009,** *98* (1), 122-134.

122.   Shoichet, B. K., Screening in a spirit haunted world. *Drug Discov. Today* **2006,** *11* (13-14), 607-615.

123.   Hopkins, A. L., Drug discovery: predicting promiscuity. *Nature* **2009,** *462* (7270), 167-168.

124.   Robinson, B., The Fischer Indole Synthesis. *Chem. Rev.* **1963,** *63* (4), 373-401.

125.   (a) Gillet, V.; Johnson, A. P.; Mata, P.; Sike, S.; Williams, P., SPROUT - A program for structure generations. *J. Comput.-Aided Mol. Des.* **1993,** *7* (2), 127-153; (b) Gillet, V. J.; Newell, W.; Mata, P.; Myatt, G.; Sike, S.; Zsoldos, Z.; Johnson, A. P., SPROUT - Recent developments in the *de-novo* design of molecules. *J. Chem. Inf. Comput. Sci.* **1994,** *34* (1), 207-217.

126.   Carlson, H. A.; McCammon, J. A., Accommodating protein flexibility in computational drug design. *Mol. Pharmacol.* **2000,** *57* (2), 213-218.

127.   Baker, S. J.; Ding, C. Z.; Akama, T.; Zhang, Y.-K.; Hernandez, V.; Xia, Y., Therapeutic potential of boron-containing compounds. *Future Med Chem* **2009,** *1* (7), 1275-1288.

128.   Fail, P. A.; Chapin, R. E.; Price, C. J.; Heindel, J. J., General, reproductive, developmental, and endocrine toxicity of boronated compounds. *Reprod. Toxicol.* **1998,** *12* (1), 1-18.

129.   Adams, J.; Kauffman, M., Development of the Proteasome Inhibitor Velcade™ (Bortezomib). *Cancer Invest.* **2004,** *22* (2), 304-311.

130.   Field-Smith, A.; Morgan, G. J.; Davies, F. E., Bortezomib (Velcade™) in the Treatment of Multiple Myeloma. *Therapeutics and Clinical Risk Management* **2006,** *2* (3), 271-279.

131.   Baker, S. J.; Tomsho, J. W.; Benkovic, S. J., Boron-containing inhibitors of synthetases. *Chem. Soc. Rev.* **2011,** *40* (8), 4279-4285.

132.   Chen, T. S. S.; Chang, C.-J.; Floss, H. G., Biosynthesis of boromycin. *The Journal of Organic Chemistry* **1981,** *46* (13), 2661-2665.

133.   Baggio, R.; Elbaum, D.; Kanyo, Z. F.; Carroll, P. J.; Cavalli, R. C.; Ash, D. E.; Christianson, D. W., Inhibition of Mn-2(2+)-arginase by borate leads to the design of a transition state analogue inhibitor, 2(S)-amino-6-boronohexanoic acid. *J. Am. Chem. Soc.* **1997,** *119* (34), 8107-8108.

134. Snyder, H. R.; Reedy, A. J.; Lennarz, W. J., Synthesis of aromatic boronic acids - Aldehydo boronic acids and a boronic acid analog of tyrosine. *J. Am. Chem. Soc.* **1958,** *80* (4), 835-838.

135. Baker, S. J.; Zhang, Y.-K.; Akama, T.; Lau, A.; Zhou, H.; Hernandez, V.; Mao, W.; Alley, M. R. K.; Sanders, V.; Plattner, J. J., Discovery of a new boron-containing antifungal agent, 5-fluoro-1,3-dihydro-1-hydroxy-2,1-benzoxaborole (AN2690), for the potential treatment of onychomycosis. *J. Med. Chem.* **2006,** *49* (15), 4447-4450.

136. Crompton, I. E.; Cuthbert, B. K.; Lowe, G.; Waley, S. G., Beta-Lactamase Inhibitors - The inhibition of serine beta-lactamases by specific boronic acids. *Biochemical Journal* **1988,** *251* (2), 453-459.

137. Weston, G. S.; Blázquez, J.; Baquero, F.; Shoichet, B. K., Structure-Based Enhancement of Boronic Acid-Based Inhibitors of AmpC β-Lactamase. *J. Med. Chem.* **1998,** *41* (23), 4577-4586.

138. Burns, C. J.; Goswami, R.; Jackson, R. W.; Lessen, T.; Li, W.; Pevear, D.; Tiruahari, P. K.; Xu, H., Beta Lactamase inhibitors *WO 2010/130708 A1* **2010**.

139. Maestro, version 9.3, Schrödinger, LLC, New York, NY.

140. Murai, N.; Miyano, M.; Yonaga, M.; Tanaka, K., One-Pot Primary Aminomethylation of Aryl and Heteroaryl Halides with Sodium Phthalimidomethyltrifluoroborate. *Org. Lett.* **2012,** *14* (11), 2818-2821.

141. Inglis, S. R.; Strieker, M.; Rydzik, A. M.; Dessen, A.; Schofield, C. J., A boronic-acid-based probe for fluorescence polarization assays with penicillin binding proteins and beta-lactamases. *Anal. Biochem.* **2012,** *420* (1), 41-47.

142. Matteson, D. S.; Sadhu, K. M., Boronic ester homologation with 99% chiral selectivity and its use in syntheses of the insect pheromones (3S,4S)-4-methyl-3-heptanol and exo-brevicomin. *J. Am. Chem. Soc.* **1983,** *105* (7), 2077-2078.

143. Burns, C. J.; Jackson, R. W.; Goswami, R.; Xu, H., Beta-lactamase inhibitors. *WO 2009/064414 A1* **2009**.

144. Cushman, D. W.; Cheung, H. S.; Sabo, E. F.; Ondetti, M. A., Design of potent competitive inhibitors of angiotensin-converting enzyme - Carboxyalkanoyl and mercaptoalkanoyl amino-acids. *Biochemistry* **1977,** *16* (25), 5484-5491.

145. Phillips, D. R.; Teng, W.; Arfsten, A.; NannizziAlaimo, L.; White, M. M.; Longhurst, C.; Shattil, S. J.; Randolph, A.; Jakubowski, J. A.; Jennings, L. K.; Scarborough, R. M., Effect of Ca2+ on GP IIb-IIIa interactions with integrilin - Enhanced GP IIb-IIIa binding and inhibition of platelet aggregation by reductions in the concentration of ionized calcium in plasma anticoagulated with citrate. *Circulation* **1997,** *96* (5), 1488-1494.

146.   Miljanich, G. P., Ziconotide: Neuronal calcium channel blocker for treating severe chronic pain. *Curr. Med. Chem.* **2004,** *11* (23), 3029-3040.

147.   Vlieghe, P.; Lisowski, V.; Martinez, J.; Khrestchatisky, M., Synthetic therapeutic peptides: science and market. *Drug Discov. Today* **2010,** *15* (1-2), 40-56.

148.   Smith, G., Filamentous fusion phage: novel expression vectors that display cloned antigens on the virion surface. *Science* **1985,** *228* (4705), 1315-1317.

149.   Lunder, M.; Bratkovič, T.; Doljak, B.; Kreft, S.; Urleb, U.; Štrukelj, B.; Plazar, N., Comparison of bacterial and phage display peptide libraries in search of target-binding motif. *Appl. Biochem. Biotechnol.* **2005,** *127* (2), 125-131.

150.   Jaworski, J. W.; Raorane, D.; Huh, J. H.; Majumdar, A.; Lee, S.-W., Evolutionary screening of biomimetic coatings for selective detection of explosives. *Langmuir* **2008,** *24* (9), 4938-4943.

151.   Frank, R., The SPOT-synthesis technique: Synthetic peptide arrays on membrane supports—principles and applications. *J. Immunol. Methods* **2002,** *267* (1), 13-26.

152.   Beyer, M.; Nesterov, A.; Block, I.; König, K.; Felgenhauer, T.; Fernandez, S.; Leibe, K.; Torralba, G.; Hausmann, M.; Trunk, U.; Lindenstruth, V.; Bischoff, F. R.; Stadler, V.; Breitling, F., Combinatorial Synthesis of Peptide Arrays onto a Microchip. *Science* **2007,** *318* (5858), 1888.

153.   Zhang, R.-z.; Xu, X.-h.; Chen, T.-b.; Li, L.; Rao, P.-f., An Assay for Angiotensin-Converting Enzyme Using Capillary Zone Electrophoresis. *Anal. Biochem.* **2000,** *280* (2), 286-290.

154.   Brem, J.; Mcdonough, M. A.; Schofield, C. J., unpublished work.

155.   Python, version 2.7.2; Python Software Foundation: Wolfeboro Falls, NH. **2011**.

156.   Weininger, D., SMILES, a chemical language and information system. 1. Introduction to methodology and encoding rules. *J. Chem. Inf. Comput. Sci.* **1988,** *28* (1), 31-36.

157.   BABEL, version 1.4; Openeye Scientific Software, Inc.: Santa Fe, NM.

158.   Hawkins, P. C. D.; Skillman, A. G.; Warren, G. L.; Ellingson, B. A.; Stahl, M. T., Conformer Generation with OMEGA: Algorithm and Validation Using High Quality Structures from the Protein Databank and Cambridge Structural Database. *J. Chem. Inf. Model.* **2010,** *50* (4), 572-584.

159.   Merrifield, R. B., Solid Phase Peptide Synthesis. I. The Synthesis of a Tetrapeptide. *J. Am. Chem. Soc.* **1963,** *85* (14), 2149-2154.

160.	ROCS, *version 3.2.0.4: OpenEye Scientific Software, Inc.: Santa Fe, NM.*

161.	EON, *version 2.2.0.5: OpenEye Scientific Software, Inc.: Santa Fe, NM.*

162.	OMEGA, *version 2.4.1; Openeye Scientific Software, Inc.: Santa Fe, NM*

163.	Lipinski, C. A., Drug-like properties and the causes of poor solubility and poor permeability. *J. Pharmacol. Toxicol. Methods* **2000,** *44* (1), 235-249.

164.	VIDA, *version 4.3.0: OpenEye Scientific Software, Santa Fe, NM.*

165.	Jain, S. K.; Agrawal, A., De novo Drug Design : An Overview. *Indian J. Pharm. Sci.* **2004,** *66* (6), 721-728.

166.	Kutchukian, P. S.; Shakhnovich, E. I., De novo design: balancing novelty and confined chemical space. *Expert Opin. Drug Discovery* **2010,** *5* (8), 789-812.

167.	Kirkpatrick, P.; Ellis, C., Chemical space. *Nature* **2004,** *432* (7019), 823-823.

168.	Gillet, V.; Johnson, A. P.; Mata, P.; Sike, S.; Williams, P., SPROUT - A program for structure generation. *J. Comput.-Aided Mol. Des.* **1993,** *7* (2), 127-153.

169.	Boehm, H. J., The computer program LUDI a new method for the de-novo design of enzyme inhibitors. *J. Comput.-Aided Mol. Des.* **1992,** *6* (1), 61-78.

170.	Goodford, P. J., A computational procedure for determining energetically favorable binding sites on biologically important macromolecules. *J. Med. Chem.* **1985,** *28* (7), 849-857.

171.	Yuan, Y.; Pei, J.; Lai, L., LigBuilder 2: A Practical de Novo Drug Design Approach. *J. Chem. Inf. Model.* **2011,** *51* (5), 1083-1091.

172.	(a) Rachelle, J. B., Overview: Fragment-Based Drug Design. In *Library Design, Search Methods, and Applications of Fragment-Based Drug Design*, American Chemical Society: 2011; Vol. 1076, pp 1-26; (b) Schneider, G.; Fechner, U., Computer-based de novo design of drug-like molecules. *Nat Rev Drug Discov* **2005,** *4* (8), 649-663.

173.	Davies, M.; Heikkila, T.; McConkey, G. A.; Fishwick, C. W. G.; Parsons, M. R.; Johnson, A. P., Structure-Based Design, Synthesis, and Characterization of Inhibitors of Human and Plasmodium falciparum Dihydroorotate Dehydrogenases. *J. Med. Chem.* **2009,** *52* (9), 2683-2693.

174.   Agarwal, A. K.; Johnson, A. P.; Fishwick, C. W. G., Synthesis of de novo designed small-molecule inhibitors of bacterial RNA polymerase. *Tetrahedron* **2008,** *64* (43), 10049-10054.

175.   Miyaura, N.; Yamada, K.; Suzuki, A., A new stereospecific cross-coupling by the palladium-catalyzed reaction of 1-alkenylboranes with 1-alkenyl or 1-alkynyl halides. *Tetrahedron Lett.* **1979,** *20* (36), 3437-3440.

176.   Niwa, N.; Yamagishi, Y.; Murakami, H.; Suga, H., A flexizyme that selectively charges amino acids activated by a water-friendly leaving group. *Bioorg. Med. Chem. Lett.* **2009,** *19* (14), 3892-3894.

177.   DMPK Group, Shanghai ChemPartner Co., Ltd. No. 3 Building, 720, Cai Lun Rd, Pudong, Shanghai, 201203, P.R. China

178.   Ward, K. E.; Archambault, R.; Mersfelder, T. L., Severe adverse skin reactions to nonsteroidal antiinflammatory drugs: A review of the literature. *Am. J. Health. Syst. Pharm.* **2010,** *67* (3), 206-213.

179.   Teng, R.; Oliver, S.; Hayes, M. A.; Butler, K., Absorption, Distribution, Metabolism, and Excretion of Ticagrelor in Healthy Subjects. *Drug Metab. Disposition* **2010,** *38* (9), 1514-1521.

180.   Viswanatha, T.; Marrone, L.; Goodfellow, V.; Dmitrienko, G., Assays for B-Lactamase Activity and Inhibition. In *New Antibiotic Targets,* Champney, W. S., Ed. Humana Press: 2008; Vol. 142, pp 239-260.

181.   Shannon, K.; Phillips, I., Beta-lactamase detection by 3 simple methods - intralactam, nitrocefin and acidimetric. *J. Antimicrob. Chemother.* **1980,** *6* (5), 617-621.

182.   Jones, R. N.; Wilson, H. W.; Novick, W. J.; Barry, A. L.; Thornsberry, C., In vitro evaluation of CENTA, a new beta-lactamase-susceptible chromogenic cephalosporin reagent. *J. Clin. Microbiol.* **1982,** *15* (5), 954-958.

183.   Gao, W. Z.; Xing, B. G.; Tsien, R. Y.; Rao, J. H., Novel fluorogenic substrates for imaging 6-lactamase gene expression. *J. Am. Chem. Soc.* **2003,** *125* (37), 11146-11147.

184.   Yao, H.; So, M.-K.; Rao, J., A bioluminogenic substrate for in vivo imaging of beta-lactamase activity. *Angew. Chem. Int. Ed.* **2007,** *46* (37), 7031-7034.

185.   Mizukami, S.; Watanabe, S.; Akimoto, Y.; Kikuchi, K., No-Wash Protein Labeling with Designed Fluorogenic Probes and Application to Real-Time Pulse-Chase Analysis. *J. Am. Chem. Soc.* **2012,** *134* (3), 1623-1629.

186.   Spencer, J.; Walsh, T. R., A New Approach to the Inhibition of Metallo-β-lactamases. *Angew. Chem. Int. Ed.* **2006,** *45* (7), 1022-1026.

187.   Yang, J.-M.; Chen, Y.-F.; Shen, T.-W.; Kristal, B. S.; Hsu, D. F., Consensus Scoring Criteria for Improving Enrichment in Virtual Screening. *J. Chem. Inf. Model.* **2005,** *45* (4), 1134-1146.

188.   PDB ID: 4BP0; Mcdonough, M. A.; Brem, J.; Schofield, C. J., The Crystal Structure of the Closed Form or Pseudomonas Aeruginosa Spm-1.

189.   Cossar, B. C.; Fields, D. L.; Fournier, J. O.; Reynolds, D. D., Perparation of Thiols. *J. Org. Chem.* **1962,** *27* (1), 93-95.

190.   Cremlyn, R. J.; Clowes, S. M., The chemistry of sulfonyl coumarin derivatives. *J. Chem. Soc. Pak.* **1988,** *10* (1), 97-104.

191.   Varma, P. P.; Sherigara, B. S.; Mahadevan, K. M.; Hulikal, V., Efficient and Straightforward Synthesis of Tetrahydrocarbazoles and 2,3-Dimethyl Indoles Catalyzed by CAN. *Synth. Commun.* **2009,** *39* (1), 158-165.

192.   Blackhall, A.; Thomson, R. H., Aromatic keto-enols. 3. Some heterocyclic quinols. *J. Chem. Soc.* **1954,** (NOV), 3916-3919.

193.   Zielinski, T.; Dydio, P.; Jurczak, J., Synthesis, structure and the binding properties of the amide-based anion receptors derived from 1H-indole-7-amine. *Tetrahedron* **2008,** *64* (3), 568-574.

194.   Islam, A. M.; Bedair, A. H.; El-Maghraby, A. A.; Aly, F. M.; Emam, H. A., Synthesis and biological activity of coumarin sulfonamides and related compounds. *Indian J. Chem., Sect B* **1982,** *21B* (5), 487-489.

Part 4

Appendices

Appendix

Assay Conditions

A1.1 Enzymatic assays

The experiments were performed by using a NovaStar microplate reader (using path length correction) and were performed at r.t. (24-25 °C). All enzymes and substrates were dissolved in the assay buffer: 50 mM HEPES-NaOH buffer (pH 7.2) supplemented with 1 µg / mL BSA (to minimize the denaturation of the enzyme), 1 µM $ZnSO_4$ and 0.01% Triton 100.

Hydrolysis of nitrocefin, CENTA, imipenem and Fluorogenic compound, was monitored by following the variation in absorbance at 492, 405 and 300 nm or fluorescence at excitation 380 nm and emission at 460 nm, respectively. In all cases 96 well flat bottom plates: µClear half area black plate for fluorescence (675096) and UV-STAR Microplate (655801) or Micro assay Plate (655095) for absorbance from Greiner Bio-One were used.

The kinetic values reported in this study are the means from at least three independent measurements. At least six different concentrations of the substrate or inhibitor were used to determinate the kinetic parameters (K_M, k_{cat} and IC_{50}). Determination of the steady state kinetic parameters for the hydrolysis of different substrates (K_M and k_{cat}) was performed by fitting the initial velocity data to the Michaelis-Menten equation using the software package Graph Prism 5.01. The IC_{50} values were determined from the plot of activity (steady state rate) versus inhibitor concentration using the same software.

IC_{50} values (concentration required to affect 50% inhibition of enzyme activity) were determined by preincubation of the appropriate amount of enzyme with the desired compound in the assay buffer for 10 min at r.t. prior to the initiation of the assay by the addition of the substrate. The compounds for inhibition study were prepared in 1 to 100 mM DMSO stock solutions. Additional tests verified that the low concentration of DMSO (0.5%) present in the reaction mixture had no inhibition effects.
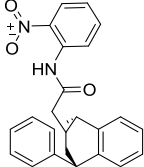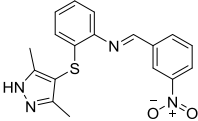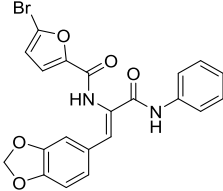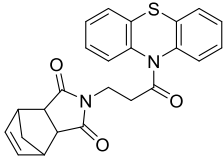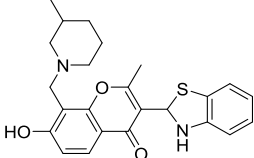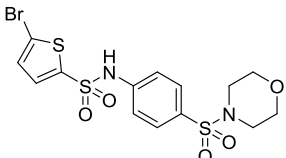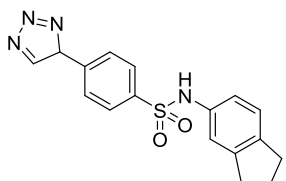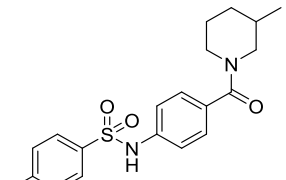
A1.2 MIC recovery determination

Minimal inhibitory concentration (MIC) values were determined by broth microdilution in cation adjusted Mueller Hinton broth (Sigma) according to Clinical Laboratory Standards Institute (CLSI) guidelines. Briefly, bacteria
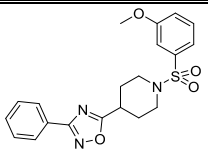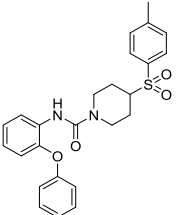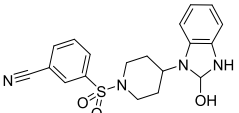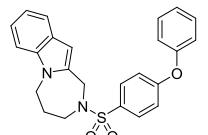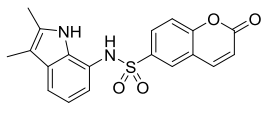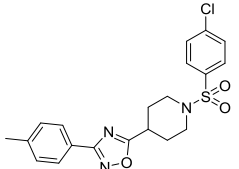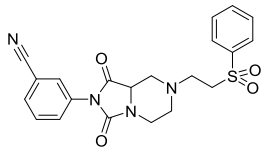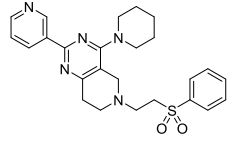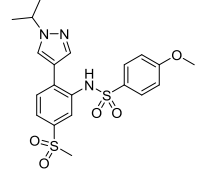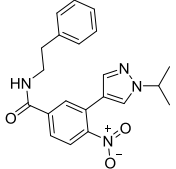
were grown overnight on Mueller-Hinton agar and several colonies resuspended in broth to give an optical density at 600 nm equivalent to a 0.5 McFarland standard. 20 μL of a 1 in 20 dilution of this suspension was inoculated into microtitre plates (Corning) containing medium plus meropenem (Sequoia Research Products, Pangbourne, U.K.) and inhibitors as appropriate. The total assay volume was 200 μL. Inhibitors were dissolved in dimethyl sulphoxide (DMSO) to 10 mg / mL and diluted in broth to a final concentration of 100 μg / mL. The concentration of DMSO in the assay was 1%. For inhibitors that were not soluble under these conditions stocks were prepared at 1 mg/mL in 50 % DMSO, giving a final DMSO concentration in the assay of 5 %. Control experiments carried out in the absence of inhibitors confirmed that susceptibility to meropenem was unaffected by DMSO at these concentrations. Plates were incubated overnight at 37 °C for 18 – 24 h and absorbance at 600 nm read on a Polarstar Omega (BMG LabTech) plate reader.

AutoDock vHTS results

A2.1 ChemBridge

Cat. No	Structure	AutoDock Score	SPROUT Score	clogP
5185088		-9.65	-6.54	5.08
5482935		-10.60	-6.70	4.61
5670808		-9.53	-6.69	3.24
5918981		-9.80	-6.77	2.93
6240983		-9.59	-6.41	4.20
7691782		-9.70	-6.94	2.18
9072094		-9.45	-6.94	3.03
9151689		-9.50	-7.19	3.49

A2.2 Peakdale

Cat. No	Structure	AutoDock Score	SPROUT Score	clogP
1011074		-9.62	-6.69	3.52
1012076		-10.40	-7.05	4.29
1017178		-9.62	-6.10	2.12
1019464		-9.67	-7.02	4.42
3001659		-9.60	-7.00	3.08
3002632		-9.65	-7.08	4.78
1015266		-9.58	-6.00	1.58
1007423		-9.50	-6.58	3.59
3001861		-10.40	-6.19	1.99
3001851		-9.50	-5.76	3.85

Peptide library generation

A3.1 Python script to generate SMILES strings

```python
import sys
import itertools
resi1=[          'A',
                 'R',
                 'N',
                 'D',
                 'C',
                 'E',
                 'Q',
                 'G',
                 'H',
                 'I',
                 'L',
                 'K',
                 'M',
                 'F',
                 'P',
                 'S',
                 'T',
                 'W',
                 'Y',
                 'V',
        ]
resi2=resi3=resi1
print 'resi1', len(resi1)
print 'resi2', len(resi2)
print 'resi3', len(resi3)

listoflists=[resi1,resi2,resi3]
print 'listoflists', len(listoflists)
crude=list(itertools.product(*listoflists))
print len(crude)

singleC=[]
for comb in crude:
        Ccheck=0
        for resi in comb:
                if resi=='C': Ccheck+=1
        if Ccheck==1: singleC.append(comb)
print singleC
print len(singleC)
```

```python
#for comb in singleC:
#       if comb[0]=='C' and comb[1]=='D' and comb[2]=='D':
#               print comb

aminodict={     'A':'C(=O)[C@H](C)N',
                'C':'C(=O)[C@H](CS)N',
                'D':'C(=O)[C@H](CC(=O)O)N',
                'E':'C(=O)[C@H](CCC(=O)O)N',
                'F':'C(=O)[C@H](C(c1ccccc1))N',
                'G':'C(=O)CN',
                'H':'C(=O)[C@H](C(C1=CN=CN1))N',
                'I':'C(=O)[C@H]([C@@H](C)(CC))N',
                'K':'C(=O)[C@H](CCCCN)N',
                'L':'C(=O)[C@H](CC(C)C)N',
                'M':'C(=O)[C@H](CCSC)N',
                'N':'C(=O)[C@H](CC(=O)N)N',
                'P':'C(=O)[C@@H]1CCCN1',
                'Q':'C(=O)[C@H](CCC(=O)N)N',
                'R':'C(=O)[C@H](CCCNC(=N)N)N',
                'S':'C(=O)[C@H](CO)N',
                'T':'C(=O)[C@H]([C@@H](C)O)N',
                'V':'C(=O)[C@H](C(C)(C))N',
                'W':'C(=O)[C@H](Cc1cNc2ccccc21)N',
                'Y':'C(=O)[C@H](Cc1ccc(O)cc1)N',
}


final=[]
for sequence in singleC:
        final.append(list(sequence))

for item in final:
        for n,letter in enumerate(item):
                if letter in aminodict.keys():
                        item[n]=aminodict[letter]
                else:
                        print 'ERRRRRRORRRRRR'
                        sys.exit()

print final

peptides=[]
for smiles in final:
        molecule=(''.join(smiles))
```

```python
        add_acid=(molecule[0:5]+'(O)'+molecule[5:])
        peptides.append(add_acid)


print peptides
print len(peptides)


output=open('output.smi', 'w+')
for molecule in peptides:
        output.write(molecule)
        output.write('\n')


print 'output.smi written'
```

The output of this program generates the SMILES strings below:

```
C(=O)(O)[C@H](C)NC(=O)[C@H](C)NC(=O)[C@H](CS)N
C(=O)(O)[C@H](C)NC(=O)[C@H](CCCNC(=N)N)NC(=O)[C@H](CS)N
C(=O)(O)[C@H](C)NC(=O)[C@H](CC(=O)N)NC(=O)[C@H](CS)N
C(=O)(O)[C@H](C)NC(=O)[C@H](CC(=O)O)NC(=O)[C@H](CS)N
C(=O)(O)[C@H](C)NC(=O)[C@H](CS)NC(=O)[C@H](C)N
C(=O)(O)[C@H](C)NC(=O)[C@H](CS)NC(=O)[C@H](CCCNC(=N)N)N
C(=O)(O)[C@H](C)NC(=O)[C@H](CS)NC(=O)[C@H](CC(=O)N)N
C(=O)(O)[C@H](C)NC(=O)[C@H](CS)NC(=O)[C@H](CC(=O)O)N
C(=O)(O)[C@H](C)NC(=O)[C@H](CS)NC(=O)[C@H](CCC(=O)O)N
C(=O)(O)[C@H](C)NC(=O)[C@H](CS)NC(=O)[C@H](CCC(=O)N)N
C(=O)(O)[C@H](C)NC(=O)[C@H](CS)NC(=O)CN
C(=O)(O)[C@H](C)NC(=O)[C@H](CS)NC(=O)[C@H](C(C1=CN=CN1))N
C(=O)(O)[C@H](C)NC(=O)[C@H](CS)NC(=O)[C@H]([C@@H](C)(CC))N
```

…

Total: 1,083 peptide SMILES strings

A3.2 Conversion of SMILES to 2D structures using Babel

```
babel -in output.smi -out output.sdf
```

A3.3 Conversion of 2D structures to 3D structures using Omega

```
omega -in output.sdf -strict -progress percent -maxconfs 1 -out 3D-
trimers.sdf
```

In silico peptide selection

A4.1 Top trimer sequences

Amino Acid Sequence	AutoDock Score	SPROUT Score	Number of AutoDock poses /20[a]
Pro-Ile-Cys	-7.40	-4.35	12
Asn-Pro-Cys	-7.00	-6.13	15
Pro-Pro-Cys	-7.50	-4.99	10
Pro-Trp-Cys	-8.40	-5.56	3
Pro-Cys-Phe	-7.76	-3.49	3
Cys-Pro-Phe	-7.30	-4.58	13
Cys-Gly-Trp	-7.60	-5.73	6
Cys-Pro-Trp	-7.60	-5.07	5
Cys-Phe-Tyr	-7.50	-4.5	4
Cys-Pro-Tyr	-7.20	-4.02	7

A4.2 Top scoring tetramers

Amino Acid Sequence	AutoDock Score	SPROUT Score	Number of AutoDock poses /20[a]
Cys-Pro-Asp-Ala	-8.00	-5.35	7
Pro-Pro-Gly-Cys	-8.00	-5.73	5
Pro-Trp-Gly-Cys	-8.50	-5.53	4
Pro-Gly-Trp-Cys	-7.70	-4.62	5
Ser-Cys-Val-Glu	-7.80	-4.61	7
Pro-Cys-Phe-Gly	-7.80	-3.17	5
Gly-Cys-Pro-Phe	-7.70	-5.94	7
Pro-Cys-Asp-Pro	-7.50	-3.6	7
Pro-Pro-Cys-Pro	-7.80	-3.17	7
Cys-Pro-Glu-Pro	-7.60	-4.34	8

A4.3 Top Scoring Dimers

Amino Acid Sequence	AutoDock Score	SPROUT Score	Number of AutoDock poses /20[a]
Asp-Cys	-7.00	-6.29	14
Glu-Cys	-7.05	-5.91	10
Gln-Cys	-6.45	-4.87	16
His-Cys	-6.40	-4.96	13
Phe-Cys	-6.44	-5.67	6
Pro-Cys	-6.68	-3.64	19
Trp-Cys	-7.80	-7.18	14
Tyr-Cys	-6.67	-3.80	14
Cys-Phe	-6.30	-3.77	6
Cys-Trp	-6.70	-6.38	9

A4.4 Worst Scoring Trimers

Amino Acid Sequence	AutoDock Score	SPROUT Score	Number of AutoDock poses /20[a]
Cys-Arg-Arg	-3.00	-2.98	2
Arg-Cys-Arg	-2.42	-1.89	2
Gln-Cys-Arg	-3.50	-2.34	2
Lys-Cys-Arg	-3.19	-4.08	1
Asp-Cys-Asp	-3.75	-4.57	1
Arg-Arg-Cys	-3.00	-2.46	2
Cys-Lys-Glu	-3.75	-3.41	2
Cys-Arg-Glu	-3.91	-5.42	3
Lys-Cys-Gln	-3.62	-2.38	2
Arg-Cys-Tyr	-3.41	-3.33	3

A4.5 Top Scoring D-L Combinations

Amino Acid Sequence	AutoDock Score	SPROUT Score	Number of AutoDock poses /20[a]
D-Cys-D-Phe-D-Tyr	-8.40	-5.49	5
D-Pro-D-Trp-D-Cys	-8.10	-3.71	6
D-Cys-D-Pro-D-Tyr	-8.00	-4.65	10
D-Pro-D-Cys-D-Phe	-8.00	-4.43	8

[a] Number of AutoDock poses out of the 20 dockings conducted for each ligand which are in the most populated cluster relating to the displayed AutoDock score.

In silico assay evaluation

A5.1 Substrate

Enzyme	Substrate	AutoDock Score	SPROUT Score	Number of AutoDock poses / 10[b]
IMP-1	Nitrocefin	-11.00	-7.95	2
	Imipenem	-6.75	-6.04	7
	Fluorogenic	-10.10	-7.63	2
	CENTA	-9.05	-8.03	1
NDM-1	Nitrocefin	-6.70	-5.11	6
	Imipenem	-6.15	-4.25	10
	Fluorogenic	-8.00	-5.69	3
	CENTA	-7.10	-4.49	2
SPM-1	Nitrocefin	2.00	-4.01	5
	Imipenem	-3.75	-2.95	3
	Fluorogenic	7.50	-4.57	2
	CENTA	2.50	-3.96	2
VIM-2	Nitrocefin	-6.00	-4.46	5
	Imipenem	-7.40	-3.39	6
	Fluorogenic	-8.00	-5.08	2
	CENTA	-7.00	-3.61	5

A5.2 Tetrahedral intermediate

Enzyme	Substrate	AutoDock Score	SPROUT Score	Number of AutoDock poses / 10[b]
IMP-1	Nitrocefin	-9.20	-6.61	3
	Imipenem	-6.92	-6.68	5
	Fluorogenic	-8.50	-6.20	2
	CENTA	-7.60	-8.54	2
NDM-1	Nitrocefin	-6.25	-5.64	1
	Imipenem	-5.40	-4.73	10
	Fluorogenic	-7.10	-6.26	2
	CENTA	-7.25	-6.06	3
SPM-1	Nitrocefin	8.00	0.96	3
	Imipenem	-3.90	0.65	6
	Fluorogenic	10.00	0.81	1
	CENTA	2.85	-4.07	1
VIM-2	Nitrocefin	-4.50	-3.69	2
	Imipenem	-6.30	-3.51	5
	Fluorogenic	-10.00	-6.32	1
	CENTA	-3.00	-3.98	2

A5.3 Hydrolysis product

Enzyme	Substrate	AutoDock Score	SPROUT Score	Number of AutoDock poses / 10[b]
IMP-1	Nitrocefin	-9.00	-8.23	1
	Imipenem	-6.20	-4.21	1
	Fluorogenic	-8.50	-7.57	2
	CENTA	-7.50	-6.79	2
NDM-1	Nitrocefin	-7.90	-7.00	3
	Imipenem	-5.50	-3.79	1
	Fluorogenic	-8.50	-7.34	1
	CENTA	-7.75	-5.38	2
SPM-1	Nitrocefin	1.00	1.27	1
	Imipenem	-4.00	0.89	3
	Fluorogenic	0.00	1.12	1
	CENTA	8.00	-3.83	1
VIM-2	Nitrocefin	-5.00	-4.86	1
	Imipenem	-7.25	-4.29	4
	Fluorogenic	-8.00	-5.13	2
	CENTA	-7.00	-6.17	2

[b] Number of AutoDock poses out of the 10 dockings conducted for each ligand which are in the most populated cluster relating to the displayed AutoDock score.